

Pickering emulsion based encapsulates stabilized by porous starch for bioactive delivery

By

Sannya Sathyan
Enrollment No:10BB17J39014

A thesis submitted to the
Academy of Scientific and Innovative Research
for the award of the degree of

DOCTOR OF PHILOSOPHY
in
SCIENCE

Under the supervision of

Dr. P. Nisha
Principal Scientist



CSIR- National Institute for Interdisciplinary Science and
Technology (CSIR-NIIST), Thiruvananthapuram
Kerala-695019, India



Academy of Scientific and Innovative Research
AcSIR Headquarters, CSIR-HRDG campus,
Sector 19, Kamla Nehru Nagar,
Ghaziabad, U. P. -201002, India

June 2023



राष्ट्रीय अंतर्विषयी विज्ञान तथा प्रौद्योगिकी संस्थान

NATIONAL INSTITUTE FOR INTERDISCIPLINARY SCIENCE AND TECHNOLOGY

वैज्ञानिक तथा औद्योगिक अनुसंधान परिषद्

Council of Scientific & Industrial Research

इंडस्ट्रियल एस्टेट पी.ओ., पाप्पनकोड, तिरुवनंतपुरम, भारत - 695 019

Industrial Estate P.O., Pappanamcode, Thiruvananthapuram, India - 695019

June, 2023

CERTIFICATE

This is to certify that the work incorporated in this Ph.D thesis entitled, "*Pickering emulsion based encapsulates stabilized by porous starch for bioactive delivery*", submitted by *Ms. Sannya Sathyan*, to the Academy of Scientific and Innovative Research (AcSIR) in fulfilment of the requirements for the award of the *Degree of Doctor of Philosophy in Sciences*, embodies original research work carried out by the student. We further certify that this work has not been submitted to any other University or Institution in part or full for the award of any degree or diploma, Research materials obtained from other sources and used in this research work have been duly acknowledged in the thesis, images, illustrations, figures, tables etc., used in the thesis from other sources, have also been duly cited and acknowledged.


20/06/2023
Sannya Sathyan


20/06/2023
Dr. P Nisha
(Thesis Supervisor)

STATEMENTS OF ACADEMIC INTEGRITY

I, **Sannya Sathyan**, a Ph.D. student of the Academy of Scientific and Innovative Research (AcSIR) with Registration No. 10BB17J39014 hereby undertake that, the thesis entitled "**Pickering emulsion based encapsulates stabilized by porous starch for bioactive delivery**" has been prepared by me and that the document reports original work carried out by me and is free of any plagiarism in compliance with the UGC Regulations on "*Promotion of Academic Integrity and Prevention of Plagiarism in Higher Educational Institutions (2018)*" and the CSIR Guidelines for "*Ethics in Research and in Governance (2020)*".


20/06/2023
Sannya Sathyan

20 June 2023

Thiruvananthapuram

It is hereby certified that the work done by the student under our supervision, is plagiarism-free in accordance with the UGC Regulations on "*Promotion of Academic Integrity and Prevention of Plagiarism in Higher Educational Institutions (2018)*" and the CSIR Guidelines for "*Ethics in Research and in Governance (2020)*".


20/06/2023
Dr. P Nisha

20 June 2023

Thiruvananthapuram

DECLARATION

I, **Sannya Sathyan.**, bearing AcSIR Registration No. 10BB17J39014 declare: that my thesis entitled, **“Pickering emulsion based encapsulates stabilized by porous starch for bioactive delivery”** is plagiarism free in accordance with the UGC Regulations on *“Promotion of Academic Integrity and Prevention of Plagiarism in Higher Educational Institutions (2018)”* and the CSIR Guidelines for *“Ethics in Research and in Governance (2020)”*.

I would be solely held responsible if any plagiarised content in my thesis is detected, which is violative of the UGC regulations 2018.


20/06/2023

Sannya Sathyan

20 June 2023

Thiruvananthapuram

20 June 2023

ACKNOWLEDGMENTS

Foremost, I thank ALMIGHTY GOD for being with me always, showering blessings and giving me strength throughout my research and academic period.

*It is my profound privilege to express my deep sense of gratitude to my supervisor **Dr. P. Nisha** Principal Scientist, Agro Processing and Technology Division, CSIR-NIIST, Trivandrum, for her valuable guidance, inspiring suggestions, continuous support, and endless patience throughout my research work. She has given me all the freedom to pursue my research, and fulfilled all necessary requirements for undertaking my work. It has been a matter of pride and profound pleasure to have worked under her kind and able supervision.*

*I am deeply grateful to **Dr. C. Anandharamakrishnan**, Director, CSIR-NIIST, **Dr. A. Ajayaghosh**, former Director of CSIR-NIIST for providing all the necessary facilities to carry out the research work in CSIR-NIIST. I am deeply obliged for the timely effects of **Dr. Karunakaran Venugopal**, current ACSIR co-ordinator and **Dr. Suresh. C.H.**, **Dr. R. Luxmi Varma**, former ACSIR co-ordinators for their kind help during academic requirements.*

*I also express my deep sense of gratitude to the members of my doctoral advisory committee, **Dr. Kaustabh Kumar Maiti**, **Dr. P. Jayamurthy** and **Dr. Binod Parameswaran** for their helpful suggestions, guidance and timely cooperation throughout my study.*

*I extend my deep sense of gratitude toward, **Dr. Dileep kumar** and **Dr. K G Raghu** (Former Heads of the Department) and **Er Venugopalan V.V.** Head of the Department, Agro Processing and Technology Division, CSIR-NIIST, Trivandrum. I am grateful to **Dr. K G Raghu** for his constant support and encouragement throughout the work.*

My deepest thanks to Dr. S. Asha Nair, Indu Ramachandran for FACS, RGCB. I also thank Mr. Peer Mohamed and Visak for Rheology and BET, Mr. Hareesh for SEM, Anju, Amal and Vipin for FTIR, DSC and XRD. Mr. Pratheesh for his generous help in APTD, Sreejith, and Merin for Academic help.

I really thank UGC for providing me Fund for my research.

Being a part of the Agro Processing and Technology Division was a wonderful pleasure. I was fortunate to get, helpful advice and support from my seniors and juniors to complete my work. I really thank my colleagues and friends, especially Dr.. Lekshmy Krishnan, Dr,Nayana, Shini, Nidhina, Sudhina, Billu, Kavya Dr. Chinthu, Abhijit, Reshma, Heeba, Dr. Arun, Dr.Resmitha, Shyam, Archana, Nisha, Sandhya, Hari, Noor, Dr. Sithara, Navami, Titto, Ramees, Treeza, Dr. Cally makebe.

I am really thankful to my dear friends Eveline, Sruthi, Anagha Anusha, Ashin, Taniya, Athira, Raveena, Roopasree, Dr. Lakshmi, Poornima, Dr. Juby, Gopika, Theertha, Drishya, Jasmina, and my seniors Dr. Soumya, Dr. Salin, Dr. Genu, Dr. Sree Lakshmi, Dr. Swapna, Dr. Anupama, Dr. Preetha, Dr. Shyni.

Most importantly, none of this would have been possible without the love, concern, support and strength provided by my family. I am greatly thankful to my parents Mr. Sathyan and Indira who are my greatest pillars, my sister and brother for the support and all other family members for their timely support. Ryan and Sayan, my two shining stars who gave me positive vibes throughout my research.

Thanks to all those who cannot fit a separate name but helped me directly or indirectly to achieve the goal.

S
20/06/2023
Sannya Sathyan

Dedicated to my pappa, amma and beloved ones..

TABLE OF CONTENTS

Sl.no.	Content	Page no.
1	Introduction and Review of Literature	1 - 61
1.1	Introduction	3
1.2	Stabilization mechanism of Pickering particle	6
1.3	Food grade Pickering particles	7
1.3.1.	Polysaccharide particles used as Pickering particles	7
1.3.1.1.	Cellulose	7
1.3.1.2.	Chitosan	9
1.3.1.3.	Starch	10
1.4.	Application of polysaccharide stabilized Pickering emulsion	11
1.4.1.	Fat substitutes	11
1.4.2.	Modulation of lipid digestion	12
1.4.3.	Encapsulation and delivery of food bioactive ingredients	12
1.5.	Porous starch	13
1.5.1.	Techniques for porous starch preparation	14
1.5.1.1.	Physical methods	14
1.5.1.1.1.	Ultrasonication	14
1.5.1.1.2.	Microwave method	15
1.5.1.1.3.	High Hydrostatic pressure (HHP)	16
1.5.1.2.	Chemical treatment	18
1.5.1.2.1.	Solvent Exchange method	18
1.5.1.2.2.	Acid and alkali treatment	18
1.5.1.3.	Enzymatic method	20
1.5.1.3.1.	α -amylase	20

1.5.1.3.2.	Glucoamylase	21
1.5.1.3.3.	Cyclodextrin glycosyltransferase	22
1.5.1.3.4.	Synergistic action of enzymes	23
1.5.2.	Characterization of porous starch	25
1.5.2.1.	Swelling power and Solubility	25
1.5.2.2.	Pasting property	25
1.5.2.3.	Rheological property	26
1.5.2.4.	Thermal property	27
1.5.2.5.	Gelatinization property	27
1.5.3.	Food application of porous starch	28
1.5.3.1.	Encapsulation of flavour and oil	28
1.5.3.2.	Encapsulation of pigments	29
1.5.3.3.	Encapsulation of probiotics	30
1.5.3.4.	Food packaging	30
1.6.	Future prospects and conclusion	36
1.7.	References	38
2	Optimization and characterization of porous corn starch and application in emulsion stabilization	63-105
2.1.	Introduction	65
2.1.1.	Objective	68
2.2	Materials and Methods	69
2.2.1	Materials	69
2.2.2	Methods	69
2.2.2.1.	Preparation of porous starch	69
2.2.2.1.1.	Optimization of concentration and incubation time of individual enzyme	69

2.2.2.1.2.	Modelling and optimization	70
2.2.2.2.	Determination of specific surface area and pore size distribution	71
2.2.2.3.	Scanning Electron Microscopy (SEM)	71
2.2.2.4.	Particle size and zeta potential	71
2.2.2.5.	Contact angle	71
2.2.2.6.	Rheology	72
2.2.2.7.	ATR-Fourier-transform infrared (FTIR) spectroscopy	72
2.2.2.8.	Differential scanning calorimetry (DSC)	72
2.2.2.9.	X-ray diffraction (XRD)	73
2.2.2.10.	Efficacy of porous starch as emulsion stabilizer	73
2.2.2.11	Fluorescence microscopy	73
2.2.2.12.	Efficacy of porous starch as bioactive carrier	74
2.3	Results and discussion	75
2.3.1.	Optimization of porous starch preparation	75
2.3.2.	Effect of combination of enzymes on porous starch preparation	78
2.3.3.	Characterization of porous starch	82
2.3.3.1.	Particle size and zeta potential	82
2.3.3.2.	Contact angle	83
2.3.3.3.	Rheological studies	84
2.3.3.3.1	Flow behaviour	84
2.3.3.4.	XRD	86
2.3.3.5.	Thermal behaviour	87
2.3.3.6	FTIR	89
2.3.3.7.	Preparation of emulsion	90
2.3.3.8.	Fluorescence microscopy	90

2.3.3.9.	Evaluation of efficacy of porous starch as carrier of bioactives	91
2.4.	Conclusion	93
2.5	References	94
3	Fabrication of Curcumin loaded encapsulates by porous starch Pickering emulsion	107-144
3.1	Introduction	109
3.1.1.	Objectives	113
3.2.	Materials and Methods	114
3.2.1.	Materials	114
3.2.2	Methods	114
3.2.2.1.	Preparation of Pickering emulsion	114
3.2.2.2.	Optimization of composition (wall and core) of emulsion.	115
3.2.2.3.	Characterization studies	115
3.2.2.3.1.	Encapsulation efficiency	115
3.2.2.3.2.	Creaming index	116
3.2.2.3.3.	Zeta potential	116
3.2.2.3.4.	Microstructure analysis and particle size	116
3.2.2.3.5.	Rheology	117
3.2.2.3.6.	ATR-Fourier-transform infrared (FTIR) spectroscopy	117
3.2.2.4.	Storage studies of emulsion	117
3.2.2.5.	Statistical analysis	118
3.3.	Results and discussion	118
3.3.1.	Standardization and optimization of core and wall materials and processing conditions of Pickering emulsion.	118
3.3.2.	Characterization studies	120

3.3.2.1.	Encapsulation efficiency	120
3.3.2.2.	Microstructure analysis by fluorescence microscopy	121
3.3.2.3.	Rheology	122
3.3.2.4.	FTIR	125
3.3.3.	Storage studies of emulsion	126
3.3.3.1.	Creaming index	126
3.3.3.2.	Particle size and Zeta potential	127
3.3.6.3.	Microstructure analysis	130
3.4.	Conclusion	132
3.5.	References	134
4	<i>In vitro</i> release kinetics and prebiotic efficacy of Curcumin Pickering emulsion	145-171
4.1	Introduction	147
4.1.1.	Objectives	149
4.2.	Materials and Methods	149
4.2.1.	Materials	150
4.2.2.	Methods	150
4.2.2.1.	<i>In vitro</i> release studies of porous starch based curcumin Pickering emulsion	150
4.2.2.2.	Prebiotic potential of fermentation metabolites (FM)	151
4.2.2.3.	Evaluation of prebiotic potential of fermentation metabolites	152
4.2.2.3.1.	Estimation of optical density	152
4.2.2.3.2.	Estimation of pH	152
4.2.2.3.3.	Colony count	152
4.2.2.3.4.	Assessment of SCFA production in FM	153
4.2.2.3.5.	Assessment of curcumin concentration in FM	153

4.2.2.4.	Statistical analysis	154
4.3.	Results and discussion	154
4.3.1.	<i>In vitro</i> release studies	154
4.3.2.	Prebiotic potential of fermentation metabolites (FM)	155
4.3.2.1.	Change in optical density	155
4.3.2.2.	Change in pH	157
4.3.2.3.	Determination of colony count	158
4.3.2.4.	Change in dry weight	159
4.3.2.5.	Determination of curcumin in fermentation metabolites	160
4.3.2.6	Quantification of short chain fatty acid production	161
4.4.	Conclusion	164
4.4.	References	165
5	<i>In vitro</i> screening of the fermentation metabolites in prevention and management of colorectal cancer	173-209
5.1.	Introduction	175
5.1.1.	Objectives	178
5.2.	Materials and Methods	179
5.2.1.	Materials	179
5.2.2.	Methods	180
5.2.2.1.	Cell culture and treatment conditions	180
5.2.2.2.	Determination of cytotoxicity effect of fermentation metabolites by MTT assay	180
5.2.2.3.	Determination of nuclear integrity by DAPI staining	181
5.2.2.4.	Wound healing assay	181
5.2.2.5.	Measurement of Reactive oxygen species (ROS)	182
5.2.2.6.	Determination of antioxidant enzyme activity	182

5.2.2.6.1	Measurement of SOD	182
5.2.2.6.2	Measurement of CAT	182
5.2.2.7.	Determination of mitochondrial membrane potential by rhodamine 123	183
5.2.2.8.	Determination of calcium by Fura- 2, AM	183
5.2.2.9.	Apoptosis assay by flow cytometry	183
5.2.2.10.	Immunoblot analysis	184
5.2.2.11.	Statistical analysis	185
5.3.	Results and discussion	185
5.3.1.	Determination of cytotoxicity fermentation metabolites (FM) by MTT Assay	185
5.3.2.	FM treatment induced chromosome condensation	187
5.3.3.	Wound Healing Assay	188
5.3.4.	Measurement of ROS by DCFDA staining	190
5.3.5.	FM treatment reduced antioxidant enzyme activity (SOD and CAT)	191
5.3.6.	FM treatment induced loss of mitochondrial membrane potential (MMP)	193
5.3.7.	Measurement of Calcium by Fura-2, AM	194
5.3.8.	Apoptosis- Annexin V-FITC	196
5.3.9.	Western blotting	197
5.4.	Conclusion	199
5.5.	Summary	200
5.6	References	201
6	Summary and Conclusion	211

List of tables

Table no.	Title	Page no.
Table 1.1	Physical treatment methods used in porous starch preparation	17
Table 1.2	Chemical treatment methods used in porous starch preparation	20
Table 1.3	Enzymatic treatment methods used in porous starch preparation	24
Table 1.4	Food applications of porous starch	31
Table 2.1	The surface area and pore size of starch treated with different concentrations of Amylase (AM) and time of incubation	75
Table 2.2	The surface area and pore size of starch treated with different concentrations of Amyloglucosidase (AMG) and time of incubation	77
Table 2.3	The surface area and pore size of starch treated with combination of enzymes, (AM/AMG) and time of incubation.	79
Table 2.4	Regression table for combination of enzymes AM and AMG	80
Table 2.5	Gelatinization temperature of native and porous starch	89
Table 3.1	Optimized conditions of stable Pickering emulsion	120
Table 3.2	Particle size of NSPE and PSPE system during storage days.	130

List of Figures

Figure no.	Title	Page no.
Fig 1.1	Mechanisms that induce emulsions instability	3
Fig 1.2	Mechanism of stability of Pickering emulsion	4
Fig 1.3 (a) and (b)	Advantages of using Pickering emulsion and Pickering emulsion delivery system.	5
Fig 1.4	Number of publications on Pickering emulsion per year (2015-2021) according to Web of science.	6
Fig 1. 5 (a) and (b)	Native and porous starch granules	14
Fig 1.6	The mechanism of enzyme treatment on starch	22
Fig 2.1	SEM images of starch treated with different concentrations and incubation time of amylase	76
Fig 2.2	SEM images of starch treated with different concentrations and incubation time of amyloglucosidase	78
Fig 2.3	SEM images of starch treated with different concentrations and incubation time of amylase and amyloglucosidase.	81
Fig 2.4 (a) and (b)	Contact angle of NS and PS	84
Fig 2.5 (a) and (b)	Shear stress vs shear rate plot and Shear rate vs Viscosity plot of NS and PS	85
Fig 2.6 (a) and (b)	Amplitude sweep of NS and PS respectively.	85
Fig 2.7 (a) and (b)	Frequency sweep of NS and PS respectively.	86
Fig 2.8 (a) (b) and (c)	XRD diffractograms and Deconvolution plots of native and porous starch	87
Fig 2.9	DSC thermograms of NS and PS.	88

Fig 2.10	FTIR spectrum of NS and PS.	89
Fig 2.11	Emulsion of NS and PS after 30 minutes, 24h and 48h.	90
Fig 2.12	Fluorescence images of porous and native starch	91
Fig 2.13 (a) (b) and (c)	HPLC chromatogram of standard Curcumin, NS and PS.	92
Fig 3.1	Fluorescence image of Native starch (NS) and Porous starch (PS) Pickering emulsion	122
Fig 3.2 (a) and (b)	Shear stress vs. shear rate plot and shear rate vs. viscosity plot of NSPE and PSPE system	123
Fig 3.3 (a) and (b)	Amplitude sweep of NSPE and PSPE system.	124
Fig 3.4 (a) and (b)	Frequency sweep of NSPE and PSPE system	125
Fig 3.5	FTIR spectrum of NSPE and PSPE system	126
Fig 3.6 (a) and (b)	Creaming index of NSPE and PSPE system	127
Fig 3.7	Light and fluorescence microscopic images of PSPE system and NSPE system on 3 rd and 15 th day	131
Fig 3.8	Mechanism of solid particle stabilized Pickering emulsion system	132
Fig 4.1	Preparation of fermentation metabolites	152
Fig 4.2	Prebiotic potential of porous starch emulsion determined by change in optical density for <i>Lactobacillus casei</i>	156
Fig 4.3	Prebiotic potential of porous starch emulsion determined by pH change for <i>Lactobacillus casei</i>	157
Fig 4.4	Colony count by pour plate method at 48h	158
Fig 4.5	Prebiotic potential of porous starch emulsion determined by colony count by pour plate method for <i>Lactobacillus casei</i> .	159
Fig 4.6	Prebiotic potential of porous starch emulsion determined by change in dry weight for <i>Lactobacillus casei</i>	160

Fig 4.7	HPLC chromatograms of standard short chain fatty acids- AA, PA and BA	162
Fig 4.8 (a), (b) and (c)	Estimation of short chain fatty acids- AA, PA and BA by HPLC	163
Fig 5.1	The pie chart shows the most prevalent cancer cases worldwide	175
Fig 5.2	Risk factors that leads to colorectal cancer	176
Fig 5.3	Relation between dietary fiber, probiotics and CRC	177
Fig 5.4	MTT cytotoxicity assay of fermentation metabolites (FM).	186
Fig 5.5	Morphological analysis of HCT 116 cells treated with different concentrations of FM by phase contrast microscopy	187
Fig 5.6	DAPI staining in HCT 116 cells.	188
Fig 5.7	<i>In vitro</i> wound healing assay.	189
Fig 5.8	Wound closure percentage of FM in HCT 116 cells	190
Fig 5.9	Determination of ROS production in HCT 116 cell lines upon pretreatment with FM via fluorescence microscopy.	191
Fig 5.10 (a) and (b)	Effect of FM on SOD activity and CAT activity in HCT 116 cell	192
Fig 5.11	Determination of MMP in HCT 116 cell upon pretreatment with FM	194
Fig 5.12	Measurement of Calcium in HCT 116 cell lines upon pretreatment with FM	195
Fig 5.13	Effect of FM on HCT 116 cell apoptosis by flow cytometry	196
Fig 5.14	Effect of FM on expression of proteins involved in apoptosis in HCT 116 cells.	199
Fig 5.15	Schematic representation of possible mechanism by which FM containing short chain fatty acids regulate signaling events to induce cell death by apoptosis in HCT 116 cells	200
Fig 6.1	Graphical representation of chapters with brief demonstration of work flow	221

ABBREVIATIONS

PS	Porous Starch
NS	Native Starch
AM	Amylase
AMG	Amyloglucosidase
PBS	Phosphate Buffered Saline
KOH	Potassium Hydroxide
SSA	Specific Surface Area
PSD	Pore Size Distribution
BET	Brunauer- Emmett-Teller
BJH	Barrett- Joiner-Halenda
DSC	Differential Scanning Calorimetry
ATR	Attenuated Total Reflection
EE	Encapsulation Efficiency
O/W	Oil In Water Emulsion
W/O	Water In Oil Emulsion
CI	Creaming Index
SGF	Simulated Gastric Fluid
SIF	Simulated Intestinal Fluid
FTIR	Fourier Transform Infrared Spectroscopy
SEM	Scanning Electron Microscopy
XRD	X-Ray Diffraction
FSO	Flax Seed Oil
NSPE	Native Starch Pickering Emulsion
PSPE	Porous Starch Pickering Emulsion
LVE	Linear Visco Elastic
ANOVA	Analysis Of Variance
SCFA	Short Chain Fatty Acids
OD	Optical Density
NaCl	Sodium Chloride
HCl	Hydrochloric Acid
CaCl	Calcium Chloride

FM	Fermentation Metabolites
HPLC	High-Performance Liquid Chromatography
SSG	Simulated Salivary Fluid
AA	Acetic Acid
PA	Propionic Acid
BA	Butyric Acid
CFU	Colony Forming Unit
CRC	Colorectal Cancer
FBS	Fetal Bovine Serum
FITC	Fluorescein IsoThiocyanate
H ₂ O ₂	Hydrogen peroxide
HRP	Horseradish Peroxidase
Bax	Bcl-2 - associated X protein
Bak	Bcl-2 Homologous Antagonist
Bcl-2	B-cell Lymphoma 2
CAT	Catalase
SOD	SuperOxide Dismutase
MMP	Mitochondrial Membrane Potential
DAPI	4',6- Diamidino-2- phenylindole
DMEM	Dulbecco's Modified Eagles's Medium
DMSO	Dimethyl sulfoxide
FACS	Fluorescence- Activated Cell Sorting
MTT	3-(4,5-dimethylthiazol-2-yl)-2,5 diphenyltetrazolium bromide
ROS	Reactive Oxygen Species
UV	Ultra Violet
Cyt C	Cytochrome C

SYMBOLS

β	Beta
α	Alpha
μ	Micro
μm	Micrometer
g	Gram
mg	Milligram
mg	Microgram
%	Percentage
$^{\circ}\text{C}$	Degree Celsius
mL	Milliliter
μl	Microliter
M	Molar
mM	Millimolar
w/v	Weight by volume
nm	Nanometre
V	Voltage
Da	Dalton
kDa	Kilo Dalton
Min	Minutes
Kb	Kilobase
h	Hour

PREFACE

The need for functional and biologically active food components is rising because of their significance in reducing the impacts of chronic and lifestyle disorders. Emulsion-based delivery systems are one strategy for safeguard, and promote absorption of biologically active food components. Mostly emulsifiers are used to modify the interfacial interactions to delay the phase separation in emulsion. The need to switch from synthetic to natural surfactants has increased as a result of rising consumer demand for environmental friendly, sustainable and natural food products. Solid particle stabilized emulsion called Pickering emulsion is an active area of research for the delivery of bioactive and nutritionally important components for food/functional and food/nutraceutical applications. Polysaccharides such as starch, cellulose and proteins are widely used as Pickering particles. Porous starch prepared by the enzymatic hydrolysis of native starch is reported for the sustained release and targeted delivery of certain drugs and bioactive.

Chapter 1 gives a general introduction and review of literature about Pickering emulsion, stabilization mechanism of Pickering particle, food grade Pickering particle and its application, techniques for porous starch preparation-physical, chemical and enzymatic method, characterization of porous starch and its food application.

Starch, has been modified to make it more efficient and functional for its use in various food applications apart from its use as stabilizing and thickening agent in industries. Porous starch is attaining great interest because of its abundant pores and increased surface area for targeted delivery and sustained release of certain drugs. Porosity of the starch granule can be tuned for various food applications including delivery of active ingredients. **Chapter 2** deals with the optimization and characterization of porous corn

starch preparation and its application studies. Porous starch was prepared enzymatically using enzymes amylase and amyloglucosidase individually and in combination. Based on the results obtained from individually treated enzymes two factorial design was performed for combination of enzymes. The enzyme concentration was optimized using surface area, pore size qualitatively and surface morphology by SEM images. Starch treated with optimized concentration of enzyme was subjected to further characterization studies such as contact angle, particle size, zeta potential, rheology, FTIR, DSC and XRD to analyze whether the porous starch act as Pickering particle and all the studies were compared with that of native starch. Further preliminary studies were conducted to evaluate the efficiency of porous starch in stabilizing emulsion by fluorescence microscopy and also as carrier of bioactive.

Solid particle stabilized surfactant free emulsion called Pickering emulsion have attracted lot of attention because it is nontoxic, biodegradable and biocompatible in nature. **Chapter 3** deals with the fabrication of curcumin loaded flax seed oil encapsulates by porous starch Pickering emulsion. O/W Pickering emulsion encapsulates were prepared by using guar gum as stabilizer and porous starch as Pickering particles. In order to ensure colon delivery porous starch was combined with guar gum, a well-known prebiotic dietary fibre, to form Pickering emulsion by encapsulating bioactive curcumin loaded in flax seed oil. The Pickering emulsion thus fabricated was characterized in terms of encapsulation efficiency, microstructure analysis by fluorescence microscopy, rheology and FTIR. The shelf stability was assessed by storing the samples for 15 days at refrigeration temperature (4 ± 2 °C). During storage studies, the samples were withdrawn every 3rd day and analyzed for creaming index, particle size, zeta potential and microstructural characteristics via fluorescence microscopy. The

results were compared with that of native starch emulsion fabricated using the same conditions replacing porous starch.

Porous starch-based Pickering emulsion can act as efficient Pickering particle and it also possess better encapsulation efficiency of curcumin. **Chapter 4** deals with the *In vitro* release kinetics and prebiotic efficacy of Curcumin Pickering emulsion. Pickering emulsion consists of curcumin loaded flax seed oil with guar gum as stabilizer and porous starch as Pickering particles. Guar gum is prebiotic in nature and is also reported to be used for colon targeted delivery of active ingredients. So in order to ensure the gut delivery of bioactive curcumin the *in vitro* release kinetics using simulated gastro intestinal conditions was performed. Pickering emulsion was fermented using probiotic species *Lactobacillus casei* and prebiotic potential of encapsulates in terms of change in OD, pH, dry weight, colony count and short chain fatty acids production using *in vitro* protocol was studied.

In vitro fermentation studies indicated the fermentation metabolites rich in SCFA, could be of great potential in maintaining the gut homeostasis, there by aids in prevention and management of CRC. **Chapter 5** deals with *in vitro* screening of the fermentation metabolites in prevention and management of colorectal cancer. The anticancer potential of fermentation metabolites was studied in HCT 116 colon cancer cell. The fermentation metabolites containing short chain fatty acids was analyzed for cytotoxic effects, nuclear integrity, mitochondrial membrane potential, antioxidant activity, ROS level, calcium level, apoptosis and finally expression of proteins by western blotting.

Chapter 1
Introduction and Review of literature

1.1. Introduction

The demand for bioactive and functional food ingredients is increasing because of their importance in mitigating chronic and lifestyle disorders such as diabetes, obesity and cancer (TMR, 2015; Lu et al., 2016). Most of the bioactives like polyphenols, tocotrienols and carotenoids are chemically unstable, retain unpleasant odours, and are sensitive to light, temperature and oxygen thus reducing their effectiveness (Mwangi et al., 2020). One strategy for safeguarding, and promoting the absorption of biologically active food components is the use of emulsion-based encapsulated delivery systems (Fu et al., 2016; Lu et al., 2016; McClements, 2007). An emulsion is a mixture of two immiscible liquids generally water and oil with one of the liquids dispersed as small spherical droplets in the other. As a result of their inherent thermodynamic instability, all emulsions eventually phase-separate by creaming, sedimentation, coalescence, flocculation and ostwald ripening (Fig 1.1) (Krishnan et al., 2023).

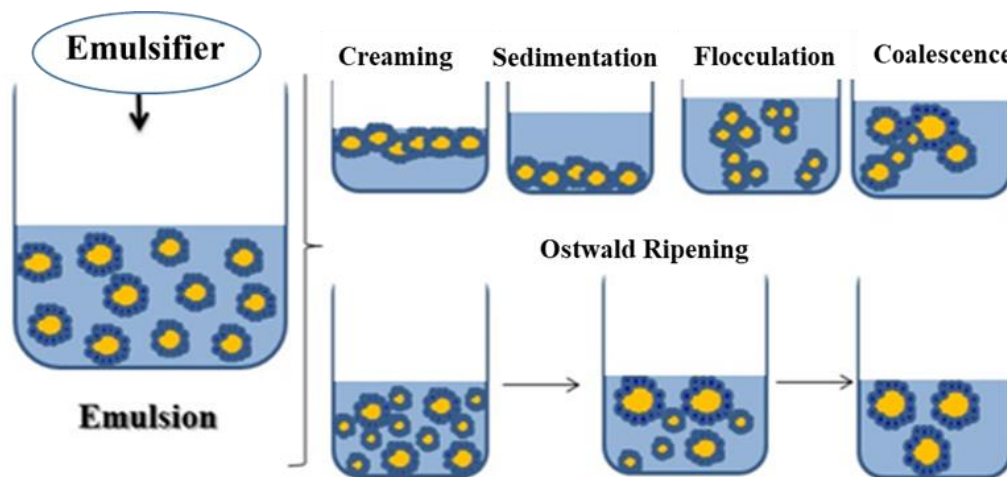


Fig 1.1: Mechanisms that induce emulsions instability (Krishnan et al., 2023).

Emulsifiers are employed to alter the interfacial interactions in order to delay the phase separation in emulsions because all emulsions are thermodynamically unstable.

Inorganic particles such as hydroxyapatite, silica, clay and latex are commonly used as stabilizers, however, their usage has been limited in the food and pharmaceutical industries due to growing concern about the biocompatibility, carcinogenicity and biodegradability of synthetic surfactants (Kierulf et al., 2020; Wang et al., 2016a, b; Wu et al., 2021b). The need to switch from synthetic to natural surfactants has increased as a result of rising consumer demand for environmentally friendly, sustainable, and natural food products and the adoption of healthier lifestyles.

The use of solid colloidal particles to generate stable emulsions is currently receiving a lot of interest. Solid particle-stabilized emulsions known as Pickering emulsions (Pickering, 1907; Ramsden, 1904; Saffarionpour, 2020), exhibit long-term stability without the addition of surfactant, as solid particles adsorb onto oil–water interface (Fig 1.2) and are regarded as promising alternatives to synthetic emulsifiers (Jiang et al., 2019; Kierulf et al., 2019).

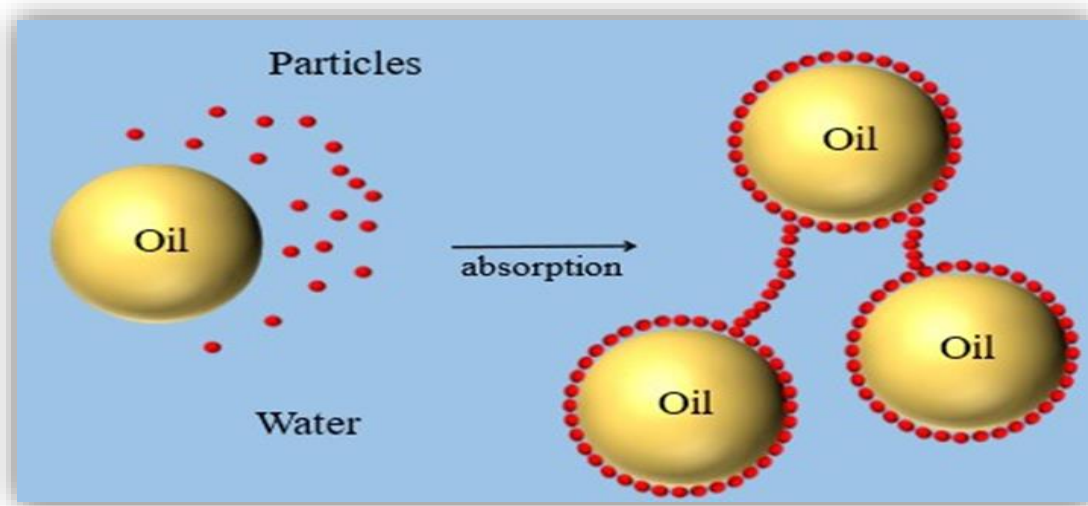


Fig 1.2: Mechanism of stability of Pickering emulsion. (Deng et al., 2022)

Further these tiny particles rearrange on the droplet surface resulting in the formation of a single or multi-layer thick solid interfacial film. The adsorption of solid particles is irreversible because the desorption energy of solid particles at the O/W interface being

significantly higher than the thermal energy. This film provides long-term stability of Pickering emulsions because it acts as a strong spatial barrier, electrostatic protection, and prevents droplet aggregation (Wang, 2020). Pickering emulsions have several advantages over other conventional emulsions (Fig 1.3a) made with surfactants, including minimal emulsifier dosage, good emulsion stability, high safety low toxicity, and reduced sensitivity to environmental factors (Jiang et al., 2020; Yang, 2017).

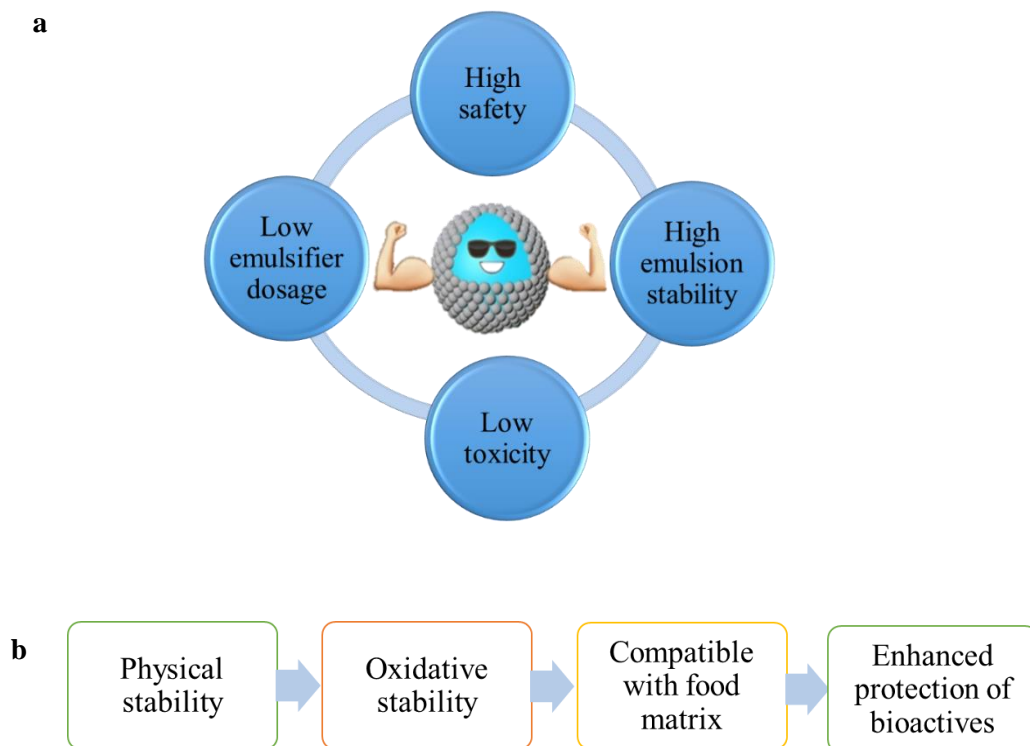


Fig 1.3: (a) Advantages of using Pickering emulsion and (b) Pickering emulsion delivery system.

Pickering emulsion based delivery system provide enhanced oxidative stability, physical stability, compatibility with food matrix and enhanced protection of labile bioactives (Fig 1.3b) (Mwangi et al., 2020). Pickering emulsions have thus gained a lot of interest from scientists and is evident from number of papers exploring Pickering emulsion has grown annually between 2008 and 2021 (Fig 1.4).

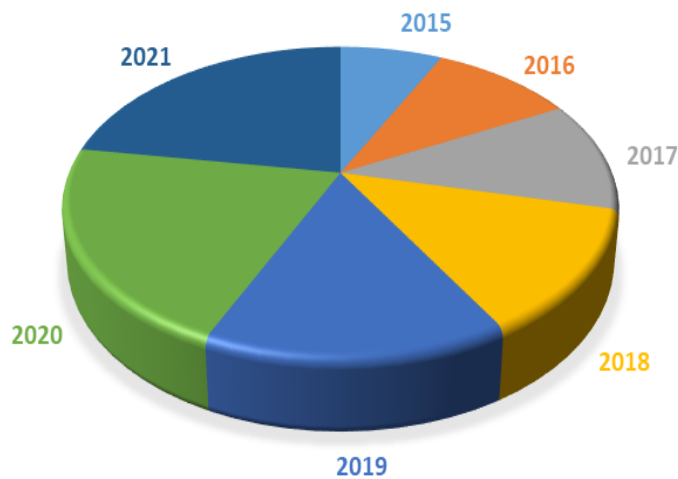


Fig 1.4: Number of publications on Pickering emulsion per year (2015-2021) according to Web of science.

1.2. Stabilization mechanism of Pickering particle

The principle of stabilization in Pickering emulsions has been described via two approaches. According to first mechanism, solid particles are adsorbed onto the interface of oil and water and generate monolayer of particle that serves as rigid film and creates a mechanical barrier to coalescence. Thus, by irreversibly attaching to oil- water interface, Pickering particles provide better stabilization to system than surfactants (Whitesides et al., 1995; Du Sorbier et al., 2015). Theoretical analysis and thermodynamic experiments, which can be found in incredibly thorough articles, provided substantial support for this mechanism (Aveyard et al., 2003; Menon et al., 1988; Binks et al., 2002). Based on the wettability of particles at interface of oil and water, the type of emulsion was determined as oil in water emulsion (O/W) or water in oil (W/O) emulsion. If the contact angle (θ) of particles is less than 90° , it may result in oil in water emulsion and contact angle (θ) greater than 90° lead to water in oil emulsion (Arditty et al., 2004; Akartuna et al., 2008; Torres et al., 2007). The development of a three-dimensional network of particles in the continuous phase is the result of particle-particle interactions, which underlie the second mechanism governing Pickering

emulsion stabilization. As a result, enhanced viscosity and increased stability of system was also observed (Lagaly et al., 1999).

1.3. Food grade Pickering particles

Pickering emulsions have been stabilized using a variety of solid particles with different functional and physicochemical characteristics. Particles of biological origin offer a competitive and promising alternative in the stabilization of food emulsions because most of them have been listed in the Code of Federal Regulations (21 CFR Parts 182 and 184) as generally regarded as safe (GRAS) by the Food and Drug Administration (FDA) (Mwangi et al., 2020). As Pickering particles for stabilizing emulsions, proteins, lipids, and polysaccharides are widely used. Most often, carbohydrates like starch and cellulose, as well as proteins like zein and soy protein, are employed. (Guida et al., 2021).

1.3.1. Polysaccharide particles used as Pickering particles

1.3.1.1. Cellulose

Cellulose, non-starch polysaccharide, is made of repeating ring of β -1,4-linked D-glucans. There are typically crystalline and non-crystalline regions in the structure of natural cellulose. The extremely asymmetric arrangement of the glucose molecules in the non-crystalline region makes it easy to see the hydroxyl groups at the ends of the chains, which gives the non-crystalline region a certain degree of hydrophilicity, while the crystalline region has a certain amount of hydrophobicity. In Pickering emulsions, cellulose particles are used as effective emulsion stabilizers. Typically, Cellulose nanofibrils (CNFs) (Winuprasith & Supphantharika, 2013), cellulose nanocrystals (CNCs) (Kalashnikova et al., 2013), bacterial cellulose and regenerated cellulose are used as cellulose particles or stabilizers. Among these, CNCs are commercially available, and Pickering emulsions made from them offer a wide range of potential application. Acid

digestion of cellulose by strong acids like HCl (hydrochloric acid), H₃PO₄ (phosphoric acid), sulfuric acid (H₂SO₄), results in the production of cellulose particles with an emulsifying action (Shang et al., 2019; Vanderfleet et al., 2018; Dai et al., 2018). Acid hydrolysis generates CNCs with higher number of negative charges on their surfaces, leading to strong electrostatic repulsion and better emulsion stabilization capacity (Salas et al., 2014). But excessive negative charge makes CNS more hydrophilic, making it difficult to prepare Pickering emulsion. To enhance emulsification efficiency of CNCs a number of chemical and physical modifications were attempted to decrease or enhance the surface hydrophobicity. Currently, chemical modification is more successful at enhancing the emulsification capabilities of cellulose particles. OSA (Octenyl Succinic anhydride) and sodium ethyl lauryl alginate modification are two commonly used chemical modification methods. Chen et al. (2018) reported that surface hydrophobicity and emulsification ability of CNC is significantly enhanced after OSA modification. Moreover, the surface characteristics and aggregation state of CNC might be improved by adding the suitable amount of sodium ethyl lauryl alginate (Bai et al., 2018).

Bai et al. (2019) formulated O/W Pickering emulsion using CNC as stabilizer and exhibited high stability against coalescence. Baek et al. (2019) fabricated Pickering emulsion using CNC (modified with phosphate groups) along with chitosan (modified with glycidyltrimethyl ammonium chloride) to improve its solubility. The results confirmed that, modified CNC-chitosan complex, leads to a stabilized Pickering emulsion compared to that of sodium tripolyphosphate (TPP) – chitosan emulsion. Food grade Pickering emulsion was also prepared using cellulose nanofibrils and chitin (Shanshan et al., 2021)

1.3.1.2. Chitosan

Chitosan (CS) is the second most prevalent polysaccharide in nature, produced by deacetylation of chitin. CS contains hydroxyl groups as its backbone along with amino groups, makes it more biocompatible and biodegradable (Wei et al., 2012). The aqueous solution of CS will undergo gelation when the level of deacetylation exceeds 75%. In an alkaline environment, CS self-assembles into aggregates with improved oil affinities and hydrophobicity (Deng et al., 2022). CS also exhibits emulsification and antibacterial properties under alkaline condition, enabling to be used as encapsulant in pharmaceuticals and cosmetics (Han et al., 2020; Lim et al., 2020). Chitosan as nanocrystals is mostly used as Pickering stabilizer. Commonly the nanocrystals are prepared by ultrasonication and acid hydrolysis methods. Self-aggregates of chitosan were also used as stabilizer since these are edible and derived naturally. The ultrasonication treatment causes depolymerization of chitosan, resulting in self-aggregation, because of formation of monodisperse smaller chitosan particles and these can stabilize Pickering emulsion containing 70% oil fraction (Ho et al., 2016). Stable chitosan-TPP (tripolyphosphate) Pickering emulsion was formulated for the delivery of bioactive curcumin (Shah et al., 2016). Wang et al. (2016b) prepared chitosan stabilized Pickering emulsion by ultrasonication, which efficiently disperse and disrupts agglomerates of chitosan. This resulted in decreased molecular weight and better emulsification of chitosan leading to a stable emulsion for about 5 months. Tian et al. (2019) formulated hydrophobic CS-TPP (Chitosan-sodium tripolyphosphate) sub microparticles under acidic conditions by ionic gelation method for the encapsulation of citral. The results indicated that the emulsion system showed better stability of citral, (about 52%) even after two weeks of storage.

1.3.1.3. Starch

Starch is the most prevalent type of carbohydrate in both human and animal diets, and in higher plants serves as a natural reserve carbohydrate. It can be found in roots, tubers, fruits, seeds, leaves, stems, and seeds. For industrial uses, the primary sources of starch are maize (82%), followed by wheat (8%), cassava (5%) and potatoes (5%) (Le et al., 2010). Starch mainly consists of linear amylose and highly branching amylopectin, both of which are formed of D-glucose units connected together via glycosidic connections ie α (1 \rightarrow 4) and α (1 \rightarrow 6) only in branch points. Mostly starch is semi crystalline in nature and its size varies from 1 μ m to 100 μ m in diameter and granules shape might range from oval or circular to polyhedral and can be indicative of a genus or a species (Tester et al., 2004; Sujka et al., 2018). Native starch has long been utilized in the pharmaceutical industry to create granules, capsules, and tablets.

Starch granules in its commercial, pure forms are usually larger in size and hydrophilic in nature. Several chemical and physical methods are employed to modify the native starch. Commonly used methods for size reduction are high-pressure treatment, organic solvent precipitation, ultrasonic treatment, acid hydrolysis and ball milling (Liu et al., 2009). Heating and ball milling to decrease the size of starch and thereby increasing its stability is some of the methods commonly employed. In order to investigate factors that determined the ability of starch granules to stabilize an emulsion, Li et al. (2013), compared four different types of native starch granules from various sources that differ in particle size, contact angle, surface morphology, surface charge, and emulsion stability. The results indicated that rice starch with smaller particle size resulted in better stabilization of Pickering emulsion. The study indicated that particle size plays an important role in starch ability to stabilize the emulsion. In order to improve the hydrophobicity of starch granules, chemical modification was performed. Studies

reported that chemical modification of starch granules by octenyl succinic anhydride (OSA), octenyl succinate, lauric acid, leads to improved hydrophobicity (Li et al., 2020; Garcia-Tejeda et al., 2018). Among this OSA modification was widely used and OSA improves their affinity to fats and oils (Agama-Acevedo., 2017). The emulsification of starch granules improves with increasing OSA modification of starch (Matos et al., 2018).

1.4. Application of polysaccharide stabilized Pickering emulsion

1.4.1. Fat substitutes

Since decades, hydrogenated vegetable oils have been employed to improve the plasticity of fats. However, this can result in the formation of trans fats, which pose substantial health concerns, raising serious questions about their safety in hydrogenated vegetable oils (Wei & Huang, 2019). Thus, it's critical to explore for high-quality, relatively inexpensive alternatives to vegetable oils that have been hydrogenated and Pickering emulsion are a possible substitute product. The high internal phase Pickering emulsion is remarkably similar to margarine in terms of content and qualities when the internal phase ratio of the emulsion is more than 80%, making it a viable margarine substitute that can successfully prevent the consumption of trans fat (Deng et al., 2022). Cream can be replaced in frozen yoghurt and ice cream with Pickering emulsions based on ethyl cellulose and camellia seed oil (Deng et al., 2022). Feng et al. (2020) reported that Pickering emulsions can be used in place of butter in cakes, reducing calorie intake and extending shelf life without affecting the flavour or texture of the cake. Zeng et al. (2017) were able to fabricate stable 83% high-internal phase Pickering emulsions, resulted in interpenetrating 3-D network structure that gave the emulsions their viscoelasticity and plasticity.

1.4.2. Modulation of lipid digestion

Pickering emulsions can be developed to regulate absorption and digestion of lipids in the gastrointestinal tract, resulting in decreased appetite and increased satiety. It has been demonstrated that by choosing the right particles to act as Pickering stabilizers, the rate and degree of lipid digestion may be controlled (Sarkar et al., 2018). Starch particles, chitin nanocrystals, cellulose nanocrystals and chitosan have been used to modify the absorption and digestion of lipids. Studies reported that cellulose nanocrystals (CNC) form a thick impenetrable coating around oil droplets and were successful in preventing merging of droplets in stomach and mouth (Bai et al., 2019). Mackie et al. (2019) reported that CNC-stabilized emulsions may be used to control lipid absorption because these Pickering emulsion results in lower absorption of saturated lipids.

1.4.3. Encapsulation and delivery of food bioactive ingredients

With the growing interest to embrace healthier life style, several functional active chemicals have been used in food systems. Bioactive ingredients such as β - carotene, coenzyme Q10 and curcumin exhibits poor water solubility and is easily oxidized and decomposed, making it challenging to include directly into food (Tumer & Tulek, 2021; Sun et al., 2022; Mota et al., 2020). Pickering emulsion is capable to load functional bioactive and also protects the active ingredients from photodegradation. Shah et al. (2016) loaded curcumin into a Pickering emulsion stabilized with chitosan-triphosphate nanoparticles; just 14% of the mass fraction of curcumin was degraded after 24 hours of dark storage, making this system substantially more protective of curcumin than traditional techniques. Zhang et al. (2018) investigated the release performance of hydrophobic calcium alginate (MCA) stabilized Pickering emulsion encapsulated with curcumin and discovered that the 4 h emulsion release in simulated gastric fluid at pH 1.5 was only 3% while the release in simulated intestinal fluid at pH 6.8 was 37%. The

results indicate that MCA-Pickering emulsions have shown delayed release and good pH sensitivity. In order to stabilize Pickering emulsions containing β -carotene, Fu et al. (2019) used Pickering emulsion made of xanthan gum and wheat gluten nanoparticles. The system showed higher bioaccessibility, with 90% of β -carotene retained after 30 days of storage. Cellulose based Pickering emulsion helps in encapsulation and protection of essential oils and the studies confirmed the antibacterial activity of eugenol, cinnamaldehyde and limonene encapsulated Pickering emulsion against the gram positive and gram negative bacteria (Mikulcova et al., 2016).

1.5. Porous starch

Porous starch is a modified form of starch that has undergone physical, chemical, and enzymatic processes that result in large amounts of surface pores that may extend into the internal of starch granules (Dura et al., 2014). Porous starch (Fig 1.5) is made up of numerous pores that are evenly spaced throughout and also expanded the interior without altering the shape of granules (Zhang et al., 2013; Gao et al., 2013). Within the starch granules, these pores can incorporate small molecules. The International Union of Pure and Applied Chemistry (IUPAC), divides pores depending on their diameter mainly into: micropores (below 2 nm), mesopores (between 2 and 50 nm), and macropores (above 50 nm) (Sujka and Jamroz, 2010). Recently porous starch has been reported to be used for delivery of various active biomolecules as the micropores can hold these biomolecules (Wu et al., 2021a; Wen et al., 2023; Ji, 2021).

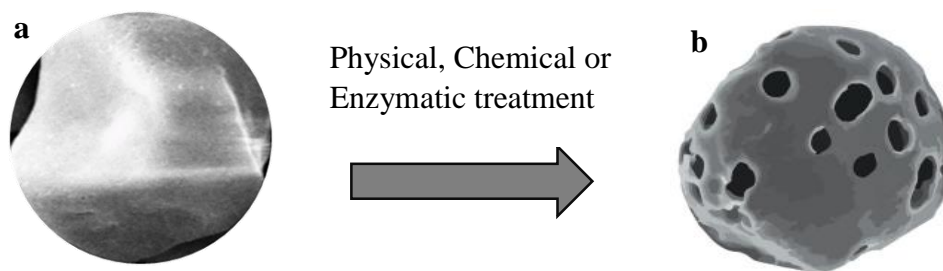


Fig 1. 5: (a) Native and (b) porous starch granules

1.5.1. Techniques for porous starch preparation

Physical, chemical, or enzymatic approaches can be used to generate porous starch, which has attracted a lot of attention recently, however studies reported that enzymatic and ultrasonic treatments are more commonly used. Different treatment methods (Physical, Chemical and Enzymatic) used for porous starch preparation is discussed in the following section.

1.5.1.1. Physical methods

Starch granules can be made porous using many techniques. The most commonly used methods are ultrasonication, microwave and hydrostatic treatment (Table 1.1).

1.5.1.1.1. Ultrasonication

An ultrasound is a sound wave with a frequency higher than 20 kHz, outside of human hearing range (Sujka & Jamroz, 2013). Ultrasound treatment is one of the most popular techniques for starch physical remodeling since it is thought to be risk-free, extremely effective, and environmentally friendly. Ultrasonic parameters (frequency, input energy, temperature) and starch preparations (concentration and type) are two key elements that determine the effectiveness of ultrasound treatment (Huang et al., 2007; Jambrak et al., 2010; Yu et al; 2013; Amini et al., 2015; Sujka et al., 2013). Many studies reported that ultrasounds physically degrade granules, leaving apparent cracks and pores on the

surface, but the granules' size and shape remain unaffected (Luo et al., 2008; Zheng et al., 2013; Amini et al., 2015). The process of particle degradation is correlated with cavitation. Starch granules are attacked by gas bubbles in the suspension medium and the granule breaks up as a result of rapidly collapsing bubbles creating shear stresses and micro-jets near to the surface (Czechowska-Biskup et al., 2005; Zuo et al., 2012; Tomasik et al., 1995). Hu et al. (2015) used dual ultrasound frequency (20 kHz + 25 kHz) for the preparation of porous starch. Sujka. (2017) treated rice, potato, wheat and corn starch with ultra sound frequency of 20 kHz and power of 170 W for 30 min that resulted in the production of new pores. Ultrasonication generated pores and cracks on the sweet potato starch surface and when the treatment time was increased from 15 to 30 min structural disorganizations were also observed. Kaur et al. (2019) also reported that ultrasonication results in generation of pores and depression in the surface of cereals such as maize, barley, wheat, rice.

1.5.1.1.2. Microwave method

Porous starch has recently been prepared using the microwave approach since it is both effective and environmentally safe. In this technique starch granules can be penetrated by a microwave-generated heat action known as molecular friction in an alternating electromagnetic field. When exposed to a microwave, starch granules can vibrate at a high frequency because the alternating electromagnetic field as positive and negative polarity are constantly switched. As a result, starch granules transform microwave radiation into heat energy. The structure of porous starch is affected by variables like intensity, duration, and amount of starch used. According to Nawaz et al. (2018) starch keep their structural reliability when intensity was between 400 and 1600 W, treatment period was under 5 min, and the weight of starch was greater than 10 g. Furthermore, Kraus et al. (2014) hypothesised that lowering system pressure while simultaneously

boosting microwave power could hasten the production of microporous starch. Despite being easy and inexpensive, the microwave approach produces starch with few pores. As a result, microwave cooking of fine porous starch is not acceptable.

1.5.1.1.3. High Hydrostatic pressure (HHP)

HHP, often uses water as pressure transmission medium with pressure varies from 100 to 800 MPa (Mujica-Paz et al., 2011). Recently, the starch modification and gelatinization processes have used this non-thermal technology (Li et al. 2012). Liu et al. (2009) found that HHP interrupts the interior assembly of starch granules and hastens the migration of water into the crystalline area, leading to the process of gelatinization. Deladino et al. (2017) found that low-pressure HHP treatment of maize starch resulted in increased pore size and volume. The organization of amylose and amylopectin structure is disrupted under low pressure conditions (Fernandez et al., 2008; Szwengiel et al., 2018). This increases the starch granules pore volume and surface area (Deladino et al., 2015).

Table 1.1: Physical treatment methods used in porous starch preparation

Starch type and concentration used	Physical treatment used	Inference
Potato starch dissolved in 10% (w/w) distilled water	Ultrasonic treatment	Compared to native starch, treated starch showed grooves and notch on the surface of starch and increased ultra-sonication power resulted in granule surface erosion. Zhu et al., (2012)
Wheat starch dissolved in 20% (w/w) distilled water	Ultrasonic treatment	Ultrasonic treatment makes the starch more rough and produce fissures and grooves on the granule of starch. Majzoobi, Hedayati, and Farahnaky, (2015)
Corn starch dissolved in 10% (w/v) deionized water	High pressure treatment	Small natural pores in native starch is increased after treatment with high pressure. Teixeira et al., (2015)
Corn starch dissolved in 10% (w/v) deionized water	High pressure treatment	Smooth granular surface of native starch had changed to more rough surface and treatment results in increase in number of pores. Deladino et al., (2015)
Corn starch dissolved in 5% (w/v) in distilled water	Ultrasonic treatment	Single treatment of native starch with solid surface and polygonal shape results in small sized pores while dual treatment results in increased size of granule and surface erosion. Hu et al., (2015)
Corn starch dissolved in 10% (w/v) deionized water	High Hydrostatic pressure	Upon treatment the small pores in native starch increased in number and have broaden pores. Deladino et al., (2017)
Corn, Wheat, Rice, Potato starch (30%) dissolved in distilled water or ethanol	Ultrasonic treatment	Sonicating potato starch in water revealed fissures and depressions on the granule surface. Treatment was more effective in large granules compared to smaller ones. For cavitation process to occur, water act as a better medium. Sujka, (2017)

1.5.1.2. Chemical treatment

Another technique for producing porous starch is chemical treatment. Starch modification frequently employs chemical processing to encourage oxidation, simple hydrolysis or cross linking (Yiu et al., 2008). Alkaline treatment and acid hydrolysis are commonly used methods for the generation of porous starch (Table 1.2).

1.5.1.2.1. Solvent Exchange method

The solvent exchange method, which prevent the hydrogel structure from collapsing and contracting under direct air drying, is based on the exchange of water with solvents like acetone and ethanol in the starch hydrogel network. During gelation, water soluble amylose gels into a network structure and a plenty of water molecules are taken up by the starch molecules. During porous starch preparation, ethanol is used to replace the water and vacuum drying is used to remove the ethanol. The porous starch structure was influenced by drying conditions and solvent concentration (Chen et al., 2020). Oliyaei et al. (2019) used higher concentration of ethanol followed by freeze drying for the preparation of porous starch. Less surface tension of a gas or liquid is preferred for homogeneous and continuous pores in starch. The major limitation of using solvent exchange method in food industries is that the porous starch shows low adsorption capacity.

1.5.1.2.2. Acid and alkali treatment

In contrast to enzyme treatment, acid hydrolysis and alkaline treatment are less efficient to create porous starch granules. While treating starch with acid or alkali, it attacks the amorphous region resulting in wide pores on granular surface and surface erosion (Deladino et al., 2017). Alkaline treatment mostly uses sodium hypochlorite, sodium hydroxide, potassium hydroxide and acid treatment use citric acid, sulfuric acid, and

hydrochloric acid (Latip et al., 2021). Falade et al. (2015) reported that side chains of granules of starch are hydrolyzed by hydrochloric acid, which modifies the surfaces of the granules. Corn starch under prolonged hydrolysis with sulfuric acid results in irregular shape due to the disruption of amylose and amylopectin chains (Utrilla et al., 2014). Avocado seed starch treated with higher concentration of lactic acid also resulted in reduced crystallinity due to hydrolysis (Delinski et al., 2017).

Sodium hydroxide treatment in the corn, potato, and sago starches become evident only after 15 days of treatment. The study indicated that alkaline treatment has an impact on the production of porous starch, which produces the amorphous and crystalline lamella based on molecular arrangement of amylopectin and amylose (Nadiha et al., 2010). Bharti et al. (2019) studied the impact of various concentrations of NaOH on three cultivars of mango kernel starches. The native starches closely resemble the starches found in corn, sorghum, and millet. Although these starch granules have amazing natural pores and grooves, their vulnerability on treatment differs. Zhou et al. (2016) used sodium hypochlorite to treat potato starch at various active chlorine concentrations. Adding more sodium hypochlorite made the pores on the surface of potato starch granules more obvious. However, the potato starch granule showed more fissures and breaks at a greater sodium hypochlorite concentration (4%).

Table 1.2: Chemical treatment methods used in porous starch preparation

Starch type and concentration used	Chemical treatment used	Inference
Corn starch 10% (w/v) in various citric acid concentration.	Hydrolysis by acid	Native corn shows small pores with polygonal shape. Treatment at 50 °C and 40 °C produced small cracks on the granule surface. Treatment at 60 °C retains the shape of granule but high temperature and citric acid results in enlarged and translucent granule. Kim & Huber (2013).
Corn starch 15% (w/v) in 3.16 M sulfuric acid solution	Hydrolysis by acid	After 3 days of treatment, the smooth polygonal starch, produced small cracks on the surface. After 9 days, pores become more visible and starch structure is completely lost after 15 days. Utrilla-Coello et al., (2014)
Corn starch 10% (w/v) in 0.1% NaOH	Alkaline treatment	Pore volume of starch increased considerably after the treatment Deladino et al., (2017)

1.5.1.3. Enzymatic method

Enzymatic method is the most efficient and popular method for the production of porous starch that results in increased number of pores on surface and the smooth surface of starch changed to rough surface due to corrosion (Fig 1.5). Different enzymes and treatment methods were used for making porous starch which was given in (Table 1.3).

1.5.1.3.1. α -amylase

The endo acting enzyme, α -amylase hydrolyzes the (1→4) glycosidic linkages of starch to quickly shorten the chains of amylose and amylopectin, increasing the number of branch and short linear chains (Xu et al., 2015). According to Ichihara et al. (2013),

granules of cassava starch that have been treated with α -amylase exhibit altered characteristics without changing size or structure. Additionally, Dura et al. (2014), described that amylase treatment causes only tiny holes to form starch granules. Following hydrolysis by α -amylase enzyme, popcorn starch (PCS) showed improved granular porous structure, decreased viscosity and gelatinization temperature compared to that of dent corn starch (DCS) (Song et al., 2020). In another study, (Zhou et al., 2021), treated V-type granular starch (VGS) with amylase enzyme in ethanol solution resulted in high adsorption capacity and high crystallinity.

1.5.1.3.2. Glucoamylase

Glucoamylase hydrolyzes single glucose molecules from amylose and amylopectin's non-reducing ends in a methodical manner. It may also hydrolyze (1,6) linkages in the branch points of amylopectin (Aggarwal & Dollimore, 2000). When amyloglucosidase concentration was raised, Aggarwal & Dollimore (2000) likewise noticed an increase in pore size, but only up to a concentration of 800 U/g starch, at which point they noticed large irregular holes and damaged starch structure. Chen and Zhang. (2012) reported that corn starch pore size grew concurrently with hydrolysis time, when treated with glucoamylase at sub-gelatinization temperatures. Benavent-gil & Rosells. (2017) found that amyloglucosidase-treated starch has broad pores and that at increasing concentrations of the enzyme, granule depression was seen as a result of the enzyme eroding activity on the starch surface. At higher enzyme concentrations and for longer periods of time, particularly at 900 and 1500 U of enzyme concentration, the shape of starch changed, being distorted into large, wide, and fragmented holes.

1.5.1.3.3. Cyclodextrin glycosyltransferase

For the purpose of producing porous starch from maize starch, Benavent-Gil & Rosell. (2017) compared the effects of α -amylase, glucoamylase, and cyclodextrin glycosyltransferase. After two hours of hydrolysis, α -amylase and glucoamylase results in better pore size compared to cyclodextrin glycosyltransferase. After enzymatic treatment of 48 h at pH 6.0, Dura & Rosell. (2016) found that maize starch granules had numerous tiny pores and rough surfaces and they discovered that in this pH range, cyclodextrin glycosyltransferase aggressively degraded the amylose chain. This shows that cyclodextrin glycosyltransferase dramatically alters the granule's amorphous area and that the inner portion of the granule has a higher enzyme action efficiency than the exterior surface of granule. (Dura et al., 2016; Dura & Rosell, 2016).

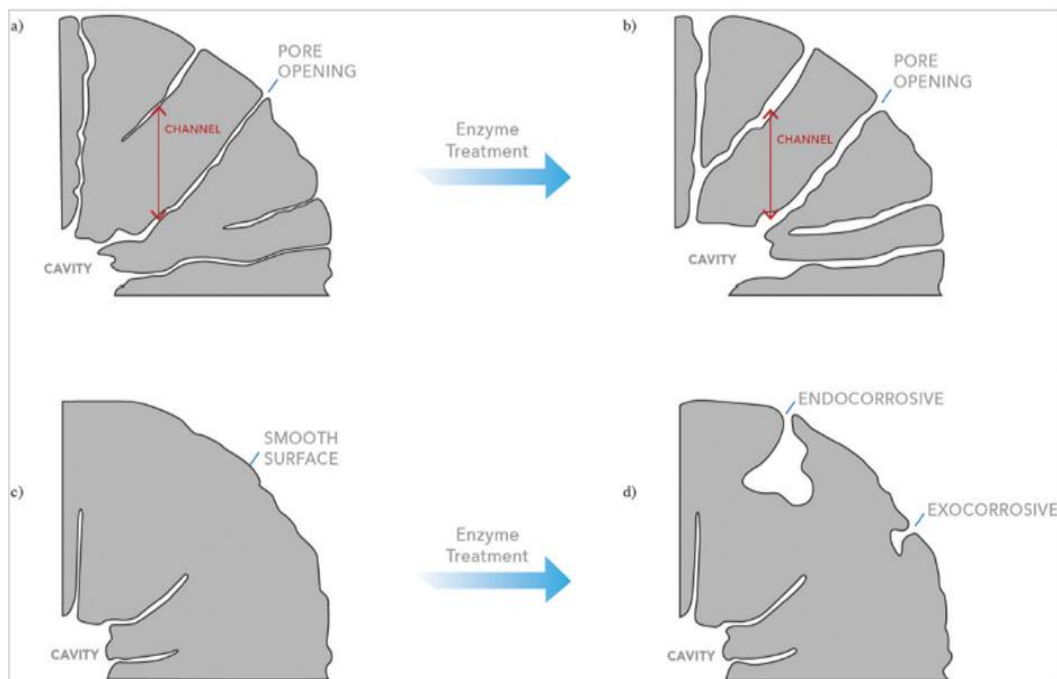


Fig 1.6: The mechanism of enzyme treatment on starch. (a) Starch granules with small natural pores changed to increased pores after treatment (b). Smooth and compact starch granule before enzyme treatment (c) and after enzyme treatment (d). Figure is adapted and reprinted from Dhital, Shrestha and Gidley (2010).

1.5.1.3.4. Synergistic action of enzymes

The efficacy of a process which is increased by combining two different types of enzymes in a process known as dual enzyme treatment (Sun et al., 2010). Dual enzyme treatment commonly uses the enzymes glucoamylase and α -amylase in the case of porous starch preparation. As previously mentioned, α -amylase randomly and quickly breaks down starch α -(1,4) glycosidic linkages, with dextrin serving as the primary end product. Thus, partial hydrolysis is all that occurs with α -amylase. Amyloglucosidase is able to completely convert glucose from the nonreducing ends of starch chains by cleaving the glycosidic linkages between α -(1,4) and α -(1,6). Amyloglucosidase, however, acts very slowly. When coupled, the enzyme α -amylase randomly separates the glucose residues on the surface of the starch and releases fresh non-reducing ends. The second stage involves the action of amyloglucosidase, which continuously releases glucose from the granules by acting on these nonreducing terminals. Thirdly, amyloglucosidase makes holes from the granule's surface to its center, giving α -amylase more access to act on additional glycosidic bonds and form pores (Sun et al., 2010). By treating maize starch with a group of enzymes, significant alterations by generating pores was observed, but with not much modification on the structure of starch granules (Zhao et al., 2018). According to Lacerda et al. (2019), more superficial attacks were seen when the enzymes amylase and amyloglucosidase were used in combination. Additionally, according to Chen et al. (2020), amylase and amyloglucosidase were typically utilized in combination for the manufacture of porous starch. Thus, the rapid hydrolysis of the whole starch is made possible by the synergistic activity.

Table 1.3: Enzymatic treatment methods used in porous starch preparation

Type of starch and concentration	Enzymes employed	Inference
Corn, Rice, Sago Tapioca, Potato starch 1% (w/v), in 50mM universal buffer (pH 6.5)	150 µl of enzyme α -amylase from <i>Bacillus aquimaris</i>)	Produced large pores in corn starch, small pores in rice starch. There was no change in the Sago tapioca and potato starch after the treatment. Puspasari et al. (2011)
Corn starch 25% (w/v) in sodium acetate buffer (pH 4.6)	Glucoamylase (11 GSHU/g starch)	Treatment produces even sized pores on granules surface. Pore size increased after elongated time of hydrolysis. Chen & Zhang (2012)
Corn starch 20% (w/v) in Monosodium phosphate buffer (pH 6.0)/sodium acetate buffer (pH 4.0)	4 U/g of Glucoamylase (AMG) and 5 U/g of fungal α -amylase (AM)	AMG produced larger pores compared to AM. Dura, Błaszczak, & Rosell (2014)
Waxy corn starch 25% in distilled water	15 mL of Distillase TM SSF (Commercial enzyme complex)	Polyhedral native waxy corn starch with smooth surface and small pores, on prolonged hydrolysis resulted in more pronounced effects. Malucelli et al. (2015)
Corn starch 20% in 20 mM sodium phosphate buffer at pH 6.0 (C6)/20 mM sodium acetate buffer at pH 4.0 (C4)	0.32 U of Cyclodextrin-glycosyl-transferase(CGTase) (<i>Thermoanaerobacter</i> sp.) (0.32 U CGTase/10 g starch)	CGTase C6 produced extensive pores compared to C4. Dura & Rosell (2016)
Corn starch 5% (w/v) in PBS buffer	Fungal α -amylase (FAM) Pancreatic α -amylase (PAM) Pancreatin (Pc)	After 30 min of treatment Pancreatin and Pancreatic α -amylase resulted in deep pores and efficiency of FAM lost after 30 min. Li et al., (2016) .
Corn starch 20% (w/v) in sodium phosphate buffer (pH 6)	Cyclodextrin glycosyltransferase(CGTase) (0.32 U CGTase/g starch)	Small and random pores were obtained when treated with enzyme at subgelatinization temperature.

Corn starch 5% in 50 mM sodium acetate buffer	Glucoamylase(AMG): pH 4.5 β-amylase (BAM): pH 5.2 α-amylase (AM): pH 5.8	Dura,Yokoyama,& Rosell, (2016). AM showed increased pore size, followed by AMG and BAM respectively, after 8 h of treatment. Jung, Lee, & Yoo (2017)
Starch 20% (w/v) in 20mM sodium acetate buffer (pH4.0)	Glycosyltransferase (CG) Glucoamylase (AMG) Branching enzyme (BE) α-amylase (AM) Cyclodextrine	Pore size increased with increased concentration of enzyme. Starch treated with AMG showed increased pore size followed by AM, BE and CG respectively. Benavent-Gil & Rosell (2017)

1.5.2. Characterization of porous starch

1.5.2.1. Swelling power and Solubility

To make native starch more soluble is one of the key goals in porous starch preparation. The breakdown of starch occurs in two steps, swelling and dissolution. Starch granules swell as the solvent molecules penetrate interior resulting in increase in the volume of the starch. With increasing solvent molecule infiltration, the macromolecular segment mobility gradually rises. To establish a stable dissolving phase, the macromolecular segment gently enters the solution by coordinated motion (Perez Rea et al., 2016, Zdanowicz et al., 2016). During the pore-forming process, the amorphous portions of native starch are disrupted, enabling unrestricted expansion of the starch granules. Numerous investigations have demonstrated that after formation of pores, native starch solubility and swelling power are increased (Zhao et al., 2018, Zhang, 2013).

1.5.2.2. Pasting property

Rapid visco analyzers are typically used to study the pasting characteristics of porous starch after the heating-cooling cycle (Balet et al., 2019). The degree of starch

modifications and retrogradation following porosity alteration can be seen by a number of characteristics that can be observed through the pasting curve (Wu et al., 2017). Generally, after pore formation the integrity of starch granules is compromised, making them more brittle and less resistant to shear stress during the heating process. The recrystallization of amylose chains may also explain why porous starch has a higher setback than native starch. According to this phenomena, fractional amylose chains can form helical structures after being leached from starch granules (Sun et al., 2017). Porous starch created via amylase catalysis resembles native starch in terms of swelling and hydration when heated and then cooled, but it has a lower peak viscosity. However, the maximal viscosity of amyloglucosidase-treated starch is higher after cooling (Dura et al., 2014). Therefore, the type of enzyme and preparation method has a significant impact on the pasting property of porous starch. This was confirmed by Benavent-Gil et al. (2017) who demonstrated a negative correlation between peak viscosity and the pore area and size of porous starch. Additionally, compared to porous starch produced by enzymatic hydrolysis, porous starch produced by freeze-thaw and enzymatic treatment displayed a lower peak viscosity. According to Fortuna et al. (2000) the specific surface area and pore volume of porous starch were strongly correlated with pasting temperature. The average pore diameter of porous starch and pasting property, however, were not shown to be correlated.

1.5.2.3. Rheological property

The rheological characteristics describe the flow behavior of starch in relation to stress (Ai and Jane, 2015). Even at large sample concentrations, native starch shows poor rheological properties. (Thirumdas et al., 2017; Wang et al., 2017). While heating starch to gelatinization temperature, starch granules, starts to lose crystalline nature, absorbs water and shows better rheological properties (Wu et al., 2016). Benavent-Gil et al.

(2019) found a correlation between the loss tangent ($\tan \delta = G''/G'$), storage modulus (G'), loss modulus (G'') and the porosity of porous starch. According to Kochkina et al. (2016) porous starch displayed solid-like behaviour since the $\tan \delta$ value increased as the porosity of the starch increased. Generally, the storage modulus and loss modulus of starch considerably rise as the temperature rises and the initial increase in storage modulus is caused by the expansion of starch granules. Due to melting of remaining starch crystallites, storage modulus further decreases as temperature increases. The porous starch loses structural integrity, which results in lower G' and G'' values.

1.5.2.4. Thermal property

Thermogravimetric analysis (TGA), which highlights crystalline structural changes and internal chemical interactions such as hydrogen bonding, is commonly used to evaluate the thermal property of starch. TGA offers information on the thermodynamic characteristics of the porous starch. Studies reported that starch granules with a high degree of crystallinity are more resistant to temperature changes (Wang et al., 2017., Fonseca et al., 2019). Porous starch loses weight early due to water loss, and then over time as the porous starch decomposes, it loses weight in stages (Liu et al., 2018). The differential thermogravimetric (DTG) analysis peak maxima reflect the greatest degree of starch loss.

1.5.2.5. Gelatinization property

The differential scanning calorimetry (DSC) method is typically used to analyze the gelatinization property. During the gelatinization process, the starch crystalline double helix structure is released and eventually get amorphous. Many studies reported that the gelatinization enthalpy of porous starch is larger than that of native starch because starch hydrolysis will result in an increase in the proportion of crystalline region and a decrease

in the proportion of amorphous region (Zhao et al., 2018; Ghavimi et al., 2015; Lacerda et al., 2018). In addition, as the temperature rises, the hydrogen bonds and double helix structure of starch are broken. Because of this, it takes more energy to shatter the crystalline region in starch

1.5.3. Food application of porous starch

Porous starch with increased pores can be used for the encapsulation and packaging of different food materials.

1.5.3.1. Encapsulation of flavour and oil

Flavours are frequently utilized to enhance the sensory characteristics of food products that have lost their distinctive flavour throughout production procedures, particularly when heat is involved. The majority of flavours are liquid mixtures of molecules in solvents, and they are frequently susceptible to deterioration when exposed to conditions such as humidity, heat and air (Salzer, 2007; Belingheri et al., 2015a). Porous starch is reported to encapsulate flavours very effectively. In a study, three techniques for turning liquid flavours into powders are used such as plating onto porous starch, spray drying and plating onto maltodextrin, and were compared for the protection they provided against heat and flavour content over shelf life, as determined by sensory and chemical tests. This work also demonstrates the critical significance that solvent selection plays in transferring liquid tastes onto porous starch; the greater the polarity-based attraction between flavour molecules and solvent, the greater the flavour retention over time. An industrial application validated the possible role of porous starch in food flavouring.

The primary goal of the flavour industry is to provide customers with flavorful products, and these products must be both enduring and profitable. As a result, the industry is continually looking for innovative, more effective, and less expensive ways to stabilize

its sensitive flavour compounds. Due to the fact that several flavor components are liposoluble and the final applications may be lipid-based, the selection of carrier oil, or solution, in which flavour components are dispersed, has a substantial impact on flavour durability during shelf life. The deterioration of carrier oils might be harmful to the product flavour because of the oxidation reaction capacity of oil to diffuse to the flavour molecules. (Leclercq et al.,2007; Belingheri et al., 2015b). Belingheri et al. (2015b) reported that for the encapsulation of sensitive oils, plating on porous starch seems to be a workable substitute to spray drying since it eliminates a heating phase that encourages oil oxidation.

The use of microencapsulation technology safeguards valuable chemicals. Studies reported that for the encapsulation of olive oil porous starch from sweet potato was used (Lei et al., 2018). The greatly increased oxidative stability of olive oil in microencapsulation is proof that the procedure is effective. Porous starch can offer a reliable delivery technique to enhance oil protection in the food sector.

1.5.3.2. Encapsulation of pigments

Porous starch along with halloysite nanotube was used as a carrier of fucoxanthin to improve its stability and to protect it from light within the matrices of porous starch. The double encapsulation of fucoxanthin results in improved encapsulation efficiency, stability and more sustained release of fucoxanthin (Oliyaei et al., 2020). Ji. (2021) fabricated porous microgels from hydrolyzed oxidised starch for the delivery of anthocyanin. The created microgels are more porous, a lot of surface area, and certain functional groups that electrostatically attract anthocyanins. These characteristics significantly increase the ability of porous microgels to adsorb anthocyanins. The study confirmed that porous microgels improve the release and stability of anthocyanins.

1.5.3.3. Encapsulation of probiotics

Li et al. (2016) studied about probiotic *Lactobacillus plantarum* 299v's ability to survive after being subjected to heat, bile, and acid treatments while being microencapsulated in either native or partially hydrolyzed maize starch. After freeze-drying the modified starch formulations had a markedly higher initial percentage of viable cells than native starch. The probiotic bacteria that were microencapsulated displayed significantly improved acid tolerance when compared to free cells. These findings show that porous starch granules allow high probiotic loading efficiency and offer improved defense against a variety of stressful situations.

1.5.3.4. Food packaging

Miao et al. (2021) formulated novel active food packaging film using maize starch-tea polyphenol (TP) loaded porous starch film forming solution which helps in controlling the delayed release of TP. The study demonstrated that PS had a good capacity for TP adsorption, and the components of the formulation were evenly distributed in the cast films. The active films also had excellent antioxidant characteristics, good mechanical qualities, UV and thermal stability. In order to extend the protection provided by the active film to the food under consideration, the delayed release of TP from the films was sustained.

Other applications

Wei, (2014) used Triton X-100 as the pore-forming agent during the free-radical polymerization of starch and acrylic acid to develop porous starch-based super absorbents. Triton X-100 enhanced the ability to absorb water as well as urine, swelling, and reswelling rates. The investigation came to the conclusion that a range of sectors that demand fast swelling might use the porous St-g-PAA super absorbents.

Table 1.4: Food applications of porous starch

	Application	Details	Inference	Reference
1.	Carrier of flavours			
a.	Tomato flavour	Tomato flavour was plated over, maltodextrin, porous starch and also spray dried for turning liquid flavours into powders.	The crucial role that solvent choice has in imprinting liquid flavours onto porous starch is revealed. The longer the flavour is retained, the higher the polarity based affinity between flavour molecules and solvent	Belingheri et al., (2015a)
b.	Clove essential oil	By employing a sacrificial template approach with potato starch and CaCO ₃ , 3D nanonetwork porous starch-based material (3D-NPS) filled CEO were created.	This new technique for making 3D-NPS is quick, safe and offers a potential basis for stabilizing and releasing chemicals such as essential oils over time. The newly created 3D-NPS offer significant promise for the pharmaceutical, cosmetics, clinical therapy, and food preservation industries.	Fang et al., (2019)
c.	Plant essential oils	The essential oil (EO) was microencapsulated using the food-grade polymer maize porous starch, and the sustained-release, antibacterial properties of PSM-EOs against <i>Penicillium roqueforti</i> and <i>Aspergillus niger</i> in bread were investigated..	PSM-EOs excelled controls in terms of sustained release, antibacterial activity and considerably increased bread shelf life. Future research should examine practical applications, including the impact on food sensory qualities and how to directly apply PSM-EOs to the surface of meals or create miniature antibacterial packages.	Ju et al., (2019)
2.	Carrier of edible oils			
a.	Carrier of oleic-sunflower oil	Oleic sunflower oil plated over porous starch instead of spray drying.	Porous starch appears to be a practical alternative to spray drying for the encapsulation of delicate that helps oil from oxidation.	Belingheri et al., (2015b)

b.	Carrier of ricinoleic acid (RA)	Ricinoleic acid was embedded into porous starch, and its release rate and its production on gamma de lactone (GDL) was investigated	PS significantly increase dispersion of RA and its controlled release thus influencing biotransformation efficiency and product yield.	Rong et al., (2018)
c.	Microencapsulation of olive oil.	Potato starch maintained in citric acid-disodium hydrogen phosphate buffer solution is preheated at different temperature to obtain porous starch encapsulated with olive oil	When compared to free olive oil, the oxidative stability of microencapsulated olive oil is greatly improved by porous starch-based material. The outcomes gained from this work might offer a strong delivery method to enhance oil preservation in the food and eventually after consumption.	Lei et al., (2018)
3.	Carrier of active ingredients			
a.	Encapsulation of fucoxanthin	Fucoxanthin was encapsulated in the pores of starch and coated with gum Arabic (GA) and maltodextrin (MD)	The alteration of PS encapsulated with fucoxanthin and coated with MD and GA agents showed better encapsulation efficiency and protection of fucoxanthin from heat and light. Fucoxanthin's double encapsulation may be beneficial for those industries that must safeguard their delicate ingredients from harsh climatic circumstances.	Oliyaei (et al), (2019)
b.	Microencapsulation of ascorbic acid	Corn starch treated with enzymes and coated with gum was used to create microcapsules (GA).	Maize starch microcapsules showed increased stability throughout storage and in vitro digestion. Thus it provides an effective way to encapsulate functional food components in microcapsules made using gum Arabic	Leyva-Lopez et al., (2019)

c	Encapsulation of β carotene	By using an esterification procedure to combine porous starch with OSA groups, it was possible to successfully manufacture porous starches that had been changed with varying degrees of substitution (DS). OSA@PS, which has exceptional emulsification capabilities, was used to create a beta-carotene emulsion.	Due to the variations in stability and emulsion particle sizes, it was shown that varied DS of samples had significant effects on the bioaccessibility of β -carotene in the emulsion. Because of this, food-grade OSA@PS with a higher DS could be used to create emulsions for the purpose of stabilizing bioactive components.	Li et al., (2020)
d	Microencapsulation of Curcumin	The wall materials for the spray dried curcumin (MEC) are β -cyclodextrin and porous starch.	The use of β -cyclodextrin and porous starch as MEC wall materials and use of spray drying to create MEC would be practical for the bakery business after careful consideration of the pH stability, solubility, interaction with the food components, and acceptable solvent system.	Huang et al. (2020)
e	Encapsulation of anthocyanin	Native maize starch was altered by sequential TEMPO oxidation and glucoamylase hydrolysis, employing trisodium phosphate (STMP) as a cross-linker, to create pH/salt-responsive porous microgel.	The created microgels have large porosity, surface area and specific functional groups that electrostatically attract anthocyanin. Furthermore, anthocyanin released from porous microgels are slowly released in simulated stomach and intestinal environments. Overall, porous microgels can improve the release and stability of anthocyanin.	Ji. (2021)
f	Adsorption of grape seed proanthocyanidins (GSP)	Enzymatically digested corn starch was moderately gelatinized	The best adsorption capacity and a comparatively low desorption percentage (49%) toward GSPs were	Wang et al., (2016a)

		to create pores, and its capacity to bind to GSPs was assessed.	demonstrated by the porous gelatinized starch. This starch can be used as a good adsorbent to enhance the use of GSPs and maintain their antioxidant activity	
g	Procyanidin adsorption	For the purpose of adsorbing procyanidin, porous chitosan-modified starch was created by easily altering the surface of porous rice starch.	Procyanidin is well adsorbed in the porous chitosan-modified starch. Chitosan was easily surface-modified on porous rice starch to create the modified starch. This surface modification could be used to create functional starches with a similar structure.	Jiang et al., (2017)
4	Encapsulation of probiotics			
a	<i>Lactobacillus plantarum</i> 299v	Probiotic bacteria <i>Lactobacillus plantarum</i> 299v was encapsulated in the porous maize starch.	In comparison to free cells, porous granules showed higher probiotic loading effectiveness and offer better protection against a variety of stressful situations	Li et al., (2016)
b	<i>Lactobacillus plantarum</i>	<i>Lactobacillus plantarum</i> was adsorbed onto porous corn and rice starch. Xanthan gum, guar gum and gelatinized starch was used as wall materials	The probiotic encapsulated in porous rice starch resulted in higher encapsulation efficiency and coated with gelatinized starch provided better yield. The α -amylase treated starch with gelatinized starch coating gives better thermal stability	Benavent-Gil et al., 2018
5.	Carrier of salt	Two potential carriers for regulated sodium release using porous corn starch produced by	Salt could not be successfully encapsulated inside the pores of porous starch. Future studies are warranted for	Christina et al., (2016)

	enzymatic method and spray drying, and lipoproteic matrix, produced by freeze drying and gelation.	various techniques for adding sodium into the pores and better drying techniques for PCS	
6. Antibacterial coating for packaging paper	Hydrophobic non crystalline porous starch (NCPS) was prepared by solvent exchange, heat treatment and alkyl ketene dimer. By combining silver nanoparticles with NCPS and employing this coating as a layer on base paper, antibacterial packaging was produced.	Antibacterial packaging paper showed excellent mechanical and barrier properties and it also showed improved antimicrobial action against <i>E. coli</i> and <i>S.aureus</i>	Dang et al., 2018

1.6. Future prospects and conclusion

With the increase in demand among the consumers for healthier food products, the development of foods containing functional ingredients has become one of the active research areas in the food industry. Solid particle stabilized emulsion called Pickering emulsion is an active area of research for the delivery of bioactive and nutritionally important components for food/functional and food/nutraceutical applications. Pickering emulsions have many benefits over conventional emulsions, such as low toxicity, excellent stability and availability of a wide range of particles, all of which have encouraged research into them and possible applications. Pickering emulsions will have superior rheological characteristics, digestibility, and freeze-thaw stability due to the modification of some colloidal particles and the formation of more nascent colloidal particles, opening up greater opportunities for their usage in food applications. Starch, has been modified to make it more efficient and functional for its use in various food applications apart from its use as stabilizing and thickening agent in industries. Recently, porous starch is attaining great interest because of its abundant pores and increased surface area for targeted delivery and sustained release of certain drugs. Porosity of the starch granule can be tuned for various food applications including delivery of active ingredients.

Based on the above gathered information and gaps identified, the present work was carried out with a hypothesis that:

- A. Porous starch act as Pickering particles in stabilization of emulsion.
- B. Porous starch with abundant pores and increased surface area, in combination with other polysaccharides such as guar gum can improve the encapsulation

efficiency for bioactive. e.g., curcumin, for colon target delivery, in the form of Pickering emulsion.

- C. Fermentation metabolites of curcumin loaded Pickering emulsion exhibit potential prebiotic and anticancer activity.

Objectives

The broad objective was to fabricate Pickering emulsion stabilized by porous starch for the delivery of bioactive. The detailed objectives are as follows:

1. To optimize fabrication of porous starch using enzyme hydrolysis.
2. To develop stable Pickering emulsion using porous starch as Pickering particle for encapsulation of bioactive using curcumin as model system for colon targeted delivery.
3. To evaluate the gastrointestinal stability and prebiotic potential of encapsulates.
4. To evaluate the anticancer potential of fermentation metabolites in prevention and management of colon cancer in HCT 116 cells.

1.7. References

- Aggarwal, P., & Dollimore, D. (2000). Degradation of starchy food material by thermal analysis. *Thermochimica acta*, 357, 57-63.
- Ai, Y., & Jane, J. L. (2015). Gelatinization and rheological properties of starch. *Starch-Stärke*, 67(3-4), 213-224.
- Akartuna, I., Studart, A. R., Tervoort, E., & Gauckler, L. J. (2008). Macroporous ceramics from particle-stabilized emulsions. *Advanced Materials*, 20(24), 4714-4718.
- Amini, A. M., Razavi, S. M. A., & Mortazavi, S. A. (2015). Morphological, physicochemical, and viscoelastic properties of sonicated corn starch. *Carbohydrate Polymers*, 122, 282-292.
- Arditty, S., Schmitt, V., Giermanska-Kahn, J., & Leal-Calderon, F. (2004). Materials based on solid-stabilized emulsions. *Journal of Colloid and Interface Science*, 275(2), 659-664.
- Aveyard, R., Binks, B. P., & Clint, J. H. (2003). Emulsions stabilised solely by colloidal particles. *Advances in Colloid and Interface Science*, 100, 503-546.
- Agama-Acevedo, E., & Bello-Perez, L. A. (2017). Starch as an emulsions stability: the case of octenyl succinic anhydride (OSA) starch. *Current Opinion in Food Science*, 13, 78-83.
- Baek, J., Wahid-Pedro, F., Kim, K., Kim, K., & Tam, K. C. (2019). Phosphorylated-CNC/modified-chitosan nanocomplexes for the stabilization of Pickering emulsions. *Carbohydrate polymers*, 206, 520-527.

- Bai, L., Xiang, W., Huan, S., & Rojas, O. J. (2018). Formulation and stabilization of concentrated edible oil-in-water emulsions based on electrostatic complexes of a food-grade cationic surfactant (ethyl lauroyl arginate) and cellulose nanocrystals. *Biomacromolecules*, *19*(5), 1674-1685.
- Bai, L., Lv, S., Xiang, W., Huan, S., McClements, D. J., & Rojas, O. J. (2019). Oil-in-water Pickering emulsions via microfluidization with cellulose nanocrystals: 1. Formation and stability. *Food Hydrocolloids*, *96*, 699-708.
- Balet, S., Guelpa, A., Fox, G., & Manley, M. (2019). Rapid Visco Analyser (RVA) as a tool for measuring starch-related physicochemical properties in cereals: A review. *Food Analytical Methods*, *12*(10), 2344-2360.
- Belingheri, C., Ferrillo, A., & Vittadini, E. (2015a). Porous starch for flavor delivery in a tomato-based food application. *LWT-Food Science and Technology*, *60*(1), 593-597.
- Belingheri, C., Giussani, B., Rodriguez-Estrada, M. T., Ferrillo, A., & Vittadini, E. (2015b). Oxidative stability of high-oleic sunflower oil in a porous starch carrier. *Food Chemistry*, *166*, 346-351.
- Benavent-Gil, Y., & Rosell, C. M. (2017). Comparison of porous starches obtained from different enzyme types and levels. *Carbohydrate polymers*, *157*, 533-540.
- Benavent-Gil, Y., Rodrigo, D., & Rosell, C. M. (2018). Thermal stabilization of probiotics by adsorption onto porous starches. *Carbohydrate polymers*, *197*, 558-564.

- Benavent-Gil, Y., Román, L., Gómez, M., & Rosell, C. M. (2019). Physicochemical properties of gels obtained from corn porous starches with different levels of porosity. *Starch-Stärke*, *71*(3-4), 1800171.
- Bharti, I., Singh, S., & Saxena, D. C. (2019). Influence of alkali treatment on physicochemical, pasting, morphological and structural properties of mango kernel starches derived from Indian cultivars. *International journal of biological macromolecules*, *125*, 203-212.
- Binks, B. P., & Clint, J. H. (2002). Solid wettability from surface energy components: relevance to Pickering emulsions. *Langmuir*, *18*(4), 1270-1273.
- Chen, G., & Zhang, B. (2012). Hydrolysis of granular corn starch with controlled pore size. *Journal of cereal science*, *56*(2), 316-320.
- Chen, J., Wang, Y., Liu, J., & Xu, X. (2020). Preparation, characterization, physicochemical property and potential application of porous starch: A review. *International journal of biological macromolecules*, *148*, 1169-1181.
- Chen, Q. H., Zheng, J., Xu, Y. T., Yin, S. W., Liu, F., & Tang, C. H. (2018). Surface modification improves fabrication of pickering high internal phase emulsions stabilized by cellulose nanocrystals. *Food Hydrocolloids*, *75*, 125-130.
- Christina, J., & Lee, Y. (2016). Modification of sodium release using porous corn starch and lipoproteic matrix. *Journal of food science*, *81*(4), E897-E905.

- Czechowska-Biskup, R., Rokita, B., Lotfy, S., Ulanski, P., & Rosiak, J. M. (2005). Degradation of chitosan and starch by 360-kHz ultrasound. *Carbohydrate Polymers*, *60*(2), 175-184.
- Dai, H., Huang, Y., & Huang, H. (2018). Enhanced performances of polyvinyl alcohol films by introducing tannic acid and pineapple peel-derived cellulose nanocrystals. *Cellulose*, *25*, 4623-4637.
- Dang, C., Yin, Y., Xu, M., & Pu, J. (2018). Hydrophobic noncrystalline porous starch (NCPS): dispersed silver nanoparticle suspension as an antibacterial coating for packaging paper. *BioResources*, *13*(1), 192-207.
- Deladino, L., A. S. Teixeira, A. S. Navarro, I. Alvarez, A. D. Molina-Garcia, and M. Martino. 2015. Corn starch systems as carriers for yerba mate (*Ilex paraguariensis*) antioxidants. *Food and Bioproducts Processing* *94*:463–72.
- Deladino, L., Teixeira, A. S., Plou, F. J., Navarro, A. S., & Molina-García, A. D. (2017). Effect of High Hydrostatic Pressure, alkaline and combined treatments on corn starch granules metal binding: Structure, swelling behavior and thermal properties assessment. *Food and Bioproducts Processing*, *102*, 241-249.
- Delinski, B. C., Henrique, W. L., Soltovski, D. O. C., Gustavo, L. L., & Schnitzler, E. (2017). Morphological and thermoanalytical study of modified avocado seeds starch with lactic acid. *Chemistry Journal of Moldova*, *12*(2), 13-18.

- Deng, W., Li, Y., Wu, L., & Chen, S. (2022). Pickering emulsions stabilized by polysaccharides particles and their applications: a review. *Food Science and Technology*, 42.
- Dhital, S., Shrestha, A. K., & Gidley, M. J. (2010). Relationship between granule size and in vitro digestibility of maize and potato starches. *Carbohydrate Polymers*, 82(2), 480-488.
- Du Sorbier, Q. M., Aimable, A., & Pagnoux, C. (2015). Influence of the electrostatic interactions in a Pickering emulsion polymerization for the synthesis of silica–polystyrene hybrid nanoparticles. *Journal of colloid and interface science*, 448, 306-314.
- Dura, A., Błaszczak, W., & Rosell, C. M. (2014). Functionality of porous starch obtained by amylase or amyloglucosidase treatments. *Carbohydrate polymers*, 101, 837-845.
- Dura, A., & Rosell, C. M. (2016). Physico-chemical properties of corn starch modified with cyclodextrin glycosyltransferase. *International Journal of Biological Macromolecules*, 87, 466-472.
- Dura, A., Yokoyama, W., & Rosell, C. M. (2016). Glycemic response to corn starch modified with cyclodextrin glycosyltransferase and its relationship to physical properties. *Plant foods for human nutrition*, 71(3), 252-258.
- Falade, K. O., & Ayetigbo, O. E. (2015). Effects of annealing, acid hydrolysis and citric acid modifications on physical and functional properties of starches from four yam (*Dioscorea* spp.) cultivars. *Food hydrocolloids*, 43, 529-539.

- Fang, Y., Fu, J., Liu, P., & Cu, B. (2020). Morphology and characteristics of 3D nanonetwork porous starch-based nanomaterial via a simple sacrifice template approach for clove essential oil encapsulation. *Industrial Crops and Products*, *143*, 111939.
- Feng, X., Sun, Y., Yang, Y., Zhou, X., Cen, K., Yu, C., ... & Tang, X. (2020). Zein nanoparticle stabilized Pickering emulsion enriched with cinnamon oil and its effects on pound cakes. *LWT*, *122*, 109025.
- Fernandez, P. P., Sanz, P. D., Martino, M. N., & García, A. M. (2008). Partially-gelatinised starches by high hydrostatic pressure as oligoelement carriers. *Spanish journal of agricultural research*, (1), 129-137.
- Fonseca, L. M., da Silva, F. T., Antunes, M. D., Mello El Halal, S. L., Lim, L. T., & Dias, A. R. G. (2019). Aging time of soluble potato starch solutions for ultrafine fibers formation by electrospinning. *Starch-Stärke*, *71*(1-2), 1800089.
- Fortuna, T., Januszewska, R., Juszczak, L., Kielski, A., & Pałasiński, M. (2000). The influence of starch pore characteristics on pasting behaviour. *International journal of food science & technology*, *35*(3), 285-291.
- Fu, D., Deng, S., McClements, D. J., Zhou, L., Zou, L., Yi, J., ... & Liu, W. (2019). Encapsulation of β -carotene in wheat gluten nanoparticle-xanthan gum-stabilized Pickering emulsions: Enhancement of carotenoid stability and bioaccessibility. *Food hydrocolloids*, *89*, 80-89.

- Fu, Y., Sarkar, P., Bhunia, A. K., & Yao, Y. (2016). Delivery systems of antimicrobial compounds to food. *Trends in food science & technology*, 57, 165-177.
- Gao, F., D. Li, C.-H. Bi, Z.-H. Mao, and B. Adhikari. 2013. The adsorption and release characteristics of CPFX in porous starch produced through different drying methods. *Drying Technology* 31 (13–14):1592–99.
- Garcia-Tejeda, Y. V., E. J. Leal-Castaneda, V. Espinosa-Solis, and V. Barrera-Figueroa. (2018). "Synthesis and characterization of rice starch laurate as food-grade emulsifier for canola oil-in-water emulsions." *Carbohydrate Polymers* 194 : 177-183.
- Ghavimi, S. A. A., Ebrahimzadeh, M. H., Shokrgozar, M. A., Solati-Hashjin, M., & Osman, N. A. A. (2015). Effect of starch content on the biodegradation of polycaprolactone/starch composite for fabricating in situ pore-forming scaffolds. *Polymer Testing*, 43, 94-102.
- Guida, C., Aguiar, A. C., & Cunha, R. L. (2021). Green techniques for starch modification to stabilize Pickering emulsions: A current review and future perspectives. *Current Opinion in Food Science*, 38, 52-61.
- Han, J., Chen, F., Gao, C., Zhang, Y., & Tang, X. (2020). Environmental stability and curcumin release properties of Pickering emulsion stabilized by chitosan/gum Arabic nanoparticles. *International Journal of Biological Macromolecules*, 157, 202-211.
- Ho, K. W., Ooi, C. W., Mwangi, W. W., Leong, W. F., Tey, B. T., & Chan, E. S. (2016). Comparison of self-aggregated chitosan particles prepared with and without

- ultrasonication pretreatment as Pickering emulsifier. *Food Hydrocolloids*, 52, 827-837.
- Hu, A., Jiao, S., Zheng, J., Li, L., Fan, Y., Chen, L., & Zhang, Z. (2015). Ultrasonic frequency effect on corn starch and its cavitation. *LWT-Food Science and Technology*, 60(2), 941-947.
- Huang, Q., Li, L., & Fu, X. (2007). Ultrasound effects on the structure and chemical reactivity of cornstarch granules. *Starch-Stärke*, 59(8), 371-378.
- Huang, C., Wang, S., & Yang, H. (2020). Evaluation of thermal effects on the bioactivity of curcumin microencapsulated with porous starch-based wall material using spray drying. *Processes*, 8(2), 172.
- Ichihara, T., Fukuda, J., Takaha, T., Yuguchi, Y., & Kitamura, S. (2013). Limited hydrolysis of insoluble cassava starch granules results in enhanced gelling properties. *Journal of Applied Glycoscience*, jag-JAG.
- Jambrak, A. R., Herceg, Z., Subaric D., Babic, J., Brncic, M., Brncic S. R., ... & Gelo, J. (2010). Ultrasound effect on physical properties of corn starch. *Carbohydrate Polymers*, 79(1), 91-100.
- Ji, Y. (2021). Synthesis of porous starch microgels for the encapsulation, delivery and stabilization of anthocyanins. *Journal of Food Engineering*, 302, 110552.
- Jiang, S., Yu, Z., Hu, H., Lv, J., Wang, H., & Jiang, S. (2017). Adsorption of procyanidins onto chitosan-modified porous rice starch. *Lwt*, 84, 10-17.

- Jiang, Y., Li, F., Li, D., Sun-Waterhouse, D., & Huang, Q. (2019). Zein/pectin nanoparticle-stabilized sesame oil pickering emulsions: Sustainable bioactive carriers and healthy alternatives to sesame paste. *Food and Bioprocess Technology*, *12*, 1982-1992.
- Jiang, H., Sheng, Y., & Ngai, T. (2020). Pickering emulsions: Versatility of colloidal particles and recent applications. *Current Opinion in Colloid & Interface Science*, *49*, 1-15.
- Ju, J., Chen, X., Xie, Y., Yu, H., Cheng, Y., Qian, H., & Yao, W. (2019). Simple microencapsulation of plant essential oil in porous starch granules: Adsorption kinetics and antibacterial activity evaluation. *Journal of food processing and preservation*, *43*(10), e14156.
- Jung, Y. S., Lee, B. H., & Yoo, S. H. (2017). Physical structure and absorption properties of tailor-made porous starch granules produced by selected amylolytic enzymes. *PloS one*, *12*(7), e0181372.
- Kalashnikova, I., Bizot, H., Bertoncini, P., Cathala, B., & Capron, I. (2013). Cellulosic nanorods of various aspect ratios for oil in water Pickering emulsions. *Soft Matter*, *9*(3), 952-959.
- Kaur, H., & Gill, B. S. (2019). Effect of high-intensity ultrasound treatment on nutritional, rheological and structural properties of starches obtained from different cereals. *International journal of biological macromolecules*, *126*, 367-375.
- Kierulf, A., Azizi, M., Eskandarloo, H., Whaley, J., Liu, W., Perez-Herrera, M., ... & Abbaspourrad, A. (2019). Starch-based Janus particles: Proof-of-concept

- heterogeneous design via a spin-coating spray approach. *Food Hydrocolloids*, *91*, 301-310.
- Kierulf, A., Whaley, J., Liu, W., Enayati, M., Tan, C., Perez-Herrera, M., ... & Abbaspourrad, A. (2020). Protein content of amaranth and quinoa starch plays a key role in their ability as Pickering emulsifiers. *Food Chemistry*, *315*, 126246.
- Kim, J. Y., & Huber, K. C. (2013). Corn starch granules with enhanced load-carrying capacity via citric acid treatment. *Carbohydrate polymers*, *91*(1), 39-47.
- Kochkina, N., & Khokhlova, Y. (2016). Viscoelastic Properties of Gelatinized Dispersions of Maize Starch Modified by Solid-State Milling. *Cereal Chemistry*, *93*(4), 395-401.
- Kraus, S., Schuchmann, H. P., & Gaukel, V. (2014). Factors Influencing the Microwave-Induced Expansion of Starch-Based Extruded Pellets under Vacuum. *Journal of Food Process Engineering*, *37*(3), 264-272.
- Krishnan, R., Mohan, K., Ragavan, K. V., & Nisha, P. (2023). Insights into headway in essential oil-based Pickering emulsions for food applications. *Sustainable Food Technology*.
- Lacerda, L. D., Leite, D. C., & da Silveira, N. P. (2019). Relationships between enzymatic hydrolysis conditions and properties of rice porous starches. *Journal of Cereal Science*, *89*, 102819.

- Lacerda, L. D., Leite, D. C., Soares, R. M., & da Silveira, N. P. (2018). Effects of α -Amylase, Amyloglucosidase, and Their Mixture on Hierarchical Porosity of Rice Starch. *Starch-Stärke*, 70(11-12), 1800008.
- Lagaly, G., Reese, M., & Abend, S. (1999). Smectites as colloidal stabilizers of emulsions: II. Rheological properties of smectite-laden emulsions. *Applied clay science*, 14(5-6), 279-298.
- Latip, D. N., Samsudin, H., Utra, U., & Alias, A. K. (2021). Modification methods toward the production of porous starch: a review. *Critical reviews in food science and nutrition*, 61(17), 2841-2862.
- Le Corre, D., Bras, J., & Dufresne, A. (2010). Starch nanoparticles: a review. *Biomacromolecules*, 11(5), 1139-1153.
- Leclercq, S., Reineccius, G. A., & Milošević, C. (2007). Effect of type of oil and addition of δ -tocopherol on model flavor compound stability during storage. *Journal of Agricultural and Food Chemistry*, 55, 9189–9194.
- Lei, M., Jiang, F. C., Cai, J., Hu, S., Zhou, R., Liu, G., ... & Xiong, X. G. (2018). Facile microencapsulation of olive oil in porous starch granules: Fabrication, characterization, and oxidative stability. *International Journal of Biological Macromolecules*, 111, 755-761.
- Leyva-Lopez, R., Palma-Rodríguez, H. M., Lopez-Torres, A., Capataz-Tafur, J., Bello-Perez, L. A., & Vargas-Torres, A. (2019). Use of enzymatically modified starch

in the microencapsulation of ascorbic acid: Microcapsule characterization, release behavior and in vitro digestion. *Food Hydrocolloids*, 96, 259-266.

Li, W., Y. Bai, S. A. S. Mousaa, Q. Zhang, and Q. Shen. (2012). Effect of high hydrostatic pressure on physicochemical and structural properties of rice starch. *Food and Bioprocess Technology* 5 (6):2233–41.

Li, C., Li, Y., Sun, P., & Yang, C. (2013). Pickering emulsions stabilized by native starch granules. *Colloids and Surfaces A: Physicochemical and Engineering Aspects*, 431, 142-149.

Li, H., Turner, M. S., & Dhital, S. (2016). Encapsulation of *Lactobacillus plantarum* in porous maize starch. *Lwt*, 74, 542-549.

Li, H., Ma, Y., Yu, L., Xue, H., Wang, Y., Chen, J., & Zhang, S. (2020). Construction of octenyl succinic anhydride modified porous starch for improving bioaccessibility of β -carotene in emulsions. *RSC advances*, 10(14), 8480-8489.

Lim, H. P., Ho, K. W., Singh, C. K. S., Ooi, C. W., Tey, B. T., & Chan, E. S. (2020). Pickering emulsion hydrogel as a promising food delivery system: Synergistic effects of chitosan Pickering emulsifier and alginate matrix on hydrogel stability and emulsion delivery. *Food Hydrocolloids*, 103, 105659.

Liu, H., Yu, L., Dean, K., Simon, G., Petinakis, E., & Chen, L. (2009). Starch gelatinization under pressure studied by high pressure DSC. *Carbohydrate polymers*, 75(3), 395-400.

- Liu, J., Wang, X., Bai, R., Zhang, N., Kan, J., & Jin, C. (2018). Synthesis, characterization, and antioxidant activity of caffeic-acid-grafted corn starch. *Starch-Stärke*, *70*(1-2), 1700141.
- Lu, W., Kelly, A. L., & Miao, S. (2016). Emulsion-based encapsulation and delivery systems for polyphenols. *Trends in Food Science & Technology*, *47*, 1-9.
- Luo, Z., Fu, X., He, X., Luo, F., Gao, Q., & Yu, S. (2008). Effect of ultrasonic treatment on the physicochemical properties of maize starches differing in amylose content. *Starch-Stärke*, *60*(11), 646-653.
- Mackie, A., Gourcy, S., Rigby, N., Moffat, J., Capron, I., & Bajka, B. (2019). The fate of cellulose nanocrystal stabilised emulsions after simulated gastrointestinal digestion and exposure to intestinal mucosa. *Nanoscale*, *11*(6), 2991-2998.
- Majzoobi, M., Hedayati, S., & Farahnaky, A. (2015). Functional properties of microporous wheat starch produced by α -amylase and sonication. *Food bioscience*, *11*, 79-84.
- Malucelli, L. C., Lacerda, L. G., da Carvalho Filho, M. A. S., Fernández, D. E. R., Demiate, I. M., Oliveira, C. S., & Schnitzler, E. (2015). Porous waxy maize starch: thermal, structural and viscographic properties of modified granules obtained by enzyme treatment. *Journal of Thermal Analysis and Calorimetry*, *120*, 525-532.
- Matos, M., Laca, A., Rea, F., Iglesias, O., Rayner, M., & Gutiérrez, G. (2018). O/W emulsions stabilized by OSA-modified starch granules versus non-ionic

- surfactant: Stability, rheological behaviour and resveratrol encapsulation. *Journal of Food Engineering*, 222, 207-217.
- McClements, D. J., Decker, E. A., & Weiss, D. J. (2007). Emulsion-based delivery systems for lipophilic bioactive components. *Journal of food science*, 72(8), R109-R124.
- Menon, V. B., & Wasan, D. T. (1988). Characterization of oil—water interfaces containing finely divided solids with applications to the coalescence of water-in-oil Emulsions: A review. *Colloids and surfaces*, 29(1), 7-27.
- Miao, Z., Zhang, Y., & Lu, P. (2021). Novel active starch films incorporating tea polyphenols-loaded porous starch as food packaging materials. *International Journal of Biological Macromolecules*, 192, 1123-1133.
- Mikulcova, V., Bordes, R., & Kasparikova, V. (2016). On the preparation and antibacterial activity of emulsions stabilized with nanocellulose particles. *Food Hydrocolloids*, 61, 780-792.
- Mota, A. H., Sousa, A., Figueira, M., Amaral, M., Sousa, B., Rocha, J., ... & Reis, C. P. (2020). Natural-based consumer health nanoproducts: Medicines, cosmetics, and food supplements. In *Handbook of functionalized nanomaterials for industrial applications* (pp. 527-578). Elsevier.
- Mujica-Paz, H., Valdez-Fragoso, A., Samson, C. T., Welti-Chanes, J., & Torres, J. A. (2011). High-pressure processing technologies for the pasteurization and sterilization of foods. *Food and Bioprocess Technology*, 4(6), 969-985.

- Mwangi, W. W., Lim, H. P., Low, L. E., Tey, B. T., & Chan, E. S. (2020). Food-grade Pickering emulsions for encapsulation and delivery of bioactives. *Trends in Food Science & Technology*, *100*, 320-332.
- Nadiha, M. N., Fazilah, A., Bhat, R., & Karim, A. A. (2010). Comparative susceptibilities of sago, potato and corn starches to alkali treatment. *Food Chemistry*, *121*(4), 1053-1059.
- Nawaz, H., Shad, M. A., Saleem, S., Khan, M. U. A., Nishan, U., Rasheed, T., ... & Iqbal, H. M. (2018). Characteristics of starch isolated from microwave heat treated lotus (*Nelumbo nucifera*) seed flour. *International journal of biological macromolecules*, *113*, 219-226.
- Oliyaei, N., Moosavi-Nasab, M., Tamaddon, A. M., & Fazaeli, M. (2019). Preparation and characterization of porous starch reinforced with halloysite nanotube by solvent exchange method. *International journal of biological macromolecules*, *123*, 682-690.
- Oliyaei, N., Moosavi-Nasab, M., Tamaddon, A. M., & Fazaeli, M. (2020). Encapsulation of fucoxanthin in binary matrices of porous starch and halloysite. *Food Hydrocolloids*, *100*, 105458.
- Perez Rea, D., Bergenståhl, B., & Nilsson, L. (2016). Development and evaluation of methods for starch dissolution using asymmetrical flow field-flow fractionation. Part II: Dissolution of amylose. *Analytical and bioanalytical chemistry*, *408*(5), 1399-1412.

- Pickering, S. U. (1907). CXCVI.—Emulsions. *Journal of the Chemical Society, Transactions*, 91(0), 2001–2021. <https://doi.org/10.1002/9781119220510.ch1>.
- Puspasari, F., Nurachman, Z., Noer, A. S., Radjasa, O. K., van der Maarel, M. J., & Natalia, D. (2011). Characteristics of raw starch degrading α -amylase from *Bacillus aquimaris* MKSC 6.2 associated with soft coral *Sinularia* sp. *Starch-Stärke*, 63(8), 461-467.
- Ramsden, W. (1904). Separation of solids in the surface-layers of solutions and ‘suspensions’(observations on surface-membranes, bubbles, emulsions, and mechanical coagulation).—Preliminary account. *Proceedings of the royal Society of London*, 72(477-486), 156-164.
- Rong, S., Wang, M., Yang, S., Li, Q., Guan, S., Cai, B., & Zhang, S. (2018). Improvement in lactone production from biotransformation of ricinoleic acid based on the porous starch delivery system. *Journal of Chemical Technology & Biotechnology*, 93(4), 1198-1205.
- Saffarionpour, S. (2020). Nanocellulose for stabilization of Pickering emulsions and delivery of nutraceuticals and its interfacial adsorption mechanism. *Food and Bioprocess Technology*, 13(8), 1292-1328.
- Salas, C., Nypelö, T., Rodriguez-Abreu, C., Carrillo, C., & Rojas, O. J. (2014). Nanocellulose properties and applications in colloids and interfaces. *Current Opinion in Colloid & Interface Science*, 19(5), 383-396.

- Salzer, U.-J. (2007). Spray drying and other methods for encapsulation of flavourings. In H. Ziegler (Ed.), *Flavourings: Production, composition, applications, regulations* (2nd ed.). (pp. 97e108). Weinheim: Wiley-VCH.
- Sarkar, A., Li, H., Cray, D., & Boxall, S. (2018). Composite whey protein–cellulose nanocrystals at oil-water interface: Towards delaying lipid digestion. *Food Hydrocolloids*, *77*, 436-444.
- Shah, B. R., Li, Y., Jin, W., An, Y., He, L., Li, Z., ... & Li, B. (2016). Preparation and optimization of Pickering emulsion stabilized by chitosan-tripolyphosphate nanoparticles for curcumin encapsulation. *Food Hydrocolloids*, *52*, 369-377.
- Shang, Z., An, X., Seta, F. T., Ma, M., Shen, M., Dai, L., ... & Ni, Y. (2019). Improving dispersion stability of hydrochloric acid hydrolyzed cellulose nanocrystals. *Carbohydrate polymers*, *222*, 115037.
- Shanshan., Zhou, H., Bai, L., Rojas, O. J., & McClements, D. J. (2021). Development of food-grade Pickering emulsions stabilized by a mixture of cellulose nanofibrils and nanochitin. *Food Hydrocolloids*, *113*, 106451.
- Song, Z., Zhong, Y., Tian, W., Zhang, C., Hansen, A. R., Blennow, A., ... & Guo, D. (2020). Structural and functional characterizations of α -amylase-treated porous popcorn starch. *Food Hydrocolloids*, *108*, 105606.
- Sujka, M., & Jamroz, J. (2010). Characteristics of pores in native and hydrolyzed starch granules. *Starch-Stärke*, *62*(5), 229-235.

- Sujka, M., & Jamroz, J. (2013). Ultrasound-treated starch: SEM and TEM imaging, and functional behaviour. *Food Hydrocolloids*, *31*(2), 413-419.
- Sujka, M. (2017). Ultrasonic modification of starch—Impact on granules porosity. *Ultrasonics Sonochemistry*, *37*, 424-429.
- Sujka, M., Pankiewicz, U., Kowalski, R., Nowosad, K., & Noszczyk-Nowak, A. (2018). Porous starch and its application in drug delivery systems. *Polimery Medycynie*, *48*(1), 25-29.
- Sun, H., Zhao, P., Ge, X., Xia, Y., Hao, Z., Liu, J., & Peng, M. (2010). Recent advances in microbial raw starch degrading enzymes. *Applied biochemistry and biotechnology*, *160*(4), 988-1003.
- Sun, J., Zuo, X. B., Fang, S., Xu, H. N., Chen, J., Meng, Y. C., & Chen, T. (2017). Effects of cellulose derivative hydrocolloids on pasting, viscoelastic, and morphological characteristics of rice starch gel. *Journal of texture studies*, *48*(3), 241-248.
- Sun, X.-F., Li, L., & Liu, Y.-B. (2022). Curcumin played an anti-cancer role in colorectal cancer via mediating circ_KIAA1199-related regulatory axis. *Food Science and Technology*, *42*, e86221. [http:// dx.doi.org/10.1590/fst.86221](http://dx.doi.org/10.1590/fst.86221).
- Szwengiel, A., Lewandowicz, G., Górecki, A. R., & Błaszczak, W. (2018). The effect of high hydrostatic pressure treatment on the molecular structure of starches with different amylose content. *Food chemistry*, *240*, 51-58.
- Teixeira, A. S., Navarro, A. S., Molina-García, A. D., Martino, M., & Deladino, L. (2015). Corn starch systems as carriers for yerba mate (*Ilex paraguariensis*)

- antioxidants: Effect of mineral addition. *Food and Bioproducts Processing*, 94, 39-49.
- Tester, R. F., Karkalas, J., & Qi, X. (2004). Starch—composition, fine structure and architecture. *Journal of cereal science*, 39(2), 151-165.
- Thirumdas, R., Trimukhe, A., Deshmukh, R. R., & Annapure, U. S. (2017). Functional and rheological properties of cold plasma treated rice starch. *Carbohydrate polymers*, 157, 1723-1731.
- Tian, H., Lu, Z., Yu, H., Chen, C., & Hu, J. (2019). Fabrication and characterization of citral-loaded oil-in-water Pickering emulsions stabilized by chitosan-tripolyphosphate particles. *Food & function*, 10(5), 2595-2604.
- TMR. (2015). Nutraceuticals market - global industry analysis, size, share, growth,trends,andforecast20152021.<http://www.transparencymarketresearch.com/global-nutraceuticals-product-market.html>.
- Tomasik, P., & Zaranyika, M. F. (1995). Nonconventional methods of modification of starch. *Advances in carbohydrate chemistry and biochemistry*, 51, 243-318.
- Torres, L. G., Iturbe, R., Snowden, M. J., Chowdhry, B. Z., & Leharne, S. A. (2007). Preparation of o/w emulsions stabilized by solid particles and their characterization by oscillatory rheology. *Colloids and Surfaces A: Physicochemical and Engineering Aspects*, 302(1-3), 439-448.

- Tumer, E., & Tulek, Y. (2021). Effects of dehydrofreezing conditions on carrot β -carotene and kinetics of β -carotene change in dehydrofrozen carrots during storage. *Food Science and Technology*, 42.
- Utrilla-Coello, R. G., Hernández-Jaimes, C., Carrillo-Navas, H., González, F., Rodríguez, E., Bello-Perez, L. A., ... & Alvarez-Ramirez, J. (2014). Acid hydrolysis of native corn starch: Morphology, crystallinity, rheological and thermal properties. *Carbohydrate polymers*, 103, 596-602.
- Vanderfleet, O. M., Osorio, D. A., & Cranston, E. D. (2018). Optimization of cellulose nanocrystal length and surface charge density through phosphoric acid hydrolysis. *Philosophical Transactions of the Royal Society A: Mathematical, Physical and Engineering Sciences*, 376(2112), 20170041.
- Wang, H., Lv, J., Jiang, S., Niu, B., Pang, M., & Jiang, S. (2016a). Preparation and characterization of porous corn starch and its adsorption toward grape seed proanthocyanidins. *Starch/starke*, 68, 1–10.
- Wang, X. Y., & Heuzey, M. C. (2016b). Chitosan-based conventional and Pickering emulsions with long-term stability. *Langmuir*, 32(4), 929-936.
- Wang, S., Xu, J., Wang, Q., Fan, X., Yu, Y., Wang, P., ... & Cavaco-Paulo, A. (2017). Preparation and rheological properties of starch-g-poly (butyl acrylate) catalyzed by horseradish peroxidase. *Process Biochemistry*, 59, 104-110.

- Wang, H., Bai, Y., & Shao, D. (2020). Study on Pickering emulsions stabilized by tea polyphenols/gelatin/chitosan nanoparticles. In *Journal of Physics: Conference Series* (Vol. 1637, No. 1, p. 012106). IOP Publishing.
- Wei, Z., Wang, C., Zou, S., Liu, H., & Tong, Z. (2012). Chitosan nanoparticles as particular emulsifier for preparation of novel pH-responsive Pickering emulsions and PLGA microcapsules. *Polymer*, *53*(6), 1229-1235.
- Wei, Q. (2014). Fast-swelling porous starch-g-poly (acrylic acid) superabsorbents. *Iranian Polymer Journal*, *23*(8), 637-643.
- Wei, Z., & Huang, Q. (2019). Developing organogel-based Pickering emulsions with improved freeze-thaw stability and hesperidin bioaccessibility. *Food Hydrocolloids*, *93*, 68-77.
- Wen, Z., Kang, L., Fu, H., Zhu, S., Ye, X., Yang, X., ... & Yang, X. (2023). Oral delivery of porous starch-loaded bilayer microgels for controlled drug delivery and treatment of ulcerative colitis. *Carbohydrate Polymers*, *314*, 120887.
- Whitesides, T. H., & Ross, D. S. (1995). Experimental and theoretical analysis of the limited coalescence process: stepwise limited coalescence. *Journal of colloid and interface science*, *169*(1), 48-59.
- Winuprasith, T., & Suphantharika, M. (2013). Microfibrillated cellulose from mangosteen (*Garcinia mangostana* L.) rind: Preparation, characterization, and evaluation as an emulsion stabilizer. *Food Hydrocolloids*, *32*(2), 383-394.

- Yiu, P. H., Loh, S. L., Rajan, A., Wong, S. C., & Bong, C. F. J. (2008). Physiochemical properties of sago starch modified by acid treatment in alcohol. *American Journal of Applied Sciences*, 5(4), 307-311.
- Yu, S., Zhang, Y., Ge, Y., Zhang, Y., Sun, T., Jiao, Y., & Zheng, X. Q. (2013). Effects of ultrasound processing on the thermal and retrogradation properties of nonwaxy rice starch. *Journal of Food Process Engineering*, 36(6), 793-802.
- Zdanowicz, M., Spychaj, T., & Mąka, H. (2016). Imidazole-based deep eutectic solvents for starch dissolution and plasticization. *Carbohydrate polymers*, 140, 416-423.
- Zeng, T., Wu, Z., Zhu, J., Yin, S., Tang, C., Wu, L., & Yang, X. (2017). Development of antioxidant Pickering high internal phase emulsions (HIPEs) stabilized by protein/polysaccharide hybrid particles as potential alternative for PHOs. *Food Chemistry*, 231, 122-130.
- Zhang, Z., Huang, J., Jiang, S., Liu, Z., Gu, W., Yu, H., & Li, Y. (2013). Porous starch based self-assembled nano-delivery system improves the oral absorption of lipophilic drug. *International journal of pharmaceutics*, 444(1-2), 162-168.
- Zhang, W., Sun, X., Fan, X., Li, M., & He, G. (2018). Pickering emulsions stabilized by hydrophobically modified alginate nanoparticles: Preparation and pH-responsive performance in vitro. *Journal of Dispersion Science and Technology*, 39(3), 367-374.
- Zhao, A. Q., Yu, L., Yang, M., Wang, C. J., Wang, M. M., & Bai, X. (2018). Effects of the combination of freeze-thawing and enzymatic hydrolysis on the

- microstructure and physicochemical properties of porous corn starch. *Food Hydrocolloids*, 83, 465-472.
- Zheng, J., Li, Q., Hu, A., Yang, L., Lu, J., Zhang, X., & Lin, Q. (2013). Dual-frequency ultrasound effect on structure and properties of sweet potato starch. *Starch-Stärke*, 65(7-8), 621-627.
- Zhou, F., Liu, Q., Zhang, H., Chen, Q., & Kong, B. (2016). Potato starch oxidation induced by sodium hypochlorite and its effect on functional properties and digestibility. *International journal of biological macromolecules*, 84, 410-417.
- Zhou, X., Chang, Q., Li, J., Jiang, L., Xing, Y., & Jin, Z. (2021). Preparation of V-type porous starch by amylase hydrolysis of V-type granular starch in aqueous ethanol solution. *International Journal of Biological Macromolecules*, 183, 890-897.
- Zhu, J., Li, L., Chen, L., & Li, X. (2012). Study on supramolecular structural changes of ultrasonic treated potato starch granules. *Food Hydrocolloids*, 29(1), 116-122.
- Zuo, Y. Y. J., Hébraud, P., Hemar, Y., & Ashokkumar, M. (2012). Quantification of high-power ultrasound induced damage on potato starch granules using light microscopy. *Ultrasonics Sonochemistry*, 19(3), 421-426.

Chapter 2

Optimization and characterization of porous corn starch and application in emulsion stabilization

2.1. Introduction

Nowadays, the application of solid colloidal particles to produce stable emulsions is gaining much attention. Solid particle-stabilized emulsions, called Pickering emulsions (Ramsden, 1903; Pickering, 1907; Saffarionpour, 2020), are regarded as a promising alternative to conventional synthetic emulsifiers as they show long-term stability without the addition of surfactant as solid particles adsorbed onto oil-water interface (Jiang et al., 2019; Kierulf et al., 2019). The widely used stabilizers are inorganic particles like latex, clay, hydroxyapatite and silica, which have been restricted within the pharmaceutical and food industries because of rising concern over the biocompatibility, carcinogenicity and biodegradability of synthetic surfactants (Wang et al., 2016; Wu et al., 2021; Kierulf et al., 2020). The Pickering particles have shown many advantages over conventional stabilizers, such as improved stability and gut health, reduced toxicity, lower contamination for the environment, and lesser irritation to the skin (Chassaing et al., 2015; Marefati et al., 2017; Marku et al., 2012; Qi et al., 2014). The addition of Pickering particles can ease the problems related with surfactants, such as air entrapment, irritancy, foaming and interaction with living matter (Frelichowska et al., 2009).

Proteins, polysaccharides and lipids are reportedly utilized as Pickering particles for stabilizing emulsions. Proteins such as soy protein, zein; and polysaccharides like cellulose and starch are commonly used (Guida et al., 2021). Among the polysaccharides, starch is widely employed because they are inexpensive, biodegradable, GRAS and non-allergenic, (Zhu, 2019). Starch composed of linear amylose chains, i.e., glucose units linked through α -(1 \rightarrow 4) bonds; and branched amylopectin, where α -(1 \rightarrow 4) glucose units linked to α -glucan by α -(1 \rightarrow 6) linkage (Pérez et al., 2009). The native starch has the ability to stabilize Pickering emulsions due to its functional and physical properties such as size, shape, amylose and amylopectin ratio content, granular structure and chemical

composition (Din et al., 2015). Previous reports also show that granule composition (Kierulf et al., 2020) and granule size (Li et al., 2013) are main factors that determine the starch emulsifying property.

In its commercial pure and native form starch will not act as a stable Pickering particle (Aveyard et al., 2003; Kierulf et al., 2020). So to enhance the ability of starch to act as a Pickering particle, it is subjected to chemical and physical modifications (Guida et al., 2021; Zhu, 2019). Physical modification cause the difference in particle size, surface properties, solubility index and functional properties like gelation ability and swelling capacity of starch (Nawaz et al., 2020). The commonly used physical modification methods are electric pulse field, ultra-high pressure, ultra-sonication, micronization, heat-moisture treatment, freezing, annealing and mild heating (Punia, 2019; C. Zhang et al., 2019). Chemical modification methods consist of oxidation, esterification, etherification, cross-linking, cationization, and hydrolysis. The chemical modification alters physical behaviour like salting, retrogradation, and gelatinization of starch (Korma et al., 2016). Among hydrolysis, the most preferred method to make porous starch is enzyme hydrolysis.

The starch is modified to produce porous starch which is obtained by physical, chemical, and enzymatic treatment, which generate large pores on the surface, that could be elongated in to the starch granules center (Dura et al., 2014). In these methods for producing porous starch, enzymatic method was broadly used because of its substrate specificity, high catalytic efficiency, and mild reaction conditions (Chen et al., 2020; Liu et al., 2018). During the past decade, due to the healthier, efficient, and environmentally friendly nature enzymatic method has received more attention (Hoon et al., 2018). The yield of porous starch depends on many factors such as source of starch, enzyme type, and reaction conditions. Enzymes like amyloglucosidase, amylase,

isoamylase, pullulanase, cyclodextrin-glycosyltransferase, and glycogen branching enzymes were mostly used for the porous starch preparation (Chen et al., 2020; Dura et al., 2014). Many previous studies suggested that synergistic action of amylase and amyloglucosidase enzymes are needed to hydrolyze starch rapidly and completely by cleaving α -1, 4- or α -1, 6 glycosidic linkages. (Dura et al., 2014; Guo et al., 2020; Sun et al., 2010).

Porous starch has many applications in pharmaceuticals, food, environment management, and other industries. In the food industry, porous starch is used for the protection of sensitive elements like vitamins, oils and food pigments, and also used as spices, sweeteners, carriers and colorants (Belingheri et al., 2015; Majzoobi et al., 2015). Zhou et al. (2021) prepared V-type Porous Starch (VPS) from V-type Granular Starch (VGS) by enzymatic treatment and observed the effects of different concentrations of starch and ethanol, and reaction temperatures on the crystal morphology, microstructure, crystallinity and adsorption properties of VGS. Results indicated that VPS exhibited better oil adsorption capacity and higher V-type crystallinity than VGS. Guo et al. (2021) prepared porous starch using three different enzymes such as amylase, branching enzyme, and glucoamylase and they reported that treated starch was found to be more efficient with improved adsorption properties. They also studied morphological characteristics (SEM), structural features (surface area, pore size, particle size), structural properties (amylose and amylopectin), and adsorption capacities (of heavy metals, pigment, oil) of porous starch. However, these studies lack characterization studies like FTIR, XRD, DSC, and rheological studies, which are very important with regard to the application in food systems. Wu et al. (2020) also prepared porous corn starch by combining enzymatic hydrolysis and extrusion technology, however they also lack rheological studies.

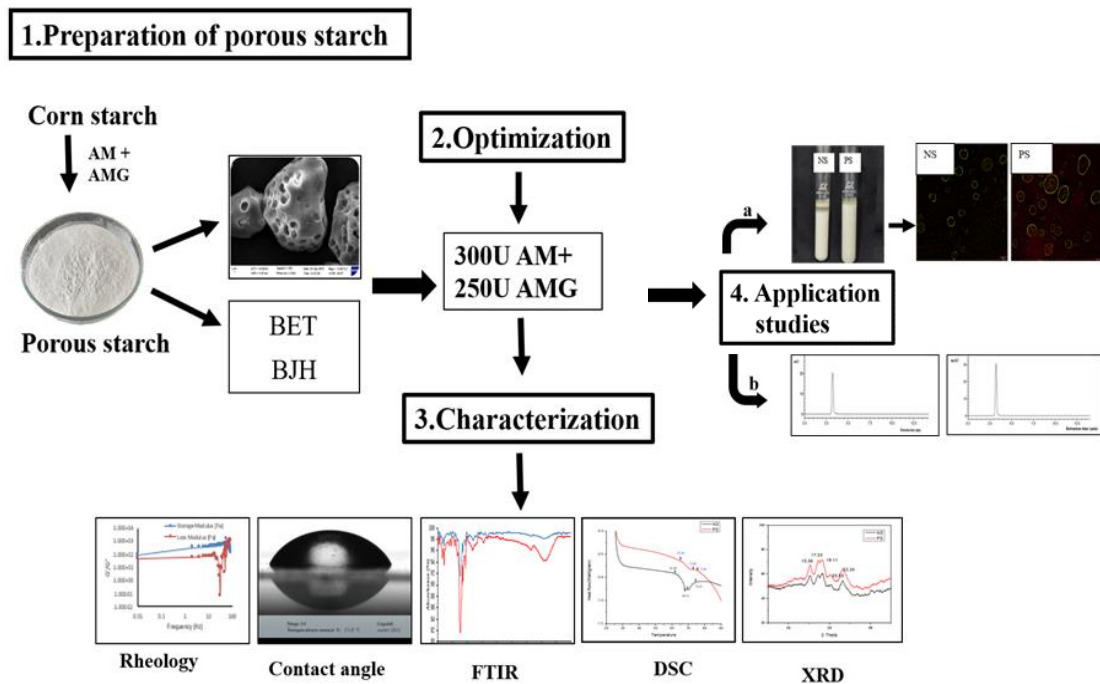
Due to the porous nature of modified starch, it could be also used as a bioactive delivery system. Belingheri et al. (2015) reported that in tomato-based food applications, porous starch was used as a flavour delivery system. Previous studies reported an effective method for colon-delivery of doxorubicin using porous starch and pectin/chitosan coating (Zhu et al 2018). Oliyaei et al. (2020) also reported the use of porous starch for the encapsulation of fucoxanthin. But, similar studies on the efficiency of porous starch as a bioactive carrier are scarce. Therefore, in the current study, we optimized the method for the production of porous starch from native corn starch by enzyme hydrolysis method. In addition, the porous starch was further subjected to thorough physico chemical characterization like particle size, zeta potential, rheology, contact angle, XRD, DSC, and FTIR; and compared to native starch characterization.

2.1.1. Objective

The main objective is to prepare porous starch enzymatically using enzymes amylase and amyloglucosidase. Porous starch thus prepared using an optimized method was further investigated for its efficiency as (1) Pickering particle in oil in water emulsion so that it can be used in other food and nutraceutical applications and (2) as a carrier of bioactive for delivery applications with curcumin as a model system.

2.2. Materials and Methods

The Experimental design for the Optimization and characterization of porous corn starch preparation and application in emulsion stabilization



2.2.1 Materials

Curcumin from *Curcuma longa*, Amyloglucosidase from *Aspergillus niger* (AMG) (≥ 260 U/mL), α -Amylase from *Aspergillus oryzae* (AM) (30U/mg), Starch from corn (CAS:9005-25-8), were purchased from Sigma-Aldrich-USA. All the other reagents used in this study were of analytical grade.

2.2.2 Methods

2.2.2.1. Preparation of porous starch

2.2.2.1.1. Optimization of concentration and incubation time of individual enzyme

The porous starch (PS) preparation was optimized based on a previously published protocol (Zhang et al., 2012) using enzymes AM and AMG with slight modifications.

Initially the PS was prepared by treating the native corn starch (NS) with AMG and AM separately. Concentration and incubation time for the treatment of each enzyme were selected based on the reported literature. Accordingly, we selected high and low concentration and incubation time for the enzyme treatment (Table 2.1 and 2.2). Enzymes (AM and AMG) at different concentrations were added to a 10% starch slurry prepared in phosphate-buffered saline (PBS) (pH-5) at 50 °C and kept under incubation for different durations of time. After completion of enzyme hydrolysis, the pH was adjusted to 10 using potassium hydroxide and starch slurry was then centrifuged at 4000 rpm for 15 minutes. The supernatant was decanted, and the precipitate was washed with distilled water 4-5 times to remove the remaining enzyme and potassium hydroxide. The residue was then dried in a petri dish at 50 °C for 5 h. The dried sample was powdered and passed through a 50-mesh sieve and was analyzed for surface area, pore size, and SEM determination.

Further, two-factorial experiment design was used to optimize porous starch preparation using combination of enzymes AM and AMG. The concentration and incubation time for the combination of enzyme treatment for the design was selected based on the preliminary results obtained from the individual enzymes.

2.2.2.1.2. Modelling and optimization

Porous starch preparation was standardized using a Two factorial experimental design against input factors of enzyme concentration, incubation time, and response parameters of surface area, pore size, and surface morphology. The experimental domain of the input parameters was defined based on the preliminary studies (2.2.2.1.1). Based on the results obtained from these experiments, two factorial experiments were designed for the combination of enzymes (Table 2.3).

2.2.2.2. Determination of specific surface area and pore size distribution

The specific surface area (SSA) and pore size distribution (PSD) was analyzed based on an N₂ adsorption–desorption process with nuance (Du et al., 2013; Jadhav & Vavia, 2017). The analysis was conducted on a TriStar II 3020 instrument (Micromeritics Instrument Corporation, GA, USA). The system was operated at a pressure (P/P₀) range of 0.1 to 1.0. The samples were degassed at 100 °C, overnight under vacuum before adsorption, and the temperature was maintained at 77 K. The SSA and PSD were calculated using Brunauer-Emmett-Teller (BET) and Barrett-Joiner-Halenda (BJH) methods.

2.2.2.3. Scanning Electron Microscopy (SEM)

PS and NS powder were adhered to an aluminum specimen holder by carbon tape. Next, a thin layer of gold was coated onto the sample under a vacuum with a gold/palladium sputter coater (SC7620, Emitech, Quorum Technologies Ltd, Kent, UK) before the microscopical evaluation. The microscopic surface texture of NS and PS was analyzed by scanning electron microscopy (ZEISS; EVO 18, Germany) under 15 kv of accelerating voltage (Da Silva Soares et al., 2021). The micrographs were recorded at 10,000X magnification.

2.2.2.4. Particle size and zeta potential

The particle size and zeta potential of PS and NS was measured using the Malvern Zetasizer (Zeta Nano-ZS; Malvern Instruments, UK), which works on the principle of dynamic light scattering (DLS) (Comunian et al., 2020).

2.2.2.5. Contact angle

The sample (5% of PS and NS in water) was heated at 85 °C for 30 min. The starch paste was then transferred to a coverslip, and the contact angle was measured using Drop

shape analyzer. (Model: DSA30E, KRUSS GmbH, Hamburg, Germany; with the KRUSS ADVANCE Software 1.7.0.8, Version 15).

2.2.2.6. Rheology

The flow behavior, amplitude sweep, and frequency sweep of NS and PS were determined using a controlled stress rheometer (MCR 102 Rheometer, Anton Paar GmbH, Ostfildern-Scharnhausen, Germany). The starch samples, NS and PS were mixed with water (38% W/V, optimized based on experiment trials), and stirred for 30 min before doing the rheological studies. The probe used for the study was a plate geometry of 25 mm diameter and 0.105 mm gap (Mohammed et al., 2021). To determine the flow behavior, the shear rate used ranged of 0.01 to 100 s⁻¹. The amplitude sweep was performed to find the LVR region by changing the strain from 0.01 to 10% for PS and 0.01 to 100% for NS. The frequency sweep was performed within the LVR region at a frequency range from 0.01 to 100 rad/s

2.2.2.7. ATR-Fourier-transform infrared (FTIR) spectroscopy

Fourier-transform infrared (FTIR) spectra of PS and NS powder was recorded using an FTIR-ATR (Attenuated Total Reflection) spectrometer (Perkin Elmer, USA) equipped with an ATR accessory with a diamond crystal at an incidence angle of 45°. The data were averaged from 32 scans recorded at 4 cm⁻¹ resolutions. Transmittances were recorded at wave numbers between 4000 and 400 cm⁻¹.

2.2.2.8. Differential scanning calorimetry (DSC)

The thermal behavior of PS and NS was evaluated by differential scanning calorimetry (DSC). DSC measurements were carried out using a differential scanning calorimeter (DSC Q2000, TA Instruments, USA) based on previous studies (Tao et al., 2016). Briefly, 3 mg of samples were weighed and placed into pre-weighted aluminum sample

pans and 6 μL of distilled water was added. The samples were scanned from 40 $^{\circ}\text{C}$ to 90 $^{\circ}\text{C}$ at a heating rate of 10 $^{\circ}\text{C}/\text{min}$ under an atmosphere of nitrogen. The temperature values obtained were the onset temperature (T_o), the peak temperature (T_p), and the conclusion temperature (T_c).

2.2.2.9. X-ray diffraction (XRD)

XEUSS SAXS/WAXS system from Xenocs was used to record the wide-angle X-ray diffraction (WAXD) measurements in the transmission mode. The powdered PS and NS samples were used for the analysis. The operating voltage was 50 kV, and the current was 0.6 mA, with Cu $K\alpha$ radiation of wavelength $\sim 1.54 \text{ \AA}$. The 2D patterns were recorded on Mar345 image plate, and the data was analyzed using the Fit2D software. The degree of crystallinity was calculated using grams software.

2.2.2.10. Efficacy of porous starch as emulsion stabilizer

The efficiency of porous starch in stabilizing emulsion was studied in terms of creaming index. For the preparation of emulsion, 10% of starch (NS and PS) was mixed with 10% flax seed oil and 80% water. The mixture was homogenized at 12,000 rpm for 150 sec to yield emulsion. The emulsion was stored at room temperature (37°C), and the creaming index of NS and PS was calculated at 24 h and 48 h. The formula calculated the creaming index, $\text{CI} (\%) = 100 \times \text{HC} / \text{HE}$, where HC is the height of the aqueous layer, and HE is the initial height.

2.2.2.11. Fluorescence microscopy

To determine whether the PS would act as Pickering particle the microstructure of starch was studied using fluorescence microscopy (Olympus fluorescence microscope IX 83, Olympus corporation of Americas, Center Valley, USA). PS and NS were stained with the dye Nile red and Safranin for staining oil and starch, respectively (Cakmak et al.,

2012; Daniel & Ana, 2020; Dean et al., 2010). 100µl of the emulsion was taken in a 96-well plate and first stained with Nile red (10%), kept for a few minutes, followed by Safranin (5mg/ml). The images were recorded using a Delta 512 EMCCD camera (Photometrics, USA).

2.2.2.12. Efficacy of porous starch as bioactive carrier

Curcumin (50µg) was added to 500 mg starch in 5 mL water. The mixture was stirred at 60 °C for 10-15 min and then centrifuged at 10000 rpm for 10 min. The supernatant was removed, the pellet was washed with methanol, vortexed for a few minutes, and again centrifuged at 10,000 rpm for 10 min. The supernatant was collected, and continued until the pellet became colorless. The supernatant was pooled together, made up to 10 mL, and curcumin content was determined using the HPLC method.

The supernatant of PS and PS was filtered through 0.22 µm PTFE filter. The analysis was performed on a Prominence Ultra- Fast Liquid Chromatography (UFLC) system containing LC-20AD system controller, Phenomenex Gemini C18 column (250×4.6mm, 5µm), a column oven (CTO-20A), an autosampler injector (SIL 20 AC) and a diode array detector (SPD-M20A). The mobile phase used for curcumin quantification was the isocratic system i.e., 100% methanol. The injection volume was 10µL, and the flow rate was kept at 1 mL/ min. The column was maintained at 40°C, and eluted fractions were monitored at 420 nm. Sample peaks (NS & PS) were identified by comparing them with the retention times of Curcumin peak. LC Lab Solutions software was used for data acquisition and analysis.

2.3 Results and discussion

2.3.1. Optimization of porous starch preparation

Initially NS was treated with AMG and AM at different concentration based on the literature to understand the optimum concentration and incubation time to yield desired porosity, which was assessed in terms of pore size (nm) and surface area (m²/g). The pore size and surface area of NS were found to be 03.457 nm and 0.202 m²/g respectively.

The pore size and surface area of starch treated with different concentrations of AM and time of incubation (Table 2.1) showed that starch treated with 300 U of enzyme exhibits greater surface area and pore size. The same result is evident from the Scanning electron micrographs of AM treated starch (Fig 2.1). α - amylase is an endo-acting enzyme that can hydrolyze the α (1 \rightarrow 4) glycosidic linkages of starch that rapidly reduce the chain length of amylose and amylopectin resulting in increase in number of short linear and branch chains (Xu et al., 2015).

Table 2.1: The surface area and pore size of starch treated with different concentrations of Amylase (AM) and time of incubation

Enzyme	Concentration (U/mL)	Time (h)	Surface area(m ² /g)	Pore size (nm)
Amylase (AM)	300	8	0.720	10.200
	300	12	0.759	09.945
	3000	8	0.581	09.554
	3000	12	0.465	06.175

From the SEM images it is clear that at lower enzyme concentration (300 U), starch showed small pores and there was no significant change in pore size when the concentration of enzyme was increased from 300 to 3000 U. Cassava starch treated with

α - amylase alters the properties of granules without altering the size and morphology (Ichihara et al., 2013). Dura et al (2014) also reported that starch treated with amylase generates small pores in the granules. These observations suggested that AM at concentrations of 300 U and below, for an incubation time of 8 h and below can result in desirable porosity.

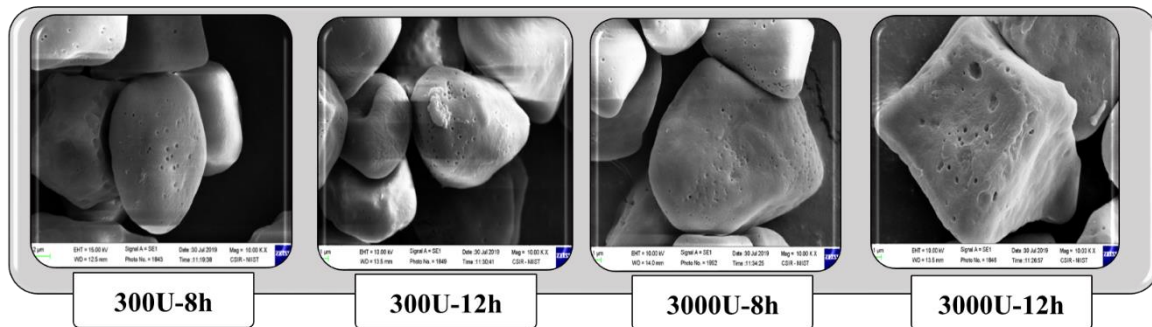


Fig 2.1: SEM images of starch treated with different concentrations and incubation time of amylase

The surface area and pore size of starch treated with different concentrations of AMG and time of incubation indicated that compared to 300 U enzyme concentration, 900 U showed decrease in surface area and porosity which is contradictory. In general, it was noted that the pore size and surface area decreased with increase in incubation time for all concentration of AMG studied. An enzyme concentration of 1500 U exhibited higher porosity and surface area (Table 2.2).

Table 2.2: The surface area and pore size of starch treated with different concentrations of Amyloglucosidase (AMG) and time of incubation

Enzyme	Concentration (U/mL)	Time (h)	Surface area(m ² /g)	Pore size(nm)
Amyloglucosidase (AMG)	300	8	1.457	28.809
	300	12	1.289	16.061
	900	8	0.981	23.219
	900	12	0.721	09.413
	1500	8	2.235	33.307
	1500	12	1.302	19.307

Amyloglucosidase hydrolyzes single glucose residues from non-reducing ends of amylose and amylopectin in a step wise manner and it can also hydrolyze α (1,6) linkages in the branch points of amylopectin (Aggarwal & Dollimore, 2000). Surface morphology of starch treated with AMG (Fig. 2.2) shows large pores and broader size distribution with increase in enzyme concentration and incubation time. At higher enzyme concentration and longer duration especially at 900 and 1500 U of enzyme concentration, the morphology of starch changed to deep and large irregular holes and broken structure. These results along with SEM images suggests that concentration of 300 U gives rise to desirable porosity. The observed results are in accordance with Benavent-gil & Rosell. (2016) who reported that amyloglucosidase treated starch shows large pores and at high amyloglucosidase concentration, depression in the granules was seen due to the eroding action of enzyme on the surface of granule. Aggarwal et al. (2000) also observed an increased pore size when amyloglucosidase concentration was increased, up to a concentration of 800 U/g starch, after which large irregular holes and broken structure of starch were observed. It was observed that porous starch, for delivery or encapsulation applications, can be obtained by treating NS with AMG at concentration 300 U for 8 h

incubation and at higher concentration of 900 U, AMG resulted in breakdown of starch structure with irregular pores making it unsuitable for such applications.

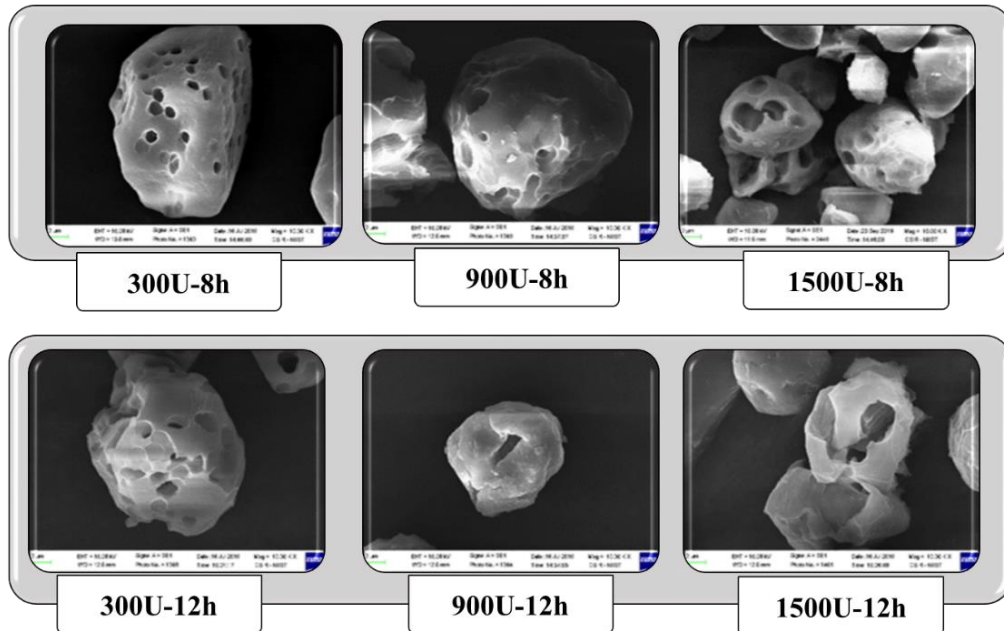


Fig 2.2: SEM images of starch treated with different concentrations and incubation time of amyloglucosidase

2.3.2. Effect of combination of enzymes on porous starch preparation

Based on the above observations acquired for individual enzymes (maximum enzyme concentration and time of 300 U and 8 h respectively), a two factorial experimental design was obtained (as given under Table 2.3) for combination of enzyme treatment. Enzyme concentration and incubation time were the input factors whereas surface area and pore size were the output parameters.

Table 2.3: The surface area and pore size of starch treated with combination of enzymes, (AM/AMG) and time of incubation.

Enzyme/s	Concentration (U/mL)	Time (h)	Surface area(m ² /g)	Pore size (nm)
Amylase/ Amyloglucosidase (AM/AMG)	150/150	6	0.900	17.389
	150/150	8	1.126	13.654
	150/300	6	0.468	48.188
	150/300	8	0.737	34.330
	300/150	6	1.781	09.165
	300/150	8	0.860	09.416
	300/300	6	0.614	40.527
	300/300	8	0.207	12.591

The regression analysis is given in (Table 2.4) and the equation for surface area and pore size are given in Eq (1) and Eq (2) respectively. As can be seen, the effect of interaction between enzyme concentration and time on surface area was more pronounced than individual effects (Table 2.4). Porosity was directly influenced by AMG enzyme, rather than by amylase and time.

$$\text{Surface area} = -5.693 + 0.04317 \text{ AM} + 0.01061 \text{ AMG} + 0.9013 \text{ Time} - 0.000096 \text{ AM*AMG} - 0.005398 \text{ AM*Time} - 0.001431 \text{ AMG*Time} + 0.000010 \text{ AM*AMG*Time} \dots\dots\dots (1)$$

$$\text{Pore Size} = 423.7 - 4.996 \text{ AM} + 0.4271 \text{ AMG} - 78.32 \text{ Time} + 0.02434 \text{ AM*AMG} + 0.7351 \text{ AM*Time} + 0.2648 \text{ AMG*Time} - 0.004015 \text{ AM*AMG*Time} \dots\dots\dots (2)$$

Table 2.4: Regression table for combination of enzymes AM and AMG

Enzymes	Surface are		Pore size	
	Effect	Coefficient	Effect	Coefficient
AM	0.057	-0.028	-104.650	-52.330
AMG	-0.660	-0.330	215.000	107.500
Time	-0.208	-0.104	-113.200	-56.600
AM*AMG	-0.250	-0.125	-42.350	-21.170
AM*Time	-0.455	-0.227	-25.230	-12.620
AMG*Time	0.139	0.069	-95.770	-47.890
AM*AMG*Time	0.118	0.059	-45.160	-22.580

The SEM images of starch treated with combination of enzymes, AM and AMG (Fig 2.3) indicated more pronounced and controlled formation of deep pores, confirming the synergistic action of these enzymes. The treatment of starch with combination of AMG and AM has already been reported to result in shallow to deep pores (Lucca Centa Malucelli, 2015). Based on the parameters analyzed and SEM images, a combination of 150/300 and 300/300 of AM/AMG for 6 hours were found to yield better porosity. Incubation time of 8 & 12 h resulted in degradation of starch molecules as evident from the SEM images. Lacerda et al. (2018) reported that 12 h of incubation time was excessive because it may result in appearance of internal canals due to exo-corrosion. Due to longer incubation time, shape of the granule also changed resulting in partial fracture, rough surface and weakened structure.

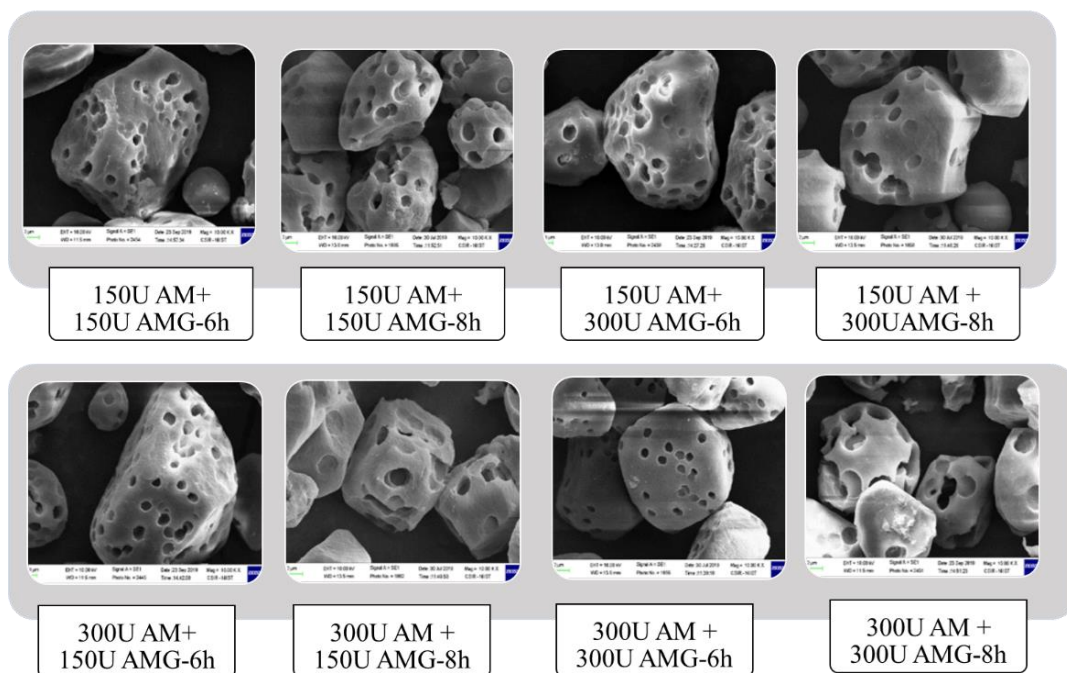


Fig 2.3: SEM images of starch treated with different concentrations and incubation time of amylase and amyloglucosidase.

As discussed earlier, α -amylase, randomly and rapidly cleaves α -(1,4) glycosidic bonds of starch with dextrin as main end product. Thus α -amylase treated starch only undergo incomplete hydrolysis. Amyloglucosidase can cleave both α -(1,4) and α -(1, 6) glycosidic bonds from the nonreducing ends of starch chains and forms entirely glucose. However, the action of amyloglucosidase is very slow. When used in combination, firstly, α -amylase randomly splits the glucose residues present on the surface of starch and releases new non reducing ends. Secondly, amyloglucosidase act on these nonreducing ends and releases glucose continuously from the granules. Thirdly, amyloglucosidase forms holes from surface to the center of granule, allowing more access of α -amylase into the interior of granule and act on more glycosidic bonds resulting in the formation of pores (Sun et al., 2010). Yu et al. (2018) also reported that treatment of corn starch with combination of enzymes creates significant changes by producing pores, but without altering the shape of starch granules. Lacerda et al. (2019) reported that while using combination of enzymes amylase and amyloglucosidase, more superficial attacks were observed. Chen

et al. (2020) also reported that for the preparation of porous starch, multiple enzyme treatment i.e., combination of amylase and amyloglucosidase was mostly used. Thus, the synergistic action of amylase and amyloglucosidase can hydrolyze the entire starch quickly.

The optimum concentration of enzymes obtained after design analysis suggested an optimum surface area and pore size at incubation time of 6 h and at an enzyme concentration of 300 U and 250 U of AM and AMG respectively. Based on the statistical analysis, porous starch was prepared using the optimum combination of enzymes i.e., 300U AM and 250U AMG for 6 hours, for further characterization and application studies.

2.3.3. Characterization of porous starch

Size of starch varies based on their origin and corn starch mostly comes under medium sized starches. Size of Pickering particles and zeta potential plays a key role in the formation of stable emulsion. Therefore, the zeta potential of NS and PS was also evaluated. It is also important to understand the wettability or hydrophobic/hydrophilic nature of the particles in order to determine the choice of emulsion type i.e., O/W or W/O, which is measured using contact angle.

2.3.3.1. Particle size and zeta potential

The particle size of PS was $2.302 \pm 0.062 \mu\text{m}$ and that of NS was $3.549 \pm 0.085 \mu\text{m}$. From the results it is clear that particle size of porous starch decreases after enzyme hydrolysis. Studies reported that during enzyme hydrolysis the native starch ruptures resulted in decreased particle size (Jiang et al., 2017; Yu et al., 2018). Decreased particle size increases the stability of Pickering emulsion (Saari et al., 2019). Rayner et al. (2012)

fabricated stable Pickering emulsion using Quinoa starch and observed that with decreased particle size droplet size also decreased.

The zeta potential of PS and NS was found to be -42 mV and -34 mV, respectively. High surface electric charge (+/-) denotes potential stability of the colloidal system (Espinosa Solis et al., 2021). The negative zeta potential values indicates negative charges on the surface of starch (Wei et al., 2014). Due to electrostatic repulsion, higher zeta potential decreases the Van der Waals force between particles (Ahmad et al., 2020; Schafer et al., 2010). High zeta potential resulted in higher particle stability due to a lower tendency for particle agglomeration (Dai et al., 2018). Starch nanoparticles also reported to exhibit negative zeta potential values (Ahmad et al., 2020). Thus PS with higher zeta potential confers better stability compared to PS.

2.3.3.2. Contact angle

Contact angle measurement is frequently used as marker to measure the degree of surface hydrophobicity or hydrophilicity. Contact angle $> 90^\circ$ denotes particle with hydrophobic nature which is suited for the formation of W/O emulsion and $< 90^\circ$ indicates hydrophilic particles that is suitable for stabilizing O/W emulsion (He et al., 2013; Su et al., 2010). Coalescence is the process where droplets combines to form large droplets and in course of time, average droplet size increases and thus decreases the stability of emulsion (Maphosa & Jideani, 2018). The contact angle of PS was found to be $63.82^\circ \pm 0.39$ and that of NS was $72.4^\circ \pm 0.14$ (Fig 2.4). Li et al. (2013) studied about emulsifying property of different native starch particles and reported that rice starch (48° contact angle) which is more hydrophilic than potato starch (63° contact angle) act as good particle emulsifier and stabilize emulsion against coalescence for several months. Hydrophobic particles stabilize water in oil emulsion whereas hydrophilic particles stabilize oil in water emulsion (Wu et al., 2016). The results showed that PS has a lower contact angle than

NS, which makes it more hydrophilic and effective emulsifier in O/W Pickering emulsions

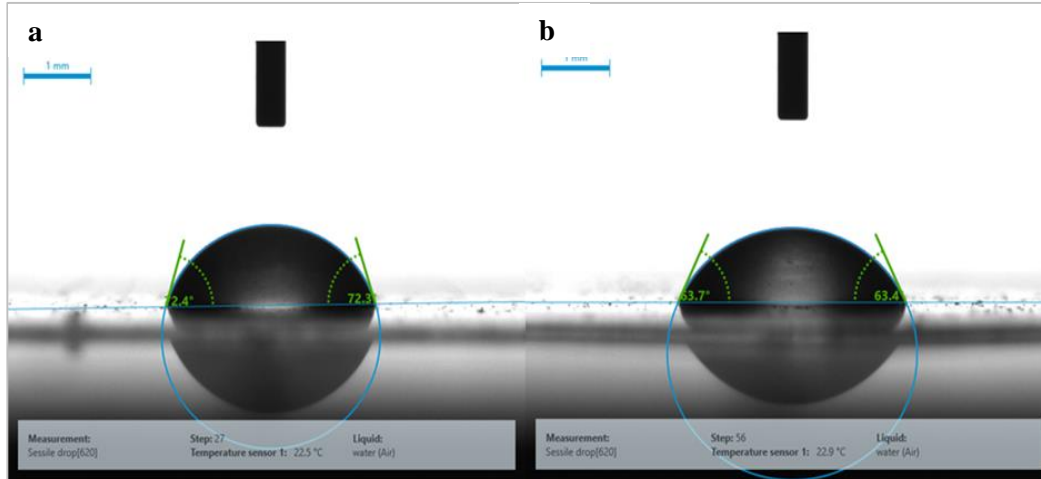


Fig 2.4: Contact angle of (a) NS and (b) PS

2.3.3.3. Rheological studies

2.3.3.3.1 Flow behaviour

The comparison of the flow ability of NS and PS of same composition of 38% W/V at 25°C is depicted in (Fig 2.5). The NS system had shown Newtonian behavior at all shear rates with viscosity 0.0285 ± 0.009 Pa.s. On the other hand, PS system shows non-Newtonian behavior with an evident shear thickening till the shear rate of 30 s^{-1} followed by shear thinning with a decreasing viscosity as the rate increases further. Shear stress vs. shear rate plot and Shear rate vs. Viscosity plot of NS and PS are given in (Fig 2.5a and b) respectively.

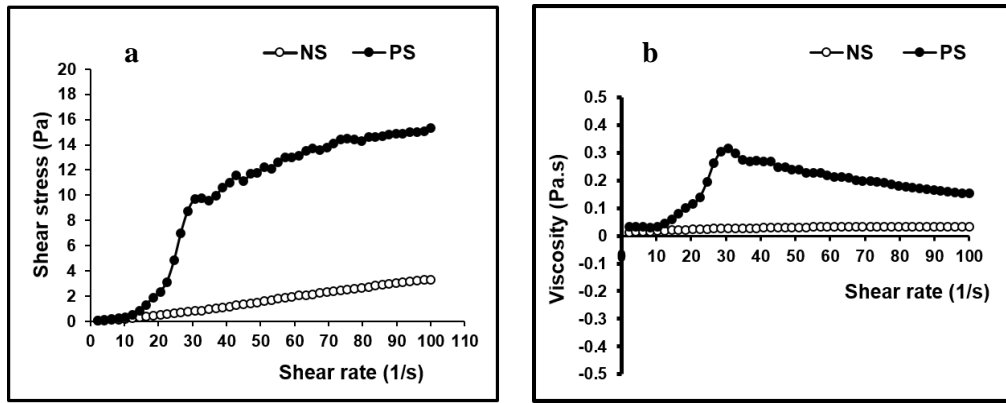


Fig 2.5: (a) Shear stress vs shear rate plot and (b) Shear rate vs Viscosity plot of NS and PS

Dynamic strain sweep determines the LVE region of the system where the properties of substances will not vary according to the deforming strain, applied shear rate or magnitude of stress. The structure of the system remains the same along the LVE region (Chen et al., 2017; Steffe, 1996). Thus, LVE region is required for the determination of the storage modulus (G'), and loss modulus (G''), of viscoelastic materials (Liu et al., 2014). Instrument could detect only G'' for NS matrix for entire range of applied strain. The PS system has shown viscoelastic nature with both G' and G'' . The LVE plateau value for the NS is observed to be less than 3% (Fig 2.6a), whereas the plateau for PS was found at strain less than 0.7% (Fig 2.6b).

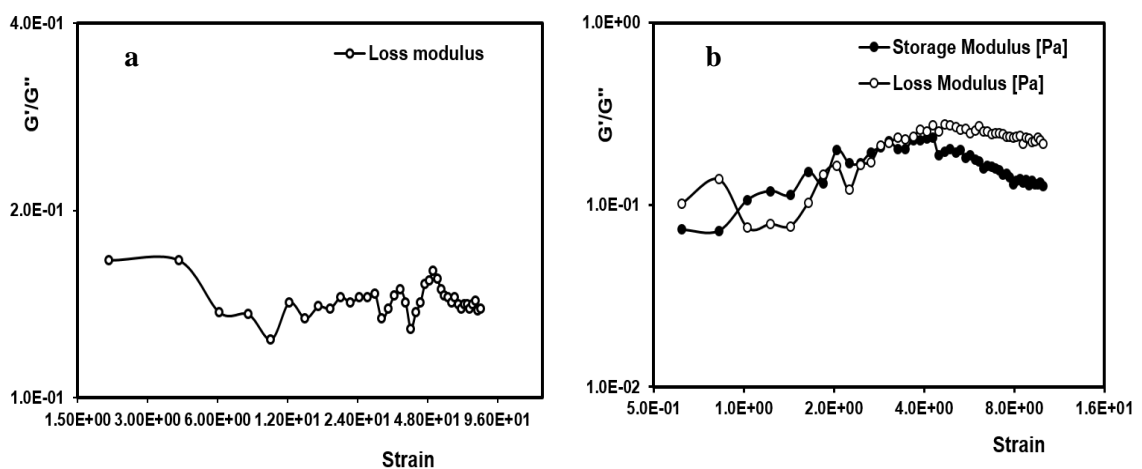


Fig 2.6: Amplitude sweep of (a) NS and PS (b) respectively.

Dynamic frequency sweep test is useful in determining the viscoelastic properties of a system in terms of time scale. G' refers the elastic property and G'' refers the viscous property of a system (Okonkwo et al., 2021). The NS has indicated that the system was not viscoelastic in nature since it has shown only the loss modulus responses (Fig 2.7a) in a similar time scale as that of the PS system. In contrast, the PS matrix has shown a viscoelastic nature with both G' and G'' (Fig 2.7b). Also, the PS system shows a higher G' value than the G'' compared to the NS system at all the frequencies up to 90 Hz. The system has shown a cross over with $G'' > G'$ only at frequency greater than 90Hz. Since the stability and emulsifying properties of the starch systems can be directly related to the elastic nature of the material, PS was observed to be a better component than NS, which can contribute more stability and elasticity to the system in which they will be incorporated. Also, we can deduce that there are more interaction forces among the PS particles than NS. These interactions in the PS matrix may help promote the formation of steric barriers that can prevent coalescence in emulsions.

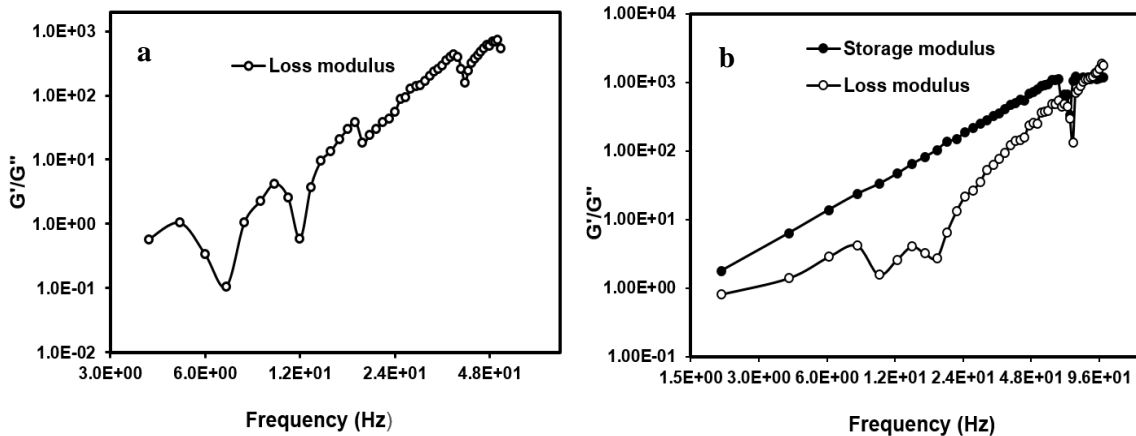


Fig 2.7: Frequency sweep of (a) NS and (b) PS respectively.

2.3.3.4. XRD

NS and PS have been analyzed by XRD to investigate the impact of enzyme treatment on the amorphous and crystalline region. From XRD diffractograms (Fig. 2.8a) it is clear

that both NS and PS exhibit A pattern, which is typical of maize starch. According to Cheng et al. (2009), a typical A pattern has two single broad peaks at 15° and 23° (2θ), a lower peak at 20° (2θ), and a dual peak at 17 - 18° (2θ). In the current study, NS and PS displayed a typical A pattern as evident from the figure 2.8a. According to the deconvolution results (Fig. 2.8b and 2.8c), the degree of crystallinity increased from 42.36% in NS to 52% in PS. Because enzymatic reactions take place mostly in the amorphous region, there is increase in the crystallinity of porous starch (Zhang, Cui et al., 2012). Sago starch nanocrystals showed enhanced crystallinity and could be employed as an effective emulsifier for O/W emulsions (Azfaralariff, 2020). Thus porous starch with increased crystallinity can be used as Pickering particle in emulsion.

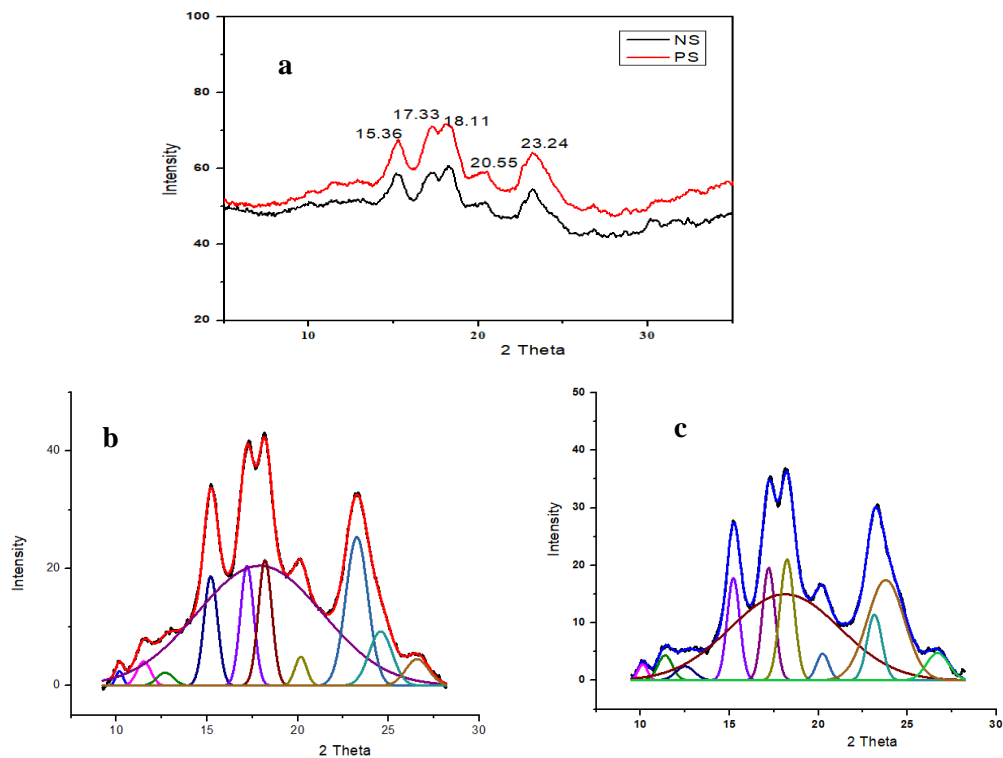


Fig 2.8: (a) XRD diffractograms and Deconvolution plots of (b) native and (c) porous starch

2.3.3.5. Thermal behaviour

It is important to understand the thermal property of NS and PS, so that it can be further

used in food and pharmaceutical applications (spray drying). Differential scanning calorimetry (DSC) was employed to analyze the thermal stability of NS and PS, and notable variations was observed in the thermograms (Fig. 2.9). According to Laura, Gomez-Mascaraque et al., (2017), thermal property is also crucial for storage stability.

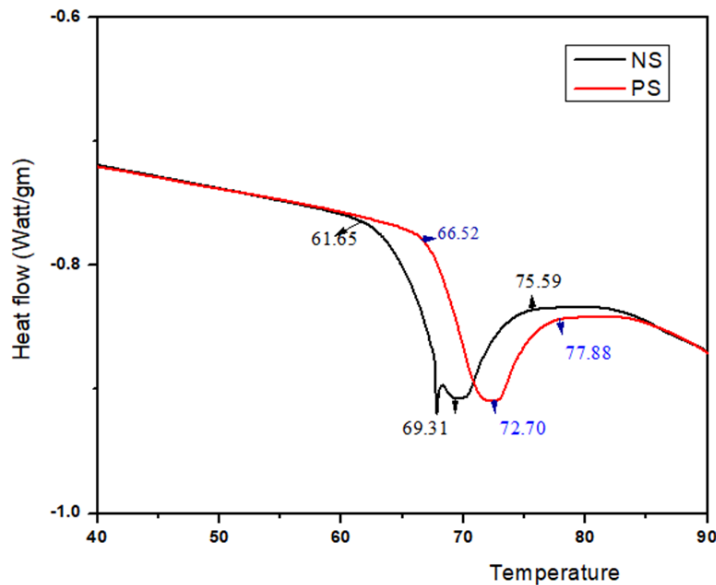


Fig 2.9: DSC thermograms of NS and PS.

The onset temperature (T_o), Peak temperature (T_p) and conclusion temperature (T_c) were analyzed by DSC and was shown in Table 2.5. NS showed delayed gelatinization compared to porous starch. During gelatinization, water is irreversibly absorbed, causing the starch granules to swell. Water can freely enter through amorphous region but in crystalline region, it happens only due to increased temperature and excess water (Yu et al., 2018). Thus the gelatinization temperature of starch granules is directly correlated with the percentage of crystalline areas and increased crystallinity resulted in higher gelatinization temperature (Zieba et al., 2011). From the results it is clear that enzyme hydrolysis makes PS more crystalline, which makes them more resistant to gelatinization. Thus thermally resistant PS can be employed for further food applications (Yu et al., 2018).

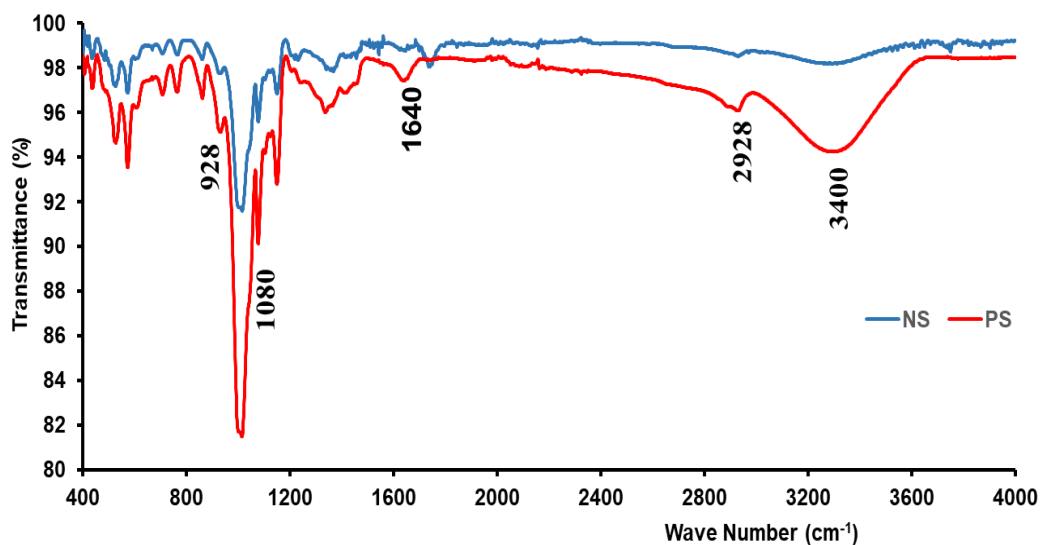
Table 2.5: Gelatinization temperature of native and porous starch

	To (°C)	Tp (°C)	Tc (°C)
Native starch	61.76 ± 0.09	69.42 ± 0.09	73.56 ± 0.7
Porous starch	65.94 ± 0.4	72.79 ± 0.07	76.78 ± 0.8

To = onset temperature; Tp = peak temperature; Tc = conclusion temperature

2.3.3.6. FTIR

The IR spectra analysis showed that the position of absorption peaks of NS and PS have not changed (Fig. 2.10). This is because after the enzymatic reaction, the molecular structure of starch remained unchanged, and as a result, the functional groups also remained the same (B. Zhang et al., 2012). FTIR spectra of NS showed peaks at 3400 cm^{-1} which indicates ($-\text{OH}$ stretching), 1080 cm^{-1} (C-O-H) bonding, 928 cm^{-1} (C-O-C) vibrations of α -1,4 glycosidic linkage, 1152 cm^{-1} (C-O , C-C) stretching, 764 cm^{-1} (C-C stretching) and 859 cm^{-1} ($-\text{CH}_2$) deformation (Wang et al., 2016). The FTIR spectra of PS also showed similar peaks which confirms that chemical structure has not changed following enzymatic hydrolysis.

**Fig 2.10: FTIR spectrum of NS and PS.**

2.3.3.7. Preparation of emulsion

Based on the results of studies mentioned above, PS can be used to stabilize O/W emulsions. Thus preliminary studies were performed to assess the emulsion stabilizing potential of PS and was evaluated based on creaming index (Hong, Kim et al., 2018; Konar, Ozarda et al., 2019).

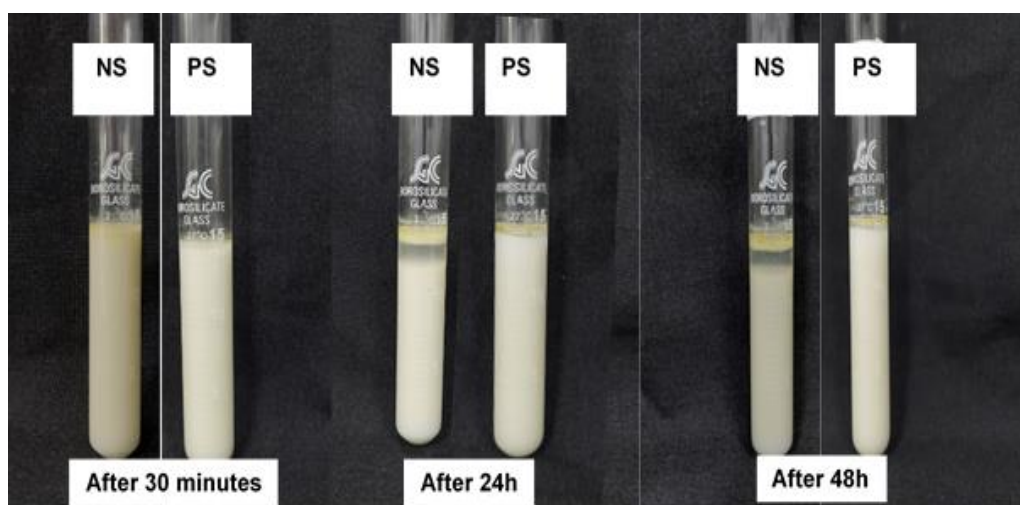


Fig 2.11: Emulsion of NS and PS after 30 minutes, 24h and 48h.

NS and PS (10%) was used to formulate emulsion (O/W) consisting of flax seed oil as dispersed phase (10%) and water as continuous phase. Following 24 hours of storage, it was observed that creaming index of PS and NS were 5.0 and 16.6% respectively, which remained stable even after 48h of storage (Fig. 2.11). In NS stabilized emulsion clear separation of dispersed and continuous phase was observed after 30 min. But PS stabilized emulsion showed greater stability compared to NS.

2.3.3.8. Fluorescence microscopy

It was understood from the previous studies that PS forms a stable emulsion by acting as a Pickering particle. In order to confirm this, fluorescence microscopy of the freshly prepared emulsion was performed.

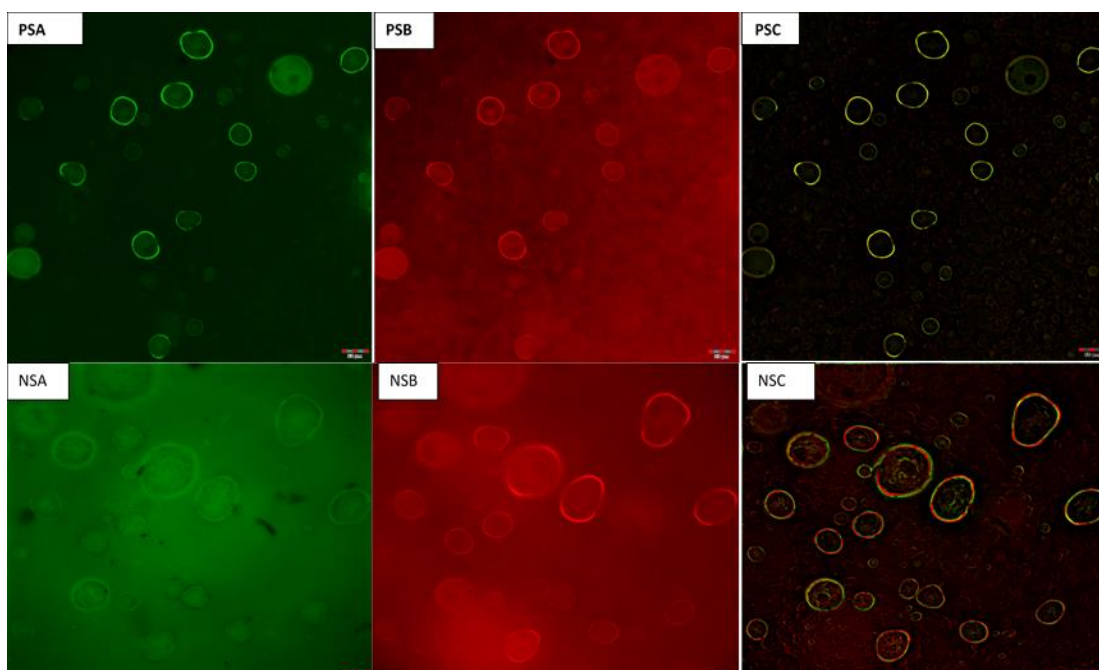


Fig 2.12: Fluorescence images of porous (PS) and native starch (NS) stained with (A) safranin (B) Nile red individually and (C) merged image of (A) and (B)

Safranin and Nile red were used to stain starch and oil in the emulsion, Fig. 2.12PS (A) and Fig. 12PS (B). From the images it is clear that the PS adsorb into interface of dispersed and continuous phase (PS as green colour) Fig. 2.12PS (C). Thus the PS solid particles entrap or protects the inner oil phase and thus acts as Pickering particle. In case of NS, the starch and oil were found on the outer core surface of emulsion resulted in emulsion destabilization Fig. 2.12 NS (A, B, C). Thus PS can protect bioactive and functional food ingredients by acting as Pickering particle.

2.3.3.9 Evaluation of efficacy of porous starch as carrier of bioactives

PS is reported to be employed for delivery of flavor, anthocyanins, doxorubicin, and controlled release of insulin for food and pharmaceutical applications (Belingheri, Ferrillo et al., 2015; Ji, 2021; Zhu, Zhong et al., 2018; Chen, Song et al., 2021). In order to understand the use of PS for delivery applications we carried out experiments using

curcumin as bioactive model system. Both NS and PS were mixed with curcumin for a predetermined time. The slurry was centrifuged so that the un-interacted curcumin (free curcumin) is left behind in the supernatant. The residue was extracted and analysed for curcumin using HPLC (Dallarmellina, Letan et al.,2021; Patil, Gutierrez et al 2017). The typical HPLC chromatograms and quantifications of curcumin, NS and PS samples are shown Fig. 2.13. The curcumin content of NS and PS were found to be $61.03 \pm 1.43 \%$ and $82.24 \pm 1.07 \%$, respectively, suggesting that PS can hold significantly higher amount of curcumin than NS. Native starch granules do not have pores on their surface, in general, and therefore cannot accommodate other moieties by adsorption and encapsulation (Choy et al., 2016). These properties can be introduced to the native starch by imparting porosity e.g., enzymatic treatment as observed in the present study. This confirms that PS could be effectively used as a carrier of nutritional compounds and bioactive for various food and nutraceutical applications.

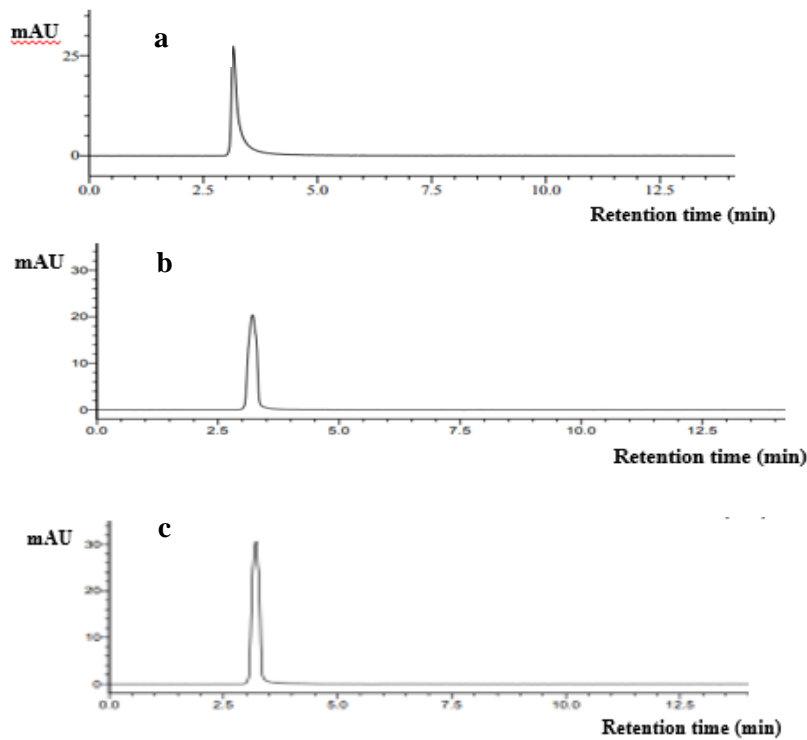


Fig 2.13: HPLC chromatogram of standard (a) Curcumin, (b) NS and (c) PS.

2.4. Conclusion

In the present study, PS was prepared enzymatically using enzymes amyloglucosidase and amylase. Based on statistical analysis, corn starch treated with 300 U amylase and 250 U amyloglucosidase for 6 h incubation, yielded PS with optimum surface area and pore size. PS was further characterized in terms of particle size, contact angle, XRD, DSC, FTIR and rheological studies. PS showed decreased particle size, more hydrophilic and crystalline nature and better thermal stability compared to native starch indicating its application in O/W emulsions. Rheological studies showed the viscoelastic nature of PS. Further studies were carried out to explore the possible application of PS as Pickering particle in stabilizing emulsion and found that PS prepared emulsion showed better stability. Fluorescence microscopy confirmed the ability of PS as Pickering particle by adsorbing into interface of water and oil in the emulsion. Finally, the efficiency of PS as bioactive carrier was ratified using curcumin as a model. Thus the results from the present study demonstrated that porous starch can act as Pickering particle for emulsion stabilization and active substance delivery application. Porous starch can act as vehicles for carrying nutritionally important compounds (e.g., vitamins, minerals, probiotics) in formulation of nutritional supplements/health foods/functional foods etc. It can also be fine-tuned as a carrier for bioactive phytochemicals and active molecules for nutraceutical and pharmaceutical applications.

2.5. References

- Aggarwal, P., & Dollimore, D. (2000). Degradation of starchy food material by thermal analysis. *Thermochimica Acta*, 358(June 1999), 57–63.
- Ahmad, M., Gani, A., Masoodi, F. A., & Rizvi, S. H. (2020). Influence of ball milling on the production of starch nanoparticles and its effect on structural , thermal and functional properties. *International Journal of Biological Macromolecules*, 151, 85–91.
- Aveyard, R., Binks, B. P., & Clint, J. H. (2003). Emulsions stabilised solely by colloidal particles. *Advances in Colloid and Interface Science*, 102, 503–546.
- Azfaralariff, A., Faiqah, F., Sisika, R., Faizan, M., & Mat, A. (2020). Food-grade particle stabilized pickering emulsion using modified sago (Metroxylon sagu) starch nanocrystal. *Journal of Food Engineering*, 280(October 2019), 109974.
- Belingheri, C., Ferrillo, A., & Vittadini, E. (2015). Porous starch for flavor delivery in a tomato-based food application. *LWT - Food Science and Technology*, 60(1), 593–597.
- Belingheri, C., Giussani, B., Rodriguez-estrada, M. T., Ferrillo, A., & Vittadini, E. (2015). Oxidative stability of high-oleic sunflower oil in a porous starch carrier. *FOOD CHEMISTRY*, 166, 346–351.
- Benavent-gil, Y., & Rosell, C. M. (2016). Comparison of porous starches obtained from different enzyme types and levels. *Carbohydrate Polymers*.
- Cakmak, T., Angun, P., Demiray, Y. E., & Ozkan, A. D. (2012). Differential Effects of Nitrogen and Sulfur Deprivation on Growth and Biodiesel Feedstock Production of *Chlamydomonas reinhardtii*. *Biotechnology and Bioengineering*,

1–11.

- Chassaing, B., Koren, O., Goodrich, J. K., Poole, A. C., Srinivasan, S., Ley, R. E., & Gewirtz, A. T. (2015). Dietary emulsifiers impact the mouse gut microbiota promoting colitis and metabolic syndrome. *Nature*, *519*(7541), 92–96.
- Chen, J., Wang, Y., Liu, J., & Xu, X. (2020). Preparation , characterization , physicochemical property and potential application of porous starch : A review. *International Journal of Biological Macromolecules*, *148*, 1169–1181.
- Chen, L., Tian, Y., Bai, Y., Wang, J., Jiao, A., & Jin, Z. (2017). Effect of frying on the pasting and rheological properties of normal maize starch. *Food Hydrocolloids*.
- Chen, Y., Song, H., Huang, K., Guan, X. (2021). Novel porous starch/ alginate hydrogel for controlled insulin release with dual response of pH and amylase. *Food Funct.* 0–27.
- Choy, S. Y., Prasad, K. N., Wu, T. Y., Raghunandan, M. E., & Ramanan, R. N. (2016). Performance of conventional starches as natural coagulants for turbidity removal. *Ecological Engineering*, *94*, 352–364.
- Comunian, T. A., da Silva Anthero, A. G., Bezerra, E. O., Moraes, I. C. F., & Hubinger, M. D. (2020). Encapsulation of pomegranate seed oil by emulsification followed by spray drying: Evaluation of different biopolymers and their effect on particle properties. *Food and Bioprocess Technology*, *13*(1), 53-66.
- Dai, L., Li, C., Zhang, J., & Cheng, F. (2018). Preparation and characterization of starch nanocrystals combining ball milling with acid hydrolysis. *Carbohydrate Polymers*, *180*(September 2017), 122–127.
- Dallarmellina, A., Letan, M., Duval, C., Contino-Pépin. (2021). One-pot solvent-free

extraction and formulation of lipophilic natural products: from curcuma to dried formulations of curcumin. *Green Chem.*

Daniel, J. F., & Ana, A. M. (2020). Rice in vitro digestion : application of INFOGEST harmonized protocol for glyceimic index determination and starch morphological study. *J Food Sci Technol*, 57(April), 1393–1404.

Da Silva Soares, B., De Carvalho, C. W. P., & Garcia-Rojas, E. E. (2021). Microencapsulation of Sacha Inchi Oil by Complex Coacervates using Ovalbumin- Tannic Acid and Pectin as Wall Materials. *Food and Bioprocess Technology*, 14(5), 817-830.

Dean, A. P., Sigeo, D. C., Estrada, B., & Pittman, J. K. (2010). Using FTIR spectroscopy for rapid determination of lipid accumulation in response to nitrogen limitation in freshwater microalgae. *Bioresource Technology*, 101(12), 4499–4507.

Din, Z.-, Xiong, H., & Fei, P. (2015). *Physical and Chemical Modification of Starches - A Review*. 8398(November).

Du, S., Wang, L., Fu, X., Chen, M., & Wang, C. (2013). Bioresource Technology Hierarchical porous carbon microspheres derived from porous starch for use in high-rate electrochemical double-layer capacitors. *Bioresource Technology*, 139, 406–409.

Dura, A., Błaszczak, W., & Rosell, C. M. (2014). Functionality of porous starch obtained by amylase or amyloglucosidase treatments. *Carbohydrate Polymers*, 101, 837–845.

- Espinosa-Solís, V., García-Tejeda, Y. V., Portilla-Rivera, O. M., & Barrera-Figueroa, V. (2021). Tailoring Olive Oil Microcapsules via Microfluidization of Pickering o/w Emulsions. *Food and Bioprocess Technology*, *14*(10), 1835-1843.
- Frelichowska, J., Bolzinger, M., & Chevalier, Y. (2009). *Colloids and Surfaces A: Physicochemical and Engineering Aspects Pickering emulsions with bare silica*. *343*, 70–74.
- Guida, C., Aguiar, A. C., & Cunha, R. L. (2021). Green techniques for starch modification to stabilize Pickering emulsions: a current review and future perspectives. *Current Opinion in Food Science*, *38*, 52–61.
- Guo, L., Li, J., Li, H., Zhu, Y., & Cui, B. (2020). The structure property and adsorption capacity of new enzyme-treated potato and sweet potato starches. *International Journal of Biological Macromolecules*, *144*, 863–873.
- Guo, L., Yuan, Y., Li, J., Tan, C., Janaswamy, S., Lu, L., Fang, Y., & Cui, B. (2021). Comparison of functional properties of porous starches produced with different enzyme combinations. *International Journal of Biological Macromolecules*, *174*(31771933), 110–119.
- He, G. J., Liu, Q., & Thompson, M. R. (2013). *Characterization of structure and properties of thermoplastic potato starch film surface cross-linked by UV irradiation*. 304–311.
- Hong, I.K., Kim, S.I., Lee, S.B. (2018). Effects of HLB value on oil-in-water emulsions: Droplet size, rheological behavior, zeta-potential, and creaming index. *J. Ind. Eng. Chem.* *67* 123–131.
- Hoon, S., Yerim, P., Jungwoo, N., Shin, K., & Kang, D. (2018). Properties and

- applications of starch modifying enzymes for use in the baking industry. *Food Science and Biotechnology*, 27(2), 299–312.
- Ichihara, T., Fukuda, J., Takaha, T., Yuguchi, Y., & Kitamura, S. (2013). Limited Hydrolysis of Insoluble Cassava Starch Granules Results in Enhanced Gelling Properties. *Journal of Applied Glycoscience*, 61(1), 15-20., 20, 15–20.
- Jadhav, N. V., & Vavia, P. R. (2017). Supercritical processed starch nanosponge as a carrier for enhancement of dissolution and pharmacological efficacy of fenofibrate. *International Journal of Biological Macromolecules*.
- Ji, Y. (2021). Synthesis of porous starch microgels for the encapsulation, delivery and stabilization of anthocyanins. *J. Food Eng.* 302 110552.
- Jiang, Y., Li, F., Li, D., Sun-Waterhouse, D., & Huang, Q. (2019). Zein/ pectin nanoparticle-stabilized sesame oil Pickering emulsions: Sustainable bioactive carriers and healthy alternatives to sesame paste. *Food and Bioprocess Technology*, 12(12), 1982–1992
- Jiang, S., Yu, Z., Hu, H., Lv, J., Wang, H., & Jiang, S. (2017). Adsorption of procyanidins onto chitosan-modified porous rice starch. *LWT - Food Science and Technology*.
- Kierulf, A., Azizi, M., Eskandarloo, H., Whaley, J., Liu, W., Perez-herrera, M., You, Z., & Abbaspourrad, A. (2019). Food Hydrocolloids Starch-based Janus particles : Proof-of-concept heterogeneous design via a spin-coating spray approach. *Food Hydrocolloids*, 91(January), 301–310.
- Kierulf, A., Whaley, J., Liu, W., Enayati, M., & Tan, C. (2020). Protein content of amaranth and quinoa starch plays a key role in their ability as Pickering emulsi

ifers. *Food Chemistry*, 315(January), 126246.

Konar, N., Ozarda, O., Senocak, S., Unluturk, N.N., Oba, S. (2019). Effects of Process Conditions on Citrus Beverage Emulsions' Creaming Index: RSM Approach. *ETP Int. J. Food Eng.* 5 22–27.

Korma, S. A., Niazi, S., Ammar, A., Zaaboul, F., & Zhang, T. (2016). *Chemically Modified Starch and Utilization in Food Stuffs.* 5(4), 264–272.

Lacerda, L. D., Leite, D. C., & Nádyá, P. (2019). Relationships between enzymatic hydrolysis conditions and properties of rice porous starches. *Journal of Cereal Science*, 89(July), 102819.

Lacerda, L. D., Leite, D. C., Soares, R. M. D., & Silveira, N. P. (2018). Effects of α - Amylase , Amyloglucosidase , and Their Mixture on Hierarchical Porosity of Rice Starch. *Starch*, 1800008, 1–7.

Laura G. Gomez-Mascaraque, Caroline Casagrande Sipoli, Lucimara Gaziola de La Torre, A. L.-R. (2017). Microencapsulation structures based on protein-coated liposomes obtained through electrospraying for the stabilization and improved bioaccessibility of curcumin. *Food Chemistry*.

Lei, L. U., De-Cheng, W. A. N. G., Jiu-Ran, Z. H. A. O., & Wei-Ping, L. U. (2009). Crystalline structure and pasting properties of starch in eight cultivars of spring- and autumn-sown waxy corn. *Acta Agronomica Sinica*, 35(3), 499-505.

Li, C., Li, Y., Sun, P., & Yang, C. (2013). Pickering emulsions stabilized by native starch granules. *Colloids and Surfaces A: Physicochemical and Engineering Aspects*, 431, 142–149.

Liu, J., Wang, X., Yong, H., Kan, J., & Jin, C. (2018). Recent advances in flavonoid-

- grafted polysaccharides: Synthesis, structural characterization, bioactivities and potential applications. *International Journal of Biological Macromolecules*, 2017.
- Liu, Q., Bao, H., Xi, C., & Miao, H. (2014). Rheological characterization of tuna myofibrillar protein in linear and nonlinear viscoelastic regions. *Journal of Food Engineering*, 121(1), 58–63.
- Lucca Centa Malucelli, Luiz Gustavo Lacerda, Marco Aurelio Silva da Carvalho Filho, Daniel Ernesto Rodriguez Fernandez, Ivo Mottin Demiate, Cristina Soltovski Oliveira, E. S. (2015). Porous waxy maize starch. *J Therm Anal Calorim* (2015), 525–532.
- Majzoobi, M., Hedayati, S., & Farahnaky, A. (2015). Functional properties of microporous wheat starch produced by α -amylase and sonication. *Food Bioscience*.
- Maphosa, Y., & Jideani, V. A. (2018). Factors Affecting the Stability of Emulsions Stabilised by Biopolymers. *Science and Technology Behind Nanoemulsions*.
- Marefati, A., Wiege, B., Haase, N. U., Matos, M., & Rayner, M. (2017). Pickering emulsifiers based on hydrophobically modified small granular starches – Part I: Manufacturing and physico-chemical characterization. *Carbohydrate Polymers*.
- Marku, D., Wahlgren, M., Rayner, M., Sjö, M., & Timgren, A. (2012). Characterization of starch Pickering emulsions for potential applications in topical formulations. *International Journal of Pharmaceutics*, 428(1–2), 1–7.
- Mohammed, A. N., Ishwarya, S. P., & Nisha, P. (2021). Nanoemulsion versus

- microemulsion systems for the encapsulation of beetroot extract: comparison of physicochemical characteristics and betalain stability. *Food and Bioprocess Technology*, 14(1), 133-150
- Nawaz, H., Waheed, R., Nawaz, M., & Shahwar, D. (2020). Physical and Chemical Modifications in Starch Structure and Reactivity. *Chemical Properties of Starch*, 9, 13–35.
- Okonkwo, V. C., Mba, O. I., Kwofie, E. M., & Ngadi, M. O. (2021). Rheological Properties of Meat Sauces as Influenced by Temperature. *Food and Bioprocess Technology*, 14(11), 2146-2160.
- Oliyai, N., Moosavi-nasab, M., & Mohammad, A. (2020). Encapsulation of fucoxanthin in binary matrices of porous starch and halloysite. *Food Hydrocolloids*, 100(May 2019), 105458.
- Patil, V.S., Gutierrez, A.M., Sunkara, M., Morris, A.J., Hilt, J.Z., Kalika, D.S., Dziubla, T.D. (2017). Curcumin Acrylation for Biological and Environmental Applications. *J. Nat. Prod.* 80 (2017) 1964–1971.
- Perez, S., Baldwin, P. M., & Gallant, D. J. (2009). Structural Features of Starch Granules I. In *Starch* (Third Edit). Elsevier Inc.
- Punia, S. (2019). Barley starch modifications: Physical, chemical and enzymatic - A review. *International Journal of Biological Macromolecules*.
- Qi, F., Wu, J., Sun, G., Nan, F., Ngai, T., & Ma, G. (2014). Systematic studies of Pickering emulsions stabilized by uniform-sized PLGA particles : preparation and stabilization mechanism . *Journal of Materials Chemistry B: Materials for Biology and Medicine*, 2, 7605–7611.

- Ramsden, W. (1903). Separation of solids in the surface-layers of solutions and 'suspensions' (observations on surface-membranes, bubbles, emulsions, and mechanical coagulation).—preliminary account. *Proc RSoc London* 72:156–164.
- Rayner, M., Sjöo, M., Timgren, A., Dejmeek, P. (2012). Quinoa starch granules as stabilizing particles for production of Pickering emulsions. *Faraday Discuss.* 158 (2012) 139–155.
- Saffarionpour, S. (2020). Nanocellulose for stabilization of Pickering emulsions and delivery of nutraceuticals and its interfacial adsorption mechanism. *Food and Bioprocess Technology*, 13(8), 1292–1328.
- Saari, H., Wahlgren, M., Rayner, M., Sjöo, M., & Matos, M. (2019). A comparison of emulsion stability for different OSA-modified waxy maize emulsifiers: Granules, dissolved starch, and non-solvent precipitates. *PloS one*, 14(2), e0210690.
- Pickering. (1907). CXCVI.—Emulsions. *J. Chem. Soc., Trans.*, 91(0), 2001–2021.
- Schafer, B., Hecht, M., Harting, J., & Nirschl, H. (2010). Agglomeration and filtration of colloidal suspensions with DVLO interactions in simulation and experiment. *Journal of Colloid and Interface Science*, 349(1), 186–195.
- Steffe, J. F. (1996). Rheological Methods In Food Process Engineering. In *East Lansing, MI 48823 USA: Freeman Press* (Second edi).
- Su, J., Huang, Z., Yuan, X., Wang, X., & Li, M. (2010). Structure and properties of carboxymethyl cellulose / soy protein isolate blend edible films crosslinked by Maillard reactions. *Carbohydrate Polymers*, 79(1), 145–153.
- Sun, H., Zhao, P., & Ge, X. (2010). Recent Advances in Microbial Raw Starch

Degrading Enzymes. *Appl Biochem Biotechnol*, 988–1003.

Tao, H., Wang, P., Wu, F., Jin, Z., & Xu, X. (2016). Particle size distribution of wheat starch granules in relation to baking properties of frozen dough. *Carbohydrate Polymers*, 137, 147–153.

Wang, H., Lv, J., Jiang, S., Niu, B., Pang, M., & Jiang, S. (2016). Preparation and characterization of porous corn starch and its adsorption toward grape seed proanthocyanidins. *Starch/Starke*, 68, 1–10.

Wang, A. J., Paterson, T., Owen, R., Sherborne, C., Dugan, J., Li, J. M., et al. (2016). Photocurable high internal phase emulsions (HIPEs) containing hydroxyapatite for additive manufacture of tissue engineering scaffolds with multi-scale porosity. *Materials Science & Engineering, C: Materials for Biological Applications*, 67, 51–58.

Wei, B., Hu, X., Li, H., Wu, C., Xu, X., Jin, Z., & Tian, Y. (2014). Effect of pHs on dispersity of maize starch nanocrystals in aqueous medium. *Food Hydrocolloids*, 36, 369–373.

Wu, J., Ma, G. (2016). Recent Studies of Pickering Emulsions : Particles Make the Difference. *Small*.

Wu, X., Li, X., Yang, L., Yuan, L., Xu, Z., Xu, J., & Li, D. (2021). Stability Enhanced Pickering Emulsions Based on Gelatin and Dialdehyde Starch Nanoparticles as Simple Strategy for Structuring Liquid Oils. *Food and Bioprocess Technology*, 1-11.

Wu, W., Jiao, A., Xu, E., Chen, Y., & Jin, Z. (2020). Effects of extrusion technology combined with enzymatic hydrolysis on the structural and physicochemical

- properties of porous corn starch. *Food and Bioprocess Technology*, 13(3), 442-451.
- Xu, E., Wu, Z., Long, J., Wang, F., Pan, X., Xu, X., ... & Jiao, A. (2015). Effect of thermostable α -amylase addition on the physicochemical properties, free/bound phenolics and antioxidant capacities of extruded hulled and whole rice. *Food and bioprocess technology*, 8(9), 1958-1973.
- Yu, L., Zhao, A., Yang, M., Wang, C., Wang, M., & Bai, X. (2018). Effects of the combination of freeze-thawing and enzymatic hydrolysis on the microstructure and physicochemical properties of porous corn starch. *Food Hydrocolloids*.
- Zhang, B., Cui, D., Liu, M., Gong, H., Huang, Y., & Han, F. (2012). Corn porous starch: Preparation, characterization and adsorption property. *International Journal of Biological Macromolecules*, 50(1), 250–256.
- Zhang, C., Lim, S., & Chung, H. (2019). Physical modification of potato starch using mild heating and freezing with minor addition of gums. *Food Hydrocolloids*, 94(February), 294–303.
- Zhou, X., Chang, Q., Li, J., Jiang, L., Xing, Y., & Jin, Z. (2021). Preparation of V-type porous starch by amylase hydrolysis of V-type granular starch in aqueous ethanol solution. *International Journal of Biological Macromolecules*, 183, 890–897.
- Zhu, F. (2019). Starch based Pickering emulsions: Fabrication, properties, and applications. *Trends in Food Science and Technology*, 85(November 2018), 129–137.
- Zhu, J., Zhong, L., Chen, W., Song, Y., & Qian, Z. (2018). Preparation and

characterization of pectin/chitosan beads containing porous starch embedded with doxorubicin hydrochloride: A novel and simple colon targeted drug delivery system. *Food Hydrocolloids*.

Zieba, T., Szumny, A., & Kapelko, M. (2011). Properties of retrograded and acetylated starch preparations: Part 1. Structure, susceptibility to amylase, and pasting characteristics. *LWT - Food Science and Technology*, 44(5), 1314–1320.

Chapter 3
Fabrication of Curcumin loaded encapsulates by
porous starch Pickering emulsion

3.1. Introduction

In recent years, Pickering emulsions have attracted a lot of attention because it is nontoxic, biodegradable and biocompatible in nature (Song et al., 2015; Ge et al., 2017; Liu et al., 2018; Zhu et al., 2020). Solid particle stabilized surfactant free emulsion called Pickering emulsion was discovered by Ramsden in 1903 (Ramsden, 1904). However, it was first published in 1907 by Pickering (Pickering, 1907). In Pickering emulsion, the solid particles, called as Pickering particles are adsorbed onto the interface between two phases of the emulsion and provide strong spatial barrier and electrostatic protection, resulting in long term stability (Wang et al., 2020). Pickering emulsions have higher environmental stability because they are stabilized by increasing steric hindrance, which changes the interface properties compared to the conventional emulsions, which are stabilized by reducing interfacial tension between the two interfaces through the adsorption of surfactant molecules (Vignati et al., 2003; Xiao et al., 2016). Many factors such as concentration of particle, particle wettability, particle size and shape, surface charge, pH and ratio of oil to water phase may influence the stability of Pickering emulsion (Duffus et al., 2016; Chevalier et al., 2013). Pickering emulsions have wide range of application in food and pharmaceutical industries. Pickering emulsion-based delivery system (PEDS) is widely used because it exerts enhanced physical and oxidative stability, enhanced protection of labile bioactive and is compatible with food matrix (Mwangi et al., 2020).

Many food grade particles like polysaccharides, lipids and proteins are reported to be used as Pickering particles for stabilizing emulsions (Guida et al., 2021). Polysaccharide such as starch, cellulose and chitosan, in their native form, possess high number of hydroxyl groups resulting in less emulsification ability (Deng et al., 2022). Therefore, these polysaccharides are subjected to physical and chemical modifications to enhance

the ability to act as a Pickering particle (Guida et al., 2021; Zhu, 2019; Deng et al., 2022). Starch is one of the polysaccharides that is frequently utilized since it is biodegradable, non-allergenic, inexpensive, and GRAS, but in its commercial pure form will act as extremely hydrophilic, making it difficult to adsorb into the interface of oil and water, thus act as poor emulsifiers (Zhu, 2019; Aveyard et al., 2003; Kierulf et al., 2020). Porous starch is a modified starch obtained by chemical, physical, and enzymatic treatment which produce abundant pores on the surface that could be extended to center of starch granules (Dura et al., 2014). Enzymatic method is widely used because of high catalytic efficiency, mild reaction condition and substrate specificity. Porous starch prepared enzymatically can function efficiently as Pickering particle for stabilization of emulsions and also for delivery of active ingredients (Sathyan et al., 2022).

Curcumin is a naturally occurring polyphenol compound obtained from the *Curcuma longa* plant which exerts many health benefits such as anticancer, antioxidant, and neuroprotective properties (Meng et al., 2021). However harsh environmental conditions like increased temperature and prolonged exposure to light may lead to degradation of curcumin (Wei et al., 2019). Encapsulation of curcumin using different carriers has been attempted to increase the bioaccessibility and stability of curcumin (Miskeen et al., 2021; Guo et al., 2021). There are reports suggesting that Pickering emulsion can be used as an effective and stable system for the delivery of curcumin. Han et al. (2020) fabricated a Pickering emulsion system stabilized by chitosan/gum arabia (CS/GA) nanoparticles, which showed better protection of bioactive curcumin, better encapsulation efficiency and sustained release of curcumin. Zhu et al. (2021) developed a system for encapsulation of curcumin using carboxymethyl cellulose (CMC), which showed decreased degradation rate. In another study, better storage stability was observed when curcumin was encapsulated in cellulose nanocrystals (Aw et al., 2022). Rice starch nanoparticle

stabilized Pickering emulsion system showed better antioxidant activity and enhanced release of curcumin at higher pH compared to acidic pH (Kamwilaisak et al., 2022). Dong et al. (2022) developed a Pickering emulsion system with better loading capacity, bioaccessibility and improved storage using ovotransferrin (OVT)–carboxymethyl chitosan (CMCS) nanoparticles (OPEOC). Flax seed oil is the rich source of essential fatty acid, alpha-linolenic acid (ALA), which is a biologic precursor to omega 3 fatty acid such as eicosapentanoic acid (EPA). Flax seed oil containing formulations was used in the pharmaceutical industry for treating cardiovascular disease, diabetes, gastrointestinal disorders, hypertension and cancer (Yakdhane, 2021). Studies reported that fabrication of Pickering emulsion using hydrophobic modified starch, V-type starch-lauric acid complexes (SLACs) and flax seed oil resulted in improved thermo-oxidative resistance and delayed oxidation of oil (Feng et al., 2022). Flax seed oil was also used as dispersed phase in fabrication of Pickering emulsion stabilized by resistant starch for the delivery of bioactive ferulic acid (Noor et al., 2022).

Studies reported that solid particles stabilized Pickering emulsion showed greater advantages over surfactants in terms of physical stability against temperature, storage, oxidation and digestion (Dickinson, 2012; Mao et al., 2015). This offers a promising platform to make use of Pickering emulsion as a delivery system. Colon targeted delivery systems is used for the delivery of various drugs and bioactives for maintaining gut health and addressing various intestinal disease conditions. Most of the bioactives cannot be delivered to colon in its pure form because they may undergo degradation while passing through gastrointestinal tract (Wang et al., 2017). Dietary fibers are polymers of carbohydrates that can tolerate the enzyme hydrolysis in small intestine (Jakobek & Matic, 2019). According to European Food safety authority dietary fiber are non-digestible carbohydrate and lignin that includes non-starch polysaccharides, fructo-

oligosaccharides, resistant starch, cellulose and pectin (Hijova et al., 2019; Padayachee et al., 2017). The colonic microbiota partially or entirely ferments dietary fibers resulting in targeted delivery of bioactive. For the delivery of bioactive curcumin, chitosan-TPP (Triphosphate) nanoparticle stabilized Pickering emulsion was formulated and the *in vitro* release studies confirmed the sustained release of curcumin (Shah et al., 2016). Zhang et al. (2022) constructed zein and PGP (peach gum polysaccharide) based nanoparticles as a delivery system of curcumin to colon. The results indicated that emulsion stabilized by zein and PGP resulted in curcumin release rate of 24 % in simulated intestinal condition.

Guar gum was used as a dietary fiber, which is a polygalactomannan, obtained from the endosperm of the bean plant *Cyamopsis tetragonolobus*, and is composed of (1-4)-linked β D-mannopyranosyl chains with one α -D-galactopyranosyl unit joined to every second main chain unit by (1-6) links (Miyazawa et al., 2006; Maier et al., 1993). It is frequently used as a gelling agent, emulsifier, stabilizer, foam stabilizer and thickener in various food industries. As a soluble dietary fibre, it acts as feed for probiotics and beneficial bacteria ferment on these fibers, resulting in production of short chain fatty acids. Guar gum has been effectively used for colon delivery of active ingredients (Garg et al., 2023; Verma et al., 2021; Hu et al., 2022). Krishnaiah et al. (2003) studied the *in vivo* availability of colon-targeted guar gum based tinidazole tablets in healthy human volunteers which suggested that the guar gum protected the drug against gastric digestion and was delivered to the colon. In another study, curcumin liquisolid tablet was developed and coated with eudragit and guar gum, which protects the drug in the upper intestinal tract ensuring colonic delivery of curcumin (Kumar et al., 2018).

From preliminary studies given in Chapter 2 (Sathyan et al., 2022), we identified that the porous starch has the ability to form stable Pickering emulsion by acting as Pickering

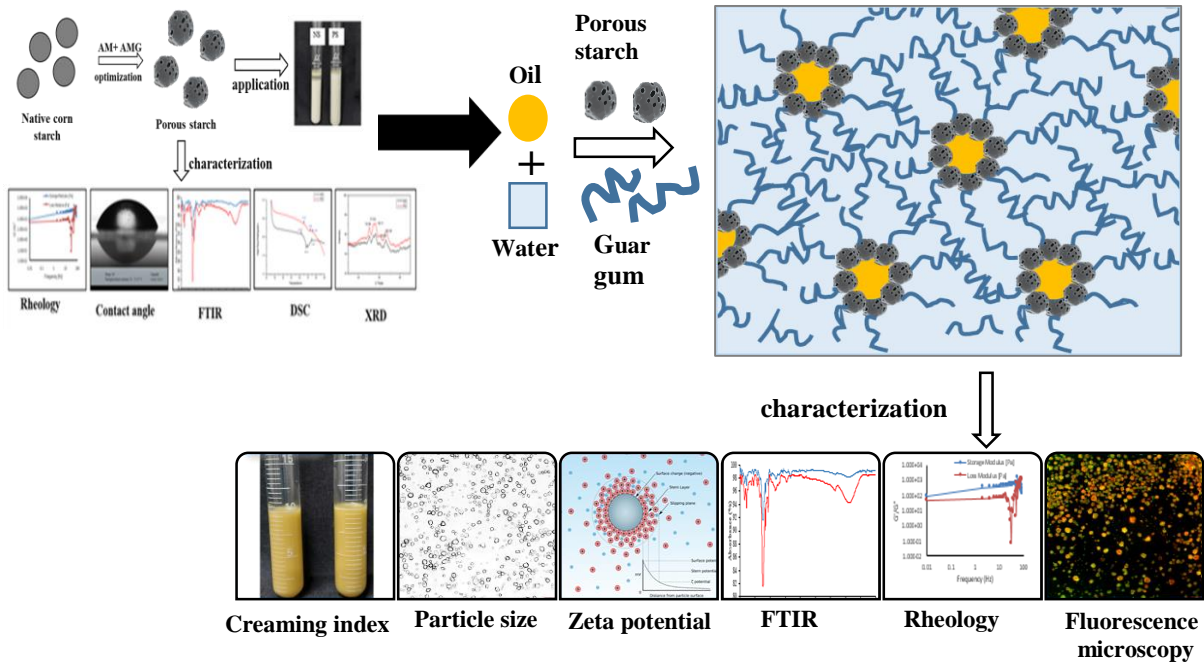
particle and also that the porous starch can adsorb curcumin. With this background, in the present study, we attempted to optimize fabrication of curcumin loaded flax seed oil O/W Pickering emulsion encapsulates stabilized by guar gum and porous starch as Pickering particles. In order to ensure colon delivery porous starch was combined with guar gum, a well-known prebiotic dietary fibre, to form Pickering emulsion by encapsulating bioactive curcumin loaded in flax seed oil. The Pickering emulsion thus fabricated was characterized in terms of encapsulation efficiency, microstructure analysis by fluorescence microscopy, rheology and FTIR. The shelf stability was assessed by storing the samples at refrigeration temperature (4 ± 2 °C).

3.1.1. Objectives

In the last chapter during preliminary studies of emulsion preparation, porous starch-based emulsion shows better stability and better bioactive loading capacity. Based on this, in the present chapter, we discuss the fabrication of curcumin loaded porous starch encapsulates by means of Pickering emulsion formation. For the preparation of Pickering emulsion, initially optimized the concentration of core and wall materials as addressed followed by optimization of homogenization speed and time. Further the characterization and the storage studies were carried out.

3.2. Materials and Methods

The experimental design for the fabrication of curcumin loaded porous starch encapsulates by Pickering emulsion and its characterization studies.



3.2.1. Materials

Starch from corn (CAS:9005-25-8) and curcumin from *Curcuma longa* were purchased from Sigma-Aldrich-USA. Flaxseed oil (FSO) was purchased from the super market in Thiruvananthapuram, Kerala, India. Guar gum was procured from Premia Food Additives, Mumbai, India. All the other reagents used in this study were of analytical grade.

3.2.2 Methods

3.2.2.1. Preparation of Pickering emulsion

O/W Pickering emulsion of curcumin loaded flax seed oil was fabricated using guar gum as stabilizer and porous starch as Pickering particle. Initially curcumin was dissolved in

flax seed oil (4000 ppm) and stirred for 2 h at 60 °C for complete dissolution. Starch was dissolved in distilled water by stirring at 40 °C for 15 min, guar gum was dissolved in boiling water, and were mixed together. To this curcumin loaded flax seed oil was added, homogenized and the emulsion so formed was characterized using various physico-chemical methods. The emulsion was stored to understand the shelf stability for 24 h.

3.2.2.2. Optimization of composition (wall and core) of emulsion.

In order to get a stable Pickering emulsion, the concentration of core and wall materials were optimized first, followed by homogenization speed and time. Pickering emulsions were prepared using porous starch and guar gum as wall material, flax seed oil loaded with curcumin as dispersed phase and water as continuous phase. Based on our earlier study (Sathyan et al., 2022), trials were attempted, varying the parameters as given in Table 3.1. During these trials, percentage of porous starch, guar gum and oil, homogenization speed and homogenization time were varied. Each sample was subjected to 24 h of creaming index analysis at room temperature. The porous starch stabilized Pickering emulsion (PSPE) fabricated using the optimized condition was subjected to storage studies for 15 days at refrigeration temperature (4 ± 2 °C). Further, the emulsion was characterized in terms of encapsulation efficiency, microstructure studies, rheology and FTIR. All the characterization studies performed was compared with that of native starch Pickering emulsion (NSPE), replaced with porous starch.

3.2.2.3. Characterization studies

3.2.2.3.1. Encapsulation efficiency

The encapsulation efficiency was determined using UV spectroscopy based on previously published protocol (Carpenter, 2019). Briefly, 7.4 mL ethanol was added to 0.6 g of emulsion (NSPE and PSPE) and the mixture was vortexed for few minutes,

centrifuged at 10,000 rpm for 10 min and the supernatant containing curcumin was analyzed at 428 nm using UV spectrophotometer (UV 2300 Shimadzu, Japan). The encapsulation efficiency (%) was calculated using the equation, $EE (\%) = Cu_e / Cu_i \times 100$ where, Cu_e is the concentration of curcumin in the stable phase of emulsions and Cu_i is the initial concentration of curcumin added.

3.2.2.3.2. Creaming index

Creaming index evaluate the physical stability of emulsion system. The NSPE and PSPE emulsion were prepared and stored in graduated test tubes at refrigeration temperature (4 ± 2 °C) for storage studies. The stability of emulsion was studied in terms of creaming index which was measured in percentage as ratio of height of serum layer to height of total emulsion. Creaming index (%) = $100 \times H_s / H_T$ where, H_s is the height of serum layer and H_T is the total height (Kwon Hong, 2018).

3.2.2.3.3. Zeta potential

The Zeta potential of NSPE and PSPE was analyzed using the Malvern Zetasizer (Zeta Nano-ZS; Malvern Instruments, UK) by using water (refractive index: 1.33) as the dispersant and employing the dynamic light scattering (DLS) technique.

3.2.2.3.4. Microstructure analysis and particle size

In order to investigate the microstructure of NSPE and PSPE system, fluorescence microscopy (Olympus fluorescence microscope IX83, Olympus corporation of Americas, Center Valley, USA) was performed. Nile red and Saffranin was used to stain oil and starch respectively. The droplet size of NSPE and PSPE system was interpreted from the bright field microscopic images using Image J- win32 software.

3.2.2.3.5. Rheology

The rheological measurements were performed on a rheometer (MCR 102 Rheometer, Anton Paar GmbH, Ostfildern-Scharnhausen, Germany) with plate geometry of 25 mm diameter and 0.105 mm gap (25-mm diameter; 0.105 mm gap). The flow curve, amplitude sweep and frequency sweep of both Native starch Pickering emulsion (NSPE) and Porous starch Pickering emulsion was studied (PSPE). To determine the shear stress, the shear rate was varied from 0.1 to 100s^{-1} . Amplitude sweep to determine the maximum deformation (% strain) attainable by the sample in the linear visco-elastic range (LVE range) was performed at strain of 2 to 100% for NSPE and PSPE, at fixed frequency of 1 Hz. Frequency sweep at constant deformation within the linear visco-elastic region at a frequency of 2 to 100 rad/s to determines the storage and loss modulus.

3.2.2.3.6. ATR-Fourier-transform infrared (FTIR) spectroscopy

The FTIR spectra of curcumin, guar gum, flax seed oil, native starch powder, porous starch powder, NSPE and PSPE was recorded using FTIR-ATR (Attenuated Total Reflection) spectrometer (Perkin Elmer, USA). The data were averaged from 32 scans recorded at 4 cm^{-1} resolutions. Transmittances were recorded at wave numbers between 4000 and 400 cm^{-1} .

3.2.2.4. Storage studies of emulsion

The emulsions (NSPE and PSPE) fabricated using optimized condition were subjected to storage studies for 15 days at refrigeration temperature ($4 \pm 2\text{ }^{\circ}\text{C}$). Samples were withdrawn at 3 days interval, for the evaluation of creaming index, particle size, zeta potential, and microstructural characteristics via fluorescence microscopy.

3.2.2.5. Statistical analysis

Data represented as mean \pm standard deviations of experiments in duplicates except for rheological studies. One-way ANOVA was used for analyzing the results using Graph Pad Prism 9.3.0 software and the significance was accepted at $P \leq 0.05$.

3.3. Results and discussion

3.3.1. Standardization and optimization of core and wall materials and processing conditions of Pickering emulsion.

Emulsions are thermodynamically unstable and the dispersed and continuous phase tend to separate on standing. The interfacial properties of the emulsifier (Pickering particles in this case) play major role in emulsion stability which also depends on the particle size of the emulsion, uniform distribution of emulsifier, droplet size, droplet surface charge, pH, phase separation, interfacial rheology etc (Badruddoza et al., 2023). In case of Pickering emulsions, due to low binding kinetics of particles, equilibration of these particles at the interface often takes a long period of time when no or weak external energy is supplied (Wu et al., 2016). Consequently, in order to drive particulate emulsifiers to the interfaces and produce stable Pickering emulsions, significant external energy is typically needed. Multiple emulsification methods like high-pressure homogenization, rotor-stator homogenization, microfluidic emulsification, ultrasonic emulsification and membrane emulsification are utilized for the production of Pickering emulsion (Pang et al., 2021; Wu et al., 2016; Kaiser et al., 2009). In the present study we have used high speed homogenization for fabrication of stable Pickering emulsion. The emulsification parameters such as the concentration of core and wall materials, homogenization speed and time were varied as given in Table 3.1 and optimized. As discussed earlier our preliminary studies suggested that emulsion with 10% porous starch and 10% oil, homogenized at 12000 rpm for 150 seconds yield a stable emulsion. From

further optimization studies using 1-10% of porous starch, it was understood that 6% of porous starch offers better emulsion stability as compared to 10 % of porous starch. As we are aiming at developing encapsulates for colon delivery, guar gum is incorporated as a wall material in order to ensure safe transit during intestinal digestion. Using, 6% of porous starch, we optimized the composition of guar gum (0.5 - 5%) in the emulsion, that can give a stable emulsion. It was observed that guar gum at 1 % level yielded a stable emulsion up to 24h at room temperature. Therefore, further studies on optimizing the dispersed phase, homogenization time and speed were carried out using emulsion with 6 % porous starch as Pickering particle and 1 % guar gum as emulsion stabilizer.

Curcumin (4000 ppm) loaded flax seed oil was used as the dispersed phase in the O/W emulsion. The dispersed phase composition was varied from 1-10%. The optimization of dispersed phase was carried out on the basis of creaming index analysis. It was found that emulsion with 2% of the flax seed oil demonstrated the highest stability. Further optimization trials were carried out to finalize the optimum homogenization speed (15000- 20000 rpm) and time (15 to 45 min). Finally, homogenization speed of 20000 rpm and time of 45 min were selected according to the stability of emulsion. Further studies were conducted using freshly prepared emulsion with optimized composition and homogenization conditions as given in (Table 3.1).

Table 3.1: Optimized conditions of stable Pickering emulsion

Sl.no.	Parameters	Components	Optimization range	Final optimized conditions
1.	Wall material composition	Starch	1-10 %	6 % (w/v) with respect to final emulsion volume
		Guar gum	0.5-5%	1% (w/v) with respect to final emulsion volume
2.	Dispersed phase	Flax seed oil loaded with 0.4% curcumin	1-10%	2% (v/v) with respect to final emulsion volume
3.	Homogenization speed		12,000 – 20,000 rpm	20,000 rpm
4.	Homogenization time		5- 45 minutes	45 minutes

The particle size of PSPE and NSPE was estimated from the microscopic images using Image J- win32 software and was found to be $6.11 \pm 0.23 \mu\text{m}$ and $8.22 \pm 0.29 \mu\text{m}$ with zeta potential of $-21.55 \pm 0.63 \text{ mV}$ and $-9.30 \pm 0.17 \text{ mV}$, respectively.

3.3.2. Characterization studies

3.3.2.1. Encapsulation efficiency

Encapsulation efficiency is the concentration of the incorporated material, detected in the formulation over the initial concentration used to make the formulation. The encapsulation efficiency of both NSPE and PSPE was analyzed using UV spectrophotometer and compared with that of standard curcumin. The PSPE showed better encapsulation efficiency of curcumin of $83.07 \pm 2.29 \%$ compared with that of NSPE of $63.20 \pm 2.18 \%$. The results showed better encapsulation efficiency compared to other reported studies. Elbially et al. (2022) reported that curcumin-loaded casein nanoparticles coated with alginate and chitosan exhibits an encapsulation efficiency of 70 % . In another study, curcumin/ β -cyclodextrin inclusion complex (CUR/ β -CD IC) nanoparticles, was effectively synthesized which exhibits better stability

and was used to encapsulate curcumin. The complex nanoparticles showed a high encapsulation efficiency of 72 % (Jiang et al., 2022). In the present study, the PSPE system showed excellent encapsulation efficiency may be due to the increased pores of porous starch, which can hold more curcumin compared to that of native starch.

3.3.2.2. Microstructure analysis by fluorescence microscopy

In order to confirm the Pickering nature of porous starch the microstructure analysis of NSPE and PSPE was performed via fluorescence microscopy (Fig 3.1). For better understanding during imaging, the emulsion was stained with Safranin (NSA and PSA) and Nile red (NSB and PSB) for staining starch and oil respectively and the merged images were given in (Fig. 3.1) (NSC and PSC). From PSC, it can be seen that the oil (reddish orange) interface is covered by the porous starch (green color) and thus clearly indicate that the porous starch has the ability to get adsorbed onto the interface between oil and water phase and thus make it an efficient Pickering particle. In addition, the guar gum in the system offer extra stability to the emulsion by increasing the viscosity of the continuous water phase via the formation of gel like structure which resists the free movement of emulsion droplets and immobilize them. Hence the droplet-droplet interaction within the emulsion will be restricted leading to higher stability and reduced destabilization (coalescence) (Sriprablom & Suphantharika, 2022). On a closure look at the NSC, it may be noticed that the polysaccharide boundary is not well defined to hold the oil phase and thus shown lesser ability to stabilize the emulsion because the oil was coming out of core, which is seen as by red colour outside the green core, (indicated by white arrows), leading to faster destabilization. This suggest that the porous starch can hold the dispersed phase more effectively that the native starch thus contributing better encapsulation and stability.

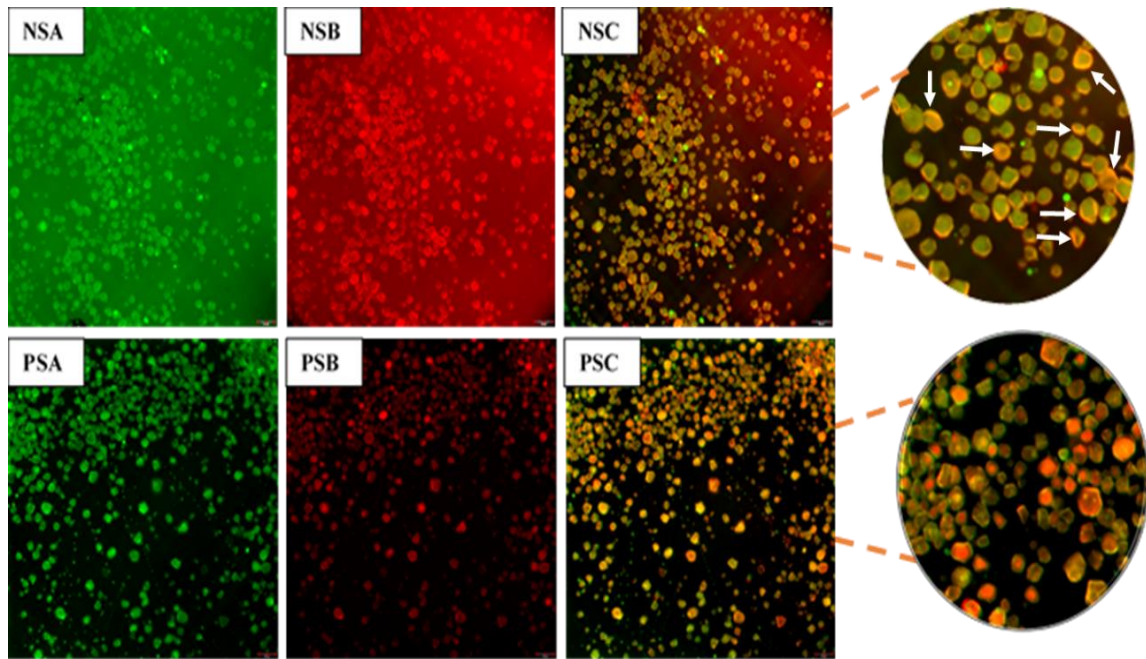


Fig 3.1: Fluorescence image of Native starch (NS) and Porous starch (PS) Pickering emulsion stained with A safranin B Nile red individually and C merged image of A and B.

3.3.2.3. Rheology

Rheology is mainly the study of flow behavior of fluid materials. It basically involves time dependent deformation of bodies caused by applied stresses. In order to understand viscoelastic properties and flow behavior of NSPE and PSPE, rheology was performed. When the elastic behavior of an emulsion is greater than its viscous behavior the emulsion is considered to be relatively stable (Tekin et al., 2020).

Flow curves [shear stress (Pa) versus shear rate (1/s)] of PSPE and NSPE are given in Fig 3.2a. It can be seen that the flow behavior of NSPE and PSPE showed non-Newtonian behavior with shear thinning property. In shear thinning or pseudoplastic flow behavior, the viscosity of fluid reduces as the shear rate increases. From the figure, it is clear that PS stabilized emulsion are offering more resistance to deformation than NS stabilized emulsion. The shear rate vs viscosity plot of emulsion system indicated that PSPE system

showed slightly higher viscosity than NSPE at low shear rate which might further increases stability of emulsion (Fig 3.2 b).

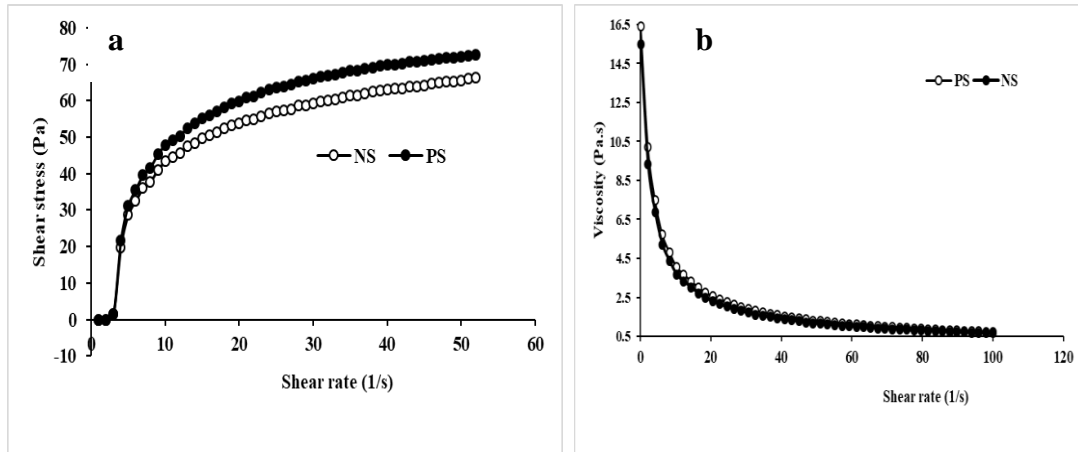


Fig 3.2: (a) Shear stress vs. shear rate plot and (b) shear rate vs. viscosity plot of NSPE and PSPE system. NS- native starch, PS- Porous starch

Dynamic strain sweep detects the LVE (Linear viscoelastic) region of the system where properties of substances do not change depending on the deforming strain, amount of stress, or applied shear rate. LVE region is the range with the lowest strain values where the test can be performed without affecting the sample's structure. In order to calculate the storage modulus (G') and loss modulus (G'') of viscoelastic materials, the LVE region is therefore necessary. At $G' > G''$ elastic fluid properties predominated, while viscous fluid properties were dominant at $G' < G''$. The LVE region of PSPE and NSPE system was found at 4% strain. From the strain sweep analysis, both the emulsion system was observed to have viscoelastic properties in which solid property seems to be higher (Fig.3.3).

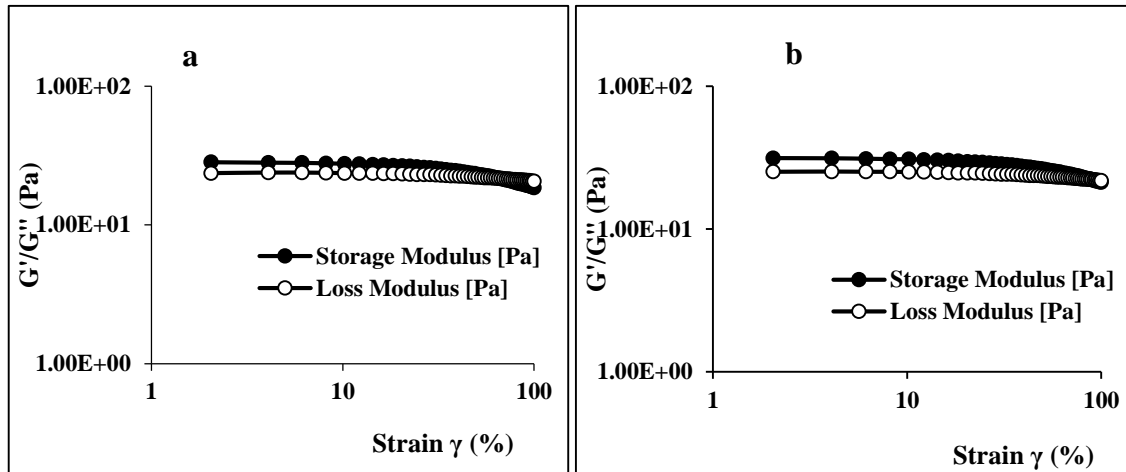


Fig 3.3: Amplitude sweep of (a) NSPE and (b) PSPE system.

Dynamic frequency sweep test was performed to determine the viscoelastic properties of the fluid. The storage modulus G' indicates the elastic property and loss modulus G'' indicates viscous property of the system. The frequency sweep analysis of NSPE (Fig 3.4a) and PSPE (Fig 3.4 b) system shows viscoelastic nature containing both G' and G'' . In NSPE system, $G' > G''$ at lower frequencies but at very high frequency (above 98 rad/s) cross over occurs where, $G'' > G'$ and the properties of fluid changed from viscoelastic to liquid nature. But PSPE system shows a very high storage modulus compared to NSPE, $G' > G''$, thus exhibiting more elastic and solid like property. Studies reported that the emulsion with higher storage modulus can confer better stability to system (Lupi et al., 2011; Khor et al., 2014). Thus PSPE system with better elastic properties, can act as barrier to coalescence and thus confer better stability to system (Wiącek et al., 2002).

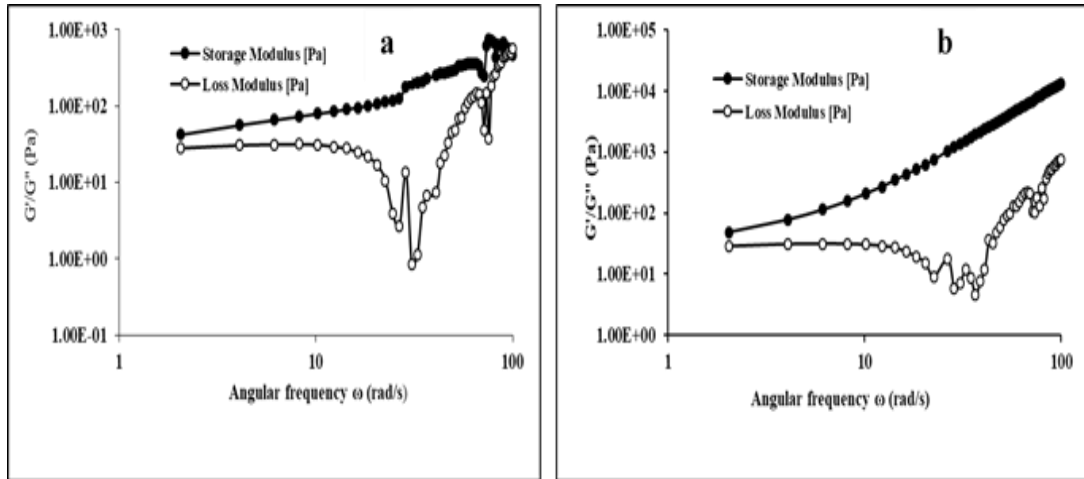


Fig 3.4: Frequency sweep of (a) NSPE and (b) PSPE system

3.3.2.4. FTIR

In order to understand the structural properties and core wall interaction of emulsion FTIR was performed (Fig 3.5). The native starch consists of characteristic absorption peaks in the fingerprint region at 3400 cm^{-1} ($-\text{OH}$ stretching) which indicates the free $\text{O}-\text{H}$ stretching vibration of OH groups in polysaccharide molecule, 1152 cm^{-1} ($\text{C}-\text{C}$, $\text{C}-\text{O}$ stretching), 1080 cm^{-1} ($\text{C}-\text{O}-\text{H}$ bonding), 928 cm^{-1} , skeletal mode vibrations of α -1,4 glycosidic linkage ($\text{C}-\text{O}-\text{C}$), 859 cm^{-1} (C (1)- H , $-\text{CH}_2$ deformation), 764 cm^{-1} ($\text{C}-\text{C}$ stretching) (Wang et al., 2016). PS also shows similar peaks with respect to NS confirming that there is no modification in chemical structure of PS and can be used for further applications. The FTIR spectrum of curcumin showed characteristic absorption peaks at 3516 cm^{-1} ($-\text{OH}$ bonding), 1602 cm^{-1} (due to stretching vibration at aromatic ring $\text{C}=\text{C}$), 1509 cm^{-1} (due to $\text{C}=\text{C}$ vibration), 1275 cm^{-1} (due to $\text{C}-\text{O}$ enol peak), 961 cm^{-1} ($-\text{CH}$) vibration (Abruzzo et al., 2016). The characteristic peaks of curcumin are not visible in both NSPE and PSPE system. This indicates that the bioactive curcumin is well encapsulated in the system.

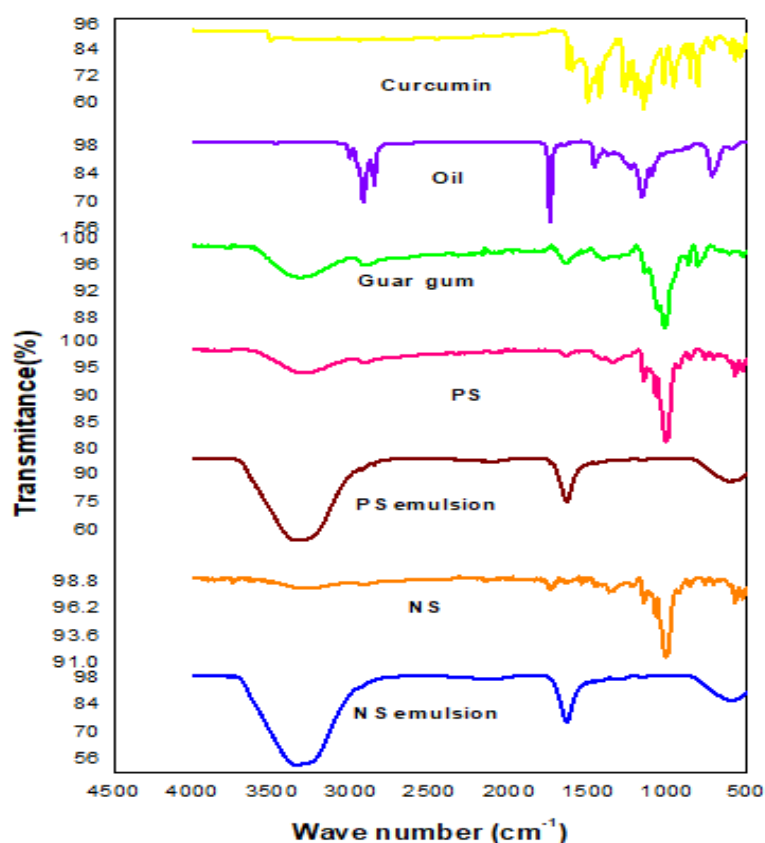


Fig 3.5: FTIR spectrum of NSPE and PSPE system. NS-native starch, PS- porous starch.

3.3.3. Storage studies of emulsion

The NSPE and PSPE system fabricated using optimized conditions was then subjected to storage studies of 15 days at refrigeration temperature (4 ± 2 °C). The samples were withdrawn every 3rd day (0th, 3rd, 6th, 9th, 12th and 15th day) and analyzed for creaming index, particle size, zeta potential, microstructural characteristics via fluorescence microscopy. The results were compared with that of native starch Pickering emulsion fabricated using the same conditions as that of PSPE, replacing porous starch.

3.3.3.1. Creaming index

Creaming index is one of the major parameter to evaluate the emulsion stability. Emulsion instability may be caused by a number of simultaneous or related processes

depending on various conditions. One of the primary ways that an emulsion becomes unstable is by creaming. Creaming is the migration of oil drops due to gravity disrupting the emulsion, which results in the formation of concentrated layer at the top most surface of the sample (Adams et al., 2007). This may further lead to destabilization of emulsion. So creaming index analysis was performed to evaluate the physical stability of emulsion system, which was measured as the percentage of height of the serum layer to the height of the entire emulsion sample. NSPE and PSPE was prepared and kept at refrigeration temperature for 15 days of storage studies. Every 3rd day the sample was analysed for creaming. The PSPE and NSPE, analyzed on 0th day and 15th day was given in (Fig: 3.6). No visible creaming was observed on NSPE and PSPE system at refrigeration temperature even after 15 days of storage.

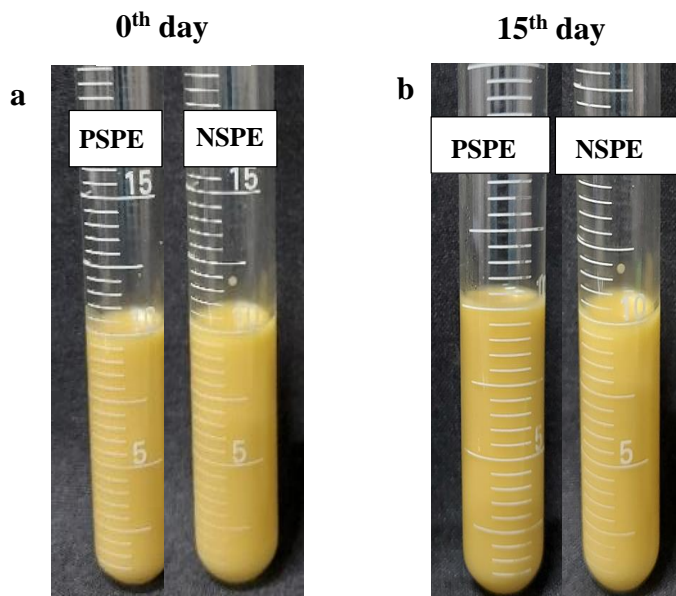


Fig 3.6: Creaming index of NSPE and PSPE system (a) 0th day (b) 15th day

3.3.3.2. Particle size and Zeta potential

The physical stability of emulsions is strongly influenced by particle size; smaller the particles the more stable is the system. A stable emulsion is produced when the particle size is reduced and more particles are spread across the interface uniformly (Tadros,

2004). The particle size of NSPE and PSPE was analyzed from the bright field microscopic images during the storage studies using Image J software. The particle size varied from 8.22 ± 0.29 to 9.29 ± 0.16 μm and 6.11 ± 0.23 to 6.66 ± 0.36 μm for NSPE and PSPE systems respectively during storage (Table 3.2).

As reported in the Chapter 2, that the porous starch exhibited reduced particle size (2.302 ± 0.062 μm) compared to that of native starch (3.549 ± 0.085 μm) (Sathyan et al., 2022). The enzymatic treatment reduces particle size as hydrolysis ruptures the native starch (Yu et al., 2018; Jiang et al., 2017). In the case of emulsion system, PSPE showed decreased droplet size which can be attributed to the lower particle size of porous starch. Compared to PSPE system, NSPE undergoes significant increase in particle size during the storage. The variation in particle size occurs due to many factors such as flocculation, creaming, sedimentation, coalescence and ostwald ripening. These processes are all interlinked to one another and may finally lead to destabilization of emulsion. (Ravera et al., 2021). Compared to NSPE, the PSPE with lower particle size demonstrated no significant variation in particle size during storage. The system becomes more unstable when particle size increases more quickly (Morais et al., 2006; Ursica et al., 2005). Lower particle size is reported to improve the stability of Pickering emulsion against creaming (Saari et al., 2019). Thus, PSPE system with lower particle size conferred better stability compared to that of NSPE system. Moreover, from the fluorescent images it was observed that the PSPE emulsion had well defined droplets with porous starch effectively encapsulated the dispersed phase and shielding the droplets from destabilization.

Zeta potential is the electrokinetic potential which measures the electrostatic attraction or repulsion between particles. The zeta potential values range between +100 mV to -100mV (Shnoudeh et al., 2019). Higher zeta potential values (positive or negative) indicate potential stability of dispersions owing to the electrostatic repulsion of distinct

particles. On the other hand, because of the van der Waals attraction forces acting on the particles, small zeta potential value might cause particle aggregation and flocculation which may lead to physical instability (Freitas et al., 1998; Hunter, 2013; Shah et al., 2014). Accordingly, zeta potential was analyzed and the values ranged from -9.30 ± 0.17 to -5.64 ± 0.23 mV and -21.55 ± 0.63 to -17.33 ± 0.12 mV for NSPE and PSPE, respectively, during storage (Table 3.2). Compared to NSPE, the PSPE system showed significantly higher zeta potential values. During storage studies, there was only slight reduction in the zeta potential of PSPE system compared to NSPE system. Greater zeta potential results in less tendency for particle agglomeration and more particle stability (Dai et al., 2018). PSPE with higher zeta potential during storage days will confer better stability compared to that of NSPE system. For the stabilization, encapsulation and delivery of anthocyanins, porous starch microgel was fabricated which exhibits decreased particle size and higher zeta potential compared to oxidized starch. The enzymatic hydrolysis cleaves the starch which resulted in decreased particle size and increased zeta potential due to exposed COO^- groups due to same (Ji, 2021; Jiang et al., 2017). Thus, porous starch with higher zeta potential, lower particles size and porous nature is proposed to hold the dispersed oil droplets in stable encapsulates protecting it from creaming and yielding a shelf stable emulsion compared to native starch.

Table 3.2: Particle size of NSPE and PSPE system during storage days.

Days	Particle size (μm)		Zeta potential (mV)	
	Native starch Pickering emulsion	Porous starch Pickering emulsion	Native starch emulsion	Porous starch emulsion
0 th	8.22 \pm 0.29 ^a	6.11 \pm 0.23 ^b	-9.30 \pm 0.17 ^a	-21.55 \pm 0.63 ^b
3 rd	8.66 \pm 0.33 ^a	6.14 \pm 0.08 ^b	-8.32 \pm 0.32 ^a	-19.53 \pm 0.26 ^b
6 th	7.44 \pm 0.04 ^a	5.32 \pm 0.27 ^b	-8.10 \pm 0.07 ^a	-19.26 \pm 0.12 ^b
9 th	8.17 \pm 0.23 ^a	6.39 \pm 0.07 ^b	-5.43 \pm 0.23 ^a	-18.46 \pm 0.28 ^b
12 th	8.88 \pm 0.11 ^a	6.40 \pm 0.06 ^b	-7.75 \pm 0.29 ^a	-17.73 \pm 0.04 ^b
15 th	9.29 \pm 0.16 ^a	6.66 \pm 0.36 ^b	-5.64 \pm 0.23 ^a	-17.33 \pm 0.12 ^b

Each value represents mean \pm SD from duplicate measurements $p \leq 0.05$ is considered significantly different.

^{a,b} Values with different alphabets in same row are significantly different for each parameter studied.

3.3.6.3. Microstructure analysis

In order to understand the structural changes during the storage studies, the NSPE and PSPE systems were analyzed by light microscopy and by fluorescence microscopy (using dye safranin). In NSPE system (Fig 3.7) it is clear that compared to 3rd day the particles agglomerate at 15th day of storage. An increase in particle size during storage can be observed in the case of NSPE, which was in accordance with particle size. But in the case of PSPE system, the droplets are found to be more uniformly distributed with lower particle agglomeration indicating better stability during the storage.

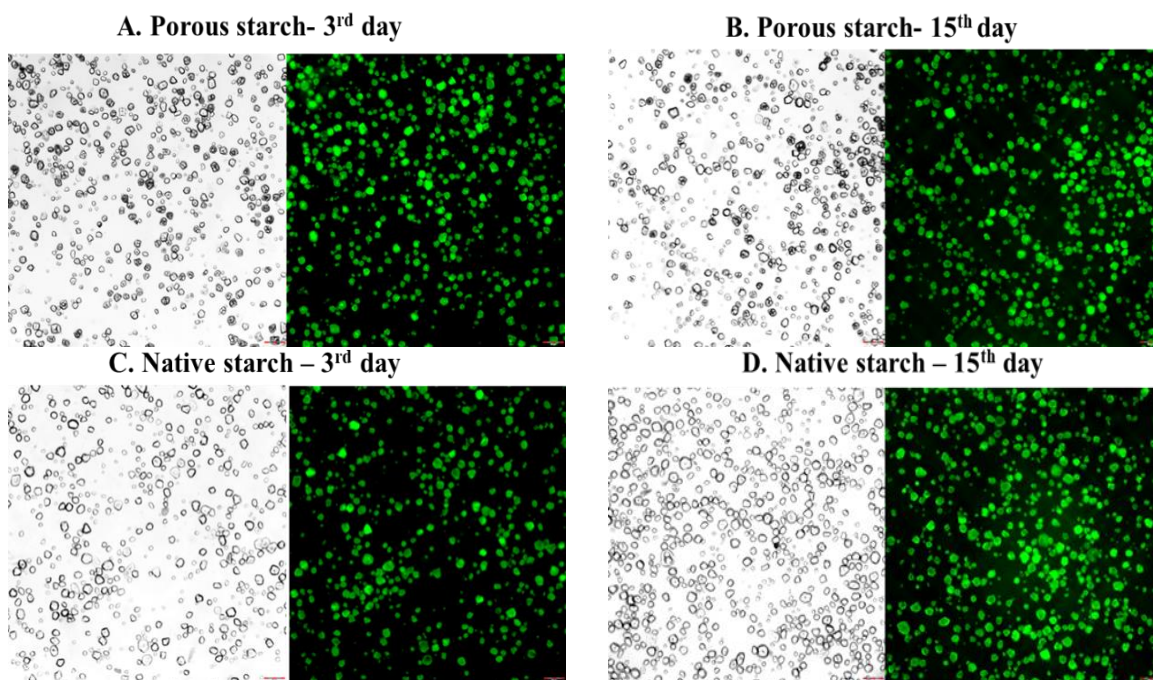


Fig 3.7: Light and fluorescence microscopic images of PSPE system on 3rd and 15th day (A and B) and NSPE system on 3rd and 15th day (C and D) respectively.

Based on the above discussions, the mechanism of stabilization of Pickering emulsion is represented in Fig 3.8. Porous starch act as Pickering particles and the dispersed phase, indicated by yellow colour loaded with curcumin, is effectively held in the stable encapsulates in the emulsion. In Pickering emulsion porous starch adsorbed into the interface of oil and water resulting in stabilized Pickering emulsion. Guar gum in the system offer extra stability to the emulsion by increasing the viscosity of the continuous water phase via the formation of gel like structure which resists the free movement of emulsion droplets and immobilize them. The droplet-droplet interaction within the emulsion will be restricted leading to higher stability and reduced destabilization

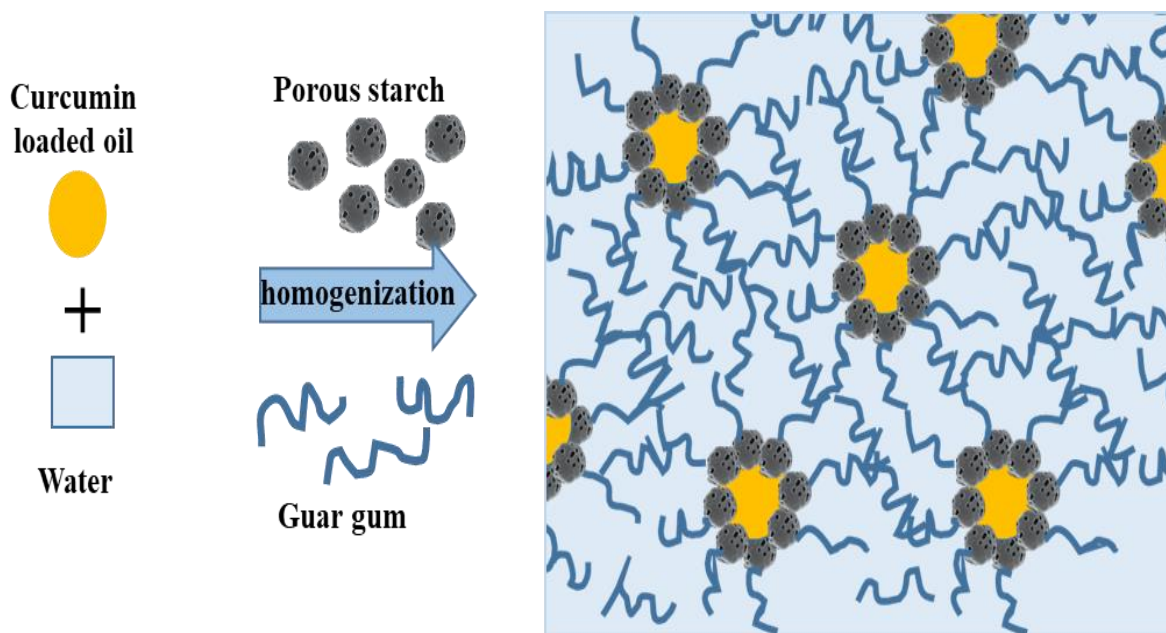


Fig 3.8: Mechanism of solid particle stabilized Pickering emulsion system

3.4. Conclusion

O/W Pickering emulsion of curcumin loaded flax seed oil with porous starch as Pickering particle and guar gum as stabilizer was fabricated. A stable emulsion was obtained with a composition of Starch 6 %, Guar gum 1 %, oil 2 % (80 ppm curcumin based on emulsion). Both native starch Pickering emulsion (NSPE) and porous starch Pickering emulsion (PSPE) system demonstrated good physical stability with zero percentage creaming index during the storage at refrigeration temperature ($4 \pm 2^\circ\text{C}$) for 15 days. Microstructure data confirmed that porous starch can act as efficient Pickering particle compared to native starch with complete encapsulation of oil phase during storage and better encapsulation efficiency in terms of curcumin retention. PSPE systems exhibited better stability in terms of droplet size and zeta potential. Both NSPE and PSPE system displayed Non-Newtonian nature and viscoelastic property with PSPE system showed prominent elastic nature. FTIR analysis indicated no chemical interaction other than hydrogen bonding happening in the emulsion system. PS emulsion showed higher

encapsulation efficiency of 83.07 ± 2.29 % compared with that of native starch of 63.20 ± 2.18 %. The developed PS system with guar gum can be used for colon target delivery and further studies to evaluate its potential as prebiotic and gastrointestinal stability is discussed in Chapter 4.

3.5. References

- Abruzzo, A., Zuccheri, G., Belluti, F., Provenzano, S., Verardi, L., Bigucci, F., ... & Calonghi, N. (2016). Chitosan nanoparticles for lipophilic anticancer drug delivery: Development, characterization and in vitro studies on HT29 cancer cells. *Colloids and Surfaces B: Biointerfaces*, *145*, 362-372.
- Adams, F., Kabalnov, A. S., Petsev, D. N., Obey, T., Vincent, B., Kunieda, H., ... & Weers, J. G. (2007). *Modern aspects of emulsion science*. Royal Society of Chemistry.
- Aveyard, R., Binks, B. P., & Clint, J. H. (2003). Emulsions stabilised solely by colloidal particles. *Advances in Colloid and Interface Science*, *100*, 503-546.
- Aw, Y. Z., Lim, H. P., Low, L. E., Singh, C. K. S., Chan, E. S., & Tey, B. T. (2022). Cellulose nanocrystal (CNC)-stabilized Pickering emulsion for improved curcumin storage stability. *LWT*, *159*, 113249.
- Badruddoza, A. Z. M., Yeoh, T., Shah, J. C., & Walsh, T. (2023). Assessing and Predicting Physical Stability of Emulsion-Based Topical Semisolid Products: A Review. *Journal of Pharmaceutical Sciences*.
- Carpenter, J., George, S., & Saharan, V. K. (2019). Curcumin encapsulation in multilayer oil-in-water emulsion: synthesis using ultrasonication and studies on stability and antioxidant and release activities. *Langmuir*, *35*(33), 10866-10876.
- Chevalier, Y., & Bolzinger, M. A. (2013). Emulsions stabilized with solid nanoparticles: Pickering emulsions. *Colloids and Surfaces A: Physicochemical and Engineering Aspects*, *439*, 23-34.

- Deng, W., Li, Y., Wu, L., & Chen, S. (2022). Pickering emulsions stabilized by polysaccharides particles and their applications: a review. *Food Science and Technology*, 42.
- Dickinson, E. (2012). Use of nanoparticles and microparticles in the formation and stabilization of food emulsions. *Trends in Food Science & Technology*, 24(1), 4-12.
- Dong, Y., Wei, Z., Wang, Y., Tang, Q., Xue, C., & Huang, Q. (2022). Oleogel-based Pickering emulsions stabilized by ovotransferrin–carboxymethyl chitosan nanoparticles for delivery of curcumin. *Lwt*, 157, 113121.
- Duffus, L. J., Norton, J. E., Smith, P., Norton, I. T., & Spyropoulos, F. (2016). A comparative study on the capacity of a range of food-grade particles to form stable O/W and W/O Pickering emulsions. *Journal of colloid and interface science*, 473, 9-21.
- Dura, A., Błaszczak, W., & Rosell, C. M. (2014). Functionality of porous starch obtained by amylase or amyloglucosidase treatments. *Carbohydrate polymers*, 101, 837-845.
- Elbially, N. S., & Mohamed, N. (2022). Fabrication of the quaternary nanocomplex curcumin-casein-alginate-chitosan as a potential oral delivery system for cancer nutraceutical therapy. *Journal of Drug Delivery Science and Technology*, 70, 103226.
- Feng, Y., Zhang, B., Fu, X., & Huang, Q. (2022). Starch-lauric acid complex-stabilised Pickering emulsion gels enhance the thermo-oxidative resistance of flaxseed oil. *Carbohydrate polymers*, 292, 119715.

- Freitas, C., & Müller, R. H. (1998). Effect of light and temperature on zeta potential and physical stability in solid lipid nanoparticle (SLN™) dispersions. *International journal of pharmaceutics*, 168(2), 221-229.
- Garg, S. S., & Gupta, J. (2023). Guar gum-based nanoformulations: Implications for improving drug delivery. *International Journal of Biological Macromolecules*.
- Ge, S., Xiong, L., Li, M., Liu, J., Yang, J., Chang, R., ... & Sun, Q. (2017). Characterizations of Pickering emulsions stabilized by starch nanoparticles: Influence of starch variety and particle size. *Food chemistry*, 234, 339-347.
- Guida, C., Aguiar, A. C., & Cunha, R. L. (2021). Green techniques for starch modification to stabilize Pickering emulsions: A current review and future perspectives. *Current Opinion in Food Science*, 38, 52-61.
- Guo, Q., Su, J., Shu, X., Yuan, F., Mao, L., Liu, J., & Gao, Y. (2021). Fabrication, structural characterization and functional attributes of polysaccharide-surfactant-protein ternary complexes for delivery of curcumin. *Food Chemistry*, 337, 128019.
- Han, J., Chen, F., Gao, C., Zhang, Y., & Tang, X. (2020). Environmental stability and curcumin release properties of Pickering emulsion stabilized by chitosan/gum Arabic nanoparticles. *International Journal of Biological Macromolecules*, 157, 202-211.
- Hijova E., Bertkova, I., & Stofilova, J. (2019). Dietary fibre as prebiotics in nutrition. *Central European journal of public health*, 27(3), 251-255.
- Hong, I. K., Kim, S. I., & Lee, S. B. (2018). Effects of HLB value on oil-in-water emulsions: Droplet size, rheological behavior, zeta-potential, and creaming index. *Journal of industrial and engineering chemistry*, 67, 123-131.

- Hu, Y., Zhang, S., Wen, Z., Fu, H., Hu, J., Ye, X., ... & Yang, X. (2022). Oral delivery of curcumin via multi-bioresponsive polyvinyl alcohol and guar gum based double-membrane microgels for ulcerative colitis therapy. *International Journal of Biological Macromolecules*, 221, 806-820.
- Hunter, R. J. (2013). *Zeta potential in colloid science: principles and applications* (Vol. 2). Academic press.
- Jakobek, L., & Matic, P. (2019). Non-covalent dietary fiber-polyphenol interactions and their influence on polyphenol bioaccessibility. *Trends in Food Science & Technology*, 83, 235-247.
- Ji, Y. (2021). Synthesis of porous starch microgels for the encapsulation, delivery and stabilization of anthocyanins. *Journal of Food Engineering*, 302, 110552.
- Jiang, S., Yu, Z., Hu, H., Lv, J., Wang, H., & Jiang, S. (2017). Adsorption of procyanidins onto chitosan-modified porous rice starch. *Lwt*, 84, 10-17.
- Jiang, L., Xia, N., Wang, F., Xie, C., Ye, R., Tang, H., ... & Liu, Y. (2022). Preparation and characterization of curcumin/ β -cyclodextrin nanoparticles by nanoprecipitation to improve the stability and bioavailability of curcumin. *LWT*, 171, 114149.
- Kaiser, A., Liu, T., Richtering, W., & Schmidt, A. M. (2009). Magnetic capsules and Pickering emulsions stabilized by core-shell particles. *Langmuir*, 25(13), 7335-7341.
- Kamwilaisak, K., Rittiwut, K., Jutakrudsada, P., Iamamorphanth, W., Pimsawat, N., Knijnenburg, J. T., & Theerakulpisut, S. (2022). Rheology, stability, antioxidant properties, and curcumin release of oil-in-water Pickering emulsions stabilized

- by rice starch nanoparticles. *International Journal of Biological Macromolecules*, 214, 370-380.
- Khor, Y. P., Koh, S. P., Long, K., Long, S., Ahmad, S. Z. S., & Tan, C. P. (2014). A comparative study of the physicochemical properties of a virgin coconut oil emulsion and commercial food supplement emulsions. *Molecules*, 19(7), 9187-9202.
- Kierulf, A., Whaley, J., Liu, W., Enayati, M., Tan, C., Perez-Herrera, M., ... & Abbaspourrad, A. (2020). Protein content of amaranth and quinoa starch plays a key role in their ability as Pickering emulsifiers. *Food Chemistry*, 315, 126246.
- Krishnaiah, Y. S. R., Muzib, Y. I., Bhaskar, P., Satyanarayana, V., & Latha, K. (2003). Pharmacokinetic evaluation of guar gum-based colon-targeted drug delivery systems of tinidazole in healthy human volunteers. *Drug delivery*, 10(4), 263-268.
- Kumar, V. S., Rijo, J., & Sabitha, M. (2018). Guargum and Eudragit® coated curcumin liquid solid tablets for colon specific drug delivery. *International journal of biological macromolecules*, 110, 318-327.
- Liu, F., Zheng, J., Huang, C. H., Tang, C. H., & Ou, S. Y. (2018). Pickering high internal phase emulsions stabilized by protein-covered cellulose nanocrystals. *Food Hydrocolloids*, 82, 96-105.
- Lupi, F. R., Gabriele, D., De Cindio, B., Sánchez, M. C., & Gallegos, C. (2011). A rheological analysis of structured water-in-olive oil emulsions. *Journal of Food Engineering*, 107(3-4), 296-303.

- Maier, H., Anderson, M., Karl, C., Magnuson, K., & Whistler, R. L. (1993). Guar, locust bean, tara, and fenugreek gums. In *industrial gums* (pp. 181-226). Academic press.
- Mao, L., & Miao, S. (2015). Structuring food emulsions to improve nutrient delivery during digestion. *Food Engineering Reviews*, 7, 439-451.
- Meng, R., Wu, Z., Xie, Q. T., Cheng, J. S., & Zhang, B. (2021). Preparation and characterization of zein/carboxymethyl dextrin nanoparticles to encapsulate curcumin: Physicochemical stability, antioxidant activity and controlled release properties. *Food Chemistry*, 340, 127893.
- Miskeen, S., An, Y. S., & Kim, J. Y. (2021). Application of starch nanoparticles as host materials for encapsulation of curcumin: Effect of citric acid modification. *International Journal of Biological Macromolecules*, 183, 1-11.
- Miyazawa, T., & Funazukuri, T. (2006). Noncatalytic hydrolysis of guar gum under hydrothermal conditions. *Carbohydrate research*, 341(7), 870-877.
- Morais, J. M., Dos Santos, O. D. H., Delicato, T., & da Rocha-Filho, P. A. (2006). Characterization and evaluation of electrolyte influence on canola oil/water nano-emulsion. *Journal of dispersion science and technology*, 27(7), 1009-1014.
- Mwangi, W. W., Lim, H. P., Low, L. E., Tey, B. T., & Chan, E. S. (2020). Food-grade Pickering emulsions for encapsulation and delivery of bioactives. *Trends in Food Science & Technology*, 100, 320-332.
- Noor, N., Gani, A., Jhan, F., Shah, M. A., & ul Ashraf, Z. (2022). Ferulic acid loaded Pickering emulsions stabilized by resistant starch nanoparticles using

- ultrasonication: Characterization, in vitro release and nutraceutical potential. *Ultrasonics Sonochemistry*, 84, 105967.
- Padayachee, A., Day, L., Howell, K., & Gidley, M. J. (2017). Complexity and health functionality of plant cell wall fibers from fruits and vegetables. *Critical reviews in food science and nutrition*, 57(1), 59-81.
- Pang, B., Liu, H., & Zhang, K. (2021). Recent progress on Pickering emulsions stabilized by polysaccharides-based micro/nanoparticles. *Advances in Colloid and Interface Science*, 296, 102522.
- Pickering, CXCVI, Umfreville CXCVI, Emulsions, J. Chem. Soc. Trans. 91 (1907) 2001–2021, <https://doi.org/10.1039/ct9079102001>.
- Ramsden, W. (1904). Separation of solids in the surface-layers of solutions and ‘suspensions’(observations on surface-membranes, bubbles, emulsions, and mechanical coagulation).—Preliminary account. *Proceedings of the royal Society of London*, 72(477-486), 156-164.
- Ravera, F., Dziza, K., Santini, E., Cristofolini, L., & Liggieri, L. (2021). Emulsification and emulsion stability: The role of the interfacial properties. *Advances in Colloid and Interface Science*, 288, 102344.
- Saari, H., Rayner, M., & Wahlgren, M. (2019). Effects of starch granules differing in size and morphology from different botanical sources and their mixtures on the characteristics of Pickering emulsions. *Food Hydrocolloids*, 89, 844-855.
- Sathyan, S., & Nisha, P. (2022). Optimization and Characterization of Porous Starch from Corn Starch and Application Studies in Emulsion Stabilization. *Food and Bioprocess Technology*, 15(9), 2084-2099.

- Shah, R., Eldridge, D., Palombo, E., & Harding, I. (2014). Optimisation and stability assessment of solid lipid nanoparticles using particle size and zeta potential. *Journal of physical science*, 25(1).
- Shah, B. R., Li, Y., Jin, W., An, Y., He, L., Li, Z., ... & Li, B. (2016). Preparation and optimization of Pickering emulsion stabilized by chitosan-tripolyphosphate nanoparticles for curcumin encapsulation. *Food Hydrocolloids*, 52, 369-377.
- Shnoudeh, A. J., Hamad, I., Abdo, R. W., Qadumii, L., Jaber, A. Y., Surchi, H. S., & Alkelany, S. Z. (2019). Synthesis, characterization, and applications of metal nanoparticles. In *Biomaterials and bionanotechnology* (pp. 527-612). Academic Press.
- Song, X., Pei, Y., Qiao, M., Ma, F., Ren, H., & Zhao, Q. (2015). Preparation and characterizations of Pickering emulsions stabilized by hydrophobic starch particles. *Food Hydrocolloids*, 45, 256-263.
- Sriprablom, J., & Suphantharika, M. (2022). Influence of xanthan gum on properties and stability of oil-in-water Pickering emulsions stabilized by zein colloidal particles. *Journal of Food Measurement and Characterization*, 16(4), 2772-2781.
- Tadros, T. (2004). Application of rheology for assessment and prediction of the long-term physical stability of emulsions. *Advances in colloid and interface science*, 108, 227-258.
- Tekin, Z. H., Avci, E., Karasu, S., & Toker, O. S. (2020). Rapid determination of emulsion stability by rheology-based thermal loop test. *LWT*, 122, 109037.

- Ursica, L., Tita, D., Palici, I., Tita, B., & Vlaia, V. (2005). Particle size analysis of some water/oil/water multiple emulsions. *Journal of pharmaceutical and biomedical analysis*, 37(5), 931-936.
- Verma, D., & Sharma, S. K. (2021). Recent advances in guar gum based drug delivery systems and their administrative routes. *International Journal of Biological Macromolecules*, 181, 653-671.
- Vignati, E., Piazza, R., & Lockhart, T. P. (2003). Pickering emulsions: interfacial tension, colloidal layer morphology, and trapped-particle motion. *Langmuir*, 19(17), 6650-6656.
- Wang, H., Lv, J., Jiang, S., Niu, B., Pang, M., & Jiang, S. (2016). Preparation and characterization of porous corn starch and its adsorption toward grape seed proanthocyanidins. *Starch/Starke*, 68, 1–10.
- Wang, Y., Li, J., & Li, B. (2017). Chitin microspheres: A fascinating material with high loading capacity of anthocyanins for colon specific delivery. *Food Hydrocolloids*, 63, 293-300.
- Wang, H., Bai, Y., & Shao, D. (2020). Study on Pickering emulsions stabilized by tea polyphenols/gelatin/chitosan nanoparticles. In *Journal of Physics: Conference Series* (Vol. 1637, No. 1, p. 012106). IOP Publishing.
- Wei, Z., Cheng, Y., Zhu, J., & Huang, Q. (2019). Genipin-crosslinked ovotransferrin particle-stabilized Pickering emulsions as delivery vehicles for hesperidin. *Food Hydrocolloids*, 94, 561-573.
- Wiącek, A. E., Chibowski, E., & Wilk, K. (2002). Studies of oil-in-water emulsion stability in the presence of new dicephalic saccharide-derived surfactants. *Colloids and Surfaces B: Biointerfaces*, 25(3), 243-256.

- Wu, J., & Ma, G. H. (2016). Recent studies of Pickering emulsions: particles make the difference. *Small*, 12(34), 4633-4648.
- Xiao, J., Gonzalez, A. J. P., & Huang, Q. (2016). Kafirin nanoparticles-stabilized Pickering emulsions: Microstructure and rheological behavior. *Food Hydrocolloids*, 54, 30-39.
- Yakdhane, A., Labidi, S., Chaabane, D., Tolnay, A., Nath, A., Koris, A., & Vatai, G. (2021). Microencapsulation of flaxseed oil—State of art. *Processes*, 9(2), 295.
- Yu, L., Zhao, A., Yang, M., Wang, C., Wang, M., & Bai, X. (2018). Effects of the combination of freeze-thawing and enzymatic hydrolysis on the microstructure and physicochemical properties of porous corn starch. *Food Hydrocolloids*.
- Zhang, R., Li, L., Ma, C., Ettoumi, F. E., Javed, M., Lin, X., ... & Luo, Z. (2022). Shape-controlled fabrication of zein and peach gum polysaccharide based complex nanoparticles by anti-solvent precipitation for curcumin-loaded Pickering emulsion stabilization. *Sustainable Chemistry and Pharmacy*, 25, 100565.
- Zhao, A. Q., Yu, L., Yang, M., Wang, C. J., Wang, M. M., & Bai, X. (2018). Effects of the combination of freeze-thawing and enzymatic hydrolysis on the microstructure and physicochemical properties of porous corn starch. *Food Hydrocolloids*, 83, 465-472.
- Zhu, F. (2019). Starch based Pickering emulsions: Fabrication, properties, and applications. *Trends in Food Science & Technology*, 85, 129-137.
- Zhu, Y., Huan, S., Bai, L., Ketola, A., Shi, X., Zhang, X., ... & Rojas, O. J. (2020). High internal phase oil-in-water pickering emulsions stabilized by chitin nanofibrils: 3D structuring and solid foam. *ACS applied materials & interfaces*, 12(9), 11240-11251.

Zhu, X., Chen, J., Hu, Y., Zhang, N., Fu, Y., & Chen, X. (2021). Tuning complexation of carboxymethyl cellulose/cationic chitosan to stabilize Pickering emulsion for curcumin encapsulation. *Food Hydrocolloids*, *110*, 106135.

Chapter 4
***In vitro* release kinetics and prebiotic efficacy of
Curcumin Pickering emulsion**

4.1. Introduction

Human intestinal tract is colonized by diverse collection of microorganisms, named as gut microbiota which consists of viruses, fungi and bacteria, which interact symbiotically with the host (Hooper et al., 2012). Gastrointestinal (GI) tract constitutes around 100 trillion bacteria which includes around thousand species (Qin et al., 2010; Floch, 2011). Three major phyla namely Firmicutes (30–50%), Bacteroidetes (20–40%) and Actinobacteria (1–10%) dominates gut microbiota (Gagniere et al., 2016). Mostly, the gut microbes interact with host by producing metabolites, predominantly the short chain fatty acids (Natarajan et al., 2014). Short chain fatty acids are produced from the anaerobic fermentation of non-digestible polysaccharides known as dietary fibres. Acetate (C₂), propionate (C₃), and butyrate (C₄) are the three primary short-chain fatty acids (SCFAs) that the gut bacteria produce in a ratio of 60:20:20, respectively (Maslowski et al., 2009; Tan et al., 2014; Thorburn et al., 2014). Dietary fibre consists of plant cell wall constituents such as hemicellulose, cellulose, structural and non-structural compounds like inulin, resistant starch (RS), chitin, β -glucan, pectin and oligosaccharides (Jha et al., 2019). Based on solubility, dietary fibre are classified into soluble (gum, pectin, inulin) and insoluble fibers (cellulose, hemicellulose) (Mudgil et al., 2013). Dietary fibre exerts many health benefits such as prevents gastrointestinal diseases, balance intestinal pH, reduces inflammation, stimulate short chain fatty acid production, add bulk to diet and protects against colon cancer. Insoluble dietary fiber passed undigested through small intestine, but absorb water and add bulk to stool. The beneficial bacteria ferment on these dietary fiber, resulting in the production of short chain fatty acids (Holscher, 2017)

Short chain fatty acids (SCFA) comprise of one to six carbons and intestinal microbiota produces different SCFAs such as valerate, caproate, succinate, lactate, formate,

hexanoate, propionate, acetate, butyrate and isobutyrate (Adom et al., 2013; Liu et al., 2021). The intestinal concentration of SCFA can reach as high as 100 mM (Maslowski et al., 2009; Tan et al., 2014; Thorburn et al., 2014; Bugaut, 1987). These SCFA helps in the regulation of cell differentiation, proliferation and apoptosis, increases mucosal blood supply and stimulate water absorption. Among the SCFA, butyrate act as key energy source of colon cells, regulates pH of lumen of colon, reduced inflammatory cytokines and also promotes apoptosis (McNabney et al., 2017)

Curcumin, also known as diferuloylmethane is the main polyphenolic bioactive present in turmeric (Stohs et al., 2020). Curcumin can regulate the intestinal microflora and also influences microbial composition and diversity. Studies reported that curcumin supplementation significantly altered the ratio of beneficial and pathogenic intestinal microflora- decreasing the bacterial load of Enterococci, Prevotellaceae, Coriobacterales and Enterobacteria and raising the quantity of Bifidobacterium and Lactobacilli (Shen et al., 2016; Shen et al., 2017). After curcumin supplementation in mice with colon cancer and colitis, decreased Coriobacterales and increased Lactobacillales were observed (McFadden et al., 2015). Studies also reported that curcumin can reduce the gut microbial dysbiosis (Vamanu et al., 2019).

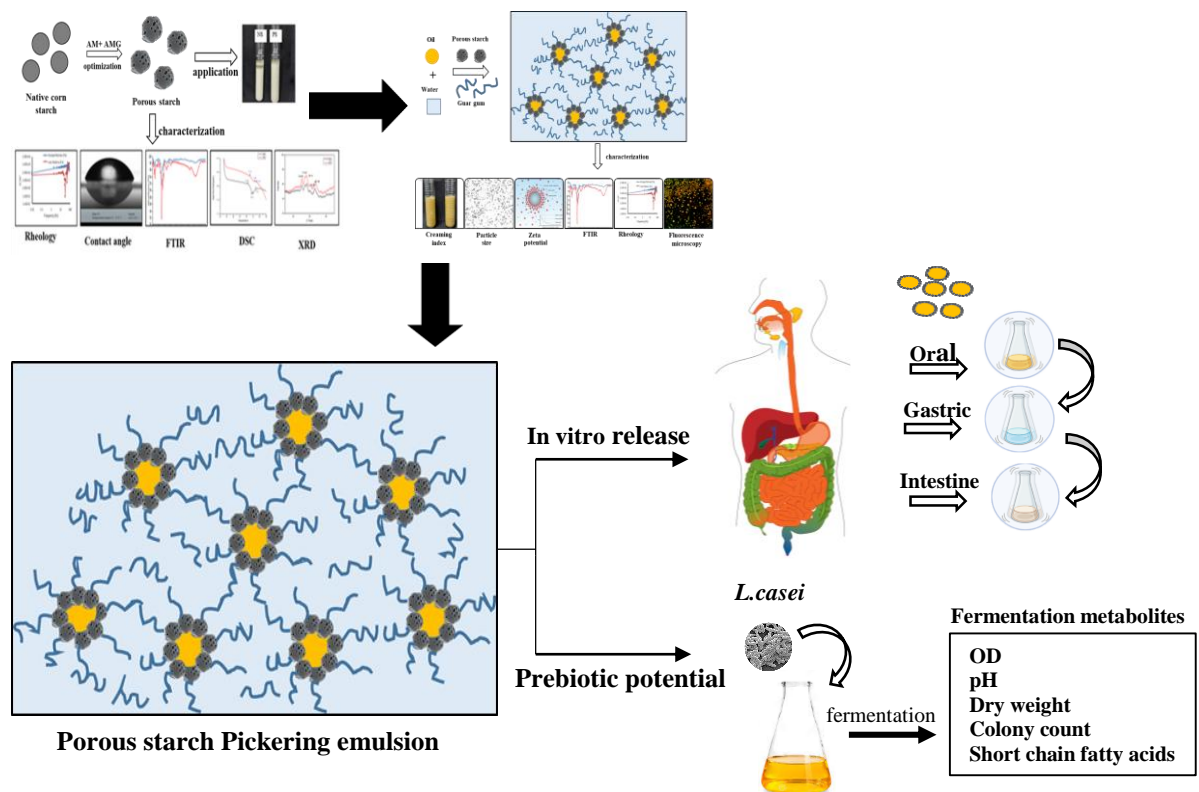
Pickering emulsion as detailed in the previous chapter consists of curcumin loaded flax seed oil with guar gum as stabilizer and porous starch as Pickering particles. Guar gum is prebiotic in nature and is also reported to be used for colon targeted delivery of active ingredients (Verma et al., 2021; Hu et al., 2022; Garg et al., 2023). Therefore, based on the finding from previous chapter, in Chapter 4, we focus on establishing the gastrointestinal stability of the developed Pickering emulsion and its prebiotic efficacy using *in vitro* protocol.

4.1.1. Objectives

From the previous chapter, it was concluded that the porous starch-based Pickering emulsion can act as efficient Pickering particle and it also possess better encapsulation efficiency of curcumin. With this background, the main objectives of this chapter are (1) To ensure the gut delivery of bioactive curcumin by studying the *in vitro* release kinetics using simulated gastro intestinal conditions (2) To evaluate the prebiotic potential of encapsulates in terms of change in OD, pH, dry weight, colony count and short chain fatty acids production using *in vitro* protocol.

4.2. Materials and Methods

The experimental design for *in vitro* release studies of curcumin loaded porous starch encapsulates by Pickering emulsion and evaluation of its prebiotic potential.



4.2.1. Materials

Freeze dried culture of *Lactobacillus casei* (NCDC 17) was procured from National Dairy Research Institute (ICAR), Karnal, Haryana, India. *Lactobacillus* MRS broth and agar powder was purchased from Himedia laboratories Pvt. Ltd (Mumbai, India). Bile salt, pancreatin from porcine pancreas, pepsin from porcine gastric mucosa, α -amylase from *Aspergillus oryzae* were purchased from Sigma-Aldrich (St. Louis, Missouri, United States). Sodium hydroxide and Sodium chloride were procured from Sisco Research Laboratories Pvt. Ltd (Mumbai, India). Calcium chloride from Spectrochem Pvt. Ltd (Mumbai, India) and Hydrochloric acid from Avantor™ Performance Material India Ltd (Haryana, India) was used. All other chemicals used were of analytical grade.

4.2.2 Methods

4.2.2.1. *In vitro* release studies of porous starch based curcumin Pickering emulsion

In vitro release studies were performed in three phases, simulated oral phase, gastric phase and intestinal phase and the preparation of each phase was described below based on previous studies with some modifications (Pan et al., 2019; Mulet-Cabero et al., 2020). The oral phase was prepared by mixing α -amylase (0.2 mg/mL), and 25 μ l of 0.3 M NaCl. Sample to simulated salivary phase taken was in the ratio 1:4. The gastric phase was prepared by combining 2 gm of NaCl and 7 mL of HCl in 1000 mL water. 20 mL of sample from oral phase was mixed with equal amount in stomach phase. To this mixture, 0.064 g of pepsin was added and the pH of the system was adjusted to 2.5. The mixture was incubated in a shaker at 37 °C for two hours at a speed of 130 rpm. After incubation 5 mL of gastric phase mixture was transferred to other tube for analysis. 30 mL of gastric phase was mixed with equal amount of intestinal phase (bile salts-1.8 g, 1.5 mL of CaCl₂-

36.7 mg/mL and NaCl- 219.1 mg/mL). To this, 1.8 g of pancreatin was added and pH of the system was adjusted to 7, followed by incubation in a shaker at 37 °C for 2 h at a speed of 130 rpm.

4.2.2.2. Prebiotic potential of fermentation metabolites (FM)

Prebiotic potential of PSPE (Porous starch based Pickering emulsion) was studied using probiotic strain, *Lactobacillus casei*, which was cultured in MRS broth for 24 h at 37 °C. The culture was diluted to obtain 80 % transmittance at 600 nm and 1mL of diluted culture was inoculated to media as follows. The culture of *Lactobacillus casei* was inoculated to MRS broth containing four treatment groups- (i) Control, (ii) Positive control- Inulin (iii) PS- Porous starch based Pickering emulsion without curcumin (iv) PSC- Porous starch based Pickering emulsion with curcumin (Fig 4.1). The PSPE and inulin were incorporated at 0.8% w/v (on basis of TSS). The treatment groups were incubated at 37 °C, resulting in the production of fermentation metabolites (FM) containing SCFA (Short chain fatty acids).

The treatment groups were incubated at 37 °C, resulting in the production of FM containing SCFA. At each time interval (24, 48 and 72 h), the FM were collected, centrifuged and supernatant was analyzed for change in OD, pH, colony count, dry weight and production of SCFA to evaluate the prebiotic potential of PSPE.

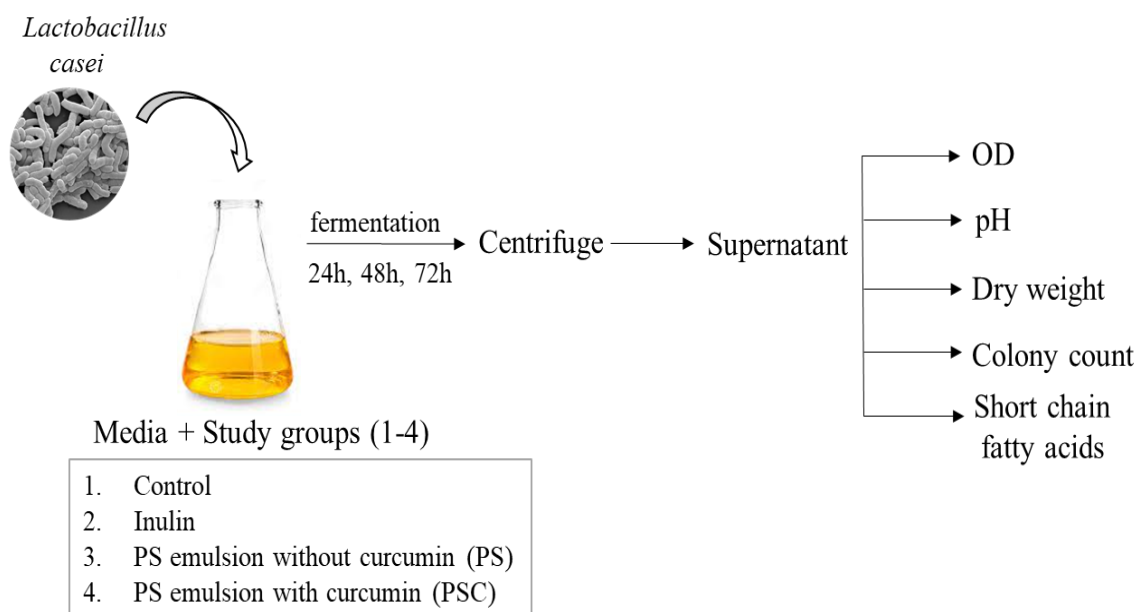


Fig 4.1: Preparation of fermentation metabolites

4.2.2.3. Evaluation of prebiotic potential of FM

The prebiotic potential was studied in terms of change in pH, OD, colony count, dry weight and by quantification of SCFA production (Madhvan et al., 2019).

4.2.2.3.1. Estimation of optical density

The OD (optical density) of samples was measured at 600 nm at particular time intervals (24, 48 and 72 h) using UV spectrophotometer (Shimadzu UV-2600, Kyoto, Japan).

4.2.2.3.2. Estimation of pH

The pH of samples was measured at particular time intervals (24, 48 and 72 h) using pH meter (Oakton, pH 700, Benchtop meter, Oakton Instruments, USA).

4.2.2.3.3. Colony count

The colony count was done at time interval of (24, 48 and 72 h) and expressed as log colony formation units (log CFU/mL). Broth from each group (1 mL) was serially diluted to obtain concentration from 10^{-1} to 10^{-8} . From this, 1 mL of the sample was used for

estimating colony count using pour plate method. The colonies were counted after incubating the plates at 37 °C for 72 h.

4.2.2.3.4. Assessment of SCFA production in FM

Short chain fatty acid (SCFA) production at each time interval was assessed and quantified by High performance Liquid Chromatography (HPLC). The fermentation medium was centrifuged at 5000 rpm for 10 min and the supernatant was used for analyzing SCFA. Standard short chain fatty acids, acetic acid, propionic acid and butyric acid and treatment groups (supernatant) were filtered through 0.45 µm filter and 10 µL was injected into the system. The analysis was performed in a Prominence UFLC (Shimadzu, Japan) containing LC 20 AD system controller, Rezex RHM-Monosaccharide H⁺ (300×7.8 mm) column, column oven (CTO-20A) and diode array detector (SPD-M20A). The mobile phase used was Milli Q water. The flow rate was 0.8ml/min, injection volume was 10 µL and the temperature of column was maintained at 50 °C. The SCFA were monitored at 230 nm. Sample peaks were determined by comparing with retention times of standard peaks. For data acquisition and analysis LC Lab Solution software was used.

4.2.2.3.5. Assessment of curcumin concentration in FM

The curcumin concentration in FM of PSC sample at 72 h incubation was analyzed using HPLC (instrumentation details same as described in 4.2.2.3.4). The fermentation medium of PSC was centrifuged and supernatant was used for determination of curcumin concentration. The mobile phase used was methanol. The flow rate was 1 mL/min, injection volume was 10 µL and the temperature of column was maintained at 33 °C. The curcumin was monitored at 420 nm. Sample peaks were determined by comparing with retention times of standard curcumin peaks.

4.2.2.4. Statistical analysis

Data represented as mean \pm standard deviations of experiments in duplicates. One-way ANOVA was used for analyzing the results using Graph Pad Prism 9.3.0 software and the significance was accepted at $P \leq 0.05$.

4.3. Results and discussion

4.3.1. *In vitro* release studies

The *in vitro* release studies of porous starch/guar gum -based Pickering emulsion (PSPE) was performed under simulated gastro intestinal conditions ie, simulated salivary fluid (SSG), simulated gastric fluid (SGF) and simulated intestinal fluid (SIF). The percentage curcumin release was 11 ± 0.01 , 17.9 ± 0.32 , and $27.9 \pm 0.01\%$ in oral, gastric and intestinal phase. The results showed the low release kinetics of curcumin in all three phases. Due to harsh environmental conditions such as low pH and digestive enzymes, significant breakdown of food materials occurs in gastric conditions. Appropriate selection of wall materials can protect the bioactive compounds from acidic gastric phase, in a stable encapsulated system (Lu et al., 2019). When the PSPE was digested with simulated gastric fluid and intestinal fluid, 17.9 and 27.9% of curcumin was released from the emulsion system after 2 h of incubation, respectively. Similar results were observed when *in vitro* studies (gastric and intestinal) were performed in Pickering emulsions stabilized by milled starch, where 20 and 28% curcumin released after gastric and intestinal digestion respectively (Lu et al., 2019). In another study, Tikekar et al. (2013) encapsulated curcumin in Pickering emulsion stabilized by silica nanoparticles and the release of curcumin in simulated gastric condition was 20% and that of simulated intestinal condition was 55.8%. The system withstands the acidic gastric condition but high release rate occurs in intestinal condition due to destabilization of emulsion. Pan et

al. (2019) fabricated succinylated whey protein hydrolysate stabilized curcumin-loaded emulsions and reported very high release of curcumin, greater than 60% in simulated intestinal phase.

The PSPE emulsion was fabricated using solid particles, porous starch and guar gum. The porous starch has the ability to get adsorbed onto the interface between oil and water phase making it an efficient Pickering particle and offers protection to the curcumin in the oil phase. Guar gum in the system offer extra stability to the emulsion by increasing the viscosity of the continuous water phase via the formation of gel like structure which resists the free movement of emulsion droplets and immobilize them. Being a soluble dietary fibre, guar gum also protects the emulsion system from gastrointestinal enzymes and helps in colonic delivery of bioactive. Thus, these particles protect the oil phase containing bioactive from interacting with harsh acidic condition. The slow release kinetics in simulated intestinal phase was due to irreversible and strong adsorption of solid particles at O/W interface and also particle interaction in continuous phase (Lu et al., 2018; Tzoumaki et al., 2013).

4.3.2. Prebiotic potential of fermentation metabolites (FM)

The fermentation metabolites were prepared using probiotic *Lactobacillus casei* (Fig 4.1). At each time interval (24, 48 and 72 h), the fermentation metabolites were collected and studied for change in OD, pH, colony count and production of SCFA to evaluate the prebiotic potential of PSPE.

4.3.2.1. Change in optical density

At particular time intervals (24, 48 and 72 h) media was withdrawn and was analyzed for optical density. The optical density directly correlates with the bacterial mass in growth media (Arun et al., 2019). If having the prebiotic potential, the growth of organisms will

be more and OD values will be higher which is measured at 600 nm. The OD measurements for different treatment groups is given in (Fig 4.2).

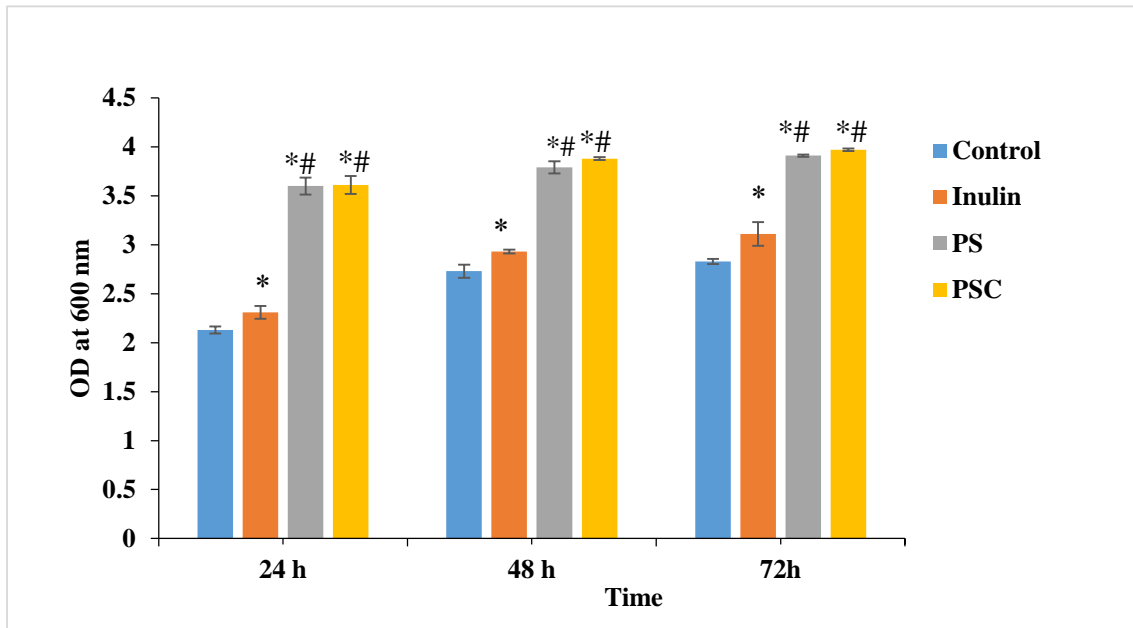


Fig 4.2: Prebiotic potential of porous starch emulsion determined by change in optical density for *Lactobacillus casei*. *p \leq 0.05 versus control. #p \leq 0.05 versus inulin. PS- Porous starch Pickering emulsion without curcumin. PSC- Porous starch based Pickering emulsion with curcumin.

From the graph, it is clear that OD value in all groups increased as the incubation time increases. Both PS and PSC treatment groups showed significant increase in OD compared to that of control and positive control groups. As can be seen, PSC showed higher OD values which ranged from 3.61 ± 0.09 to 3.97 ± 0.01 compared to inulin 2.31 ± 0.06 to 3.11 ± 0.12 as the incubation time increases from 24 to 72 h. The results clearly indicate that porous starch based Pickering emulsion, promotes the growth of probiotics, there by increases turbidity of media. Curcumin is a known antimicrobial agent, however, the antimicrobial effect was not visible as no significant difference was observed in OD between the PS and PSC treatment groups.

4.3.2.2. Change in pH

The fermentation of samples by probiotic strain, *Lactobacillus casei*, results in the production of SCFA. The SCFA are secondary metabolites and its production results in reduction of pH, that can be correlated with the prebiotic activity of samples (Rios-Covian et al., 2016). Therefore, pH was estimated at different time intervals (24, 48 and 72 h) which is given in (Fig 4.3). From the graph, it is clear that pH value in all treatment groups decreases as the incubation time increases. Among the treatment groups, PSC groups showed lower pH of 4.42 ± 0.01 to 4.11 ± 0.01 , as the incubation time increases from 24 to 72 h. The pH, of both PS and PSC treatment groups reduced significantly compared to that of positive control and control groups. The results demonstrate that the samples significantly promote growth of probiotic bacteria which can be correlated with the production of SCFA.

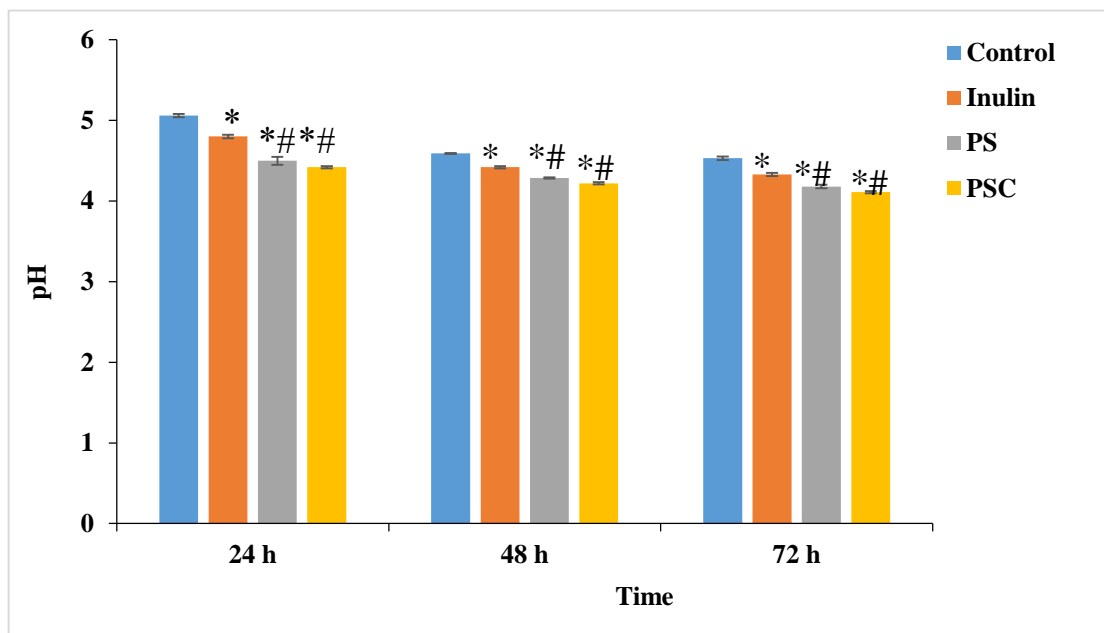


Fig 4.3: Prebiotic potential of porous starch emulsion determined by pH change for *Lactobacillus casei*. *p \leq 0.05 versus control. #p \leq 0.05 versus inulin. PS- Porous starch Pickering emulsion without curcumin. PSC- Porous starch Pickering emulsion with curcumin.

4.3.2.3. Determination of colony count

For enumeration of microorganism, the most ideal and preferable method was colony count method. Quantification of bacteria can be attained by growing the organisms on an agar plate after serial dilution and calculating the number of CFU (colony forming units) (Davis. 2014). Hence we performed pour plate method for the growth of microorganisms and the number of colonies was analyzed by colony forming unit. The colony counts of different treatment groups on 48 h with dilution factor of 10^{-8} respectively was given in (Fig 4.4). The colony counts of different treatment groups expressed in log values was given in (Fig 4.5). The number of colonies were increased in all experimental group as the incubation time increases from 24 to 48 h. However, a slight decrease in colony count was observed at 72 h of incubation. The PSC treatment groups showed highest number of colonies varied from 9.2 ± 0.01 to 9.9 ± 0.01 log CFU/mL at 48 h incubation. But when the incubation time was increased to 72 h, the number of colonies was decreased to 9.75 ± 0.05 log CFU/mL.

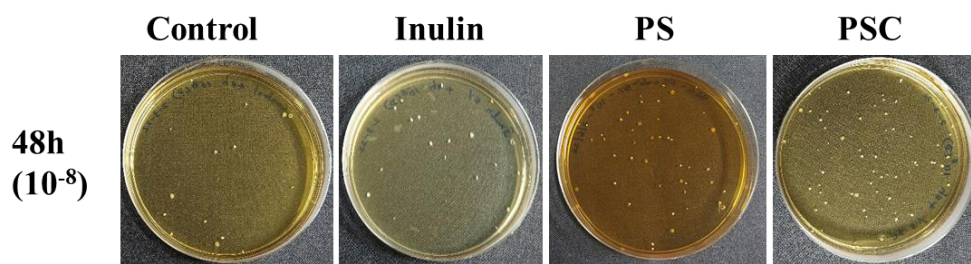


Fig 4.4: Colony count by pour plate method at 48h. PS- Porous starch based Pickering emulsion without curcumin. PSC- Porous starch based Pickering emulsion with curcumin.

Bacterial growth progresses mainly through four stages, lag, exponential, stationary and death phase. Exponential phase is the growth stage where maximum cell growth and division occurs, followed by stationary phase where cell division and growth declines, but the bacteria survives (Wang et al., 2015). Rezvani et al. (2017) studied the growth

kinetics of five *Lactobacillus* strains including *Lactobacillus casei* and reported that the exponential phase or maximum cell growth occurs in a period of 25-45 h for the *Lactobacillus* strain. The decrease in colonies after 48 h incubation might be due to the decline in exponential phase, as the growth stage of *Lactobacillus casei* has changed from exponential to the stationary phase.

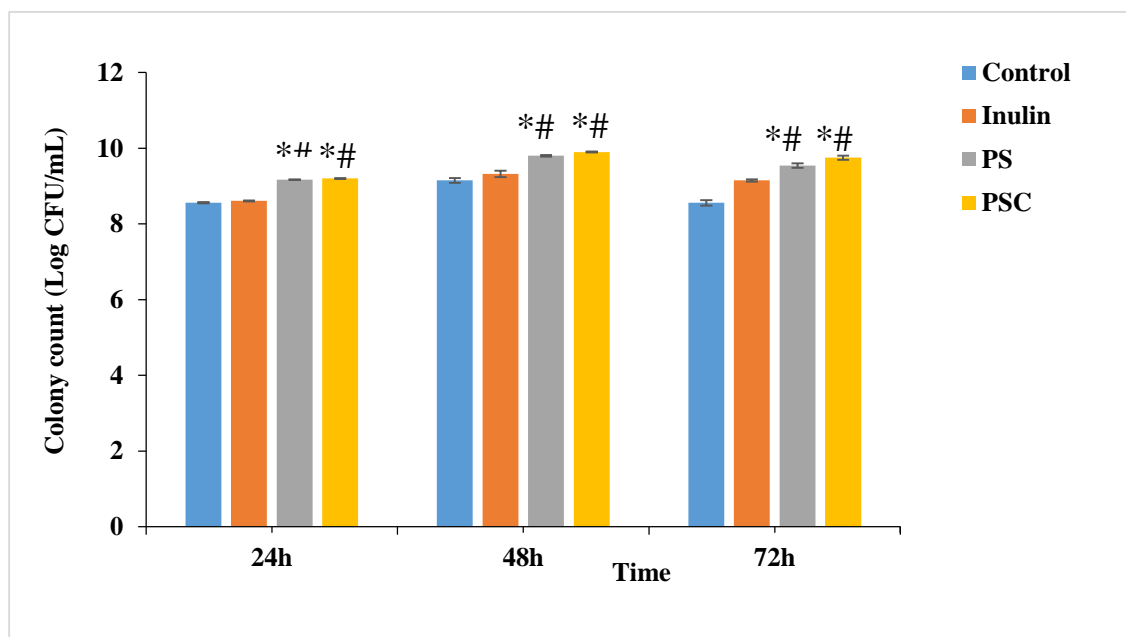


Fig 4.5: Prebiotic potential of porous starch emulsion determined by colony count by pour plate method for *Lactobacillus casei*. * $p \leq 0.05$ versus control. # $p \leq 0.05$ versus inulin.

4.3.2.4 Change in dry weight

The samples after fermentation were centrifuged and the residue was freeze dried and the weight of the residue directly indicates the mass of bacteria in the media. The dry mass of all the groups were found to increase with incubation (Fig 4.6). For PSC the dry mass increased from 57.68 ± 1.05 to 73.03 ± 0.35 mg/mL compared to inulin $43.39 \pm .95$ to $60.65 \pm .61$ mg/mL respectively as the incubation time increases from 24 to 72h. This significant increase in the dry weight of PSC with inulin group indicate that PSC support the growth of probiotics.

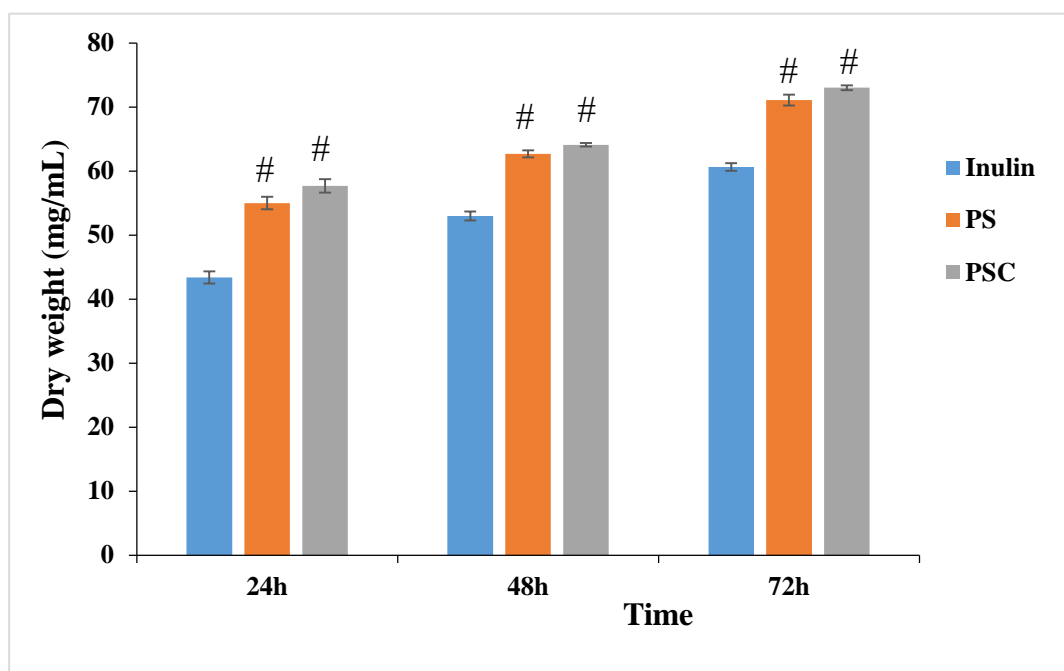


Fig 4.6: Prebiotic potential of porous starch emulsion determined by change in dry weight for *Lactobacillus casei*. #p \leq 0.05 versus inulin.

Even though decrease in bacterial growth was found at 72 h of plate count, the dry weight increased as the incubation time increases from 24 to 72 h. This might due to the fact that bacterial growth continued after 48 h of incubation but at 72 h, growth phase might have shifted to stationary phase. Thus 72 h of incubation resulted in increased dry weight and decreased growth of *Lactobacillus casei*.

4.3.2.5 Determination of curcumin in fermentation metabolites

The curcumin concentration in the FM of PSC sample at 72 h incubation was analyzed using HPLC which was found to be 6.14 ± 0.28 ppm (compared to initial concentration of 40ppm). Studies reported that there is bidirectional interaction between gut microbiota and curcumin. Curcumin can be transformed into many active metabolites by the action of enzymes generated by gut microbiota (Tsuda, 2018). Mostly gut microbiota transforms curcumin by hydroxylation, reduction, acetylation, demethylation resulted in different metabolites such as demethylcurcumin and bis-demethylcurcumin. The enzyme

NADPH-dependent curcumin/dihydrocurcumin reductase transforms curcumin to dihydrocurcumin and tetrahydrocurcumin (Lou et al., 2015; Chen et al., 2016; Pinkaew et al., 2016). It has been reported that metabolites of curcumin exhibit many biological properties such as anti-inflammatory, anti-oxidant and anti-tumor activities. The microorganisms such as *Bifidobacteria longum*, *Lactobacillus casei*, *Lactobacillus acidophilus*, *Enterococcus faecalis* are reported to metabolize curcumin (Carmody et al., 2014; Scazzocchio et al., 2020). In recent *in vivo* study, the oral administration of curcumin resulted in eight different metabolites by the transformation of intestinal microbiota (Sun et al., 2020). The decreased concentration of curcumin in FM of PSC sample may be attributed due to transformation of curcumin to its metabolites by the probiotic organism under study.

4.3.2.6 Quantification of short chain fatty acid production

Metabolism of undigested carbohydrate by probiotic bacteria results in the production of SCFA which was analyzed by HPLC. The HPLC chromatogram of standard SCFA viz., acetic acid (AA), propionic acid (PA) and butyric acid (BA) are shown in (Fig 4.6) The retention time of SCFA was found to be 10.593, 12.995 and 14.826 min for AA, PA and BA respectively. Short chain fatty acids produced by different experimental groups at different time intervals were identified and quantified. The results indicate that the SCFA production was increased in all treatment groups when the incubation time was increased from 24 to 72 h.

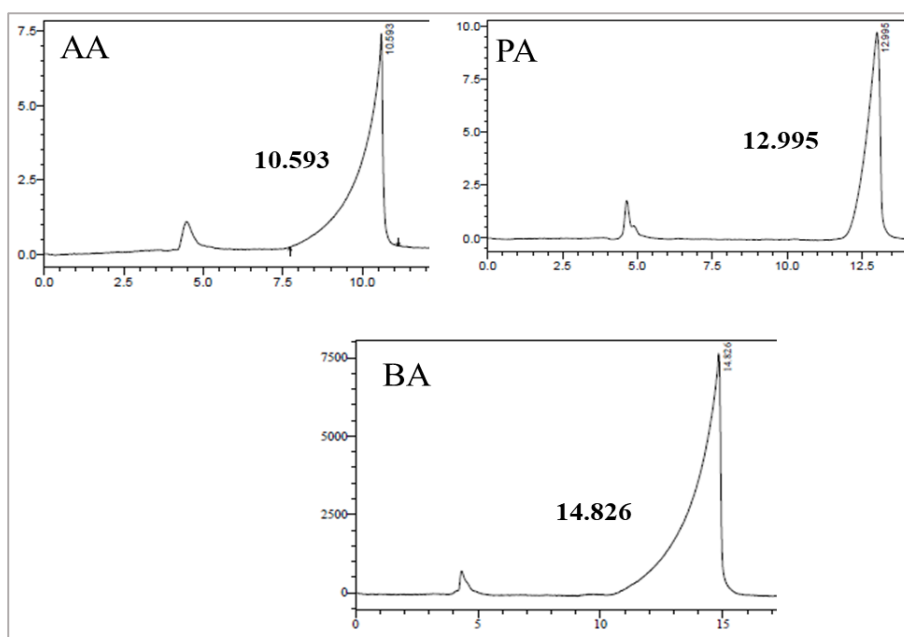


Fig 4.7: HPLC chromatograms of standard short chain fatty acids and their retention time- AA (Acetic acid), PA (Propionic acid), BA (Butyric acid).

Fermentation metabolites produced by porous based curcumin Pickering emulsion incubated for 72 h has showed the highest SCFA production. Fig 4.7 shows the graphical representation of SCFA, acetic acid, propionic acid and butyric acid produced when different groups were incubated with *Lactobacillus casei* for 24 to 72 h. Porous based curcumin Pickering emulsion incubated for 37 °C showed highest concentration of acetic acid (20.65mg/mL), propionic acid (18.33 mg/mL) and butyric acid 1.28 (mg/mL) was used for further studies. These results confirmed the prebiotic property of porous based curcumin Pickering emulsion.

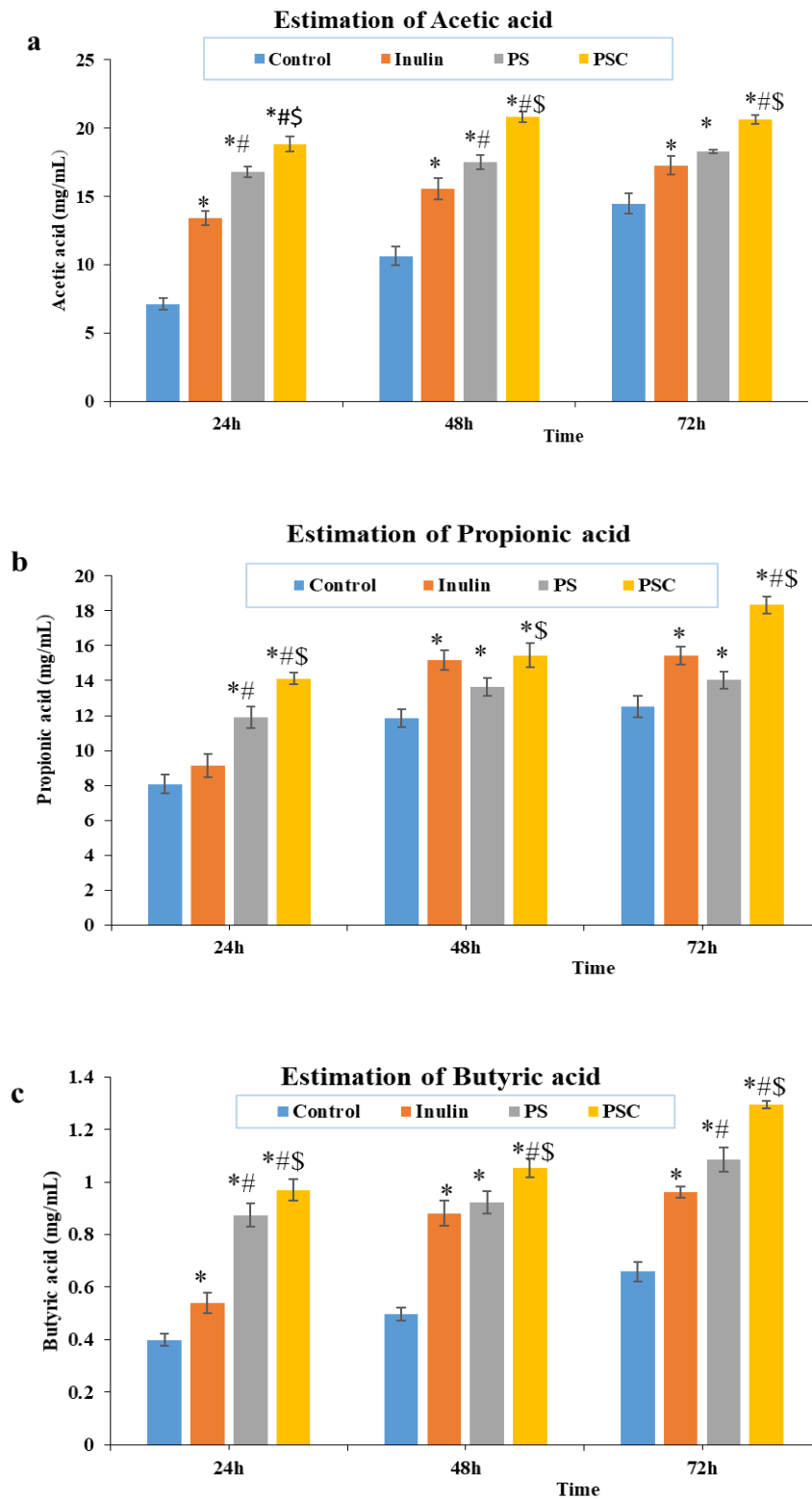


Fig 4.8: Estimation of short chain fatty acids (a) Acetic acid (b) Propionic acid (c) Butyric acid by HPLC. * $p \leq 0.05$ versus control. # $p \leq 0.05$ versus inulin. \$ $p \leq 0.05$ versus PS emulsion.

The prebiotic property of porous starch based Pickering emulsion (PS and PSC) can be attributed to the soluble dietary fibre, guar gum. *In vitro* studies reported that partially hydrolyzed guar gum can promote growth of probiotics *Lactobacillus* and *Bifidobacterium* (Koecher et al., 2014; Carlson et al., 2015; Carlson et al., 2016). Curcumin can also modify the intestinal microflora. Studies demonstrated that oral administration of curcumin promotes the growth of *Lactobacilli* and inhibit the growth of *Enterobacteria*, *Prevotellaceae*, *Rikenellaceae* and *Coriobacteriales* (McFadden et al., 2015; Chatelier et al., 2013; Shen et al., 2017; Scazzocchio et al., 2020). In another study administration of nano-bubble curcumin extract (NCE) resulted in improved growth of *Lactobacilli* and *Proteobacteria* and leads to increased short chain fatty acid production (Chen et al., 2020). Thus combined effect of both curcumin and guar gum in PSC emulsion resulted in significant increase in SCFA compared to PS emulsion which is devoid of curcumin.

4.4. Conclusion

The core release studies of porous starch based Pickering emulsion showed low release of curcumin in simulated gastro intestinal conditions. The porous starch Pickering emulsion was fermented using *Lactobacillus casei* and the prebiotic potential was confirmed in terms of increased optical density, colony count, dry weight and decreased pH. Quantification of short chain fatty acids by HPLC further confirmed the prebiotic potential of porous starch based Pickering emulsion. PSPE showed significant increase in short chain fatty acid production compared to other treatment groups. Based on this we have decided to undertake further studies to evaluate the potential of the fermentation supernatant enriched with fermentation metabolites against the mitigation and control of colorectal cancer which forms the content for the next chapter, chapter 5.

4.5. References

- Adom, D., & Nie, D. (2013). Regulation of autophagy by short chain fatty acids in colon cancer cells. *Autophagy—A Double-Edged Sword—Cell Survival or Death*, 235-247.
- Bugaut, M. (1987). Occurrence, absorption and metabolism of short chain fatty acids in the digestive tract of mammals. *Comparative Biochemistry and Physiology Part B: Comparative Biochemistry*, 86(3), 439-472.
- Carlson, J., Hospattankar, A., Deng, P., Swanson, K., & Slavin, J. (2015). Prebiotic effects and fermentation kinetics of wheat dextrin and partially hydrolyzed guar gum in an in vitro batch fermentation system. *Foods*, 4(3), 349-358.
- Carlson, J., Gould, T., & Slavin, J. (2016). In vitro analysis of partially hydrolyzed guar gum fermentation on identified gut microbiota. *Anaerobe*, 42, 60-66.
- Carmody, R. N., & Turnbaugh, P. J. (2014). Host-microbial interactions in the metabolism of therapeutic and diet-derived xenobiotics. *The Journal of clinical investigation*, 124(10), 4173-4181.
- Chen, P. T., Chen, Z. T., Hou, W. C., Yu, L. C., & Chen, R. P. Y. (2016). Polyhydroxycurcuminoids but not curcumin upregulate neprilysin and can be applied to the prevention of Alzheimer's disease. *Scientific Reports*, 6(1), 1-12.
- Chen, Y. M., Chiu, W. C., Chiu, Y. S., Li, T., Sung, H. C., & Hsiao, C. Y. (2020). Supplementation of nano-bubble curcumin extract improves gut microbiota composition and exercise performance in mice. *Food & function*, 11(4), 3574-3584.

- Davis, C. (2014). Enumeration of probiotic strains: review of culture-dependent and alternative techniques to quantify viable bacteria. *Journal of microbiological methods*, 103, 9-17.
- Floch, M. H. (2011). Intestinal microecology in health and wellness. *Journal of clinical gastroenterology*, 45, S108-S110.
- Gagniere, J., Raisch, J., Veziat, J., Barnich, N., Bonnet, R., Buc, E., ... & Bonnet, M. (2016). Gut microbiota imbalance and colorectal cancer. *World journal of gastroenterology*, 22(2), 501-518.
- Garg, S. S., & Gupta, J. (2023). Guar gum-based nanoformulations: Implications for improving drug delivery. *International Journal of Biological Macromolecules*.
- Holscher, H. D. (2017). Dietary fiber and prebiotics and the gastrointestinal microbiota. *Gut microbes*, 8(2), 172-184.
- Hooper, L. V., Littman, D. R., & Macpherson, A. J. (2012). Interactions between the microbiota and the immune system. *science*, 336(6086), 1268-1273.
- Hu, Y., Zhang, S., Wen, Z., Fu, H., Hu, J., Ye, X., ... & Yang, X. (2022). Oral delivery of curcumin via multi-bioresponsive polyvinyl alcohol and guar gum based double-membrane microgels for ulcerative colitis therapy. *International Journal of Biological Macromolecules*, 221, 806-820.
- Jha, R., Fohse, J. M., Tiwari, U. P., Li, L., & Willing, B. P. (2019). Dietary fiber and intestinal health of monogastric animals. *Frontiers in veterinary science*, 6, 48.

- KB, A., Madhavan, A., TR, R., Thomas, S., & Nisha, P. (2019). Short chain fatty acids enriched fermentation metabolites of soluble dietary fibre from *Musa paradisiaca* drives HT29 colon cancer cells to apoptosis. *PloS one*, *14*(5), e0216604.
- Koecher, K. J., Noack, J. A., Timm, D. A., Klosterbuer, A. S., Thomas, W., & Slavin, J. L. (2014). Estimation and interpretation of fermentation in the gut: coupling results from a 24 h batch in vitro system with fecal measurements from a human intervention feeding study using fructo-oligosaccharides, inulin, gum acacia, and pea fiber. *Journal of agricultural and food chemistry*, *62*(6), 1332-1337.
- Le Chatelier, E., Nielsen, T., Qin, J., Prifti, E., Hildebrand, F., Falony, G., ... & Pedersen, O. (2013). Richness of human gut microbiome correlates with metabolic markers. *Nature*, *500*(7464), 541-546.
- Liu, P., Wang, Y., Yang, G., Zhang, Q., Meng, L., Xin, Y., & Jiang, X. (2021). The role of short-chain fatty acids in intestinal barrier function, inflammation, oxidative stress, and colonic carcinogenesis. *Pharmacological research*, *165*, 105420.
- Lou, Y., Zheng, J., Hu, H., Lee, J., & Zeng, S. (2015). Application of ultra-performance liquid chromatography coupled with quadrupole time-of-flight mass spectrometry to identify curcumin metabolites produced by human intestinal bacteria. *Journal of Chromatography B*, *985*, 38-47.
- Lu, X., Li, C., & Huang, Q. (2019). Combining in vitro digestion model with cell culture model: Assessment of encapsulation and delivery of curcumin in

- milled starch particle stabilized Pickering emulsions. *International journal of biological macromolecules*, *139*, 917-924.
- Lu, X., Xiao, J., & Huang, Q. (2018). Pickering emulsions stabilized by media-milled starch particles. *Food Research International*, *105*, 140-149.
- Maslowski, K. M., Vieira, A. T., Ng, A., Kranich, J., Sierro, F., Yu, D., ... & Mackay, C. R. (2009). Regulation of inflammatory responses by gut microbiota and chemoattractant receptor GPR43. *Nature*, *461*(7268), 1282-1286.
- McFadden, R. M. T., Larmonier, C. B., Shehab, K. W., Midura-Kiela, M., Ramalingam, R., Harrison, C. A., ... & Kiela, P. R. (2015). The role of curcumin in modulating colonic microbiota during colitis and colon cancer prevention. *Inflammatory bowel diseases*, *21*(11), 2483-2494.
- McNabney, S. M., & Henagan, T. M. (2017). Short chain fatty acids in the colon and peripheral tissues: a focus on butyrate, colon cancer, obesity and insulin resistance. *Nutrients*, *9*(12), 1348.
- Mudgil, D., & Barak, S. (2013). Composition, properties and health benefits of indigestible carbohydrate polymers as dietary fiber: A review. *International journal of biological macromolecules*, *61*, 1-6.
- Mulet-Cabero, A. I., Egger, L., Portmann, R., Ménard, O., Marze, S., Minekus, M., ... & Mackie, A. (2020). A standardised semi-dynamic in vitro digestion method suitable for food—an international consensus. *Food & function*, *11*(2), 1702-1720.
- Natarajan, N., & Pluznick, J. L. (2014). From microbe to man: the role of microbial short chain fatty acid metabolites in host cell biology. *American Journal of Physiology-Cell Physiology*, *307*(11), C979-C985.

- Pan, Y., Xie, Q. T., Zhu, J., Li, X. M., Meng, R., Zhang, B., ... & Jin, Z. Y. (2019). Study on the fabrication and in vitro digestion behavior of curcumin-loaded emulsions stabilized by succinylated whey protein hydrolysates. *Food Chemistry*, 287, 76-84.
- Pinkaew, D., Changtam, C., Tocharus, C., Govitrapong, P., Jumnonprakhon, P., Suksamram, A., & Tocharus, J. (2016). Association of Neuroprotective Effect of Di-O-Demethylcurcumin on A β 25–35-Induced Neurotoxicity with Suppression of NF- κ B and Activation of Nrf2. *Neurotoxicity research*, 29, 80-91.
- Qin, J., Li, R., Raes, J., Arumugam, M., Burgdorf, K. S., Manichanh, C., ... & Wang, J. (2010). A human gut microbial gene catalogue established by metagenomic sequencing. *nature*, 464(7285), 59-65.
- Rezvani, F., Ardestani, F., & Najafpour, G. (2017). Growth kinetic models of five species of Lactobacilli and lactose consumption in batch submerged culture. *brazilian journal of microbiology*, 48, 251-258.
- Rios-Covian, D., Ruas-Madiedo, P., Margolles, A., Gueimonde, M., De Los Reyes-gavilan, C. G., & Salazar, N. (2016). Intestinal short chain fatty acids and their link with diet and human health. *Frontiers in microbiology*, 7, 185
- Scazzocchio, B., Minghetti, L., & D'Archivio, M. (2020). Interaction between gut microbiota and curcumin: a new key of understanding for the health effects of curcumin. *Nutrients*, 12(9), 2499.
- Shen, L., & Ji, H. F. (2016). Intestinal microbiota and metabolic diseases: pharmacological Implications. *Trends in Pharmacological Sciences*, 37(3), 169-171.

- Shen, L., Liu, L., & Ji, H. F. (2017). Regulative effects of curcumin spice administration on gut microbiota and its pharmacological implications. *Food & nutrition research*, *61*(1), 1361780.
- Stohs, S. J., Chen, O., Ray, S. D., Ji, J., Bucci, L. R., & Preuss, H. G. (2020). Highly bioavailable forms of curcumin and promising avenues for curcumin-based research and application: a review. *Molecules*, *25*(6), 1397.
- Sun, Z. Z., Li, X. Y., Wang, S., Shen, L., & Ji, H. F. (2020). Bidirectional interactions between curcumin and gut microbiota in transgenic mice with Alzheimer's disease. *Applied microbiology and biotechnology*, *104*, 3507-3515.
- Tan, J., McKenzie, C., Potamitis, M., Thorburn, A. N., Mackay, C. R., & Macia, L. (2014). The role of short-chain fatty acids in health and disease. *Advances in immunology*, *121*, 91-119.
- Thorburn, A. N., Macia, L., & Mackay, C. R. (2014). Diet, metabolites, and "western-lifestyle" inflammatory diseases. *Immunity*, *40*(6), 833-842.
- Tikekar, R. V., Pan, Y., & Nitin, N. (2013). Fate of curcumin encapsulated in silica nanoparticle stabilized Pickering emulsion during storage and simulated digestion. *Food Research International*, *51*(1), 370-377.
- Tsuda, T. (2018). Curcumin as a functional food-derived factor: degradation products, metabolites, bioactivity, and future perspectives. *Food & function*, *9*(2), 705-714
- Tzoumaki, M. V., Moschakis, T., Scholten, E., & Biliaderis, C. G. (2013). In vitro lipid digestion of chitin nanocrystal stabilized o/w emulsions. *Food & Function*, *4*(1), 121-129.

- Vamanu, E., Gatea, F., Sârbu, I., & Pelinescu, D. (2019). An in vitro study of the influence of *Curcuma longa* extracts on the microbiota modulation process, in patients with hypertension. *Pharmaceutics*, *11*(4), 191.
- Verma, D., & Sharma, S. K. (2021). Recent advances in guar gum based drug delivery systems and their administrative routes. *International Journal of Biological Macromolecules*, *181*, 653-671.
- Wang, L., Fan, D., Chen, W., & Terentjev, E. M. (2015). Bacterial growth, detachment and cell size control on polyethylene terephthalate surfaces. *Scientific reports*, *5*(1), 15159.

Chapter 5

***In vitro* screening of the fermentation metabolites in prevention and management of colorectal cancer**

5.1. Introduction

Cancer is the major cause of death worldwide and is characterized by uncontrolled division of abnormal cells. Colorectal cancer (CRC) or bowel cancer is the uncontrolled growth of cells in the colon, rectum, or appendix (Kumar et al., 2018) which is the third most commonly diagnosed and is the second largest lethal cancer worldwide (American Cancer Society, 2023; Rawla et al., 2019) (Fig 5.1). The incidence of colorectal cancer has increased intensively in the last 60 years (Pericleous et al., 2013) and by 2030, the global burden of CRC is predicted to cause 2.2 million new cases and 1.1 million annual deaths (Rawla et al., 2019).

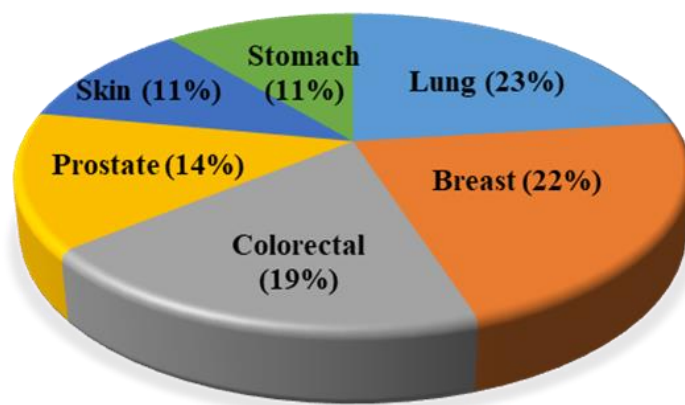


Fig 5.1: The pie chart shows the most prevalent cancer cases worldwide.

Common symptoms of colorectal cancer include bleeding in the rectum, presence of blood in stool, abdominal pain, loss of appetite and weight loss. Loss of blood might lead to anemia, resulting in tiredness and shortness of breath (American Cancer Society, 2023). There are many factors that lead to colon cancer such as family history and genetics, low physical activity, inflammatory bowel disease, overweight and obesity, consumption of red meat, consumption of alcohol and intake of low dietary fibre (Fig 5.2) (World Cancer Research Fund/American Institute for Cancer Research, 2018).



Fig 5.2: Risk factors that lead to colorectal cancer

According to reports, diet and lifestyle factors are linked to the development of colorectal cancer in which dietary factors accounts for 70 to 90% of colorectal cancer mortality (Pericleous et al., 2013; Arun et al., 2018). The hypothesis of high dietary fibre intake and reduced colon cancer was postulated after a study in African populations who consumed large levels of fibre and had a low incidence of colon cancer (Burkitt et al., 1972; MacDonald et al., 2012). Due to the presence of high content of phytochemicals, the consumption of vegetables, fruits, soy and green tea are reported to reduce the colorectal cancer risk (Tantamango et al., 2011; Yan et al., 2010; Butt et al., 2009). Diet rich in whole grains and fibre have also been associated with lower risk of colon cancer (Haas et al., 2009).

The anaerobic fermentation of carbohydrates such as nondigestible polysaccharides and dietary fibers by gut microbiota results in the production of short-chain fatty acids (SCFAs) such as isobutyrate, valerate, formate, hexanoate, butyrate, acetate and propionate. These SCFA usually contains an aliphatic tail with 1 to 6 carbons and the concentration of SCFAs in the intestine can range from 10 to 100 mM (Miller et al., 1996). Acetate interacts with the G protein-coupled receptor (GPCR43, 41) in adipose tissue and immune cells to improve ileal motility, increase colonic blood flow, and plays role in adipogenesis and the host immune system (Hong et al., 2005; Brown et al., 2003). Propionate has been proven in both animal and human studies to decrease food intake

and promote fullness by enhancing the satiety hormone leptin and by activating GPCR43, 41 (Xiong et al., 2004; Samuel et al., 2008). Butyrate plays a major role in regulating colonic cell growth and differentiation (Macfarlane et al., 2011). Studies reported that butyrate can induce apoptosis in colon cancer cells by downregulating Bcl-xL, Bcl-2 and cyclin D1 (Thangaraju et al., 2009; Tang et al., 2011). Butyrate can also inhibit colonic cell growth and proliferation. Colorectal cancer cells are more sensitive to SCFA than normal intestinal cells and butyrate can selectively inhibit the growth of colorectal cancer cells. Wang et al. (2020) reported that sodium butyrate selectively decreased the expression of Thioredoxin in CRC but not in normal colon cells. This resulted in upregulated ROS generation, reduced cell growth and apoptosis. The probiotics inhibit the growth of pathogenic bacteria and maintain gut barrier integrity and modulate gut immunity (Loke et al., 2020) (Fig 5.3)

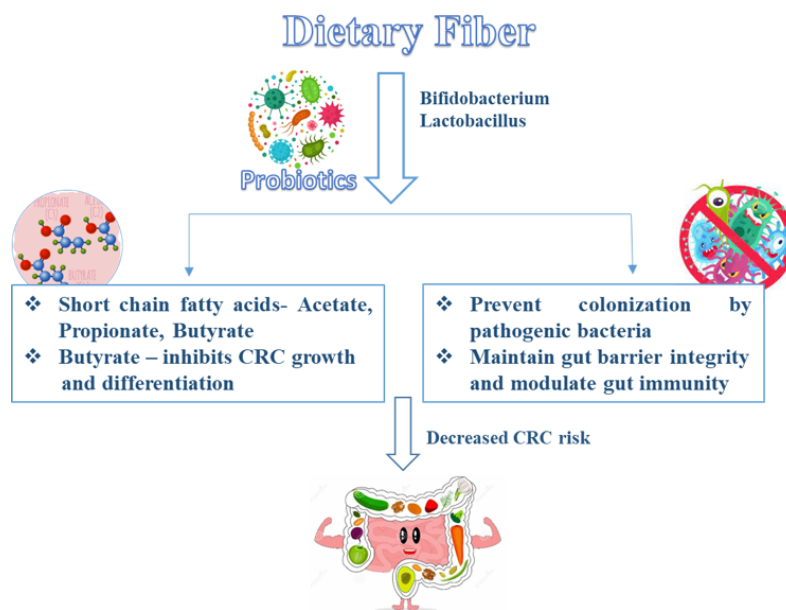


Fig 5.3: Relation between dietary fiber, probiotics and CRC. The intake of dietary fiber and fermentation by gut microbiota resulted in the production of short chain fatty acids which ultimately leads to decreased colorectal cancer risk.

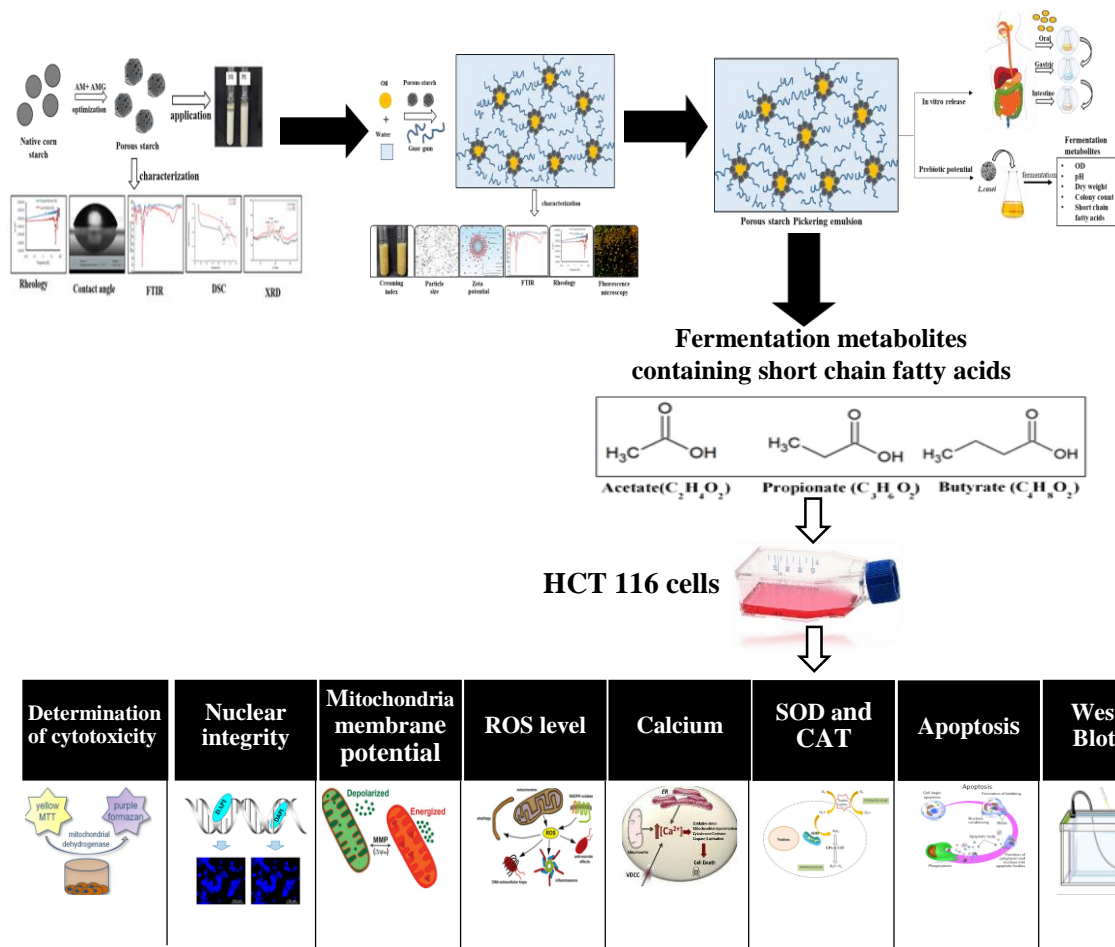
Findings from the previous chapter, chapter 4, ensured the prebiotic properties of Pickering emulsion and colon delivery of curcumin. As evident from the *in vitro* studies, fermentation metabolites rich in SCFA, could be of great potential in maintaining gut homeostasis, and there by aiding in the prevention and management of CRC. Therefore, chapter 5 deals with the studies on investigating the potential of the fermentation metabolites in the management of CRC in HCT 116 cells.

5.1.1. Objectives

In chapter 4 the probiotic fermentation of Pickering emulsion resulted in the production of fermentation metabolites containing short chain fatty acids. The main objective of this chapter is to elucidate the anticancer potential of fermentation metabolites in HCT 116 colon cancer cells by investigating cytotoxicity, nuclear fragmentation, ROS generation, antioxidant activity, mitochondrial membrane potential and apoptosis.

5.2. Materials and Methods

The experimental design for the assessment of the anticancer potential of fermentation metabolites in HCT 116 colon cancer cells



5.2.1. Materials

Dulbecco's modified eagle's media (DMEM), MTT (3-(4, 5-dimethylthiazol-2-yl)-2, 5-diphenyl tetrazolium bromide), Dimethyl sulfoxide (DMSO), 2,7-Dichlorodihydrofluorescein diacetate (DCFH-DA), Rhodamine 123 (Rh123), DAPI ((4',6-diamidino-2-phenylindole) were purchased from Sigma-Aldrich Chemicals (St Louis, MO, USA). Trypsin-EDTA, Antibiotic-antimycotic, Fetal bovine serum (FBS) was procured from Gibco Invitrogen (Carlsbad, CA, USA). Camptothecin was purchased

from Tokyo chemical industry (India) Pvt, Chennai, Tamil Nadu, India. Fura-2, AM, Catalase assay kit, Superoxide Dismutase assay kit and Annexin V – FITC assay kit were purchased from Cayman Chemicals (MI-USA). Primary antibodies (β actin, Bcl 2, Bak, Bax,) and corresponding secondary antibodies for immunoblotting were purchased from Immunotag, St. Louis, USA. cPARP and caspase 3 were procured from Cell signaling, Danvers, Massachusetts, USA. All other chemicals used were of the standard analytical grade.

5.2.2. Methods

5.2.2.1. Cell culture and treatment conditions

HCT 116 (human colon carcinoma) cells were purchased from National Centre for Cell Science, Pune, India. Cells were cultured in DMEM with 10% Fetal bovine serum and 1% antibiotic-antimycotic solution at 37 °C under 5% CO₂. The cells were treated with different concentrations of fermentation metabolites (50 μ L and 100 μ L) for 24 h. Camptothecin (25 μ M) was used as positive control. After incubation, the cells were collected by using Trypsin EDTA solution and used for further studies.

5.2.2.2. Determination of cytotoxicity by MTT assay

The cytotoxic effect of fermentation metabolites was determined by MTT assay. MTT (3-(4, 5-dimethylthiazol-2-yl)-2, 5-diphenyl tetrazolium bromide) measures cellular metabolic activity as an indicator of cell viability. The HCT 116 cells were seeded in 96 well plate and treated with different concentrations of fermentation metabolites (25, 50, 75, 100 and 125 μ L) for a period of 24 h. The images of treated cells at various concentrations were taken by using phase-contrast microscope using NIS-Elements 3.21.00 imaging software (Nikon Eclipse TS 100). The cells treated with media were taken as control. The cells were exposed to MTT reagent (0.2 mg/mL) and incubated for

4 h at 37 °C. The formazan crystals formed were dissolved in DMSO. After incubation for 20 min in a shaker (Orbit plate shaker, Labnet International, USA), the absorbance was read at 570 nm (Synergy 4 Biotek multiplate reader, USA) and the percentage cell viability was calculated (Wilson, 2000).

5.2.2.3. Determination of nuclear integrity by DAPI staining

The DNA was stained with blue fluorescent dye DAPI (4', 6- diamidino-2-phenylindole) to examine the DNA condensation during apoptotic cell death. Briefly, the HCT 116 cells were seeded in 96 well plate and treated with different concentrations of fermentation metabolites (50 µL and 100µL). Camptothecin (25 µM) was used as positive control. The treated cells were stained with 1 µg/mL DAPI dye and incubated for 15 min at 37 °C. The incubated cells were rinsed with PBS (Phosphate- buffered saline) for 2 to 3 times and the fluorescence intensity was measured using a fluorescence microscope (Olympus fluorescence microscope IX83, Olympus corporation of Americas, Center Valley, USA).

5.2.2.4. Wound healing assay

The invasiveness and metastatic potential of cancer cells are correlated with cell migration and motility (Yamazaki et al., 2005). Scratch wound assay was done to analyze the effect of fermentation metabolites on the migration of HCT 116 cells. The HCT 116 cells were seeded on 6 well plate and treated with different concentration of fermentation metabolites (50 µL and 100 µL) for 24 h after creating a wound over the confluent monolayer of cells. Images were taken at 0 and 24 h, and the recover of scratch area was compared. The images were taken using phase-contrast microscope using NIS-Elements 3.21.00 imaging software (Nikon Eclipse TS 100). The results obtained were compared with untreated cells and positive control camptothecin.

5.2.2.5. Measurement of Reactive oxygen species (ROS)

ROS (Reactive oxygen species) are commonly used as mediators in the apoptotic pathway. The cell permeable H₂DCFDA (2,7-Dichlorodihydrofluorescein diacetate) probe, was used to analyze the intracellular ROS, which was transformed into a highly fluorescent 2',7'-dichlorofluorescein (DCF) in the presence of ROS (Yang et al., 2014). Using a cell-permeable H₂DCFDA probe that was intracellularly transformed into a highly fluorescent 2',7'-dichlorofluorescein (DCF) following reaction with ROS, the levels of intracellular ROS were assessed. Briefly, the HCT cells were seeded in 96 well plate and then treated with different concentration of fermentation metabolites. The treated cells were then stained with 20 μM DCFDA and kept at 37 °C for 20 min. The cells were then rinsed with PBS for 2 to 3 times and the fluorescence intensity was measured using a fluorescence microscope (Olympus fluorescence microscope IX83, Olympus corporation of Americas, Center Valley, USA).

5.2.2.6. Determination of antioxidant enzyme activity

5.2.2.6.1. Measurement of Superoxide dismutase (SOD)

Activity of SOD was analyzed by using an SOD assay kit (Cayman chemical company, USA). The kit utilizes a tetrazolium salt for the detection of superoxide radicals generated by hypoxanthine and xanthine oxidase. The absorbance was read at 450 nm using a plate reader.

5.2.2.6.2. Measurement of Catalase (CAT)

Activity of CAT was analyzed using catalase assay kit (Cayman chemical company, USA). The kit utilizes the peroxidatic function of CAT for analyzing enzyme activity. In this method catalase reacts with methanol in presence of an optimal concentration of hydrogen peroxide. The formaldehyde is measured colorimetrically with purpald as

chromogen. Purpald upon oxidation changes from colourless to purple colour. The absorbance was read at 540 nm using a plate reader.

5.2.2.7. Determination of mitochondrial membrane potential by rhodamine 123

The mitochondrial membrane potential was analyzed by staining the HCT-116 cells using a cationic dye Rhodamine 123. In normal cells with polarized mitochondrial membrane, the dye binds and resulted in green fluorescence. Loss of membrane potential resulted in decreased fluorescence as the dye washed out of the membrane. The HCT 116 cells were seeded in 96 well plate and treated with different concentration of fermentation metabolites (50 and 100 μ L). Camptothecin (25 μ M) was used as positive control. The treated cells were stained with 10 μ g/mL rhodamine 123 and incubated for 15 min at 37 $^{\circ}$ C. The incubated cells were rinsed with PBS for 2 to 3 times and the fluorescence intensity was measured using fluorescence microscope (Olympus fluorescence microscope IX83, Olympus corporation of Americas, Center Valley, USA).

5.2.2.8. Determination of calcium by Fura- 2, AM

The amount of calcium was determined by Fura -2 dye. Briefly, the HCT 116 cells were seeded in 96 well plate and treated with different concentration of fermentation metabolites. After treatment the cells were stained with 5 μ M Fura 2-AM dye and kept in dark for 45 min at 37 $^{\circ}$ C. This is followed by three times wash with HBSS and cells were resuspended in plain DMEM medium. The fluorescence intensity was measured using fluorescence microscope.

5.2.2.9. Apoptosis assay by flow cytometry

The effect of fermentation metabolites on apoptosis in HCT 116 cells was analyzed using Annexin V-fluorescein isothiocyanate (FITC)/propidium iodide staining assay kit (Cayman chemical company, USA). This kit employs a FITC-conjugated annexin V as

a probe for phosphatidylserine on the outer membrane of apoptotic cells. Propidium iodide (PI) is used as marker of cell membrane permeability. The HCT 116 cells were seeded in a 6 well plate and treated using fermentation metabolites. After 24 h, the cells were trypsinized, washed with 10% HBSS, centrifuged at 3000 rpm for 5 min and flick out supernatant. The cells were suspended in binding buffer and thoroughly mixed. Centrifuged again for 5 min and resuspend the cells in Annexin V FITC/ PI staining solution, mixed well and incubated in dark for 15 min at room temperature. After incubation add binding buffer and then analyzed by flow cytometry using Becton Dickinson fluorescence-activated cell sorting (BD FACS) Aria II (BD Biosciences) and fluorescence intensities were analyzed by BD FACS DIVA software.

5.2.2.10. Immunoblot analysis

The HCT 116 cells were grown on T25 flask and treated with various concentrations of fermentation metabolites. After treatment, the cells were harvested and lysed in ice-cold lysis buffer containing protease inhibitor cocktail and the homogenate was centrifuged at 10,000×g for 15 min at 4 °C. The total protein concentration in the supernatant was quantified using a BCA protein assay kit (Thermo scientific, Pierce™ BCA protein assay kit, USA) and the protein concentration were equalized and stored at 80 °C until use. The expression of proteins β -actin, Bcl-2, c-PARP, Bax, Bak, Caspase-3, were analyzed by immunoblotting. The protein samples along with loading dye were heated in dry bath heat blocks (Benchmark, USA) for 5 min at 95 °C. Proteins were separated by SDS PAGE in 10% SDS polyacrylamide gel. Samples (25 μ L) were loaded into each well. The protein in the gel was transferred to a PVDF transfer membrane (Immobilon P™, Millipore154 R, USA) using Trans-Blot Turbo™ transfer system (Bio-Rad Laboratories, Germany). After transfer of proteins the membrane was blocked in 5% skimmed milk in TBST (Tris-buffered saline with 0.1% Tween 20 detergent) for 1 h at room temperature,

membrane was washed 3 times with TBST followed by incubation with primary antibodies (β -actin, Bcl-2, c-PARP, Bax, Bak, Caspase-3) in the ratio (1:1000) with gentle agitation at 4 °C overnight. The incubation is followed by three time wash with TBST, and then incubated with HRP linked secondary antibodies (1:2000) at 4 °C. The blot bound antibodies were detected using SuperSignal™ West Pico PLUS chemiluminescent (ECL) horseradish peroxidase (HRP) substrate, ThermoScientific, Rockford, U.S.A and measured by densitometry using a ChemiDoc XRS digital imaging system and the Multi- Analyst software from Bio-Rad Laboratories (United States).

5.2.2.11. Statistical analysis

Data represented as mean \pm standard deviations of experiments in duplicates. One-way ANOVA was used for analyzing the results using Graph Pad Prism 9.3.0 software and the significance was accepted at $P \leq 0.05$.

5.3. Results and discussion

The fermentation metabolites (FM) as described in the previous chapter was found to contain promising SCFA which was further investigated for its potential in prevention and management of CRC using HCT 116 cells.

5.3.1. Determination of cytotoxicity of fermentation metabolites(FM) by MTT

Assay

The cytotoxic effect of FM was determined by MTT assay. MTT measures cellular metabolic activity as an indicator of cell viability. In live cells, MTT, the yellow-coloured dye is changed to purple formazan which was measured calorimetrically. The OD of the untreated cell was assumed to be 100%, and the percentage reduction of OD in the treated cells was then calculated. After growing the cells for 24 h, they were treated with different concentrations (25- 125 μ L) of FM. From the results it was found that the FM

exert cytotoxic effects against HCT 116 colon cancer cells, in a dose dependent manner (Fig 5.4) and the cell viability was decreased by 88, 73, 57, 50 and 8 % respectively.

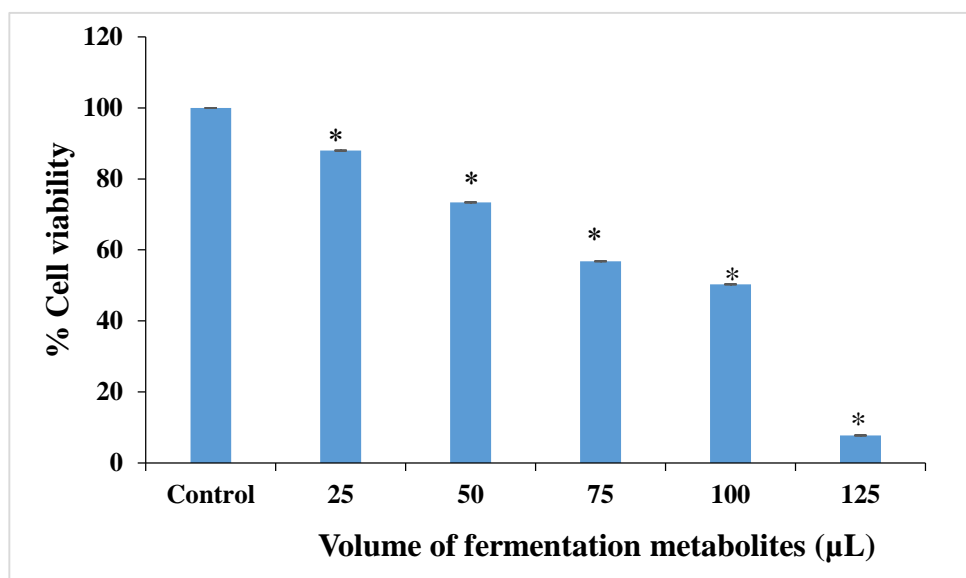


Fig 5.4: MTT cytotoxicity assay of fermentation metabolites (FM). HCT 116 cells were treated with various concentration of fermentation metabolites (25, 50, 75, 100 and 125 µL) for a period of 24 hours and the cytotoxicity of FM was determined by MTT assay. * $p \leq 0.05$ versus control.

Morphological analysis of HCT 116 cells treated with different concentrations of FM was observed by using phase contrast microscopy, as shown in the Fig 5.5. From the figure it is clear that the morphology of cell has changed as the concentration of FM has increased. At low concentrations (25 and 50 µL) the morphology of cells did not alter much and they appeared similar to that of control cells. But at higher concentrations especially at (100 and 125 µL), the cell number was reduced and cells shape was distorted indicating the cytotoxicity activity of FM against HCT 116 cells.

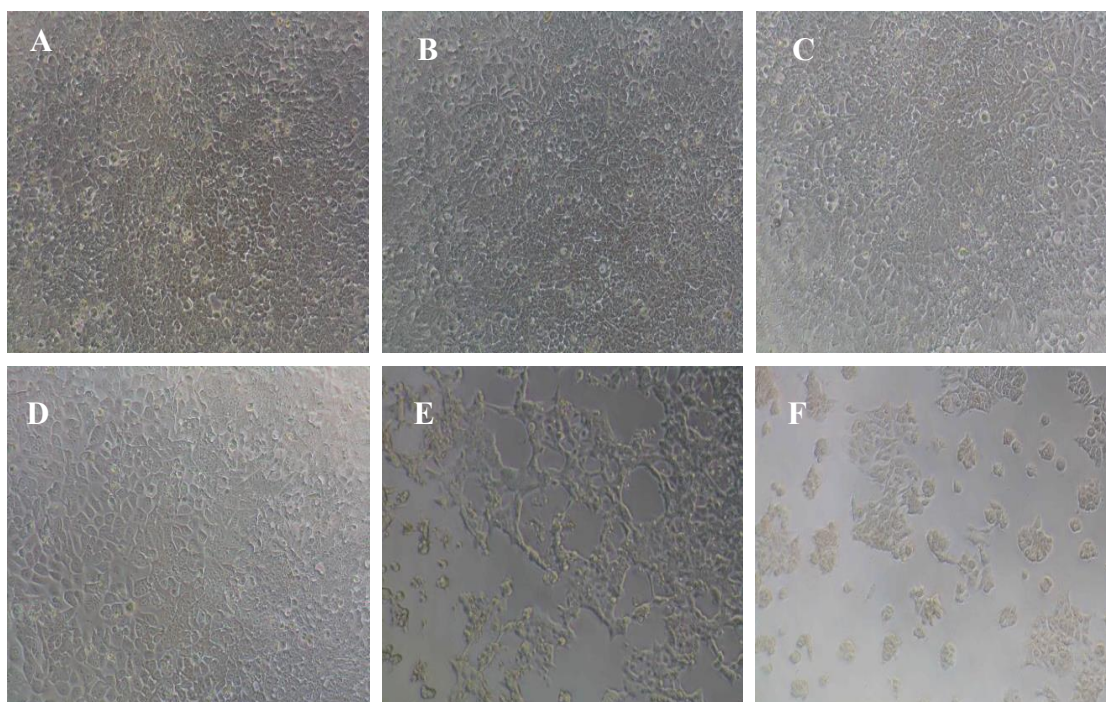


Fig 5.5: Morphological analysis of HCT 116 cells treated with different concentrations of FM by phase contrast microscopy. A - Untreated; B – 25 μ L; C – 50 μ L; D – 75 μ L; E - 100 μ L; F – 125 μ L.

The cytotoxicity studies clearly demonstrated that cell viability decreased significantly in FM treated cells in dose dependent manner. Two concentration-50 μ L (exhibits 75% cell viability) and 100 μ L (exhibits 50% cell viability) was used for further studies. After cytotoxicity studies various parameters were analyzed that results in FM treated cell death in following sections.

5.3.2. FM treatment induced chromosome condensation

Nuclear changes such as DNA fragmentation and chromatin condensation are the hall mark of apoptosis. In order to examine formation of apoptotic bodies, HCT 116 cells were treated with FM and then stained with DAPI (4',6-diamidino-2-phenylindole). DAPI is a blue fluorescent dye that fluorescence upon binding to AT regions of double stranded DNA. In cells with damaged cell membrane more DAPI enters the cell and

stains blue colour. Also, the chromosome condensation and fragmentation can be visualized (Atale et al., 2014). Camptothecin (25 μ M) was used as positive control. From the Fig 5.6, it is clear that that compared to intact and regular nuclei of untreated cells, the cells treated with FM showed higher degree of chromatin condensation, which is the hall mark of apoptosis (Maraming et al., 2019).

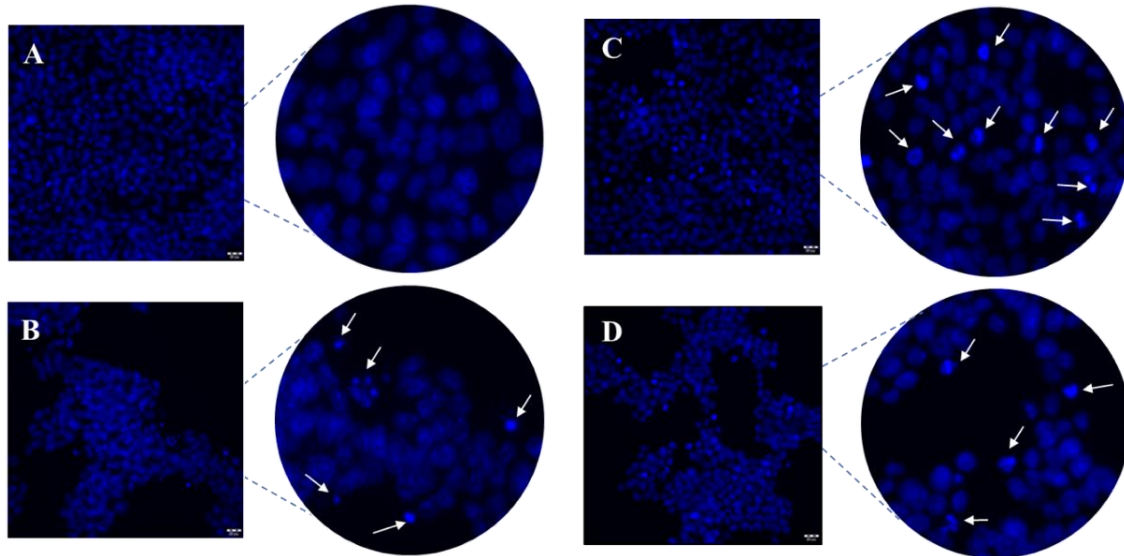


Fig 5.6: DAPI staining in HCT 116 cells. Effect of FM on DNA damage in HCT 116 cells. The arrow indicates chromatin condensation which is a hall mark of apoptosis. A - Untreated; B - Camptothecin (25 μ M); C - 50 μ L FM; D - 100 μ L FM.

5.3.3. Wound Healing Assay

Depending on the type of cell and level of differentiation, cancer cells can migrate in different ways. Cell migration is a crucial stage in tumour invasion and metastasis (Dangroo et al., 2017). To investigate this, wound healing assay was done to examine the effects of FM on HCT 116 cell migration. HCT 116 cells were scratched and treated with FM for 24 h and the area of wound was calculated using Image J software (Fig 5.7).

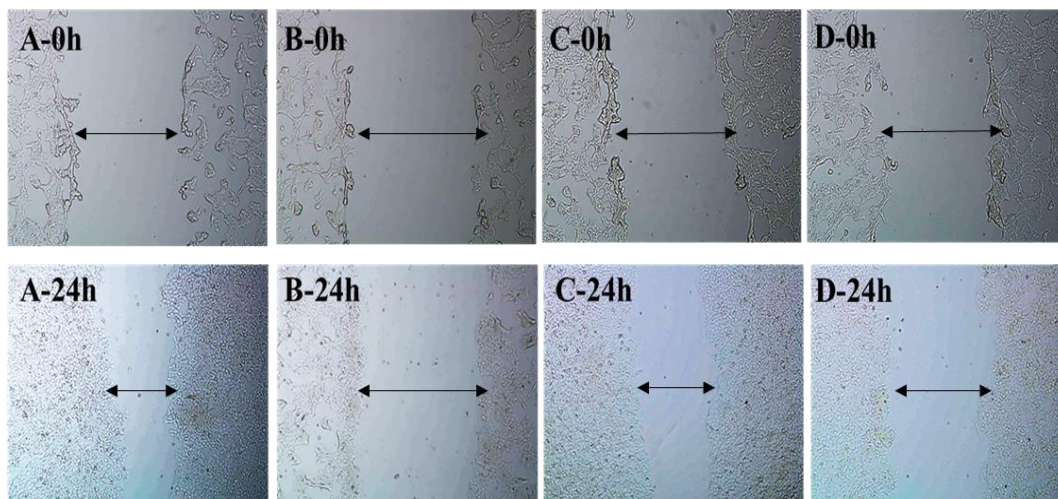


Fig 5.7: *In vitro* wound healing assay. HCT 116 cells were scratched and treated with different concentrations of sample for 24 h and area of wound was measured at 0 and 24 h using Image J software. A - Untreated; B - Camptothecin (25 μ M); C – 50 μ L FM; D – 100 μ L FM.

The percentage increase in cell migration was measured as how much scratch area was recovered in comparison with that of 0 h. Higher the cell density in the scratch area, higher will be the migration. The results were plotted as percentage wound closure which is given in Fig 5.8. After incubation for 24 h, cells in untreated group started growing in the wound area (53%), whereas treatment of cells with FM reduced the cell migration in the wound area significantly and the cell density was severely reduced as the concentration of FM was increased (39 and 28 % respectively for 50 and 100 μ L). The percentage increase in cell migration after 24 h of incubation with the positive control camptothecin was 18%. Results demonstrated that FM containing short chain fatty acids blocked the migration of HCT 116 cell lines.

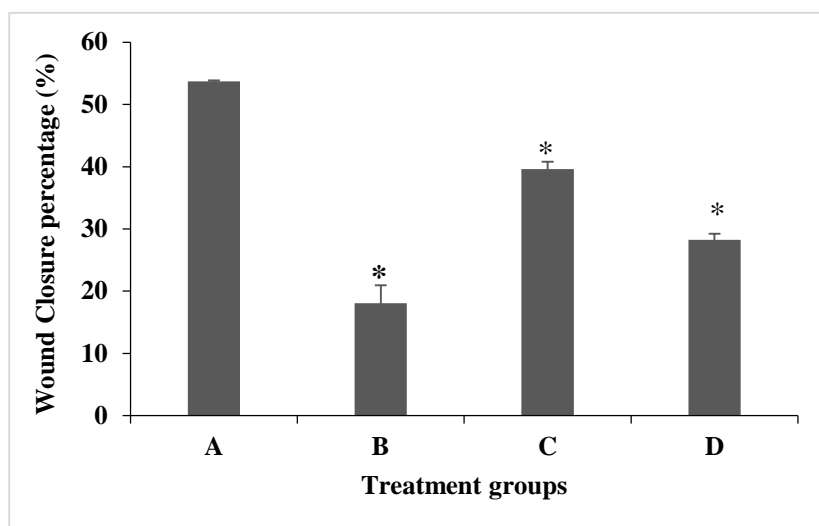


Fig 5.8: Wound closure percentage of FM in HCT 116 cells. A - Untreated; B – Camptothecin (25 μ M); C – 50 μ L FM; D – 100 μ L FM.

5.3.4. Measurement of ROS by DCFDA staining

Generation of reactive oxygen species (ROS) is one of the main factors that lead to apoptosis. Therefore, intracellular ROS level were estimated by DCFH-DA (Dichlorodihydro-fluorescein diacetate) staining assay in order to understand the inducing mechanism of increased cellular cytotoxicity by the FM. DCFH-DA is a non-fluorescent dye, but after entering the cell, cellular esterase cleaves the acetyl group and in the presence of ROS, it is oxidized to fluorescent molecule, DCF (2',7'-dichlorofluorescein) (Sen et al., 2000; Nova et al., 2020). The DCF emits green fluorescence which was measured and the amount of fluorescence produced is directly linked to ROS generation. From the Fig 5.9a, it is clear that cells treated with FM showed a higher fluorescence, which indicates a higher ROS production compared to untreated cells. The analysis of fluorescence intensity (Fig 5.9b) showed that the fluorescence increased with increase in concentration of FM indicating higher generation of ROS.

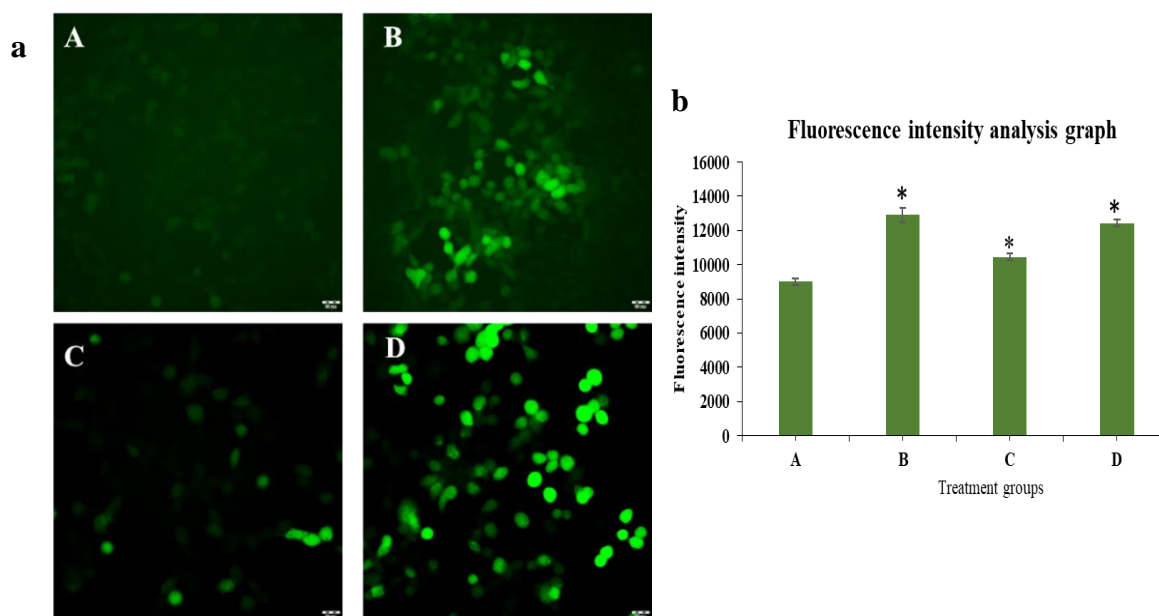


Fig 5.9: (a) Determination of ROS production in HCT 116 cell lines upon pretreatment with FM via fluorescence microscopy. (b) Fluorescence intensity analysis graph demonstrating increase in ROS in treated groups. * $p \leq 0.05$ versus untreated. A - Untreated; B – Camptothecin (25 μM); C – 50 μL FM; D – 100 μL FM.

Studies reported that short chain fatty acids induce ROS production. Arun et al. (2018) reported that fermentation supernatant obtained from dietary fibre of *Musa paradisiaca* inflorescence containing short chain fatty acid induces ROS production. Acetate exhibits cytotoxicity and induce ROS production in thymic origin tumor cells (Pandey et al., 2019). Sodium propionate and butyrate also showed increased ROS production which ultimately triggers apoptosis (Pant et al., 2017; Park et al., 2021). The results clearly demonstrated that FM containing acetate, propionate and butyrate increased ROS production leading to the onset of apoptosis in HCT 116 cells in the present study.

5.3.5. FM treatment reduced antioxidant enzyme activity (SOD and CAT)

SOD (Superoxide dismutase) and CAT (Catalase) are first line defense antioxidant enzymes. These enzymes scavenge reactive oxygen species and help to maintain cellular homeostasis. SOD is the most potent antioxidant in the cell and first enzyme involved in detoxification. It catalyses the dismutation of two superoxide anion molecules (O_2^-) into

hydrogen peroxide (H₂O₂) and molecule oxygen (O₂), hence making it less hazardous (Ighodaro et al., 2018; Fridovich. 1995). SOD is a metalloenzyme that requires metal ions such as copper, zinc, manganese, iron for its activity (Gill et al., 2010). The antioxidant enzyme CAT is found in every biological tissue that uses oxygen. The enzyme catalyses the breakdown or reduction of hydrogen peroxide (H₂O₂) to water and molecular oxygen and uses either iron or manganese as cofactor (Chelikani et al., 2004; Marklund. 1984). The activity of FM on antioxidant enzymes was studied to understand the fate of SOD and CAT on treatment with FM. The results are expressed as percentage inhibition (Fig 5. 10) for both the enzymes and the cells on pretreatment with the FM resulted in inhibition of SOD and CAT activity in a dose dependent manner.

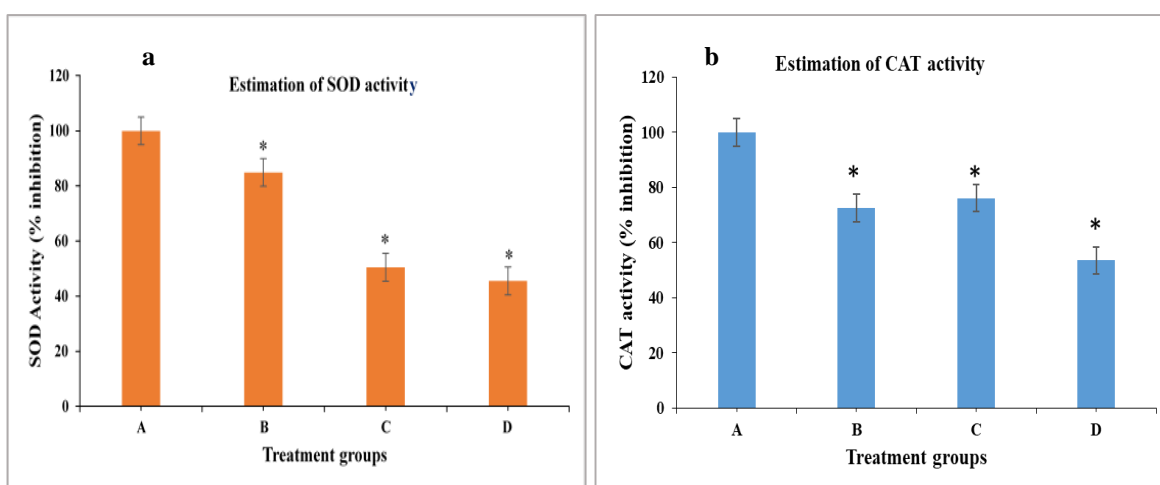


Fig 5.10: Effect of FM on (a) SOD activity and (b) CAT activity in HCT 116 cell. *p≤ 0.05 versus untreated. A - Untreated; B – Camptothecin (25 μM); C – 50 μL FM; D – 100 μL FM.

Increased ROS production in cells often resulted in an elevated oxidative stress. The level of stress developed can be determined by the antioxidant activity of enzymes SOD and CAT. Excess ROS generation resulted in decreased level of antioxidant activity of SOD and CAT (Shi et al., 2016; Ali et al., 2021). The reduction in innate antioxidant enzyme

activity such as SOD and CAT may be correlated with the increased oxidative stress caused by excessive accumulation of ROS.

5.3.6. FM treatment induced loss of mitochondrial membrane potential (MMP)

Cellular homeostasis is significantly influenced by mitochondria. Mitochondria are commonly known as the power house of the cell because they act as energy source for cells by synthesizing ATP. Mitochondria are also crucial for maintaining cell survival. It is also involved in two types of neuronal death, necrosis and apoptosis (Nicholls et al., 2000). High ROS generation in cells may results in compromised membrane potential in mitochondria and to investigate this, we further analyzed the mitochondrial membrane potential of cells treated with FM using Rhodamine 123. Rhodamine 123 is a cationic fluorescent dye which accumulates at matrix of intact mitochondria. In depolarized mitochondria the dye will released into the cytosolic compartment resulting in decreased fluorescence intensity (Toescu, et al., 2000). The cells were treated with different concentrations of FM and then stained with Rhodamine 123. The mitochondrial membrane potential was evaluated using fluorescence microscopy (Fig 5.11a) and the amount of fluorescence produced is directly linked to membrane potential.

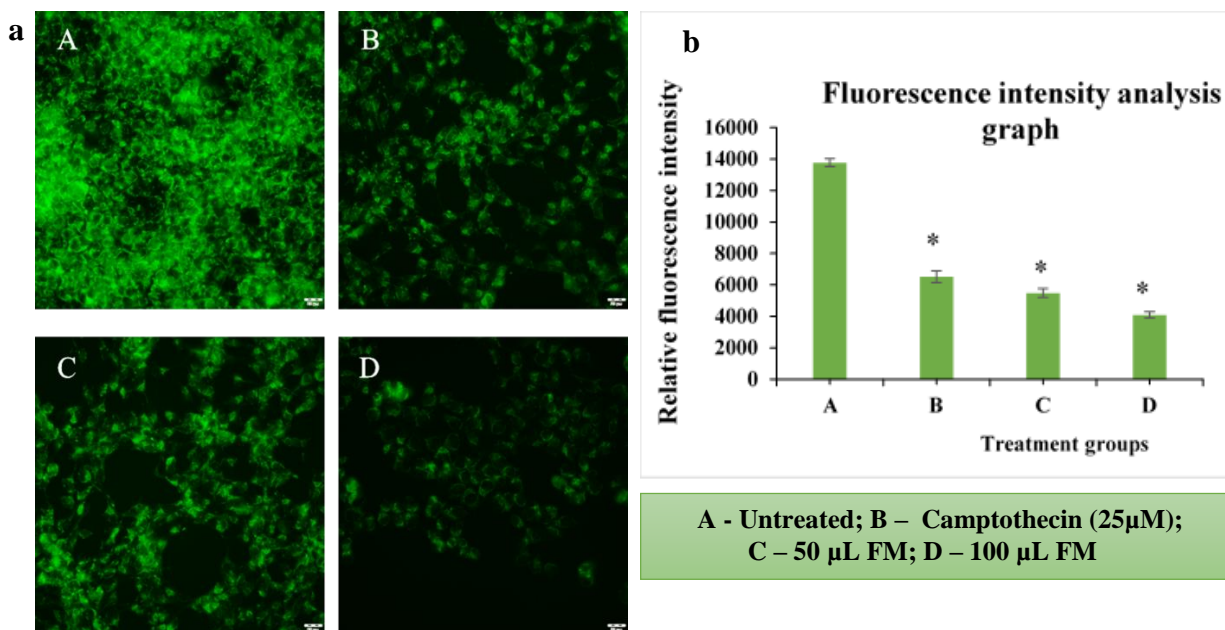


Fig 5.11: (a) Determination of MMP in HCT 116 cell upon pretreatment with FM. (b) Fluorescence intensity analysis graph demonstrating loss of mitochondrial membrane potential in treated groups. * $p \leq 0.05$ versus untreated. A - Untreated; B – Camptothecin (25 μM); C – 50 μL FM; D – 100 μL FM.

The untreated cells showed higher fluorescence intensity due to intact mitochondrial membrane. But in cells treated with FM, the fluorescence intensity decreased in dose dependent manner due to loss of membrane potential (Fig 5.11b). Studies reported that ROS generation can lead to dysfunction of mitochondria which ultimately leads to apoptosis (Witayateeraporn et al., 2022; Karnan et al., 2020). From the results it is clear that the FM disrupt mitochondrial membrane potential which triggers cellular death by apoptosis.

5.3.7. Measurement of Calcium by Fura-2, AM

Calcium plays important role in apoptosis induction and apoptotic signalling pathway modulation. An elevated calcium level was linked to apoptosis brought on by various toxic insults. Calcium was measured using Fura-2, AM. Fura-2, AM (acetoxymethyl ester), is a membrane permeable derivative of fura-2, which is a calcium indicator. It is

an aminopolycarboxylic acid fluorescent dye which binds to free intracellular calcium and the amount of fluorescence will be proportional to calcium concentration (Martinez et al., 2017). HCT 116 cells were pretreated with FM followed by staining with Fura -2, AM, and the fluorescence was measured (Fig 5.12a). From the images it is clear that FM treated cells showed higher fluorescence intensity compared to untreated cells (Fig 5.12b). The results clearly demonstrated that cells treated with FM showed increase in intracellular calcium level as evidenced from increased fluorescence intensity.

Loss of mitochondrial membrane potential or mitochondrial dysfunction might lead to imbalance of cytoplasmic Ca^{2+} homeostasis. The overload of intracellular calcium leads to opening of mitochondrial permeability transition pore (PTP), which resulted in Ca^{2+} efflux to cytoplasm, swelling of mitochondria and apoptosis (Foster et al., 2006; Qin et al., 2008; Wang et al., 2020). In our study, loss of membrane potential in FM treated cells leads to high cellular calcium resulted in high fluorescence intensity whereas untreated cells with intact membrane showed lower fluorescence.

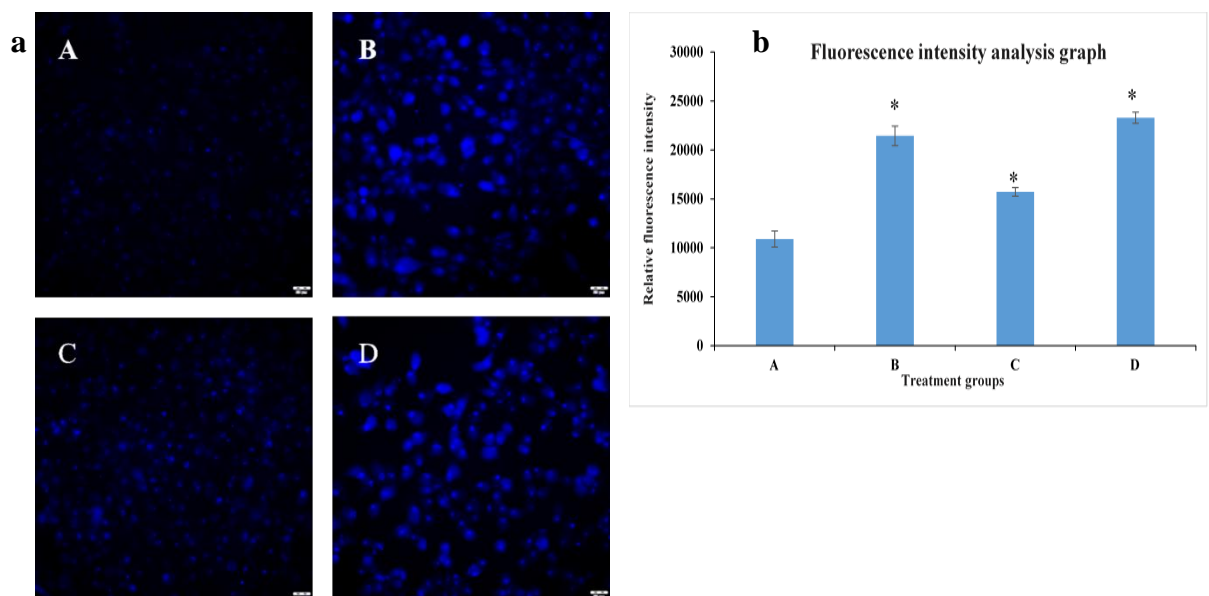


Fig 5.12: (a) Measurement of Calcium in HCT 116 cell lines upon pretreatment with FM. (b) Fluorescence intensity analysis graph demonstrating increase in Calcium in treated groups. * $p \leq 0.05$ versus untreated. A - Untreated; B – Camptothecin (25 μM); C – 50 μL FM; D – 100 μL FM.

5.3.8. Apoptosis- Annexin V-FITC

To confirm cell death, we studied apoptosis by Annexin V FITC assay kit. The redistribution of phosphatidyl serine and phosphatidyl ethanolamine, which are membrane phospholipids, to outer leaflet of membrane is one of the hall marks of apoptosis. Annexin V, phospholipid binding protein, was conjugated with FITC, act as probe for phosphatidylserine residues located on outer plasma membrane. The apoptotic cells bounded with fluorochrome labeled Annexin V was analyzed using flow cytometry. Briefly, the HCT 116 cells were treated with different concentrations of FM for 24h. Flow cytometry analysis showed that the rate of apoptosis increased in FM treated cells in dose dependent manner (Fig 5.13a). The early and late apoptotic rate was determined and expressed in percentage cell number (Fig 5.13b).

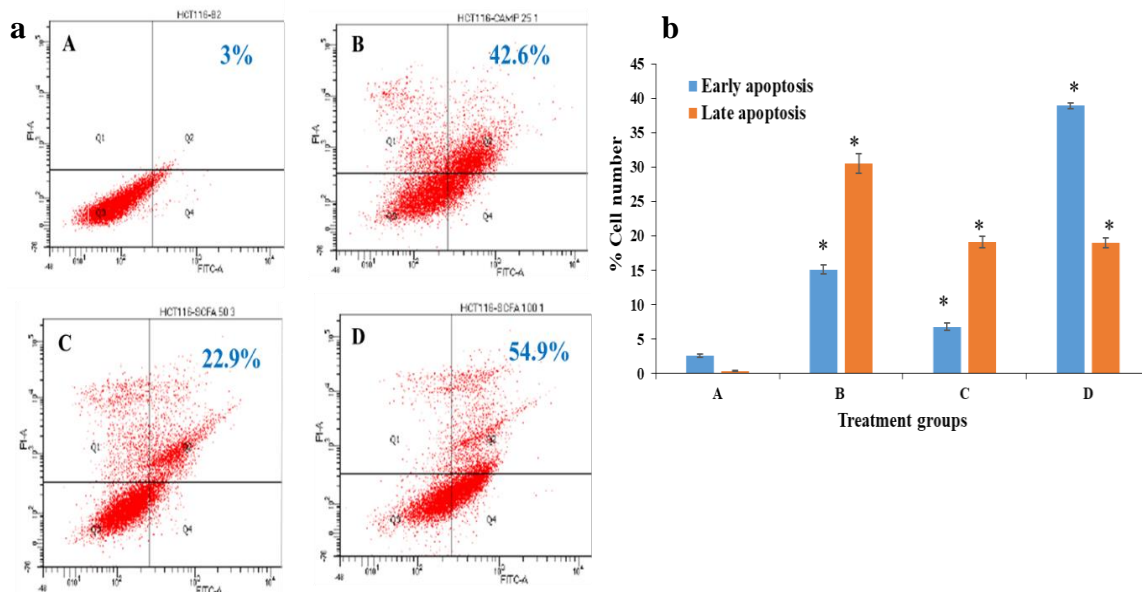


Fig 5.13: (a) Effect of FM on HCT 116 cell apoptosis by flow cytometry. (b) The apoptosis rate was expressed as % cell number. * $p \leq 0.05$ versus untreated. A - Untreated; B - Camptothecin (25 μ M); C - 50 μ L FM; D - 100 μ L FM.

The percentage apoptotic cells of untreated cells were found as 3%, but in the case of treated cells the apoptotic cells increased from 22.9% to 54.9%, for low and high concentrations of FM respectively. Studies reported that short chain fatty acids produced from the fermentation of dietary fiber can result in prevention of colon cancer. Among short chain fatty acids, butyrate can induce DNA fragmentation and apoptosis (Zeng et al., 2015; Zeng et al., 2017). Butyrate also inhibits invasion and growth of colorectal cancer cells while also inducing apoptosis (Bordonaro et al., 2015; Hu et al., 2015; McNabney et al., 2017; Zeng et al., 2019). Thus, it is evident that the FM treatment in HCT 116 cells leads to excess ROS generation, loss of mitochondrial membrane potential which ultimately leads to apoptosis.

5.3.9. Western blotting

The results from different assays demonstrated that FM containing short chain fatty acids exhibit significant anticancer activities by inducing apoptosis. The expression of some of the major proteins in apoptotic pathway was analyzed using western blot. Apoptosis or programmed cell death leads to many morphological changes such as nuclear, cytoplasmic and mitochondrial changes. From the above discussed experiments it was found that the cell death follows mitochondrial or intrinsic pathway mediated apoptosis. So the expression of some of the proteins associated in this pathway was investigated. The expression of various proteins like Bcl-2, c-PARP, Bax, Bak, and Caspase-3 was studied. The intrinsic apoptotic pathway is mainly regulated by BCL2 family of pro and anti-apoptotic proteins. Bcl 2 is an antiapoptotic protein, prevent apoptosis either by sequestering caspase or by inhibiting the release of cytochromes C from mitochondria. The proapoptotic proteins like Bax and Bak can initiate the release of cytochrome C from mitochondria, which ultimately leads to caspase activation (Wolf et al., 2022). Caspases 3 is an effector caspase which helps in the activation of apoptosis. Activated Caspase 3

can cleave many cellular substrates like PARP (poly ADP-ribose polymerase), resulted in cleaved PARP (c-PARP). PARP cleavage, which is catalysed by caspase-3, is regarded as one of the biomarkers for the detection of apoptosis and has a positive regulatory role in the apoptosis of numerous cell lines (Qiu et al., 2019).

Briefly, HCT 116 were treated with different concentration of FM and the expression of different proteins like Bax, Bak, Caspase-3, Bcl-2 and c-PARP were analyzed (Fig 5.14). The expression of proteins like Bax, Bak, Caspase-3 and c-PARP was increased and antiapoptotic protein Bcl-2 was decreased after treatment with FM in HCT 116 cell. The activation of Bax/Bak might initiated the release of cytochrome C from mitochondria. Cytochrome C in the cytosol activates Caspase 3 which further activates PARP cleavage. Mondal & Bennett. (2016) reported that resveratrol along with antioxidant sorafenib induced apoptosis in MCF7 breast cancer cells through ROS generation and by PARP and caspase 3 cleavage. Ropivacaine activates caspase 3 and PARP, which inhibits proliferation and promotes apoptosis in hepatocellular carcinoma (HCC) cells (Wang et al., 2019). Thus in present study treatment with FM activates proapoptotic proteins Bax/Bak, release of Cytochrome C from mitochondria, caspase 3 activation, which further activates PARP by cleavage (cPARP) and promotes apoptosis in HCT 116 cancer cells.

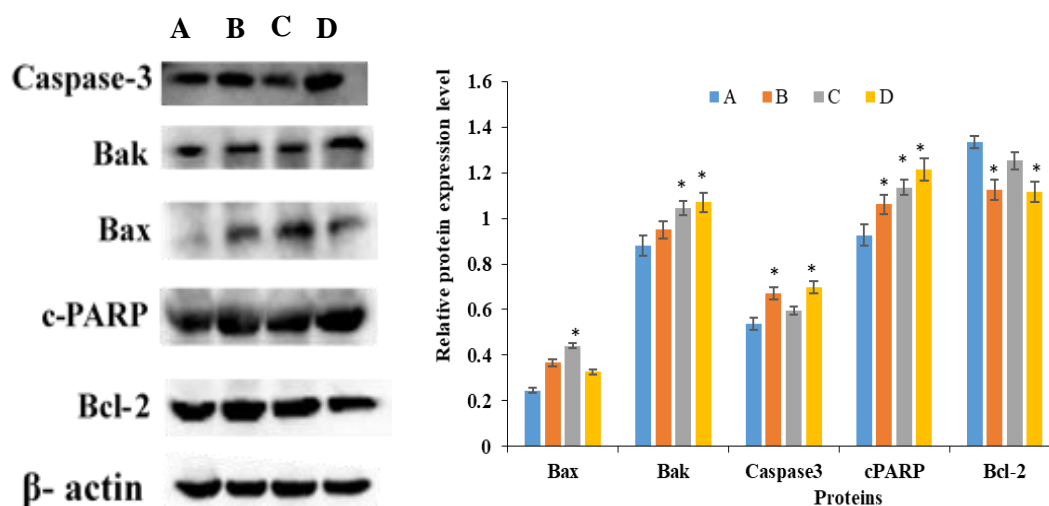


Fig 5.14: Effect of FM on expression of proteins involved in apoptosis in HCT 116 cells. The results were compared with that of untreated cells and positive control camptothecin. A- Untreated, B- camptothecin (25 μM), C- 50 μL FM, D – 100 μL FM. (a) Protein expression level and (b) Quantification of expressed proteins Bcl-2, c-PARP, Bax, Bak and caspase 3. * $p \leq 0.05$ versus untreated.

5.4. Conclusion

The anticancer potential of fermentation metabolites in HCT 116 cells were explored and found that fermentation metabolites containing short chain fatty acids exhibited cytotoxic effects. The metabolites induced DNA damage and effectively obstructed the motility and migration proficiency of HCT 116 cell lines. Suppression of antioxidant enzymes like SOD and CAT, over production of ROS and calcium levels, loss of mitochondrial membrane integrity, ultimately induced apoptosis in HCT 116 cells. The apoptosis was further confirmed by flow cytometry analysis. The protein expression studies confirmed that the fermentation metabolites can induce apoptosis by downregulating expression of Bcl-2 family protein and upregulating expression of Bax, Bak, caspase-3 and c-PARP. Thus, the present study established the fact that the probiotic fermentation metabolites of O/W Pickering emulsion of curcumin loaded flax seed oil with porous starch as Pickering particles, distinctively induced apoptosis in HCT 116 cells. This could be a potential

strategy for delivering bioactive phytochemicals and prebiotics to the gut for maintaining homeostasis and to prevent as well as manage the onset of chronic diseases.

5.5. Summary

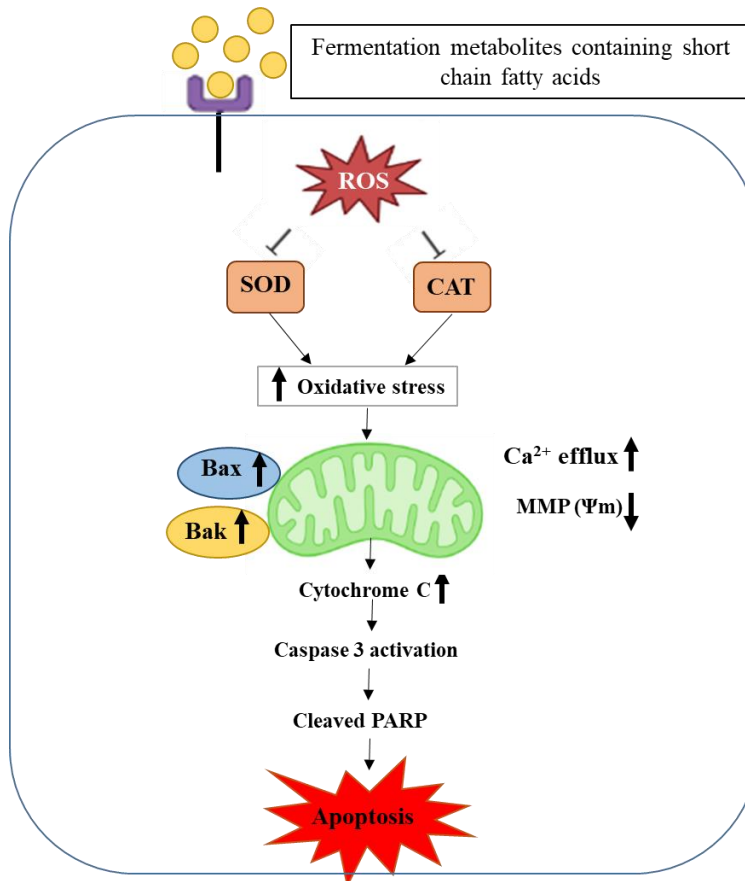


Fig 5.15: Schematic representation of possible mechanism by which FM containing short chain fatty acids regulate signaling events to induce cell death by apoptosis in HCT 116 cells

5.6. References

- Ali, I., Yang, M., Wang, Y., Yang, C., Shafiq, M., Wang, G., & Li, L. (2021). Sodium propionate protect the blood-milk barrier integrity, relieve lipopolysaccharide-induced inflammatory injury and cells apoptosis. *Life Sciences*, 270, 119138.
- American Cancer Society. *Cancer Facts & Figures 2023*.
- Arun, K. B., Madhavan, A., Reshmitha, T. R., Thomas, S., & Nisha, P. (2018). Musa paradisiaca inflorescence induces human colon cancer cell death by modulating cascades of transcriptional events. *Food & Function*, 9(1), 511-524.
- Atale, N., Gupta, S., Yadav, U. C. S., & Rani, V. (2014). Cell-death assessment by fluorescent and nonfluorescent cytosolic and nuclear staining techniques. *Journal of microscopy*, 255(1), 7-19.
- Bordonaro, M., & Lazarova, D. L. (2015). CREB-binding protein, p300, butyrate, and Wnt signaling in colorectal cancer. *World journal of gastroenterology: WJG*, 21(27), 8238.
- Brown, A. J., Goldsworthy, S. M., Barnes, A. A., Eilert, M. M., Tcheang, L., Daniels, D., ... & Dowell, S. J. (2003). The Orphan G protein-coupled receptors GPR41 and GPR43 are activated by propionate and other short chain carboxylic acids. *Journal of Biological Chemistry*, 278(13), 11312-11319.

- Burkitt, D. P., Walker, A. R. P., & Painter, N. S. (1972). Effect of dietary fibre on stools and transit-times, and its role in the causation of disease. *The Lancet*, *300*(7792), 1408-1411.
- Butt, M. S., & Sultan, M. T. (2009). Green tea: nature's defense against malignancies. *Critical reviews in food science and nutrition*, *49*(5), 463-473.
- Chelikani, P., Fita, I., & Loewen, P. C. (2004). Diversity of structures and properties among catalases. *Cellular and Molecular Life Sciences CMLS*, *61*, 192-208.
- Dangroo, N. A., Singh, J., Rath, S. K., Gupta, N., Qayum, A., Singh, S., & Sangwan, P. L. (2017). A convergent synthesis of novel alkyne–azide cycloaddition congeners of betulinic acid as potent cytotoxic agent. *Steroids*, *123*, 1-12.
- Foster, K. A., Galeffi, F., Gerich, F. J., Turner, D. A., & Müller, M. (2006). Optical and pharmacological tools to investigate the role of mitochondria during oxidative stress and neurodegeneration. *Progress in neurobiology*, *79*(3), 136-171.
- Fridovich, I. (1995). Superoxide radical and superoxide dismutases. *Annual review of biochemistry*, *64*(1), 97-112
- Gill, S. S., & Tuteja, N. (2010). Reactive oxygen species and antioxidant machinery in abiotic stress tolerance in crop plants. *Plant physiology and biochemistry*, *48*(12), 909-930.
- Haas, P., Machado, M. J., Anton, A. A., Silva, A. S. S., & De Francisco, A. (2009). Effectiveness of whole grain consumption in the prevention of colorectal cancer: meta-analysis of cohort studies. *International journal of food sciences and nutrition*, *60*(sup6), 1-13.

- Hong, Y. H., Nishimura, Y., Hishikawa, D., Tsuzuki, H., Miyahara, H., Gotoh, C., ... & Sasaki, S. (2005). Acetate and propionate short chain fatty acids stimulate adipogenesis via GPCR43. *Endocrinology*, *146*(12), 5092-5099.
- Hu, S., Liu, L., Chang, E. B., Wang, J. Y., & Raufman, J. P. (2015). Butyrate inhibits pro-proliferative miR-92a by diminishing c-Myc-induced miR-17-92a cluster transcription in human colon cancer cells. *Molecular cancer*, *14*(1), 1-15.
- Ighodaro, O. M., & Akinloye, O. A. (2018). First line defence antioxidants-superoxide dismutase (SOD), catalase (CAT) and glutathione peroxidase (GPX): Their fundamental role in the entire antioxidant defence grid. *Alexandria journal of medicine*, *54*(4), 287-293.
- Karanam, G., & Arumugam, M. K. (2020). Reactive oxygen species generation and mitochondrial dysfunction for the initiation of apoptotic cell death in human hepatocellular carcinoma HepG2 cells by a cyclic dipeptide Cyclo (-Pro-Tyr). *Molecular Biology Reports*, *47*(5), 3347-3359.
- Kumar, V. S., Rijo, J., & Sabitha, M. (2018). Guar gum and Eudragit® coated curcumin liquid solid tablets for colon specific drug delivery. *International journal of biological macromolecules*, *110*, 318-327.
- Loke, Y. L., Chew, M. T., Ngeow, Y. F., Lim, W. W. D., & Peh, S. C. (2020). Colon carcinogenesis: The interplay between diet and gut microbiota. *Frontiers in Cellular and Infection Microbiology*, *10*, 603086.
- MacDonald, R. S., & Wagner, K. (2012). Influence of dietary phytochemicals and microbiota on colon cancer risk. *Journal of agricultural and Food Chemistry*, *60*(27), 6728-6735.

- Macfarlane, G. T., & Macfarlane, S. (2011). Fermentation in the human large intestine: its physiologic consequences and the potential contribution of prebiotics. *Journal of clinical gastroenterology*, *45*, S120-S127.
- Marklund, S. L. (1984). Extracellular superoxide dismutase and other superoxide dismutase isoenzymes in tissues from nine mammalian species. *Biochemical Journal*, *222*(3), 649-655.
- Maraming, P., Klaynongsruang, S., Boonsiri, P., Peng, S. F., Daduang, S., Leelayuwat, C., ... & Daduang, J. (2019). The cationic cell-penetrating KT2 peptide promotes cell membrane defects and apoptosis with autophagy inhibition in human HCT 116 colon cancer cells. *Journal of Cellular Physiology*, *234*(12), 22116-22129.
- Martínez, M., Martínez, N. A., & Silva, W. I. (2017). Measurement of the intracellular calcium concentration with fura-2 AM using a fluorescence plate reader. *Bio-protocol*, *7*(14), e2411-e2411.
- McNabney, S. M., & Henagan, T. M. (2017). Short chain fatty acids in the colon and peripheral tissues: a focus on butyrate, colon cancer, obesity and insulin resistance. *Nutrients*, *9*(12), 1348.
- Miller, T. L., & Wolin, M. J. (1996). Pathways of acetate, propionate, and butyrate formation by the human fecal microbial flora. *Applied and environmental microbiology*, *62*(5), 1589-1592.
- Mondal, A., & Bennett, L. L. (2016). Resveratrol enhances the efficacy of sorafenib mediated apoptosis in human breast cancer MCF7 cells through ROS, cell cycle inhibition, caspase 3 and PARP cleavage. *Biomedicine & Pharmacotherapy*, *84*, 1906-1914.

- Nicholls, D. G., & Budd, S. L. (2000). Mitochondria and neuronal survival. *Physiological reviews*, *80*(1), 315-360.
- Nova, Z., Skovierova, H., Strnadel, J., Halasova, E., & Calkovska, A. (2020). Short-term versus long-term culture of A549 cells for evaluating the effects of lipopolysaccharide on oxidative stress, surfactant proteins and cathelicidin LL-37. *International Journal of Molecular Sciences*, *21*(3), 1148.
- Pandey, S. K., Yadav, S., Goel, Y., & Singh, S. M. (2019). Cytotoxic action of acetate on tumor cells of thymic origin: role of MCT-1, pH homeostasis and altered cell survival regulation. *Biochimie*, *157*, 1-9.
- Pant, K., Yadav, A. K., Gupta, P., Islam, R., Saraya, A., & Venugopal, S. K. (2017). Butyrate induces ROS-mediated apoptosis by modulating miR-22/SIRT-1 pathway in hepatic cancer cells. *Redox Biology*, *12*, 340-349.
- Park, H. S., Han, J. H., Park, J. W., Lee, D. H., Jang, K. W., Lee, M., ... & Myung, C. S. (2021). Sodium propionate exerts anticancer effect in mice bearing breast cancer cell xenograft by regulating JAK2/STAT3/ROS/p38 MAPK signaling. *Acta Pharmacologica Sinica*, *42*(8), 1311-1323.
- Pericleous, M., Mandair, D., & Caplin, M. E. (2013). Diet and supplements and their impact on colorectal cancer. *Journal of Gastrointestinal Oncology*, *4*(4), 409.
- Qin, X. J., Li, Y. N., Liang, X., Wang, P., & Hai, C. X. (2008). The dysfunction of ATPases due to impaired mitochondrial respiration in phosgene-induced pulmonary edema. *Biochemical and biophysical research communications*, *367*(1), 150-155.

- Qiu, D., Zhou, M., Lin, T., Chen, J., Wang, G., Huang, Y., ... & Chen, H. (2019). Cytotoxic components from hypericum elodeoides targeting RXR α and inducing HeLa cell apoptosis through caspase-8 activation and PARP cleavage. *Journal of natural products*, 82(5), 1072-1080.
- Rawla, P., Sunkara, T., & Barsouk, A. (2019). Epidemiology of colorectal cancer: incidence, mortality, survival, and risk factors. *Gastroenterology Review/Przeegląd Gastroenterologiczny*, 14(2), 89-103.
- Samuel, B. S., Shaito, A., Motoike, T., Rey, F. E., Backhed, F., Manchester, J. K., ... & Gordon, J. I. (2008). Effects of the gut microbiota on host adiposity are modulated by the short-chain fatty-acid binding G protein-coupled receptor, Gpr41. *Proceedings of the National Academy of Sciences*, 105(43), 16767-16772.
- Sen, C. K., Packer, L., & Hänninen, O. (2000). Oxidative stress indices: analytical aspects and significance. *Handb. Oxid. antioxidants Exerc*, 433.
- Shi, H., Guo, Y., Liu, Y., Shi, B., Guo, X., Jin, L., & Yan, S. (2016). The in vitro effect of lipopolysaccharide on proliferation, inflammatory factors and antioxidant enzyme activity in bovine mammary epithelial cells. *Animal nutrition*, 2(2), 99-104.
- Tang, Y., Chen, Y., Jiang, H., Robbins, G. T., & Nie, D. (2011). G-protein-coupled receptor for short-chain fatty acids suppresses colon cancer. *International journal of cancer*, 128(4), 847-856.
- Tantamango, Y. M., Knutsen, S. F., Beeson, W. L., Fraser, G., & Sabate, J. (2011). Foods and food groups associated with the incidence of colorectal polyps: the Adventist Health Study. *Nutrition and cancer*, 63(4), 565-572.

- Thangaraju, M., Cresci, G. A., Liu, K., Ananth, S., Gnanaprakasam, J. P., Browning, D. D., ... & Ganapathy, V. (2009). GPR109A is a G-protein–coupled receptor for the bacterial fermentation product butyrate and functions as a tumor suppressor in colon. *Cancer research*, 69(7), 2826-2832.
- Toescu, E. C., & Verkhratsky, A. (2000). Assessment of mitochondrial polarization status in living cells based on analysis of the spatial heterogeneity of rhodamine 123 fluorescence staining. *Pflügers Archiv*, 440, 941-947.
- Wang, C., Nie, G., Yang, F., Chen, J., Zhuang, Y., Dai, X., ... & Zhang, C. (2020). Molybdenum and cadmium co-induce oxidative stress and apoptosis through mitochondria-mediated pathway in duck renal tubular epithelial cells. *Journal of hazardous materials*, 383, 121157.
- Wang, W., Zhu, M., Xu, Z., Li, W., Dong, X., Chen, Y., ... & Li, M. (2019). Ropivacaine promotes apoptosis of hepatocellular carcinoma cells through damaging mitochondria and activating caspase-3 activity. *Biological Research*, 52(1), 1-10.
- Wilson, A. P. (2000). Cytotoxicity and viability assays. *Animal cell culture: a practical approach*, 1, 175-219.
- Witayateeraporn, W., Nguyen, H. M., Ho, D. V., Nguyen, H. T., Chanvorachote, P., Vinayanuwattikun, C., & Pongrakhananon, V. (2022). Aspiletrein A Induces Apoptosis Cell Death via Increasing Reactive Oxygen Species Generation and AMPK Activation in Non-Small-Cell Lung Cancer Cells. *International Journal of Molecular Sciences*, 23(16), 9258.

- Wolf, P., Schoeniger, A., & Edlich, F. (2022). Pro-apoptotic complexes of BAX and BAK on the outer mitochondrial membrane. *Biochimica et Biophysica Acta (BBA)-Molecular Cell Research*, 119317.
- World Cancer Research Fund/American Institute for Cancer Research (2018). Diet, Nutrition, Physical Activity and Cancer: A Global Perspective. Continuous Update Project Expert Report. Available at: dietandcancerreport.org.
- Xiong, Y., Miyamoto, N., Shibata, K., Valasek, M. A., Motoike, T., Kedzierski, R. M., & Yanagisawa, M. (2004). Short-chain fatty acids stimulate leptin production in adipocytes through the G protein-coupled receptor GPR41. *Proceedings of the National Academy of Sciences*, 101(4), 1045-1050.
- Yamazaki, D., Kurisu, S., & Takenawa, T. (2005). Regulation of cancer cell motility through actin reorganization. *Cancer science*, 96(7), 379-386.
- Yan, L., Spitznagel, E. L., & Bosland, M. C. (2010). Soy consumption and colorectal cancer risk in humans: a meta-analysis. *Cancer epidemiology, biomarkers & prevention*, 19(1), 148-158.
- Yang, C., Jiang, L., Zhang, H., Shimoda, L. A., DeBerardinis, R. J., & Semenza, G. L. (2014). Analysis of hypoxia-induced metabolic reprogramming. *Methods in enzymology*, 542, 425-455.
- Zeng, H., Claycombe, K. J., & Reindl, K. M. (2015). Butyrate and deoxycholic acid play common and distinct roles in HCT116 human colon cell proliferation. *The Journal of nutritional biochemistry*, 26(10), 1022-1028.

Zeng, H., Taussig, D. P., Cheng, W. H., Johnson, L. K., & Hakkak, R. (2017).

Butyrate inhibits cancerous HCT116 colon cell proliferation but to a lesser extent in noncancerous NCM460 colon cells. *Nutrients*, 9(1), 25.

Zeng, H., Umar, S., Rust, B., Lazarova, D., & Bordonaro, M. (2019). Secondary bile

acids and short chain fatty acids in the colon: a focus on colonic microbiome, cell proliferation, inflammation, and cancer. *International journal of molecular sciences*, 20(5), 1214.

6. Summary and Conclusion

Biologically active and functional dietary ingredients are currently in high demand due to their ability to delay the onset and reduce the impacts of majority of chronic and lifestyle diseases, including obesity, diabetes, and cancer. One strategy to protect, encapsulate and promote the uptake of biologically active food components is emulsion-based delivery systems. All emulsions are thermodynamically unstable and emulsifiers are used to modify the interfacial interactions to delay the phase separation in emulsion. Due to increasing demand for eco- friendly, natural, sustainable food products and to embrace healthier life styles there has been increased need to replace synthetic surfactants with natural alternatives. Solid particle stabilized emulsion called Pickering emulsion is attaining great interest due to increased physical stability, oxidative stability, compatibility with food matrix and enhanced protection of bioactives. Starch has been modified to make it more efficient and functional for its use in various food applications apart from its use as stabilizing and thickening agent in industries. Recently, Porous starch is attaining great interest because of its abundant pores (extending to the centre of the starch granule) and increased surface area, for targeted delivery and sustained release of certain drugs. Porosity of the starch granule can be tuned for various food applications including delivery of active ingredients.

With the increase in demand among the consumers for healthier food products, the development of foods containing functional ingredients has become one of the active research areas in the food industry. Solid particle stabilized emulsion called Pickering emulsion is an active area of research for the delivery of bioactive and nutritionally important components for food/functional and food/nutraceutical applications. Porous starch prepared by the hydrolysis of native starch is reported for the sustained release and targeted delivery of certain drugs and bioactives. Based on the above gathered information and gaps identified we focussed on whether (1) Porous starch act as

Pickering particles in stabilization of emulsion (2) Porous starch with abundant pores and increased surface area, in combination with other polysaccharides such as guar gum can improve the encapsulation efficiency for bioactive E.g., curcumin and can ensure colon delivery by forming a Pickering emulsion (3) Fermentation metabolites of curcumin loaded Pickering emulsion exhibit potential prebiotic and anticancer activity.

In the present study entitled “**Pickering emulsion based encapsulates stabilized by porous starch for bioactive delivery**” we attempted to optimize fabrication of porous starch using enzymatic hydrolysis. Further, the prepared porous starch was studied for its efficacy as a Pickering particle in stabilization of O/W emulsion and as a bioactive carrier for delivery applications using curcumin as model system. The prepared curcumin loaded emulsion was further studied for its gastro intestinal stability and prebiotic potential. The fermentation supernatant from the prebiotic studies were evaluated for its efficacy in management of colon cancer in HCT 116 cells.

Chapter 1 gives a general introduction and review of literature about Pickering emulsion, stabilization mechanism of Pickering particle, food grade Pickering particle and its application, techniques for porous starch preparation-physical, chemical and enzymatic method, characterization of porous starch and its food application.

Chapter 2 entitled ‘**Optimization and characterization of porous corn starch and application in emulsion stabilization**’ deals with the optimization of conditions for porous starch preparation, its characterization and application studies in emulsion stabilization. Porous starch was prepared enzymatically using amyloglucosidase (AMG) and amylase (AM). Two factorial experimental design was used to standardized porous preparation in terms of pore size and surface area. The formation of pores in the starch was confirmed by SEM images. Based on pore size, surface area and statistical analysis optimized conditions for porous starch preparation was drawn with enzyme

concentration of 300 U AM and 250 U AMG for 6 h incubation. Native and porous starch were compared for physicochemical characteristics such as contact angle, zeta potential, rheology, XRD, FTIR & DSC and the results indicated that porous starch can act as stabilizer for O/W emulsions. Further studies such as emulsion stabilizing efficiency in terms of creaming index, fluorescence microscopy images of emulsion to confirm Pickering emulsion formation and studies using curcumin as model system confirmed that porous starch act as Pickering particle and better bioactive carrier compared to native starch.

Chapter 3 deals with **Fabrication of Curcumin loaded flax seed oil encapsulates by porous starch Pickering emulsion.** O/W Pickering emulsion of curcumin loaded flax seed oil with porous starch-Guar gum as Pickering particle was fabricated. A stable emulsion (PSPE) was obtained with a composition of porous starch (6% w/v) and guar gum (1% w/v) as wall material and flax seed oil (2% v/v) loaded with curcumin (80 ppm) as dispersed phase. The optimized emulsion was stored at $(4 \pm 2 \text{ }^\circ\text{C})$ for 15 days and characterization studies were performed and compared with that of native starch Pickering emulsion (NSPE). PSPE with decreased particle size and high zeta potential conferred better stability than NSPE. Rheological studies confirmed that PSPE retained better elastic property than NSPE. Microstructure data confirmed porous starch can act as efficient Pickering particle compared to native starch with complete encapsulation of oil phase during the spectrum of storage and better encapsulation efficiency in terms of curcumin retention. FTIR analysis indicated no chemical interaction other than hydrogen bonding happening in the emulsion system. PSPE showed better encapsulation efficiency of curcumin ($83.07 \pm 2.29\%$) than NSPE ($63.20 \pm 2.18\%$). In conclusion, PSE encapsulates can be used as carrier of curcumin for food and nutraceutical applications

Chapter 4 entitled '***In vitro* release kinetics and prebiotic efficacy of Curcumin Pickering emulsion**' focus on the evaluation of *in vitro* release studies of curcumin in simulated gastrointestinal condition and to investigate the prebiotic potential of PSPE. The core release studies of porous starch Pickering emulsion showed low release in simulated gastro intestinal conditions. Pickering emulsion was fermented using probiotic species *Lactobacillus casei* and the prebiotic potential was investigated in terms of change in pH, optical density, colony count, dry weight and by quantification of short chain fatty acids. The results confirmed the prebiotic potential of encapsulates.

Chapter 5 is the '***In vitro* screening of the fermentation metabolites in prevention and management of colorectal cancer**'. This chapter explored the anticancer potential of fermentation metabolites in HCT 116 colon cancer cells. The fermentation metabolites containing short chain fatty acids exhibited cytotoxic effects. The metabolites induced DNA damage and effectively obstructed the motility and migration proficiency of HCT 116 cell lines. Suppression of antioxidant enzymes like SOD and CAT, over production of ROS and calcium levels, loss of mitochondrial membrane integrity, ultimately induced apoptosis in HCT 116 cells. The flow cytometry analysis was performed to confirm the same. The protein expression studies by western blotting confirmed that the short chain fatty acids containing fermentation metabolites induces apoptosis by upregulating expression of Bax, Bak, caspase-3 and c-PARP and downregulating Bcl-2 protein.

CONCLUSIONS

- Conditions for enzymatic modification of native starch to porous starch was standardised.
- The porous starch can act as Pickering particle for emulsion stabilization.
- Porous starch can also bind bioactive compounds and could be explored for delivery application.
- Porous starch based encapsulates in the form of Pickering emulsion showed better encapsulation efficiency of curcumin and showed low release kinetics in simulated gastro intestinal conditions, indicating its application in colon delivery of active ingredients.
- The encapsulates with guar gum as stabilizer (also dietary fibre) and porous starch as Pickering particle displayed potential prebiotic properties which ultimately helps in sustaining gut homeostasis.
- The fermentation metabolites of Pickering emulsion enriched with short chain fatty acids induced apoptosis in HCT 116 colon cancer cells.
- Porous starch based Pickering emulsion could be a promising strategy for delivering bioactive phytochemicals and prebiotics to the gut for maintaining homeostasis and to prevent and manage chronic diseases.

FUTURE ASPECTS

- There is a great potential for porous starch-based delivery systems for application in food, functional food, nutraceutical and pharmaceutical applications. Further research is warranted to establish the health benefits using in vivo studies.
- The pore size can be finetuned for various target groups, which needs to be further studied.
- Application of the developed emulsions and fabrication of newer emulsions based on the same strategy should be explored for other bioactives.
- Short chain fatty acids, key mediators of gut brain communication, can be utilized for further studies in prevention and management of life style diseases.

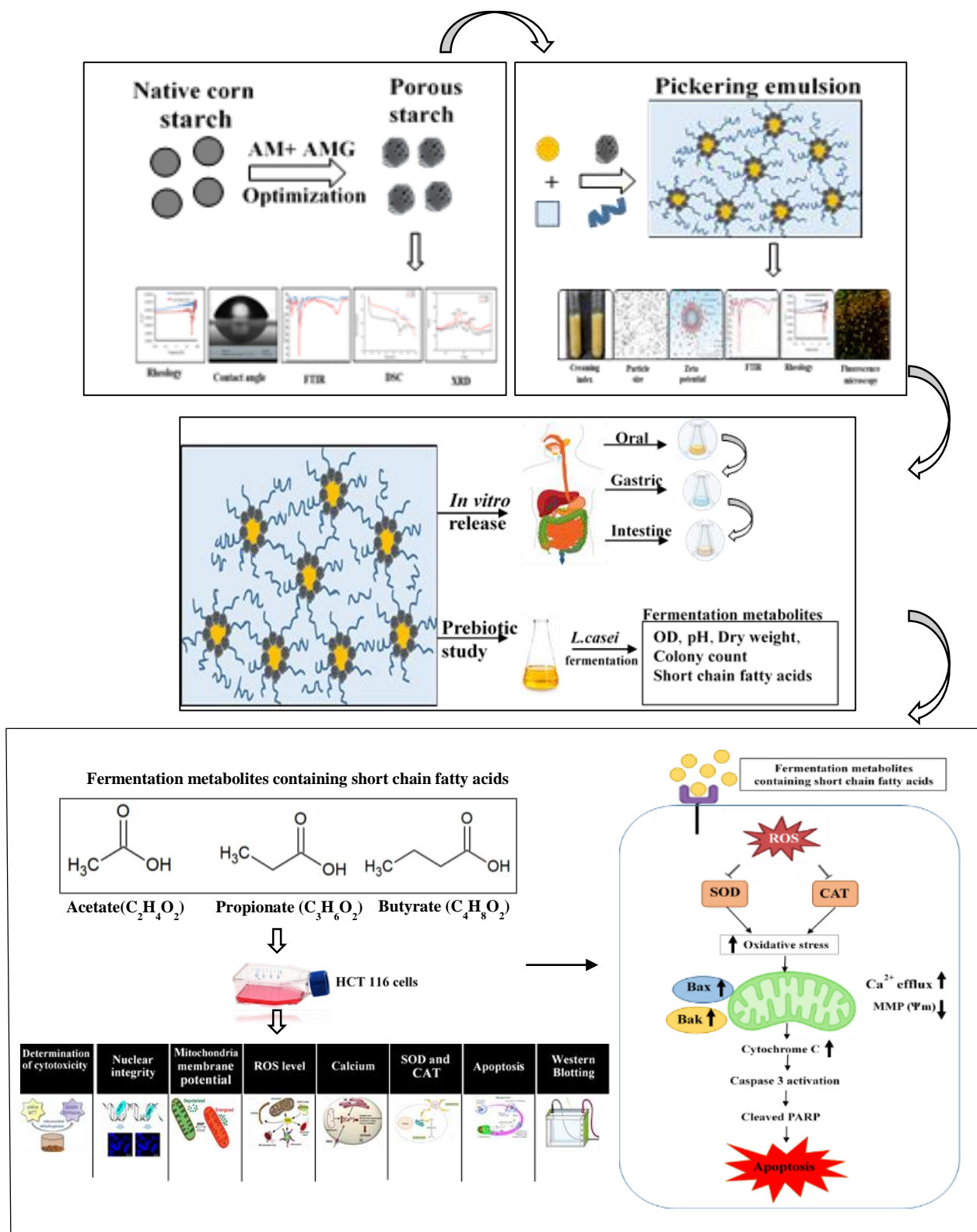


Fig 6.1: Graphical representation of chapters with brief demonstration of work flow

APPENDIX

Sl.No	Instruments	Manufacturer
1	Overhead stirrer	Remi, RQ126/D, with 40V, Mumbai, India
2	Spectrophotometer	Shimadzu UV-2600, Japan
3	Hot air oven	Globe Tex, Digital Laboratory Hot Air Oven, Ghaziabad, India
4	Microplate reader	Synergy 4 Biotek, USA
5	Homogenizer	T25 ULTRA-TURRAX digital; dispersing tool: S 25 N -8G: IKA, Private Limited, China
6	Gel electrophoresis system	Bio-Rad Laboratories, Germany
7	Water activity meter	Rotronic HygroPalm23-AW-A, Switzerland
8	HPLC	Shimadzu, Japan
9	FACS	BD FACS Aria II, BD Bioscience, USA
10	Scanning Electron Microscope	Carl Zeiss EVO-18, Germany
11	Oven	Bajaj OTG, 4500 TMCSS, Mumbai, India
12	Confocal Microscopy	Pathway 855, BD Bioscience, USA
13	Malvem Zeta sizer	Zeta Nano-ZS; Malvern Instruments, UK
14	Gel Doc	Bio-Rad Laboratories, Germany
15	Oakton pH 700	Benchtop Meter, Oakton Instruments, USA
16	FTIR-ATR spectrometer	Perkin Elmer, Spectrum Two, US
17	Rheometer	Anton Paar GmbH. Ostfildern-Scharnhausen, Germany
18	Drop shape analyser	KRÜSS GMBH, Hamburg, Germany
19	Fluorescence microscope	Olympus IX83, Olympus Corporation of the Americas, Center Vally, PA, USA
20	BET	Micromerities Instrument Corporation, GA, USA
21	Refrigerated Centrifuge	Beckman Coulter, Pasadena, CA, USA

ABSTRACT

Name of the student: Sannya Sathyan	Registration No.: 10BB17J39014
Faculty of study: Biological Sciences	Year of submission: 2023
ACSIR academic centre/CSIR Lab: CSIR-NIIST	Name of supervisor: Dr. P Nisha
Title of the thesis: “Pickering emulsion based encapsulates stabilized by porous starch for bioactive delivery”	

Biologically active compounds play vital role such as reducing and inhibiting the risk of noncommunicable diseases as it exhibits many health benefits. Solid particle stabilized emulsion called Pickering emulsion can be used for the delivery of bioactive and nutritionally important components. Polysaccharides and protein were commonly used as Pickering particle. Porosity of the starch granule can be tuned for various food applications including delivery of active ingredients. Porous starch (PS) prepared enzymatically using AM and AMG and standardized using two factorial experimental design. Based on surface area, pore size and statistical analysis 300 U AM and 250 U AMG for 6 h incubation were suggested for PS preparation. The physicochemical characterization studies such as contact angle, zeta potential, rheology, XRD, FTIR and DSC indicated that PS can act as stabilizer for O/W emulsions. Further microstructure studies confirmed that PS act as Pickering particle and efficient bioactive carrier system. A stable O/W porous starch based Pickering emulsion (PSPE) was obtained with a composition of porous starch (6% w/v) and guar gum (1% w/v) as wall material and flax seed oil (2% v/v) loaded with curcumin (80 ppm) as dispersed phase. Characterization studies confirmed that PSPE showed better stability, elastic property, encapsulation efficiency and can act as efficient Pickering particle than NSPE. The core release studies of PSPE showed low release kinetics in simulated gastro intestinal conditions. The PSPE was fermented using *Lactobacillus casei* and the prebiotic potential was confirmed in terms of change in pH, OD, colony count and by quantification of SCFA. Finally, anticancer potential of FM was studied in HCT 116 colon cancer cells and studies confirmed that the probiotic FM of PSPE induced DNA damage, increased ROS and calcium levels and obstructs cell motility. Loss of mitochondrial membrane integrity ultimately induced apoptosis in HCT 116 cells which is confirmed by protein expression studies by western blotting. Thus present study could be a potential strategy for delivering bioactive phytochemicals and prebiotics to the gut for maintaining homeostasis and also to prevent and manage the onset of chronic diseases.

LIST OF PUBLICATIONS

Related to thesis published

- **Sathyan, S., & Nisha, P.** (2022). Optimization and Characterization of Porous Starch from Corn Starch and Application Studies in Emulsion Stabilization. *Food and Bioprocess Technology*, 15(9), 2084-2099.

Manuscript under preparation

- **Sathyan, S., & Nisha, P.** Fabrication of porous starch based Pickering emulsion for the encapsulation of curcumin- Characterization and *invitro* stability studies (Manuscript under preparation)
- **Sathyan, S., & Nisha, P.** Preliminary screening of curcumin based porous starch encapsulates for the management of colon cancer (Manuscript under preparation)

Published – Not related to thesis

- Arun, K. B., Dhanya, R., Chandran, J., Abraham, B., **Satyan, S., & Nisha, P.** (2020). A comparative study to elucidate the biological activities of crude extracts from rice bran and wheat bran in cell line models. *Journal of food science and technology*, 57(9), 3221-3231.

LIST OF CONFERENCES

- **Sannya Sathyan, Dr. P. Nisha.** Porous starch as Pickering particles in stabilization of emulsion (2023)- 29th ICFoST by AFSTI, Trivandrum (Received best poster award).
- **Sannya Sathyan, Dr. P. Nisha.** Preparation of porous corn starch: Optimization, Characterization and its application studies (2022) – AAFS, Bengaluru (Poster presentation)



Optimization and Characterization of Porous Starch from Corn Starch and Application Studies in Emulsion Stabilization

Sannya Sathyan^{1,2} · P. Nisha^{1,2}

Received: 6 January 2022 / Accepted: 31 May 2022

© The Author(s), under exclusive licence to Springer Science+Business Media, LLC, part of Springer Nature 2022

Abstract

Preparation of porous starch (PS) from corn starch (NS) using enzymes amylase (AM) and amyloglucosidase (AMG) was standardized using two factorial experimental design in terms of surface area and pore size distribution. SEM micrographs confirmed the formation of porous structures in the granules. Based on surface area, pore size and statistical analysis 300 U AM and 250 U AMG for 6 h incubation were suggested for porous starch preparation. Physicochemical characteristics of NS and PS were compared using zeta potential, contact angle, rheology, FTIR, XRD, and DSC which suggested the potential of PS as a stabilizer for O/W emulsions. Further studies confirmed emulsion stabilizing efficacy of PS with creaming index of 5.0% against 16.6% for NS. The fluorescence microscopy images of the emulsion after staining with specific dyes revealed that PS acts as a Pickering particle. Furthermore, studies using curcumin as model system indicated that PS acts as better bioactive carrier as compared to NS. The curcumin holding capacities of PS and NS were 82.24 ± 1.07 and $61.03 \pm 1.43\%$, respectively. The study suggested that PS can be effectively used as Pickering particle and bioactive carrier in various food, nutraceutical, and pharmaceutical applications.

Keywords Porous starch · Pickering particle · Fluorescence microscopy · Bioactive carrier

Introduction

The application of solid colloidal particles to produce stable emulsions is gaining lot of attention at present. Solid particle-stabilized emulsions, called Pickering emulsions (Pickering, 1907; Ramsden, 1903; Saffarionpour, 2020), show long-term stability without the addition of surfactant as solid particles adsorbed onto oil–water interface and regarded as promising alternative to conventional synthetic emulsifiers (Jiang et al., 2019; Kierulf et al., 2019). Inorganic particles like clay, latex, silica, and hydroxyapatite are widely used as stabilizers but their use have been restricted within the food and pharmaceutical industries because of growing concern over biodegradability, biocompatibility, and carcinogenicity of synthetic surfactants

(Kierulf et al., 2020; Wang et al., 2016a, b; Wu et al., 2021). Pickering particles shown to have several advantages over conventional stabilizers such as lower toxicity and improved gut health, improved stability, lower irritation to the skin, and lower contamination for the environment (Chassaing et al., 2015; Marefati et al., 2017; Marku et al., 2012; Qi et al., 2014). Addition of Pickering particles can alleviate the problems associated with surfactants including air entrapment, foaming, irritancy, and interaction with the living matter (Frelichowska et al., 2009).

Proteins, lipids, and polysaccharides are reported to be used as Pickering particles for stabilizing emulsions. Proteins like zein, and soy protein and, polysaccharides like starch, and cellulose are commonly used (Guida et al., 2021). Among polysaccharides, starch are widely used because they are inexpensive, non-allergenic, biodegradable, and GRAS (Zhu, 2019). Starch consists of linear amylose chains, i.e., glucose units with α - (1 \rightarrow 4) linkage) and branched amylopectin, α -(1 \rightarrow 4) glucose units linked to α -glucan with α -(1 \rightarrow 6) bonds (Pérez et al., 2009). The ability of native starch to stabilize Pickering emulsions are due to different physical and functional properties such as shape, size, granular structure, ratio between amylose and amylopectin

✉ P. Nisha
bp.nisha@yahoo.com; pnisha@niist.res.in

¹ Agro Processing and Technology Division, CSIR – National Institute for Interdisciplinary Science and Technology (NIIST), Thiruvananthapuram 695019, Kerala, India

² Academy of Scientific and Innovative Research (AcSIR), Ghaziabad 201002, India

content, and chemical composition (Din et al., 2015). Previous studies also show that granule size (Li et al., 2013) and granule composition (Kierulf et al., 2020) are important factors that determine the emulsifying property of starch.

Native starch in its commercial, pure, native form will not act as a stable Pickering particle (Aveyard et al., 2003; Kierulf et al., 2020). Starch is subjected to physical and chemical modifications to enhance the ability of starch to act as a Pickering particle (Guida et al., 2021; Zhu, 2019). Physical modification results in difference in surface properties, particle size, solubility index, and functional properties like swelling capacity and gelation ability of starch (Nawaz et al., 2020). Commonly used physical modification methods are micronization, pulse electric field, ultra-sonication, ultra-high pressure, heat-moisture treatment, annealing, freezing, and mild heating (Punia, 2019; Zhang et al., 2019). Methods of chemical modification include oxidation, etherification, esterification, cationization, cross linking, and hydrolysis. Chemical modification results in change in physical behavior like salting, retro gradation, and gelatinization of starch (Korma et al., 2016). Among hydrolysis enzyme, hydrolysis is most preferred method to make it porous.

Porous starch is a modified starch obtained by chemical, physical, and enzymatic treatment which produce abundant pores on the surface that could be extended to center of starch granules (Dura et al., 2014). Among different methods used for the production of porous starch, enzymatic method was widely used because of high catalytic efficiency, substrate specificity, and mild reaction conditions (Chen et al., 2020; Liu et al., 2018). During past decade, enzyme catalysis method has received increased attention, because it is more efficient, healthier, and environmentally friendly (Hoon et al., 2018). Various factors like enzyme type, source of starch, and reaction conditions will influence the yield of porous starch. Enzymes amylase, amyloglucosidase, pululanase, isoamylase, glycogen branching enzymes, and cyclodextrin-glycosyltransferase were commonly used for the preparation of porous starch (Chen et al., 2020; Dura et al., 2014). Amylase and amyloglucosidase hydrolyzed starch by cleaving α -1, 4- or α -1, 6 glucosidic bonds and many studies suggested that synergistic action of these enzymes are required to hydrolyze starch completely and rapidly (Dura et al., 2014; Guo et al., 2020; Sun et al., 2010).

Porous starch has many applications in food, pharmaceuticals, environment management, and other industries. In food industry, porous starch is used for protection of sensitive elements like vitamins, oils, and food pigments which are sensitive to light and also used as colorants, spices, and sweeteners carriers (Belingheri et al., 2015a, b; Majzoobi et al., 2015). In recent studies, Zhou et al. (2021) prepared V-type porous starch (VPS) from V-type granular starch (VGS) and the effects of different concentrations of starch and ethanol and reaction

temperatures on the microstructure, crystal morphology, crystallinity, and adsorption properties of VGS before and after enzymatic hydrolysis were studied and reported that VPS exhibited higher V-type crystallinity and better oil adsorption capacity. Guo et al. (2021) prepared porous starch using three different enzymes and reported that starch treated with combination of three enzymes, amylase, branching enzyme, and glucoamylase was found to be most efficient with improved adsorption capacities. The authors studied structural properties (amylose and amylopectin), morphological characteristics (SEM), structural features (particle size, pore size, surface area), and adsorption capacities (of oil, pigment, heavy metals) of porous starch. However, these studies lack characterization studies like FTIR, XRD, DSC, and rheological studies which are very important with respect to the application of these in food systems. Wu et al. (2020) also prepared porous corn starch by combining extrusion technology followed by enzymatic hydrolysis but the study also lacks the rheological studies.

The porous starch could also be used for bioactive delivery. (Belingheri et al., 2015a, b) used porous starch for flavor delivery in tomato-based food application. Zhu et al. (2018) reported an effective method for colon-targeted delivery of doxorubicin using porous starch along with pectin/chitosan coating. Oliyai et al. (2020) reported encapsulation of fucoxanthin in porous starch. However, similar studies on the efficiency of porous starch as bioactive carrier is scarce. Therefore, in the present study, we optimized the method of preparation of porous starch from native corn starch by enzyme hydrolysis method, which and was further subjected to detailed physicochemical characterization in terms of particle size, zeta potential, contact angle, rheology, DSC, XRD, and FTIR and compared it with native starch. The porous starch thus prepared using optimized method was further investigated for its efficiency as (1) Pickering particle in oil in water emulsion so that it can be used in further food and nutraceutical applications and (2) as a carrier of bioactive for delivery applications with curcumin as a model system.

Materials and Methods

Materials

Starch from corn (CAS:9005–25-8), α -amylase from *Aspergillus oryzae* (AM) (30 U/mg), amyloglucosidase from *Aspergillus niger* (AMG) (≥ 260 U/mL), and curcumin from *Curcuma longa* were purchased from Sigma-Aldrich-USA. All the other reagents used in this study were of analytical grade.

Preparation of Porous Starch

Optimization of Concentration and Incubation Time of Individual Enzyme

The preparation of porous starch (PS) was optimized based on previously published protocol (Zhang et al., 2012) using enzymes AMG and AM with slight modifications. Initially, the PS was prepared by treating the native corn starch (NS) with AM and AMG separately. Concentration and incubation time for treatment of each of the enzyme were selected based on the reported literature. Accordingly, we selected a low and high concentration and incubation time for the enzymes treatment (Table 1). Enzymes (AMG and AM) at different concentrations were added to starch slurry (10%) prepared in phosphate-buffered saline (PBS) (pH-5) at 50 °C and kept under incubation for different durations of time. After completion of enzyme hydrolysis, the pH was adjusted to 10 with 1 M KOH. The starch slurry was then centrifuged at 4000 rpm for 15 min. The supernatant was decanted, and the precipitate was washed with distilled water 4–5 times to remove the remaining enzyme and potassium hydroxide. The residue was then transferred to a Petri dish and dried at 50 °C for 5 h. The dried sample was powdered and passed through as 50-mesh sieve and was analyzed for surface area, pore size, and SEM determination.

Furthermore, porous starch preparation using enzyme combination was optimized using a two factorial experiment design. The concentration and incubation time for the combination of enzymes treatment for the design were

selected based on the preliminary results obtained from the individual enzymes.

Modeling and Optimization

Porous starch preparation was standardized using a two factorial experimental design (34–36) against input factors of enzyme concentration, incubation time, and response parameters of surface area, pore size, and surface morphology. The experimental domain of the input parameters was defined based on the preliminary studies (Optimization of concentration and incubation time of individual enzyme). Based on the results obtained from these experiments, two factorial experiments were designed for the combination of enzymes (Table 2).

Determination of Specific Surface Area and Pore Size Distribution

The pore structures of the starch granules including the specific surface area (SSA) and pore size distribution (PSD) were analyzed based on an N₂ adsorption–desorption process with nuance (Du et al., 2013; Jadhav & Vavia, 2017). The analysis was carried out on a TriStar II 3020 instrument (Micromeritics Instrument Corporation, GA, USA). The system was operated at pressure (P/P₀) range of 0.1 to 1.0. The samples were degassed at 100 °C overnight under vacuum before adsorption and the temperature was maintained at 77 K. The SSA and PSD were calculated using Brunauer–Emmett–Teller (BET) and Barrett–Joiner–Halenda (BJH) methods.

Table 1 The surface area and pore size of starch treated with different concentrations of enzymes, (AM, AMG) and time of incubation

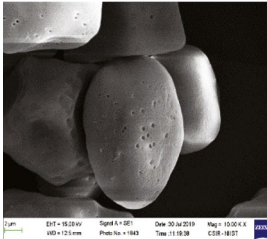
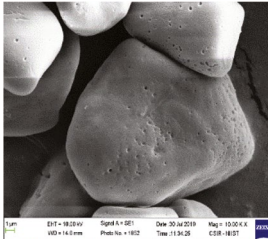
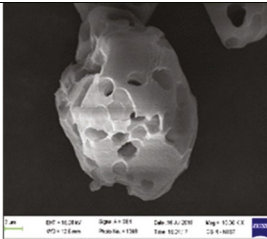
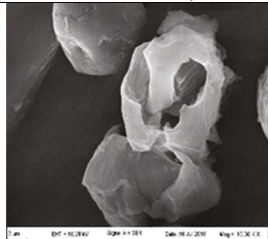
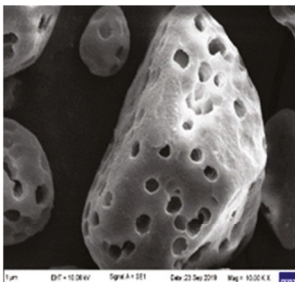
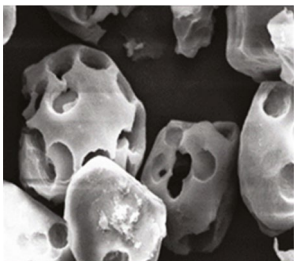
Enzyme/s	Concentration (U/mL)	Time (h)	Surface area(m ² /g)	Pore size (nm)		
Amylase (AM)	300	8	0.720	10.200	 <p>AM 300U/mL, 8h</p>	 <p>AM 3000U/mL, 8h</p>
	300	12	0.759	09.945		
	3000	8	0.581	09.554		
	3000	12	0.465	06.175		
Amyloglucosidase (AMG)	300	8	1.457	28.809	 <p>AMG 300 U/mL, 12 h</p>	 <p>AMG 1500 U/mL, 12 h</p>
	300	12	1.289	16.061		
	900	8	0.981	23.219		
	900	12	0.721	09.413		
	1500	8	2.235	33.307		
	1500	12	1.302	19.307		

Table 2 The surface area and pore size of starch treated with combination of enzymes, (AM/AMG) and time of incubation

Enzyme/s	Concentration (U/mL)	Time (h)	Surface area(m ² /g)	Pore size (nm)	SEM Images	
Amylase/ Amyloglucosidase (AM/AMG)	150/150	6	0.900	17.389		
	150/150	8	1.126	13.654		
	150/300	6	0.468	48.188		
	150/300	8	0.737	34.330		
	300/150	6	1.781	09.165		
	300/150	8	0.860	09.416		
	300/300	6	0.614	40.527		
	300/300	8	0.207	12.591		

Scanning Electron Microscopy (SEM)

NS and PS powder were adhered to an aluminum specimen holder by carbon tape. Next, a thin layer of gold was coated on to the sample under vacuum with a gold/palladium sputter coater (SC7620, Emitech, Quorum Technologies Ltd, Kent, UK) prior to the microscopical evaluation. The microscopic surface texture of these samples was evaluated by scanning electron microscopy (ZEISS; EVO 18, Germany) under 15 kv of accelerating voltage (Da Silva Soares et al., 2021). The micrographs were recorded at 10,000X magnification.

Particle Size and Zeta Potential

The size and zeta potential of NS and PS were calculated using the Malvern Zetasizer (Zeta Nano-ZS; Malvern Instruments, UK), which works on the principle of dynamic light scattering (DLS) (Comunian et al., 2020).

Contact Angle

The sample (5% of NS and PS in water) was heated at 85 °C for 30 min. The starch paste was then transferred to a coverslip and the contact angle was measured in a Drop shape analyzer. (Model: DSA30E, KRUSS GmbH, Hamburg, Germany; with the KRUSS ADVANCE Software 1.7.0.8, Version 15).

Rheology

The flow behavior, amplitude sweep and frequency sweep of NS and PS, was determined using a controlled stress rheometer (MCR 102 Rheometer, Anton Paar GmbH, Ostfildern-Scharnhausen, Germany). The starch samples, NS and PS, were mixed with water (38% W/V, optimized based on experiment trials), and stirred for 30 min before doing the rheological studies. The probe used for the study

was plate geometry of 25 mm diameter and 0.105 mm gap (Mohammed et al., 2021). To determine the flow behavior, the shear rate used was in the range from 0.01 to 100 s⁻¹. The amplitude sweep was performed to find the LVR region by changing the strain from 0.01 to 10% for PS and 0.01 to 100% for NS. The frequency sweep was performed within the LVR region at a frequency range from 0.01 to 100 rad/s.

ATR-Fourier-Transform Infrared (FTIR) Spectroscopy

Fourier-transform infrared (FTIR) spectroscopy of NS and PS was recorded using an FTIR-ATR (attenuated total reflection) spectrometer (Perkin Elmer, USA), equipped with an ATR accessory with a diamond crystal at an incidence angle of 45°. Transmittances were recorded at wave numbers between 4000 and 400 cm⁻¹.

Differential Scanning Calorimetry (DSC)

The thermal behavior of NS and PS was evaluated by differential scanning calorimetry (DSC). DSC measurements were carried out using a differential scanning calorimeter (DSC Q2000, TA Instruments, USA) based on previous studies (Tao et al., 2016). Briefly, 3 mg of samples was weighed

Table 3 Regression table for combination of enzymes AM and AMG

Enzymes	Surface area		Pore size	
	Effect	Coefficient	Effect	Coefficient
AM	0.057	-0.028	-104.650	-52.330
AMG	-0.660	-0.330	215.000	107.500
Time	-0.208	-0.104	-113.200	-56.600
AM*AMG	-0.250	-0.125	-42.350	-21.170
AM*time	-0.455	-0.227	-25.230	-12.620
AMG*time	0.139	0.069	-95.770	-47.890
AM*AMG*time	0.118	0.059	-45.160	-22.580

and distilled water was added (6 μL), and placed into pre-weighted aluminum sample pans. The samples were scanned from 40 to 90 $^{\circ}\text{C}$ at a heating rate of 10 $^{\circ}\text{C}/\text{min}$ under an atmosphere of nitrogen. The temperature values obtained were the onset temperature (T_o), the peak temperature (T_p), and the conclusion temperature (T_c).

X-Ray Diffraction (XRD)

XEUSS SAXS/WAXS system from Xenocs was used to record the wide-angle X-ray diffraction (WAXD) measurements in the transmission mode. The powdered NS and PS samples were used for the analysis. The operating voltage was 50 kV, and the current was 0.6 mA, with Cu $K\alpha$ radiation of wavelength $\sim 1.54 \text{ \AA}$. The 2D patterns were recorded on a Mar345 image plate and the data was analyzed using the Fit2D software. The degree of crystallinity was calculated using grams software.

Efficacy of Porous Starch as Emulsion Stabilizer

The efficiency of porous starch in stabilizing emulsion was studied in terms of creaming index. For the preparation of emulsion, 10% of starch (NS and PS) was mixed with 10% flax seed oil and 80% water. The mixture was homogenized at 12,000 rpm for 150 s to yield emulsion. The emulsion was stored at room temperature (37 $^{\circ}\text{C}$) and creaming index of NS and PS was calculated at 24 h and 48 h. The creaming index was calculated by the formula, $CI (\%) = 100 \times HC / HE$, where HC is the height of aqueous layer, HE is the initial height.

Fluorescence Microscopy

Fluorescence microscopy was performed to determine whether the PS would act as Pickering particle (Olympus fluorescence microscope IX83, Olympus corporation of Americas, Center Valley, USA). PS and NS were stained with dye Nile red and safranin for staining oil and starch respectively (Cakmak et al., 2012; Daniel & Ana, 2020; Dean et al., 2010). One hundred microliter of emulsion was taken in a 96 well plate and first stained with Nile red (10%), kept for few minutes, followed by safranin (5 mg/ml). The images were recorded using a delta 512 EMCCD camera (photometrics, USA).

Efficacy of Porous Starch as Bioactive Carrier

Curcumin (50 μg) was added to 500 mg starch taken in 5 mL water. The mixture was stirred at 60 $^{\circ}\text{C}$ for 10–15 min and then centrifuged at 10,000 rpm for 10 min. The supernatant was removed and the pellet was washed with methanol, vortexed for few minutes, and again centrifuged at 10,000 rpm

for 10 min. The supernatant was collected and the process was continued until the pellet become colorless. The supernatant was pooled together, made up to 10 mL and curcumin content was determined using HPLC method.

The supernatant of NS and PS was filtered through 0.22 μm PTFE filter. The analysis was performed on a prominence ultra-fast liquid chromatography (UFLC) system containing LC-20AD system controller, Phenomenex Gemini C18 column (250 \times 4.6 mm, 5 μm), a column oven (CTO-20A), an auto sampler injector (SIL 20 AC), and a diode array detector (SPD-M20A). The mobile phase used for curcumin quantification was isocratic system, i.e., 100% methanol. The injection volume was 10 μL , and the flow rate was kept at 1 mL/min. The column was maintained at 40 $^{\circ}\text{C}$ and eluted fractions were monitored at 420 nm. Sample peaks (NS and PS) were identified by comparing with retention times of curcumin peak. LC Lab solutions software was used for data acquisition and analysis.

Results and Discussion

Optimization of Porous Starch Preparation

Initially, NS was treated with AM and AMG at different concentrations based on the literature to understand the optimum concentration and incubation time to yield desired porosity, which was assessed in terms of surface area (m^2/g) and pore size (nm). The surface area and pore size of NS were 0.202 m^2/g and 03.457 nm respectively.

The surface area and pore size of starch treated with different concentrations of AM and time of incubation (Table 1) showed that starch treated with 300 U of enzyme exhibits greater surface area and pore size. It is also evident from the scanning electron micrographs of AM-treated starch (Table 1 and Supplementary Fig. 1). α -Amylase is an endo-acting enzyme that can hydrolyze the α (1 \rightarrow 4) glycosidic linkages of starch that rapidly reduce the chain length of amylose and amylopectin resulting in increase in number of short linear and branch chains (Xu et al., 2015). From the SEM images, it is clear that at lower enzyme concentration (300 U) starch shows small pores and there was no significant change in pore size when the enzyme concentration was increased from 300 to 3000 U. Ichihara et al. (2013) reported that α -amylase treated cassava starch granules results in changes in properties of granules without changing the size and morphology. Dura et al. (2014) also reported that amylase treatment produces small pores in starch granules. These observations suggested that AM at concentrations of 300 U and below, for an incubation time of 8 h and below can result in desirable porosity.

The surface area and pore size of starch treated with different concentrations of AMG and time of incubation

indicated that compared to 300 U enzyme concentration, 900 U showed decrease in surface area and porosity which is contradictory. In general, it was noted that the pore size and surface area decreased with increase in incubation time for all concentration of AMG studied. An enzyme concentration of 1500 U exhibited higher porosity and surface area (Table 1). Amyloglucosidase hydrolyzes single glucose residues from non-reducing ends of amylose and amylopectin in a step wise manner and it can also hydrolyze α (1,6) linkages in the branch points of amylopectin (Aggarwal & Dollimore, 2000). Surface morphology of starch treated with AMG (Table 1 and Supplementary Fig. 2) shows large pores and broader size distribution with increase in enzyme concentration and incubation time. At higher enzyme concentration and longer duration especially at 900 and 1500 U of enzyme concentration, the morphology of starch changed to deep and large irregular holes and broken structure. These results along with SEM images suggest that concentrations of 300 U give rise to desirable porosity. The observed results are in accordance with Benavent-gil and Rosell (2016) who reported that amyloglucosidase-treated starch shows large pores and at high amyloglucosidase concentration, depression in the granules was seen due to the eroding action of enzyme on the surface of granule. Aggarwal and Dollimore (2000) also observed an increased pore size when amyloglucosidase concentration was increased, up to a concentration of 800 U/g starch, after which large irregular holes and broken structure of starch were observed. It was observed that porous starch, for delivery/encapsulation applications, can be obtained by treating NS with AMG at concentration 300 U for 8 h incubation and at higher concentration of 900 U, AMG resulted in breakdown of starch structure with irregular pores making it unsuitable for such applications.

Effect of Combination of Enzyme on Porous Starch Preparation

Based on the above observations acquired for individual enzymes (maximum enzyme concentration and time of 300 U and 8 h respectively), a two factorial experimental design was obtained (as given under Table 2) for combination of enzyme treatment. Enzyme concentration and incubation time were the input factors whereas surface area and pore size were the output parameters. The regression analysis is given in (Table 3) and the equation for surface area and pore size are given in Eqs. (1) and (2) respectively. As can be seen, the effect of interaction between enzyme concentration and time on surface area was more pronounced than individual effects (Table 2). Porosity was directly influenced by AMG enzyme, rather than by amylase and time.

$$\begin{aligned} \text{Surface area} = & -5.693 + 0.04317 AM + 0.01061 AMG \\ & + 0.9013 Time - 0.000096 AM * AMG \\ & + -0.005398AM * Time - 0.001431 AMG * Time \\ & + 0.000010 AM * AMG * Time \end{aligned} \quad (1)$$

$$\begin{aligned} \text{Pore size} = & 423.7 - 4.996 AM + 0.4271AMG \\ & - 78.32 Time + 0.02434AM * AMG \\ & + 0.7351AM * Time + 0.2648 AMG \\ & * Time - 0.004015AM * AMG * Time \end{aligned} \quad (2)$$

The SEM images of starch treated with combination of enzymes, AM and AMG (Table 2 and Supplementary Fig. 3), indicated more pronounced and controlled formation of deep pores, confirming the synergistic action of these enzymes. The treatment of starch with combination of AM and AMG has already been reported to result in shallow to deep pores (Malucelli et al., 2015). Based on the parameters analyzed and SEM images, a combination of 150/300 and 300/300 of AM/AMG for 6 h was found to yield better porosity incubation time of 8 and 12 h resulted in degradation of starch molecules as evident from the SEM images. Lacerda et al. (2018) reported that 12 h of incubation time was excessive because it may result in appearance of internal canals due to exo-corrosion. Due to longer incubation time, shape of the granule also changed resulting in partial fracture, rough surface, and weakened structure.

As discussed earlier, α -amylase randomly and rapidly cleaves α -(1,4) glycosidic bonds of starch with dextrin as main end product. Thus, α -amylase only undergo incomplete hydrolysis. Amyloglucosidase can cleave both α -(1,4) and α -(1, 6) glycosidic bonds from the nonreducing ends of starch chains and forms entirely glucose. However, the action of amyloglucosidase is very slow. When used in combination, firstly, α -amylase randomly splits the glucose residues present on the surface of starch and releases new non reducing ends. Secondly, amyloglucosidase act on these nonreducing ends and releases glucose continuously from the granules. Thirdly, amyloglucosidase forms holes from surface to the center of granule, allowing more access of α -amylase into the interior of granule and act on more glycosidic bonds resulting in the formation of pores (Sun et al., 2010). Yu et al. (2018) also reported that treatment of corn starch with combination of enzymes creates significant changes by producing pores, but without altering the shape of starch granules. Lacerda et al. (2019) reported that while using combination of enzymes amylase and amyloglucosidase, more superficial attacks were observed. Chen et al. (2020) also reported that for the preparation of porous starch, multiple enzyme treatment, i.e., combination of amylase and amyloglucosidase was mostly used. Thus, the synergistic action of amylase and amyloglucosidase can hydrolyze the entire starch quickly.

The optimum concentration of enzymes obtained after design analysis suggested an optimum surface area and pore size at incubation time of 6 h and at an enzyme concentration of 300 U and 250 U of AM and AMG respectively. Based on the statistical analysis, porous starch was prepared using the optimum combination of enzymes, i.e., 300 U AM and 250 U AMG for 6 h, for further characterization and application studies.

Characterization of Porous Starch

Size of starch varies based on their origin and corn starch mostly comes under medium-sized starches. Size of Pickering particles and zeta potential plays a key role in the formation of stable emulsion. Therefore, the zeta potential of NS and PS was also evaluated. It is also important to understand the wettability or hydrophobic/hydrophilic nature of the particles in order to determine the choice of emulsion type, i.e., O/W or W/O, which is measured using contact angle.

Particle Size and Zeta Potential

The particle size of NS was found to be $3.549 \pm 0.085 \mu\text{m}$ whereas the same for PS was $2.302 \pm 0.062 \mu\text{m}$. As can be seen, the particle size decreases after the enzyme treatment. The results obtained were in accordance with previous reports that the enzymatic treatment reduces particle size efficiently, as hydrolysis ruptures the NS (Jiang et al., 2017; Yu et al., 2018). Hisfazilah Saari and Marilyn Rayner (2019) reported that decreased particle size of starch increased the stability of Pickering emulsion against creaming. Quinoa starch yielded a stable Pickering emulsion which is attributed to its smaller particle size and the droplet size decreased with decreased particle size (Rayner et al., 2012).

The zeta potential of NS and PS was -34 mV and -42 mV , respectively. In a colloidal system, higher surface electric charge (+/-) indicates potential stability of the system (Espinosa Solis et al., 2021). The negative zeta potential values signify the negative charges on the surface of starch particles (Wei et al., 2014). A higher zeta potential reduces the Van der Waals force because of electrostatic repulsion between the particles (Ahmad et al., 2020; Schafer et al., 2010). Dai et al. (2018) reported that higher zeta potential leads to less tendency for particle agglomeration and hence lead to higher particle stability. Ahmad et al. (2020) also reported negative zeta potential values for starch nanoparticles. Thus, the high zeta potential value of PS confers upon its greater stability relative to NS.

Contact Angle

Contact angle measurement provides a significant way to analyze the surface properties of starch and used usually as a marker to measure the degree of surface hydrophobicity or hydrophilicity. Contact angle of $< 90^\circ$ denotes hydrophilic particles that is suitable for stabilizing O/W emulsion and $> 90^\circ$ indicates particle with hydrophobic nature which is suited for the formation of W/O emulsion (He et al., 2013; Su et al., 2010). Coalescence is the process where droplets come into contact and combine to form large droplets and in course of time, this increases the average droplet size and thus reduces the stability of emulsion (Maphosa & Jideani, 2018). Accordingly, the contact angle of NS was $72.4^\circ \pm 0.14$ and that of PS was $63.82^\circ \pm 0.39$ (Fig. 1). Li et al. (2013) studied about emulsifying ability of different native starch granules and reported that rice starch (contact angle 48°) which is more hydrophilic than potato starch (contact angle 63°) showed to be a good particle emulsifier and stabilize

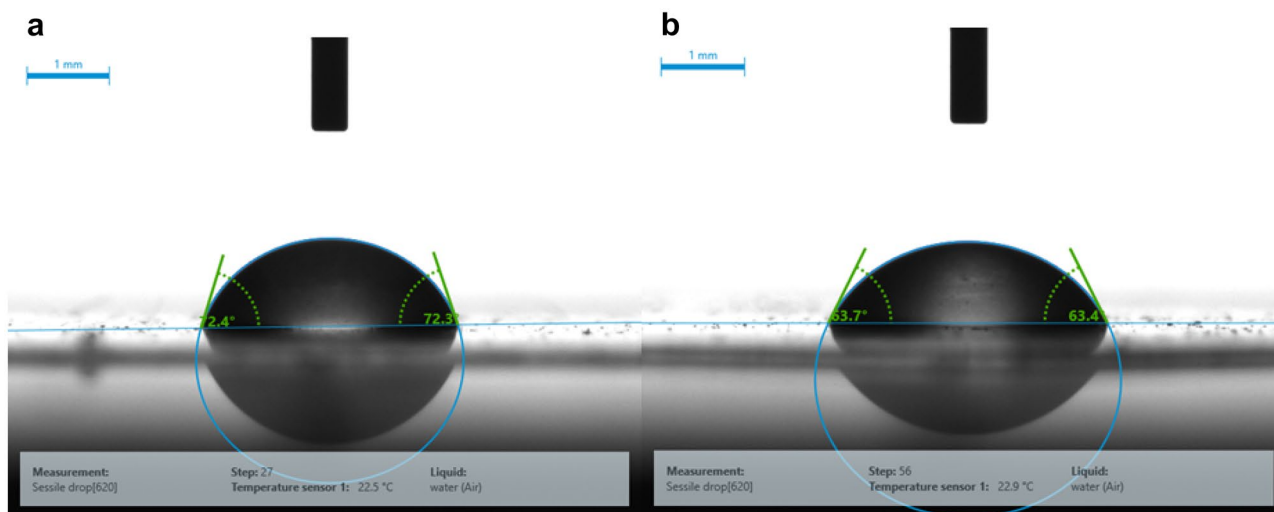


Fig. 1 Contact angle of NS (a) and PS (b)

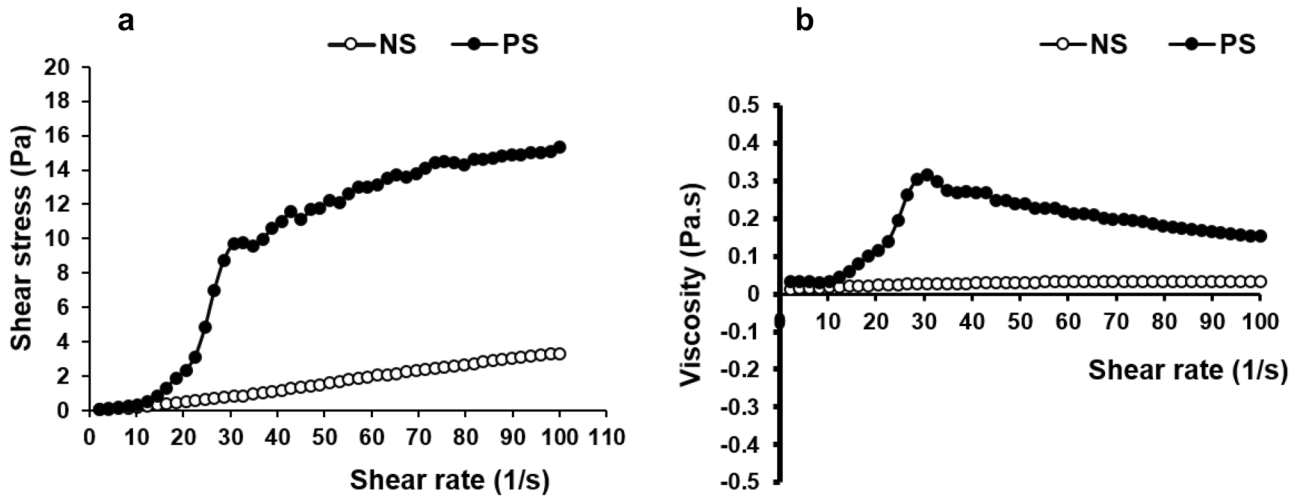


Fig. 2 Shear stress vs. shear rate plot and shear rate vs. viscosity plot of NS and PS are given in Fig. 2a and b respectively

emulsion against coalescence for several months. Hydrophilic particles stabilize oil in water emulsion as most of the particles would be structured in aqueous phase whereas hydrophobic particles stabilize water in oil emulsion (Wu & Ma, 2016). Our results indicated that the contact angle of the PS is lower than that of NS, which makes PS more hydrophilic which makes it more effective as a solid emulsifier in oil in water Pickering emulsions with respect to emulsion stability.

Rheological Studies

Flow Behavior The comparison of the flow ability of NS and PS of same composition of 38% W/V at 25 °C is depicted in Fig. 2. The NS system had shown Newtonian behavior at all shear rates with viscosity 0.0285 ± 0.009 Pa.s. On the other hand, PS system shows non-Newtonian behavior with an

evident shear thickening till the shear rate of 30 s^{-1} followed by shear thinning with a decreasing viscosity as the rate increases further. Shear stress vs. shear rate plot and shear rate vs. viscosity plot of NS and PS are given in (Fig. 2a and b) respectively.

Dynamic strain sweep determines the LVE region of the system where the properties of substances will not vary according to the magnitude of stress, deforming strain or applied shear rate. The structure of the system remains the same along the LVE region (Chen et al., 2017; Steffe, 1996). Thus, LVE region is required for the determination of the storage modulus (G'), and loss modulus (G''), of viscoelastic materials (Liu et al., 2014). Instrument could detect only G'' for NS matrix for entire range of applied strain. The PS system has shown viscoelastic nature with both G' and G'' and the nature was predominantly elastic at lower strain values, which then changed to viscous with increasing strain. The

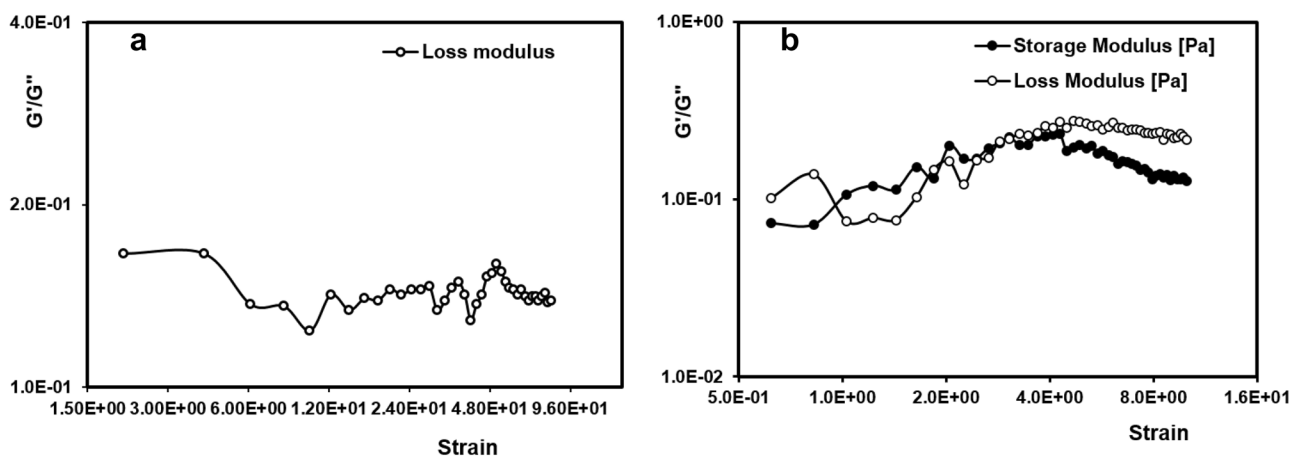


Fig. 3 Amplitude sweep of NS (a) and PS (b) respectively

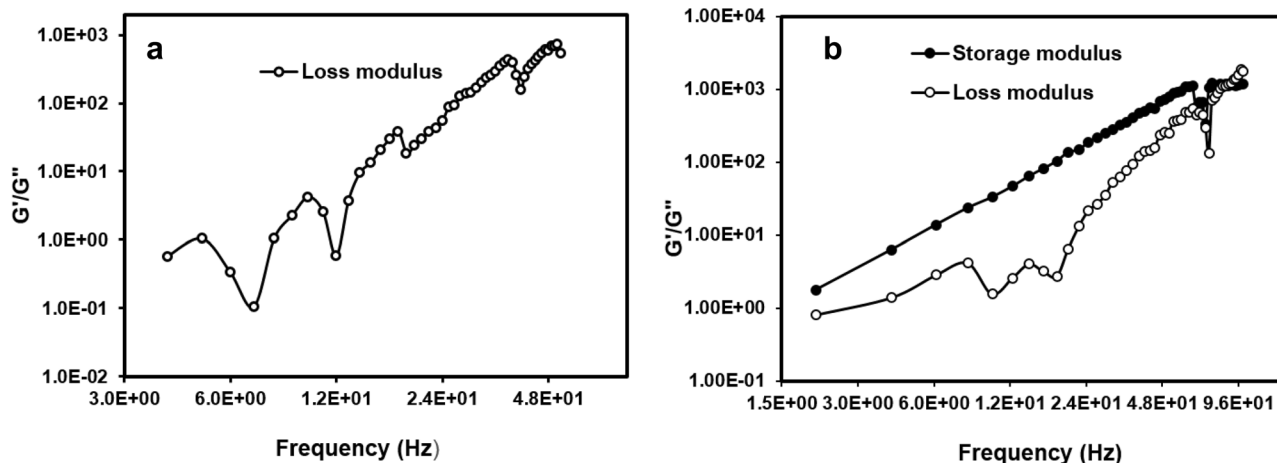


Fig. 4 Frequency sweep of NS (a) and PS (b) respectively

LVE plateau value for the NS is observed to be less than 3% (Fig. 3a), whereas the plateau for PS was found at strain less than 0.7% (Fig. 3b).

Dynamic frequency sweep test is useful in determining the viscoelastic properties of a system in terms of time scale. G' refers the elastic property and G'' refers the viscous property of a system (Okonkwo et al., 2021). The NS has indicated that the system was not viscoelastic in nature since it has shown only the loss modulus responses (Fig. 4a) in a similar time scale as that of the PS system. In contrast, the PS matrix has shown a viscoelastic nature with both G' and G'' (Fig. 4b). Also, the PS system shows a higher G' value than the G'' compared to the NS system at all the frequencies up to 90 Hz. The system has shown a cross over with $G'' > G'$ only at frequency greater than 90 Hz. Since the stability and emulsifying properties of the starch systems can be directly related to the elastic nature of the material, PS was observed to be a better component than NS, which can contribute more stability and elasticity to the system in which they will be incorporated. Also, we can deduce that there are more interaction forces among the PS particles than NS. These interactions in the PS matrix may help promote the formation of steric barriers that can prevent coalescence in emulsions.

XRD

In order to study the effect of enzyme treatment on the amorphous and crystalline region, NS and PS were analyzed by XRD. XRD diffractograms are shown in the (Fig. 5a) and it is evident from the figure that both NS and PS show A pattern, which is characteristic of corn starch. A typical A pattern shows two single broad peaks at 15 and 23 (2θ), lower peak at 20 (2θ), and dual peak at 17–18 (2θ) (Lei et al., 2009). NS and PS in the present study showed

typical A pattern with strong reflections at 2θ of 15, 17, 18, 20, and 23. The deconvolution results show that degree of crystallinity increased from 42.36% in NS to 52% in PS (Fig. 5b and c). The crystallinity of porous starch is increased because enzymatic reaction mainly happens in the amorphous region resulting in increased crystalline region and decreased amorphous region (Zhang et al., 2012). In a recent study, Azfaralariff et al. (2020) reported that starch nanocrystals prepared from sago starch showed increased crystallinity and can be effectively used as emulsifier in oil in water emulsion. This suggests that porous starch with increased crystallinity should be employed for the evaluation as Pickering particle in emulsion.

Thermal Behavior

As the porous starch-based Pickering emulsions could be further converted in to powder form by means of spray drying or freeze drying for application in food, nutraceutical, and pharmaceutical applications, it is important to determine the thermal behavior (especially for spray drying as the sample has to pass through hot air currents) of NS and PS which was assessed by differential scanning calorimetry (DSC) (Fig. 6). Thermal behavior is also important with respect to storage stability (Laura, Gomez-Mascaraque et al., 2017). As can be seen, notable differences were observed between the thermograms of NS and PS. The onset temperature (T_o), peak temperature (T_p), and conclusion temperature (T_c) are given in Table 4 and a delayed gelatinization of NS is observed as in the case of previous reports. Gelatinization is the breaking of intermolecular and intramolecular hydrogen bonds of starch due to excess water and heat. As a result, water is absorbed in an irreversible manner leading to swelling of starch granules. Water can freely enter through amorphous region but in crystalline region, it happens only due to

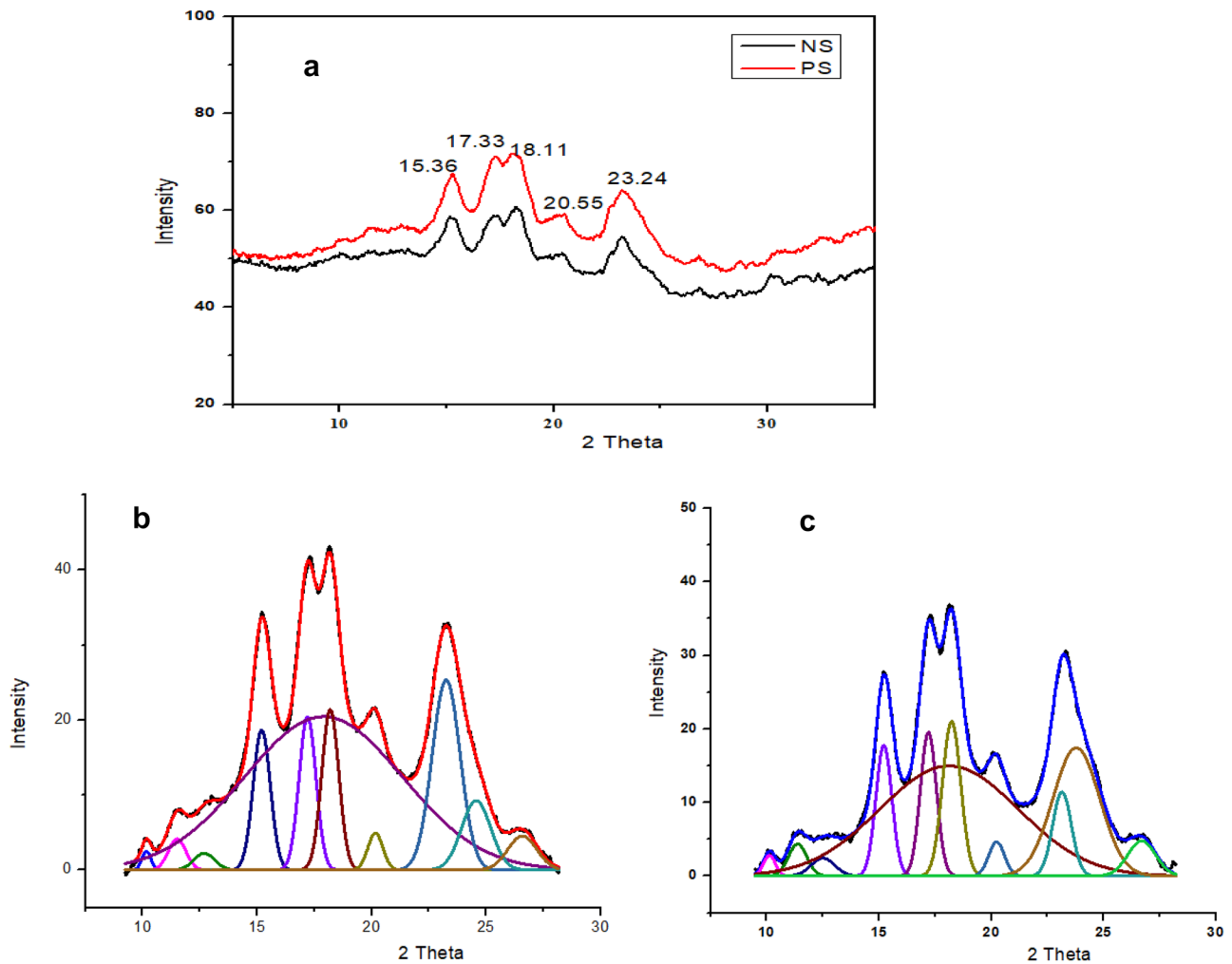


Fig. 5 XRD diffractograms of native and porous starch (a). Deconvolution plots of native and porous starch (b) and c respectively

increased temperature and excess water (Yu et al., 2018). So gelatinization of starch granules is closely related to the proportion of crystalline regions, and more crystallinity results in a higher gelatinization temperature (Zieba et al., 2011). The XRD studies indicated that enzyme hydrolysis results in more crystalline region in PS and therefore, they are more resistant to gelatinization. Therefore, the PS obtained through enzymatic hydrolysis are more thermally resistant and thus can be used for further food applications (Yu et al., 2018).

FTIR The IR spectra of NS and PS are shown in the (Fig. 7). As it is evident from the figure, there is no obvious change in the positions of characteristic absorption peak of NS and PS. This is because the molecular structure of starch did not change after the enzymatic reaction and so the functional groups were also the same (Zhang et al., 2012). The FTIR spectra contain the characteristic peaks for NS in the fingerprint region at 3400 cm^{-1} (–OH stretching) which indicates the free O–H stretching vibration of OH groups in polysaccha-

ride molecule, 1152 cm^{-1} (C–C, C–O stretching), 1080 cm^{-1} (C–O–H bonding), 928 cm^{-1} , skeletal mode vibrations of α -1,4 glycosidic linkage (C–O–C), 859 cm^{-1} (C (1)–H, –CH₂ deformation), 764 cm^{-1} (C–C stretching) (Wang et al., 2016a, b). PS also shows similar peaks with respect to NS confirming that there is no modification in chemical structure of PS and can be used for further applications.

Preparation of Emulsion

Above studies suggested that PS thus prepared could be employed as an emulsifier/stabilizer for O/W emulsions. Therefore, we conducted preliminary studies to evaluate the efficacy of the PS in stabilizing the emulsions. The stability of the emulsion was assessed in terms of creaming index which was measured in terms of height of total emulsion and aqueous layer (Hong et al., 2018; Konar et al., 2019). O/W emulsion was prepared using NS and PS with 10% flax seed oil and 80% water and

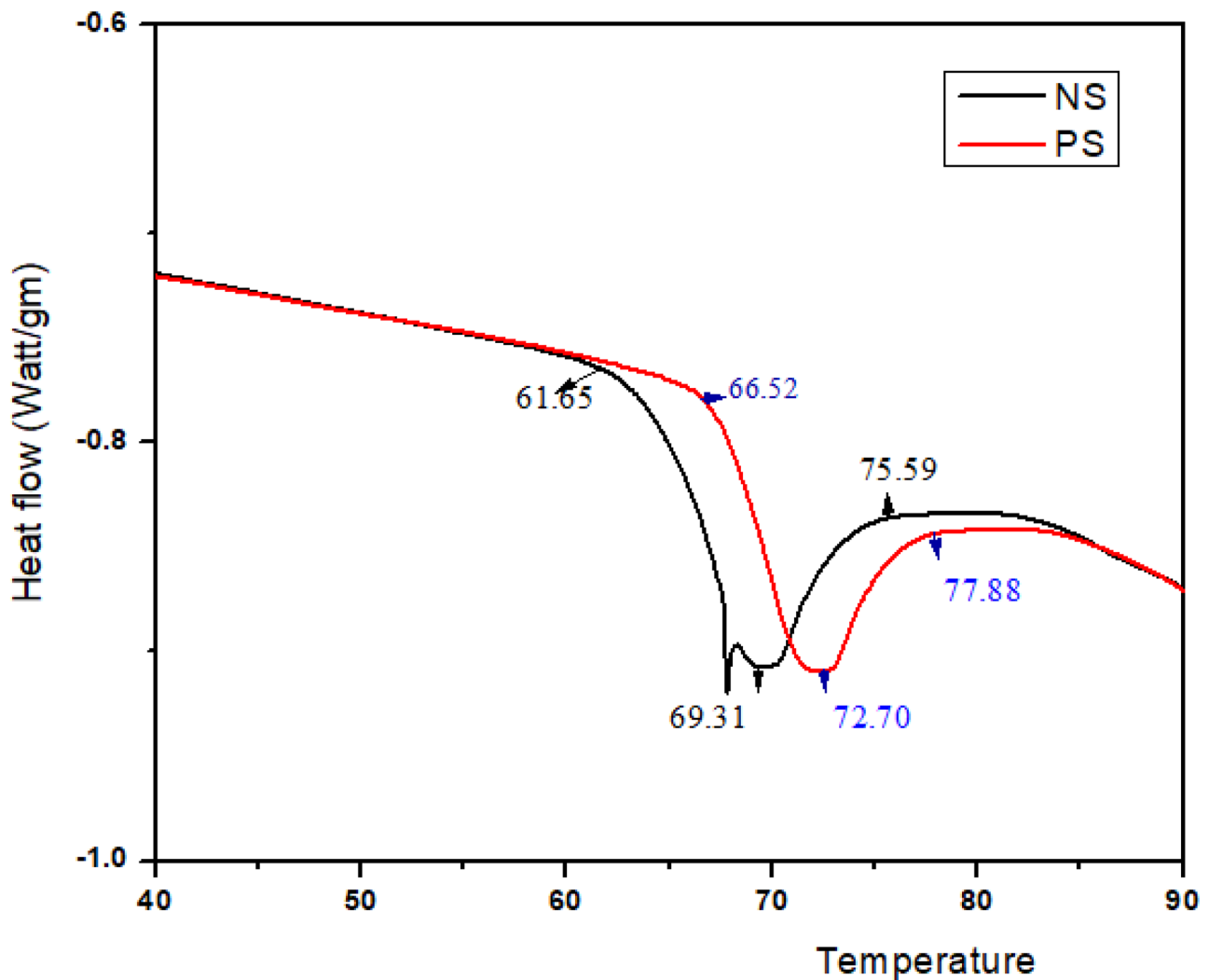


Fig. 6 DSC thermograms of NS and PS

was observed for 48 h of storage. It was found that the creaming index of NS and that of PS after 24 h of storage was 16.6 and 5.0%, respectively, which did not change on further storage (Fig. 8). As can be seen, for emulsion prepared using NS, the oil layer was clearly visible at the top after 30 min itself. However, the PS-stabilized emulsion exhibited significantly higher stability as compared to NS.

The characterization studies in the previous sections suggested better emulsion stabilizing properties of PS as compared to NS. Thus, PS can be more effectively used as Pickering particle in emulsion as compared to NS.

Fluorescence Microscopy

It was understood from the previous studies that PS forms a stable emulsion by acting as a Pickering particle. In order to confirm this, fluorescence microscopy of the freshly

prepared emulsion was performed. The emulsion was stained with safranin and nile red for staining the starch Fig. 9PS (A) and oil Fig. 9PS (B) respectively. Images clearly demonstrate that PS adsorb onto interface between two phases (green color) with inner oil phase (red) and the merged image Fig. 9PS (C) clearly depicts the entrapment of oil by the PS particles, thus acting as Pickering particle. Whereas, in NS-stabilized Pickering emulsion, there was no distinguished layer separation observed. The starch

Table 4 Gelatinization temperature of native and porous starch

	To (°C)	Tp (°C)	Tc (°C)
Native starch	61.76 ± 0.09	69.42 ± 0.09	73.56 ± 0.7
Porous starch	65.94 ± 0.4	72.79 ± 0.07	76.78 ± 0.8

To onset temperature, Tp peak temperature, Tc conclusion temperature

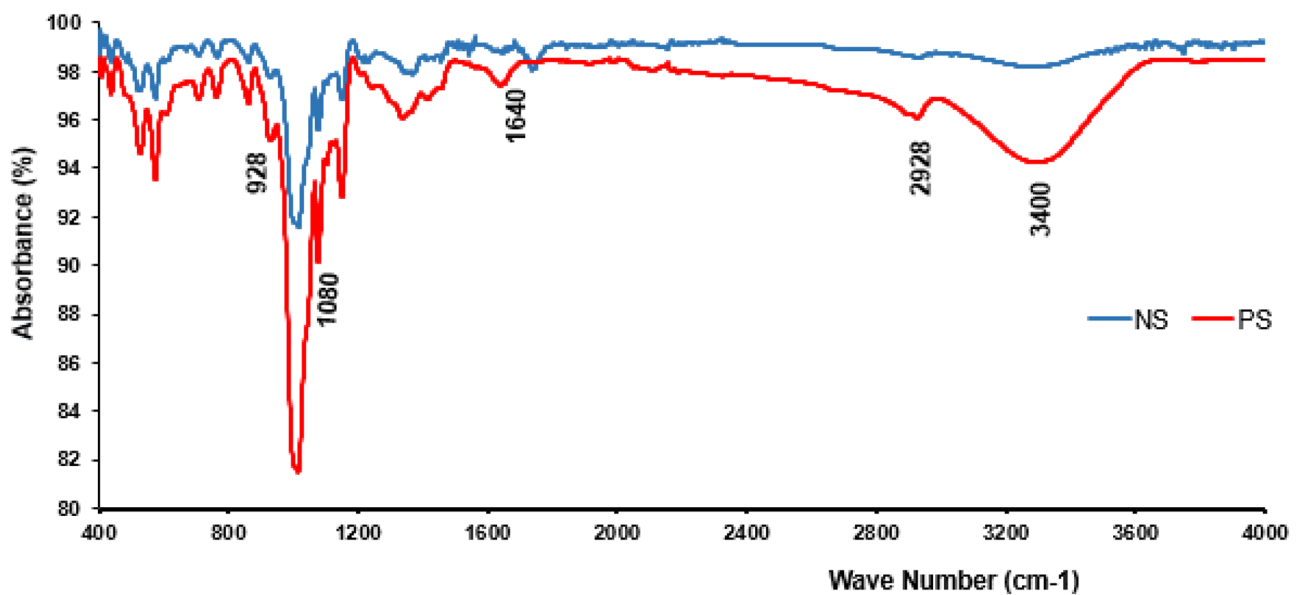


Fig. 7 FTIR spectrum of NS and PS

particles were also found in the core portion of emulsion. Images also demonstrate the presence of oil on the outer surface of starch particles thus leading to the destabilization of the emulsion Fig. 9 NS (A), NS (B), and NS (C). This suggests that PS as Pickering particle can protect nutritionally and biologically active substances by providing a protecting layer surrounding them.

Evaluation of Efficacy of Porous Starch as Carrier of Bioactives

PS is reported to be employed for delivery of flavor, anthocyanins, doxorubicin, and controlled release of insulin for

food and pharmaceutical applications (Belingeri et al., 2015a, b; Ji, 2021; Zhu et al., 2018; Chen et al., 2021). In order to understand the use of PS for delivery applications, we carried out experiments using curcumin as bioactive model system. Both NS and PS were mixed with curcumin for a predetermined time. The slurry was centrifuged so that the un-interacted curcumin (free curcumin) is left behind in the supernatant. The residue was extracted and analyzed for curcumin using HPLC (Dallarmellina et al., 2021; Patil et al., 2017). The typical HPLC chromatograms and quantifications of curcumin, NS and PS samples are shown in Supplementary Fig. 4. The curcumin content of NS and PS were found to $61.03 \pm 1.43\%$ and $82.24 \pm 1.07\%$,

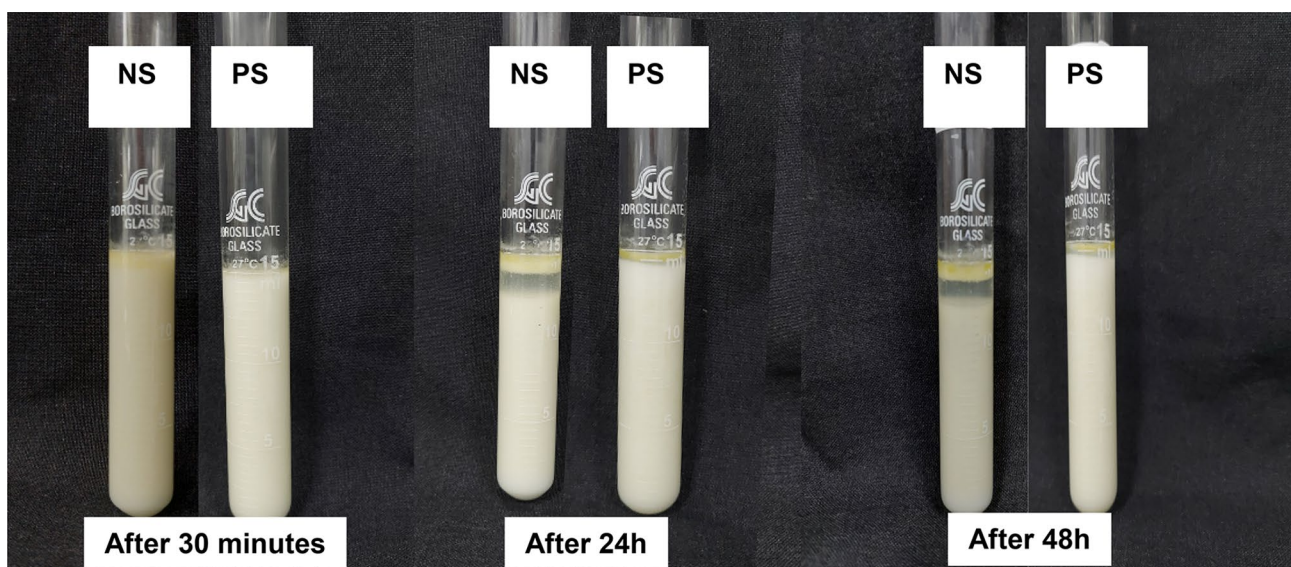


Fig. 8 Emulsion of NS and PS after 30 min, 24 h and 48 h

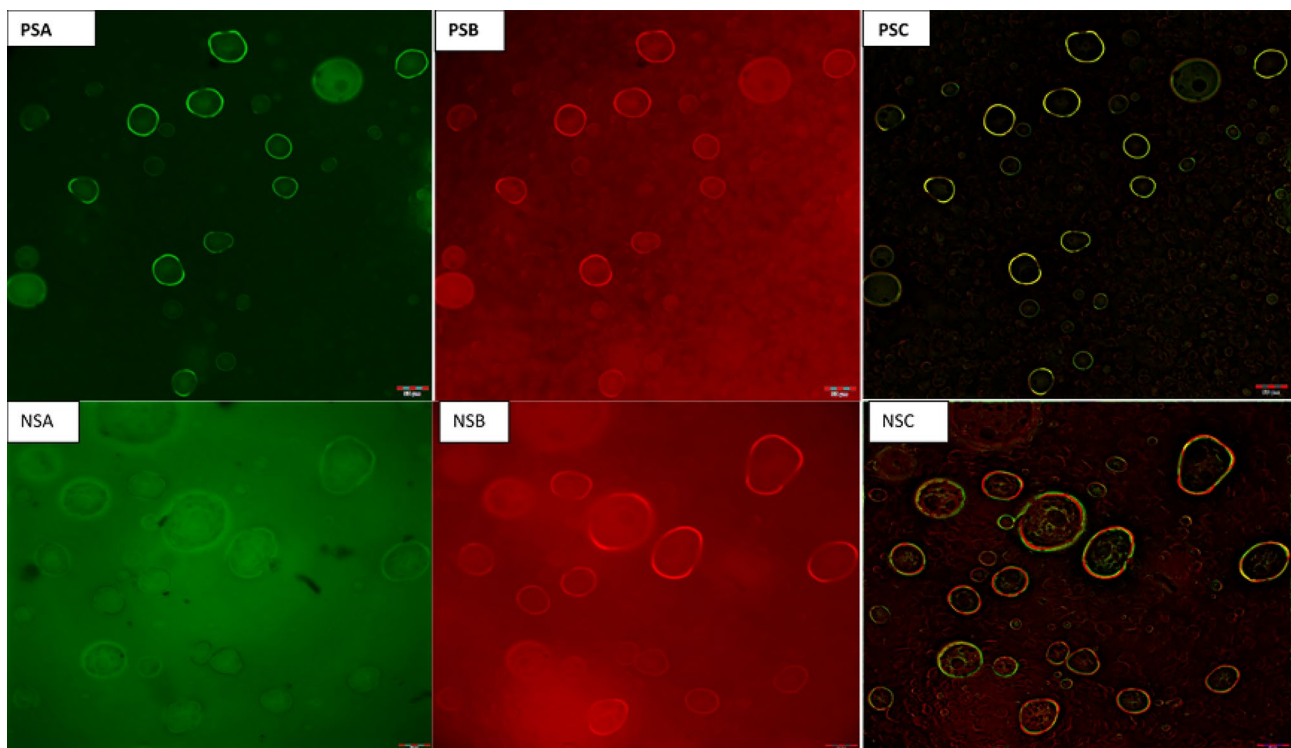


Fig. 9 Fluorescence images of porous (PS) and native starch (NS) stained with **A** safranin **B** Nile red individually and **C** merged image of **A** and **B**

respectively, suggesting that PS can hold significantly higher amount of curcumin than NS. Native starch granules do not have pores on their surface, in general, and therefore cannot accommodate other moieties by adsorption and encapsulation (Choy et al., 2016). These properties can be introduced to the native starch by imparting porosity, e.g., enzymatic treatment as observed in the present study. This confirms that PS could be effectively used as a carrier of nutritional compounds and bioactive for various food and nutraceutical applications.

Conclusion

In the present study, PS was produced from corn starch enzymatically using amylase and amyloglucosidase. Based on statistical analysis, corn starch treated with 300 U amylase and 250 U amyloglucosidase for 6 h incubation yielded PS with optimum surface area and pore size. PS was further characterized in terms of particle size, contact angle, XRD, DSC, FTIR, and rheological studies. PS showed decreased particle size, more hydrophilic and crystalline nature, and better thermal stability compared to native starch indicating its application in O/W emulsions. Rheological studies showed the viscoelastic nature of PS. Further studies were carried out to explore the possible application of PS

as Pickering particle in stabilizing emulsion and found that PS prepared emulsion showed better stability. Fluorescence microscopy confirmed the ability of PS as Pickering particle by adsorbing into interface of water and oil in the emulsion. Finally, the efficiency of PS as bioactive carrier was ratified using curcumin as a model. Thus, the results from the present study demonstrated that porous starch can act as Pickering particle for emulsion stabilization and active substance delivery application. Porous starch can act as vehicles for carrying nutritionally important compounds (e.g., vitamins, minerals, probiotics) in formulation of nutritional supplements/health foods/functional foods, etc. It can also be fine-tuned as a carrier for bioactive phytochemicals and active molecules for nutraceutical and pharmaceutical applications.

Supplementary Information The online version contains supplementary material available at <https://doi.org/10.1007/s11947-022-02843-y>.

Acknowledgements Sannya Sathyan is grateful to the University Grants Commission (UGC, India) for Fellowship and CSIR for the facilities.

Data Availability Data may be made available on request.

Declarations

Conflict of Interest The authors declare no competing interests.

References

- Aggarwal, P., & Dollimore, D. (2000). Degradation of starchy food material by thermal analysis. *Thermochimica Acta*, 358(June 1999), 57–63
- Ahmad, M., Gani, A., Masoodi, F. A., & Rizvi, S. H. (2020). Influence of ball milling on the production of starch nanoparticles and its effect on structural, thermal and functional properties. *International Journal of Biological Macromolecules*, 151, 85–91. <https://doi.org/10.1016/j.ijbiomac.2020.02.139>
- Aveyard, R., Binks, B. P., & Clint, J. H. (2003). Emulsions stabilised solely by colloidal particles. *Advances in Colloid and Interface Science*, 102, 503–546.
- Azfaralariff, A., Faiqah, F., Sisika, R., Faizan, M., & Mat, A. (2020). Food-grade particle stabilized pickering emulsion using modified sago (Metroxylon sagu) starch nanocrystal. *Journal of Food Engineering*, 280(October 2019), 109974. <https://doi.org/10.1016/j.jfoodeng.2020.109974>
- Belingheri, C., Ferrillo, A., & Vittadini, E. (2015a). Porous starch for flavor delivery in a tomato-based food application. *LWT - Food Science and Technology*, 60(1), 593–597. <https://doi.org/10.1016/j.lwt.2014.09.047>
- Belingheri, C., Giussani, B., Rodriguez-estrada, M. T., Ferrillo, A., & Vittadini, E. (2015b). Oxidative stability of high-oleic sunflower oil in a porous starch carrier. *FOOD CHEMISTRY*, 166, 346–351. <https://doi.org/10.1016/j.foodchem.2014.06.029>
- Benavent-gil, Y., & Rosell, C. M. (2016). Comparison of porous starches obtained from different enzyme types and levels. *Carbohydrate Polymers*. <https://doi.org/10.1016/j.carbpol.2016.10.047>
- Cakmak, T., Angun, P., Demiray, Y. E., & Ozkan, A. D. (2012). Differential effects of nitrogen and sulfur deprivation on growth and biodiesel feedstock production of *Chlamydomonas reinhardtii*. *Biotechnology and Bioengineering*, 1–11. <https://doi.org/10.1002/bit.24474>
- Chassaing, B., Koren, O., Goodrich, J. K., Poole, A. C., Srinivasan, S., Ley, R. E., & Gewirtz, A. T. (2015). Dietary emulsifiers impact the mouse gut microbiota promoting colitis and metabolic syndrome. *Nature*, 519(7541), 92–96. <https://doi.org/10.1038/nature14232>
- Chen, J., Wang, Y., Liu, J., & Xu, X. (2020). Preparation, characterization, physicochemical property and potential application of porous starch: A review. *International Journal of Biological Macromolecules*, 148, 1169–1181. <https://doi.org/10.1016/j.ijbiomac.2020.02.055>
- Chen, L., Tian, Y., Bai, Y., Wang, J., Jiao, A., & Jin, Z. (2017). Effect of frying on the pasting and rheological properties of normal maize starch. *Food Hydrocolloids*. <https://doi.org/10.1016/j.foodhyd.2017.09.024>
- Chen, Y., Song, H., Huang, K., & Guan, X. (2021). Novel porous starch/alginate hydrogel for controlled insulin release with dual response of pH and amylase. *Food & Function*, 0–27. <https://doi.org/10.1039/D1FO01411K>
- Choy, S. Y., Prasad, K. N., Wu, T. Y., Raghunandan, M. E., & Ramanan, R. N. (2016). Performance of conventional starches as natural coagulants for turbidity removal. *Ecological Engineering*, 94, 352–364. <https://doi.org/10.1016/j.ecoleng.2016.05.082>
- Comunian, T. A., da Silva Anthero, A. G., Bezerra, E. O., Moraes, I. C. F., & Hubinger, M. D. (2020). Encapsulation of pomegranate seed oil by emulsification followed by spray drying: Evaluation of different biopolymers and their effect on particle properties. *Food and Bioprocess Technology*, 13(1), 53–66.
- Da Silva Soares, B., De Carvalho, C. W. P., & Garcia-Rojas, E. E. (2021). Microencapsulation of Sacha Inchi oil by complex coacervates using ovalbumin-tannic acid and pectin as wall materials. *Food and Bioprocess Technology*, 14(5), 817–830
- Dai, L., Li, C., Zhang, J., & Cheng, F. (2018). Preparation and characterization of starch nanocrystals combining ball milling with acid hydrolysis. *Carbohydrate Polymers*, 180(September 2017), 122–127. <https://doi.org/10.1016/j.carbpol.2017.10.015>
- Dallarmellina, A., Letan, M., Duval, C., & Contino-Pépin. (2021). One-pot solvent-free extraction and formulation of lipophilic natural products: From curcuma to dried formulations of curcumin. *Green Chemistry*. <https://doi.org/10.1039/d1gc00587a>
- Daniel, J. F., & Ana, A. M. (2020). Rice in vitro digestion: Application of INFOGEST harmonized protocol for glycemic index determination and starch morphological study. *Journal of Food Science and Technology*, 57(April), 1393–1404. <https://doi.org/10.1007/s13197-019-04174-x>
- Dean, A. P., Sigee, D. C., Estrada, B., & Pittman, J. K. (2010). Using FTIR spectroscopy for rapid determination of lipid accumulation in response to nitrogen limitation in freshwater microalgae. *Biore-source Technology*, 101(12), 4499–4507. <https://doi.org/10.1016/j.biortech.2010.01.065>
- Din, Z.-, Xiong, H., & Fei, P. (2015). Physical and chemical modification of starches - A review. 8398(November). <https://doi.org/10.1080/10408398.2015.1087379>
- Du, S., Wang, L., Fu, X., Chen, M., & Wang, C. (2013). Bioresource technology hierarchical porous carbon microspheres derived from porous starch for use in high-rate electrochemical double-layer capacitors. *Biore-source Technology*, 139, 406–409. <https://doi.org/10.1016/j.biortech.2013.04.085>
- Dura, A., Błaszczak, W., & Rosell, C. M. (2014). Functionality of porous starch obtained by amylase or amyloglucosidase treatments. *Carbohydrate Polymers*, 101, 837–845. <https://doi.org/10.1016/j.carbpol.2013.10.013>
- Espinosa-Solís, V., García-Tejeda, Y. V., Portilla-Rivera, O. M., & Barrera-Figueroa, V. (2021). Tailoring olive oil microcapsules via microfluidization of Pickering o/w emulsions. *Food and Bioprocess Technology*, 14(10), 1835–1843.
- Frelichowska, J., Bolzinger, M., & Chevalier, Y. (2009). *Colloids and Surfaces A: Physicochemical and Engineering Aspects Pickering Emulsions with Bare Silica*, 343, 70–74. <https://doi.org/10.1016/j.colsurfa.2009.01.031>
- Gomez-Mascaraque, L. G., Sipoli, C. C., Gaziola, L., & de La Torre, A.L.-R. (2017). Microencapsulation structures based on protein-coated liposomes obtained through electrospraying for the stabilization and improved bioaccessibility of curcumin. *Food Chemistry*. <https://doi.org/10.1016/j.foodchem.2017.04.133>
- Guida, C., Aguiar, A. C., & Cunha, R. L. (2021). Green techniques for starch modification to stabilize Pickering emulsions: A current review and future perspectives. *Current Opinion in Food Science*, 38, 52–61. <https://doi.org/10.1016/j.cofs.2020.10.017>
- Guo, L., Li, J., Li, H., Zhu, Y., & Cui, B. (2020). The structure property and adsorption capacity of new enzyme-treated potato and sweet potato starches. *International Journal of Biological Macromolecules*, 144, 863–873. <https://doi.org/10.1016/j.ijbiomac.2019.09.164>
- Guo, L., Yuan, Y., Li, J., Tan, C., Janaswamy, S., Lu, L., Fang, Y., & Cui, B. (2021). Comparison of functional properties of porous starches produced with different enzyme combinations. *International Journal of Biological Macromolecules*, 174(31771933), 110–119. <https://doi.org/10.1016/j.ijbiomac.2021.01.165>
- He, G. J., Liu, Q., & Thompson, M. R. (2013). Characterization of structure and properties of thermoplastic potato starch film surface cross-linked by UV irradiation. 304–311. <https://doi.org/10.1002/star.201200097>
- Hong, I. K., Kim, S. I., & Lee, S. B. (2018). Effects of HLB value on oil-in-water emulsions: Droplet size, rheological behavior, zeta-potential, and creaming index. *Journal of Industrial and Engineering Chemistry*, 67, 123–131. <https://doi.org/10.1016/j.jiec.2018.06.022>
- Hoon, S., Yerim, P., Jungwoo, N., Shin, K., & Kang, D. (2018). Properties and applications of starch modifying enzymes for use in

- the baking industry. *Food Science and Biotechnology*, 27(2), 299–312. <https://doi.org/10.1007/s10068-017-0261-5>
- Ichihara, T., Fukuda, J., Takaha, T., Yuguchi, Y., & Kitamura, S. (2013). Limited hydrolysis of insoluble cassava starch granules results in enhanced gelling properties. *Journal of Applied Glycoscience*, 61(1), 15–20. <https://doi.org/10.5458/jag.jag>
- Jadhav, N. V., & Vavia, P. R. (2017). Supercritical processed starch nanosponge as a carrier for enhancement of dissolution and pharmacological efficacy of fenofibrate. *International Journal of Biological Macromolecules*. <https://doi.org/10.1016/j.ijbiomac.2017.03.002>
- Ji, Y. (2021). Synthesis of porous starch microgels for the encapsulation, delivery and stabilization of anthocyanins. *Journal of Food Engineering*, 302, 110552. <https://doi.org/10.1016/j.jfoodeng.2021.110552>
- Jiang, S., Yu, Z., Hu, H., Lv, J., Wang, H., & Jiang, S. (2017). Adsorption of procyanidins onto chitosan-modified porous rice starch. *LWT - Food Science and Technology*. <https://doi.org/10.1016/j.lwt.2017.05.047>
- Jiang, Y., Li, F., Li, D., Sun-Waterhouse, D., & Huang, Q. (2019). Zein/pectin nanoparticle-stabilized sesame oil Pickering emulsions: Sustainable bioactive carriers and healthy alternatives to sesame paste. *Food and Bioprocess Technology*, 12(12), 1982–1992.
- Kierulf, A., Azizi, M., Eskandarloo, H., Whaley, J., Liu, W., Perez-herrera, M., You, Z., & Abbaspourrad, A. (2019). Food hydrocolloids starch-based Janus particles : Proof-of-concept heterogeneous design via a spin-coating spray approach. *Food Hydrocolloids*, 91(January), 301–310. <https://doi.org/10.1016/j.foodhyd.2019.01.037>
- Kierulf, A., Whaley, J., Liu, W., Enayati, M., & Tan, C. (2020). Protein content of amaranth and quinoa starch plays a key role in their ability as Pickering emulsi fi ers. *Food Chemistry*, 315(January), 126246. <https://doi.org/10.1016/j.foodchem.2020.126246>
- Konar, N., Ozarda, O., Senocak, S., Unluturk, N. N., & Oba, S. (2019). Effects of process conditions on citrus beverage emulsions' creaming index: RSM approach. *ETP International Journal of Food Engineering*, 5, 22–27. <https://doi.org/10.18178/ijfe.5.1.22-27>
- Korma, S. A., Niazi, S., Ammar, A., Zaaboul, F., & Zhang, T. (2016). Chemically modified starch and utilization in food stuffs. 5(4), 264–272. <https://doi.org/10.11648/j.ijnfs.20160504.15>
- Lacerda, L. D., Leite, D. C., & Nádyá, P. (2019). Relationships between enzymatic hydrolysis conditions and properties of rice porous starches. *Journal of Cereal Science*, 89(July), 102819. <https://doi.org/10.1016/j.jcs.2019.102819>
- Lacerda, L. D., Leite, D. C., Soares, R. M. D., & Silveira, N. P. (2018). Effects of α -amylase, amyloglucosidase, and their mixture on hierarchical porosity of rice starch. *Starch*, 1800008, 1–7. <https://doi.org/10.1002/star.201800008>
- Lei, W.-C., & Zhao Jiu-Ran, L.W.-P. (2009). Crystalline structure and pasting properties of starch in eight cultivars of spring- and autumn-sown waxy corn. *Acta Agronomica Sinica*, 35(3), 499–505. [https://doi.org/10.1016/S1875-2780\(08\)60070-X](https://doi.org/10.1016/S1875-2780(08)60070-X)
- Li, C., Li, Y., Sun, P., & Yang, C. (2013). Pickering emulsions stabilized by native starch granules. *Colloids and Surfaces a: Physicochemical and Engineering Aspects*, 431, 142–149. <https://doi.org/10.1016/j.colsurfa.2013.04.025>
- Liu, J., Wang, X., Yong, H., Kan, J., & Jin, C. (2018). Recent advances in flavonoid-grafted polysaccharides: Synthesis, structural characterization, bioactivities and potential applications. *International Journal of Biological Macromolecules*, 2017. <https://doi.org/10.1016/j.ijbiomac.2018.05.149>
- Liu, Q., Bao, H., Xi, C., & Miao, H. (2014). Rheological characterization of tuna myofibrillar protein in linear and nonlinear viscoelastic regions. *Journal of Food Engineering*, 121(1), 58–63. <https://doi.org/10.1016/j.jfoodeng.2013.08.016>
- Majzoobi, M., Hedayati, S., & Farahnaky, A. (2015). Functional properties of microporous wheat starch produced by α -amylase and sonication. *Food Bioscience*. <https://doi.org/10.1016/j.fbio.2015.05.001>
- Malucelli, L. C., Lacerda, L. G., da Carvalho Filho, M. A. S., Fernández, D. E. R., Demiate, I. M., Oliveira, C. S., & Schnitzler, E. (2015). Porous waxy maize starch. *Journal of Thermal Analysis and Calorimetry*, 2015, 525–532. <https://doi.org/10.1007/s10973-015-4483-6>
- Maphosa, Y., & Jideani, V. A. (2018). Factors affecting the stability of emulsions stabilised by biopolymers. *Science and Technology behind Nanoemulsions*. <https://doi.org/10.5772/intechopen.75308>
- Marefati, A., Wiege, B., Haase, N. U., Matos, M., & Rayner, M. (2017). Pickering emulsifiers based on hydrophobically modified small granular starches – Part I : Manufacturing and physico-chemical characterization. *Carbohydrate Polymers*. <https://doi.org/10.1016/j.carbpol.2017.07.044>
- Marku, D., Wahlgren, M., Rayner, M., Sjöö, M., & Timgren, A. (2012). Characterization of starch Pickering emulsions for potential applications in topical formulations. *International Journal of Pharmaceutics*, 428(1–2), 1–7. <https://doi.org/10.1016/j.ijpharm.2012.01.031>
- Mohammed, A. N., Ishwarya, S. P., & Nisha, P. (2021). Nanoemulsion versus microemulsion systems for the encapsulation of beetroot extract: Comparison of physicochemical characteristics and betalain stability. *Food and Bioprocess Technology*, 14(1), 133–150.
- Nawaz, H., Waheed, R., Nawaz, M., & Shahwar, D. (2020). Physical and chemical modifications in starch structure and reactivity. *Chemical Properties of Starch*, 9, 13–35. <https://doi.org/10.5772/intechopen.88870>
- Okonkwo, V. C., Mba, O. I., Kwofie, E. M., & Ngadi, M. O. (2021). Rheological properties of meat sauces as influenced by temperature. *Food and Bioprocess Technology*, 14(11), 2146–2160.
- Oliyaee, N., Moosavi-nasab, M., & Mohammad, A. (2020). Encapsulation of fucoxanthin in binary matrices of porous starch and halloysite. *Food Hydrocolloids*, 100(May 2019), 105458. <https://doi.org/10.1016/j.foodhyd.2019.105458>
- Patil, V. S., Gutierrez, A. M., Sunkara, M., Morris, A. J., Hilt, J. Z., Kalika, D. S., & Dziubla, T. D. (2017). Curcumin acrylation for biological and environmental applications. *Journal of Natural Products*, 80(2017), 1964–1971. <https://doi.org/10.1021/acs.jnatprod.6b00951>
- Perez, S., Baldwin, P. M., & Gallant, D. J. (2009). *Structural features of starch granules I*. Elsevier Inc. <https://doi.org/10.1016/B978-0-12-746275-2.00005-7>
- Pickering, S. U. (1907). CXCVI.—Emulsions. *Journal of the Chemical Society, Transactions*, 91(0), 2001–2021. <https://doi.org/10.1002/9781119220510.ch15>
- Punia, S. (2019). Barley starch modifications: Physical, chemical and enzymatic - A review. *International Journal of Biological Macromolecules*. <https://doi.org/10.1016/j.ijbiomac.2019.12.088>
- Qi, F., Wu, J., Sun, G., Nan, F., Ngai, T., & Ma, G. (2014). Systematic studies of Pickering emulsions stabilized by uniform-sized PLGA particles : Preparation and stabilization mechanism †. *Journal of Materials Chemistry b: Materials for Biology and Medicine*, 2, 7605–7611. <https://doi.org/10.1039/C4TB01165A>
- Ramsden, W. (1903). Separation of solids in the surface-layers of solutions and 'suspensions' (observations on surface-membranes, bubbles, emulsions, and mechanical coagulation).—preliminary account. *Proceeding of the Royal Society London*, 72, 156–164.
- Rayner, M., Sjöo, M., Timgren, A., & Dejmek, P. (2012). Quinoa starch granules as stabilizing particles for production of Pickering emulsions. *Faraday Discussions*, 158(2012), 139–155. <https://doi.org/10.1039/c2fd20038d>
- Saari, H., & Marilyn Rayner, M. W. (2019). Effects of starch granules differing in size and morphology from different botanical sources

- and their mixtures on the characteristics of Pickering emulsions. *Food Hydrocolloids*. <https://doi.org/10.1016/j.foodhyd.2018.11.063>
- Saffarionpour, S. (2020). Nanocellulose for stabilization of Pickering emulsions and delivery of nutraceuticals and its interfacial adsorption mechanism. *Food and Bioprocess Technology*, 13(8), 1292–1328.
- Schafer, B., Hecht, M., Harting, J., & Nirschl, H. (2010). Agglomeration and filtration of colloidal suspensions with DVLO interactions in simulation and experiment. *Journal of Colloid and Interface Science*, 349(1), 186–195. <https://doi.org/10.1016/j.jcis.2010.05.025>
- Steffe, J. F. (1996). Rheological methods in food process engineering. In *East Lansing, MI 48823 USA: Freeman Press* (Second ed.). <https://doi.org/10.1016/b978-1-4832-3245-4.50016-9>
- Su, J., Huang, Z., Yuan, X., Wang, X., & Li, M. (2010). Structure and properties of carboxymethyl cellulose / soy protein isolate blend edible films crosslinked by Maillard reactions. *Carbohydrate Polymers*, 79(1), 145–153. <https://doi.org/10.1016/j.carbpol.2009.07.035>
- Sun, H., Zhao, P., & Ge, X. (2010). Recent advances in microbial raw starch degrading enzymes. *Applied Biochemistry and Biotechnology*, 988–1003. <https://doi.org/10.1007/s12010-009-8579-y>
- Tao, H., Wang, P., Wu, F., Jin, Z., & Xu, X. (2016). Particle size distribution of wheat starch granules in relation to baking properties of frozen dough. *Carbohydrate Polymers*, 137, 147–153. <https://doi.org/10.1016/j.carbpol.2015.10.063>
- Wang, H., Lv, J., Jiang, S., Niu, B., Pang, M., & Jiang, S. (2016a). Preparation and characterization of porous corn starch and its adsorption toward grape seed proanthocyanidins. *Starch/starke*, 68, 1–10. <https://doi.org/10.1002/star.201600009>
- Wang, A. J., Paterson, T., Owen, R., Sherborne, C., Dugan, J., Li, J. M., et al. (2016b). Photocurable high internal phase emulsions (HIPEs) containing hydroxyapatite for additive manufacture of tissue engineering scaffolds with multi-scale porosity. *Materials Science & Engineering, c: Materials for Biological Applications*, 67, 51–58.
- Wei, B., Hu, X., Li, H., Wu, C., Xu, X., Jin, Z., & Tian, Y. (2014). Effect of pHs on dispersity of maize starch nanocrystals in aqueous medium. *Food Hydrocolloids*, 36, 369–373. <https://doi.org/10.1016/j.foodhyd.2013.08.015>
- Wu, J., & Ma, G. (2016). Recent studies of Pickering emulsions : Particles make the difference. *Small*, 1–16. <https://doi.org/10.1002/smll.201600877>
- Wu, W., Jiao, A., Xu, E., Chen, Y., & Jin, Z. (2020). Effects of extrusion technology combined with enzymatic hydrolysis on the structural and physicochemical properties of porous corn starch. *Food and Bioprocess Technology*, 13(3), 442–451.
- Wu, X., Li, X., Yang, L., Yuan, L., Xu, Z., Xu, J., & Li, D. (2021). Stability enhanced Pickering emulsions based on gelatin and dialdehyde starch nanoparticles as simple strategy for structuring liquid oils. *Food and Bioprocess Technology*, 1–11
- Xu, E., Wu, Z., Long, J., Wang, F., Pan, X., Xu, X., ... & Jiao, A. (2015). Effect of thermostable α -amylase addition on the physicochemical properties, free/bound phenolics and antioxidant capacities of extruded hulled and whole rice. *Food and Bioprocess Technology*, 8(9), 1958–1973
- Yu, L., Zhao, A., Yang, M., Wang, C., Wang, M., & Bai, X. (2018). Effects of the combination of freeze-thawing and enzymatic hydrolysis on the microstructure and physicochemical properties of porous corn starch. *Food Hydrocolloids*. <https://doi.org/10.1016/j.foodhyd.2018.04.041>
- Zhang, B., Cui, D., Liu, M., Gong, H., Huang, Y., & Han, F. (2012). Corn porous starch: Preparation, characterization and adsorption property. *International Journal of Biological Macromolecules*, 50(1), 250–256. <https://doi.org/10.1016/j.ijbiomac.2011.11.002>
- Zhang, C., Lim, S., & Chung, H. (2019). Physical modification of potato starch using mild heating and freezing with minor addition of gums. *Food Hydrocolloids*, 94(February), 294–303. <https://doi.org/10.1016/j.foodhyd.2019.03.027>
- Zhou, X., Chang, Q., Li, J., Jiang, L., Xing, Y., & Jin, Z. (2021). Preparation of V-type porous starch by amylase hydrolysis of V-type granular starch in aqueous ethanol solution. *International Journal of Biological Macromolecules*, 183, 890–897. <https://doi.org/10.1016/j.ijbiomac.2021.05.006>
- Zhu, J., Zhong, L., Chen, W., Song, Y., & Qian, Z. (2018). Preparation and characterization of pectin/chitosan beads containing porous starch embedded with doxorubicin hydrochloride: A novel and simple colon targeted drug delivery system. *Food Hydrocolloids*. <https://doi.org/10.1016/j.foodhyd.2018.04.042>
- Zhu, F. (2019). Starch based Pickering emulsions: Fabrication, properties, and applications. *Trends in Food Science and Technology*, 85(November 2018), 129–137. <https://doi.org/10.1016/j.tifs.2019.01.012>
- Zieba, T., Szumny, A., & Kapelko, M. (2011). Properties of retrograded and acetylated starch preparations: Part 1. Structure, susceptibility to amylase, and pasting characteristics. *LWT - Food Science and Technology*, 44(5), 1314–1320. <https://doi.org/10.1016/j.lwt.2010.12.018>

Publisher's Note Springer Nature remains neutral with regard to jurisdictional claims in published maps and institutional affiliations.